VOLUME 39 NOVEMBER 1961 NUMBER 11

Canadian Journal of Chemistry

Editor: LÉO MARION

Associate Editors:

E. BAER, *University of Toronto*
D. H. EVERETT, *University of Bristol*
R. U. LEMIEUX, *University of Alberta*
D. J. LE ROY, *University of Toronto*
C. A. McDOWELL, *University of British Columbia*
E. W. R. STEACIE, *National Research Council of Canada*
R. W. TAFT, Jr., *The Pennsylvania State University*
H. G. THODE, *McMaster University*
A. E. VAN ARKEL, *University of Leiden*

Published by THE NATIONAL RESEARCH COUNCIL

OTTAWA CANADA

Canadian Journal of Chemistry

Under the authority of the Chairman of the Committee of the Privy Council on Scientific and Industrial Research, the National Research Council issues THE CANADIAN JOURNAL OF CHEMISTRY and five other journals devoted to the publication, in English or French, of the results of original scientific research. Matters of general policy concerning these journals are the responsibility of a joint Editorial Board consisting of: members representing the National Research Council of Canada; the Editors of the Journals; and members representing the Royal Society of Canada and four other scientific societies.

The Chemical Institute of Canada has chosen the Canadian Journal of Chemistry as its medium of publication for scientific papers.

EDITORIAL BOARD

Representatives of the National Research Council

I. McT. Cowan (Chairman), *University of British Columbia*
Léo Marion, *National Research Council*
H. G. Thode, *McMaster University*
D. L. Thomson, *McGill University*

Editors of the Journals

D. L. Bailey, *University of Toronto*
T. W. M. Cameron, *Macdonald College*
F. E. Chase, *Ontario Agricultural College*
H. E. Duckworth, *McMaster University*
Léo Marion, *National Research Council*
J. F. Morgan, *Department of National Health and Welfare, Ottawa*
J. A. F. Stevenson, *University of Western Ontario*

Representatives of Societies

D. L. Bailey, *University of Toronto*
Royal Society of Canada
T. W. M. Cameron, *Macdonald College*
Royal Society of Canada
H. E. Duckworth, *McMaster University*
Royal Society of Canada
Canadian Association of Physicists
P. R. Gendron, *University of Ottawa*
Chemical Institute of Canada
D. J. Le Roy, *University of Toronto*
Royal Society of Canada
J. F. Morgan, *Department of National Health and Welfare, Ottawa*
Canadian Biochemical Society
R. G. E. Murray, *University of Western Ontario*
Canadian Society of Microbiologists
J. A. F. Stevenson, *University of Western Ontario*
Canadian Physiological Society

Ex officio

Léo Marion (Editor-in-Chief), *National Research Council*
J. B. Marshall (Administration and Awards), *National Research Council*

Manuscripts for publication should be submitted to Dr. Léo Marion, Editor-in-Chief, Canadian Journal of Chemistry, National Research Council, Ottawa 2, Canada.
(For instructions on preparation of copy, see **Notes to Contributors** (inside back cover).)

Proof, correspondence concerning proof, and orders for reprints should be sent to the Manager, Editorial Office (Research Journals), Division of Administration and Awards, National Research Council, Ottawa 2, Canada.

Subscriptions, renewals, requests for single or back numbers, and all remittances should be sent to Division of Administration and Awards, National Research Council, Ottawa 2, Canada. Remittances should be made payable to the Receiver General of Canada, credit National Research Council.

The journals published, frequency of publication, and subscription prices are:

Canadian Journal of Biochemistry and Physiology	Monthly	$9.00 a year
Canadian Journal of Botany	Bimonthly	$6.00 a year
Canadian Journal of Chemistry	Monthly	$12.00 a year
Canadian Journal of Microbiology	Bimonthly	$6.00 a year
Canadian Journal of Physics	Monthly	$9.00 a year
Canadian Journal of Zoology	Bimonthly	$5.00 a year

The price of regular single numbers of all journals is $2.00.

Canadian Journal of Chemistry

Issued by THE NATIONAL RESEARCH COUNCIL OF CANADA

VOLUME 39 NOVEMBER 1961 NUMBER 11

DIELECTRIC RELAXATION IN LIQUIDS

II. ISOMERIC PENTANEDIOLS[1]

D. W. DAVIDSON

ABSTRACT

For five pentanediols the infrared spectra, the dipole moments, and the static dielectric constants show an increasing degree of internal hydrogen bonding with increasing proximity of the OH groups. The dielectric dispersion loci at low temperatures are skewed arcs over most of the dispersion range. Values of the parameter β decrease from ca. 1 to 0.55 in the series 1,5-, 1,4-, 1,2-, 2,4-, and 2,3-pentanediol, which is also the order of increasing relaxation time τ_0 at low temperatures. Increased τ_0 is associated with increased irregularity of intermolecular hydrogen bonding, an effect which supports the view that relaxation proceeds by a co-operative mechanism which is facilitated by regularity in the liquid structure. At temperatures of "structural relaxation", values of log τ_0 are linear in $(T-T_\infty)^{-1}$; the proportionality constants, but not the T_∞'s, are the same for all five diols.

The experimental behavior at relatively high frequencies departs from both the skewed-arc and Glarum equations, although less from the latter. These departures are compared with the high frequency dispersion regions in *n*-propanol.

In a previous paper (1) the ability of the skewed-arc expression to represent the results of dielectric relaxation measurements of liquids has been discussed. Most mono-hydroxyl alcohols exhibit a principal dispersion region which is, within the experimental errors, of the classical Debye type ($\beta = 1$ in the skewed-arc representation). This is in contrast to the relaxation behavior of such polyhydroxyl alcohols as have been studied, for which values of β considerably smaller than unity must be invoked. It is natural to attempt to relate this qualitative difference in the relaxation behavior to the absence in the polyhydroxyl liquids of the same degree of regularity in *inter*molecular hydrogen bonding that exists in the simple alcohols. In order to examine the role played by *intra*-molecular hydrogen bonding and steric factors in the extent and regularity of the hydrogen bonding between polyhydroxyl molecules, we have studied the relaxation behavior of five isomeric pentanediols. With one exception, the pentanediols may be cooled sufficiently to bring the dispersion regions within the frequency range required for bridge measurements.

Information about the extent of *intra*molecular hydrogen bonding was provided by an examination of the hydroxyl-group stretching bands in the infrared spectra of dilute solutions of the pentanediols in carbon tetrachloride and by measurement of the dipole moments of the pentanediols in dioxane solution.

EXPERIMENTAL METHODS

1,2-Pentanediol was prepared by bromohydrination of pentene-1 with N-bromo-succinimide, conversion to the epoxide (b.p. 76–78°), and hydrolysis to the diol with Dowex 50 resin.

[1]*Manuscript received May 25, 1961.*
Contribution from the Division of Applied Chemistry, National Research Council, Ottawa, Canada.
Issued as N.R.C. No. 6503.

The infrared spectrum of a commercial sample of 2,3-pentanediol showed a strong spurious band at 1733 cm^{-1}, which disappeared after saponification with sodium hydroxide. An authentic sample of the 2,3-diol was prepared from pentene-2 (which gas-chromatographic analysis showed to consist of roughly equal proportions of the trans and cis forms) by performic acid oxidation and hydrolysis. The product (*B*) consisted of approximately equal amounts of *threo* and *erythro* isomers. Its infrared spectrum was almost identical with that of the saponified commercial product (*A*).

The other pentanediols were commercial products.

All the pentanediols were fractionated in a Todd still. The boiling ranges and refractive indices are given in Table I.

TABLE I

Pentanediol		Boiling range (p, mm)	n_D
1,2		83–84° (3)	1.4387 (23°)
2,3	*A*	70–71° (3.5)	1.4404 (20°)
	B		1.4405 (20°)
1,4		221–222° (748)	
		103° (4)	1.4451 (25°)
2,4	*A*	199–200° (757)	1.4329 (25°)
	B	83° (5)	1.4329 (25°)
1,5		239° (759)	
		121° (6)	1.4495 (25°)

1,4-Dioxane was refluxed for several hours over calcium hydride and distilled.

The dielectric constant and loss measurements at frequencies up to 500 kc/sec and the temperature measurement and control were essentially as outlined previously (2). Less accurate measurements at higher frequencies were made in the case of 1,5-pentanediol with (*a*) a Model 260A Boonton Q-Meter and a cell consisting of two parallel-plate platinum electrodes mounted in a glass vessel, and (*b*) a Model 250A Boonton RX-Meter and a cell constructed of two coaxial stainless steel electrodes with Teflon insulation.

Measurements of the dipole moments of the pentanediols in dioxane were made by the method previously described (3). Infrared spectra of the carbon tetrachloride solutions were obtained with a Perkin–Elmer Model 112 infrared spectrometer equipped with sodium chloride and calcium fluoride optics.

RESULTS AND DISCUSSION

Intramolecular Hydrogen Bonding

(a) OH Stretching Vibrations

The fundamental OH stretching vibration region of the infrared spectra of solutions of the pentanediols in carbon tetrachloride is shown in Fig. 1. Following Kuhn (4) and others, one may associate the presence in this region of two bands of concentration-independent relative intensity at low concentrations (less than 0.1% or 0.015 molar) with the presence of both free and *intra*molecularly hydrogen-bonded OH groups. The frequencies of free OH groups and of those taking part in *intra*molecular and, at higher concentrations, in *inter*molecular hydrogen bonds are given in Table II. The latter are somewhat concentration dependent; the values given are for concentrations in the range 0.2 to 0.6%.

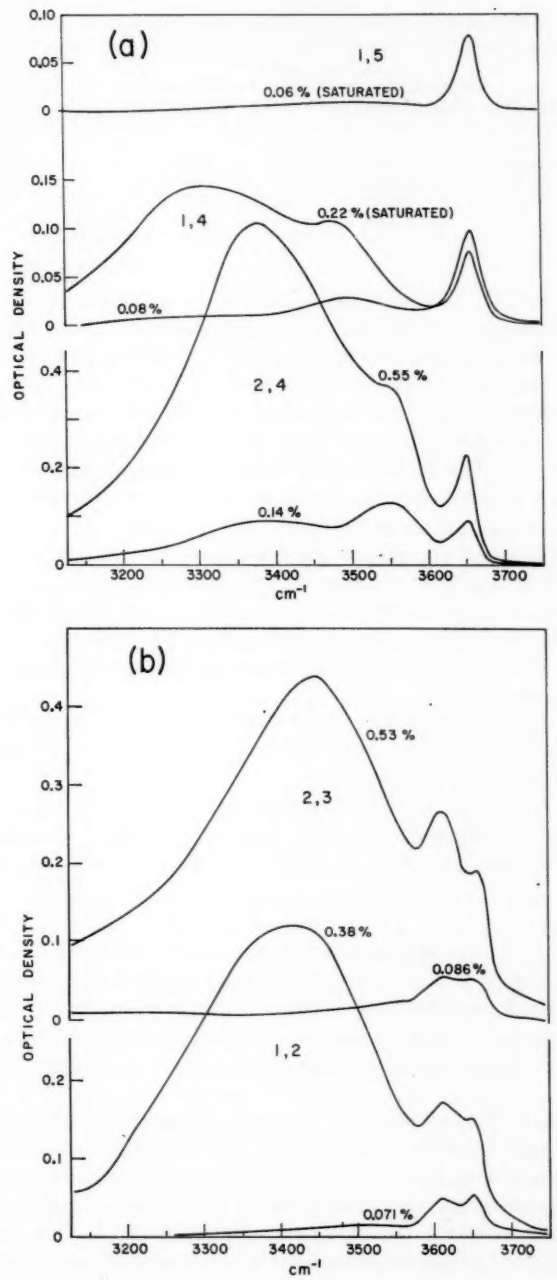

FIG. 1(*a*) and (*b*). OH stretching vibration region of the infrared spectra of the pentanediols in CCl_4.

TABLE II

OH stretching vibration bands of pentanediols in CCl_4

Diol	Frequencies (cm^{-1})			Approx. fraction of free OH groups*
	Free OH	*Intra*bonded OH	*Inter*bonded OH	
1,5	3639			1
1,4	3638	3464	3292	0.85
2,4	3639	3538	3369	0.65
1,2	3646	3604	3407	0.55
2,3	3646	3600	3437	0.50

*At low concentrations.

Like 1,6-hexanediol (4), 1,5-pentanediol shows no evidence of internal hydrogen bonding. A small degree of internal bonding takes place in 1,4-pentanediol, as shown by the presence of a weak band whose frequency shift from the free OH band ($\Delta\tilde{\nu}$ = 174 cm^{-1}) is similar to that shown by 1,4-butanediol (156 cm^{-1} (4); 170 cm^{-1} (5)). More extensive *intra*molecular hydrogen bonding takes place in 2,4-pentanediol; the frequency difference (101 cm^{-1}) is somewhat larger than for 1,3-propanediol (78 cm^{-1} (4)) or 1,3-butanediol (80 cm^{-1} (5)). The bands arising from internally bonded OH groups in the vicinal pentanediols are about as strong as those arising from the free OH groups. The frequency shifts are similar to those found in other *vic*-diols.

In view of the well-known correlation between $\Delta\tilde{\nu}$ and hydrogen bond "strength", it is a fair inference that, although the number of molecules which are *intra*molecularly bonded *increases*, the strength of the bonds *decreases* in the sequence 1,4- to *vic*-diol. The frequencies associated with the broad bands due to *inter*molecular hydrogen bonding (Table II, column 4) likewise suggest that the bonds between molecules become somewhat weaker in the same sequence.

The estimates of the fraction of free OH groups given in the last column of Table II are based on the approximation that the extinction coefficient is the same for the free OH stretching band in all five pentanediols.

With increasing concentration the *intra*molecular hydrogen-bonding bands become obscured by the strong *inter*molecular ones. Solutions of the pentanediols in dioxane all show strong bands with peaks near 3480 cm^{-1} arising from association with the solvent.

(b) Dipole Moments

Because of the limited solubility of some of the pentanediols in CCl_4 and other inert solvents and the tendency of diol molecules in such solvents to associate even at low concentrations, the dipole moments were measured for solutions in dioxane. The results, based on measurements of 6 to 8 solutions in the weight fraction range between 0.005 and 0.08, are given in Table III. The dipole moments of some other diols are included for comparison.

Two primary solvent effects are to be expected: an enhanced moment for each OH group which is hydrogen bonded to the solvent, and a change (usually a reduction) in the molecular moment arising from the effect on the extent of *intra*molecular hydrogen bonding of the competition provided by bonding to dioxane. To get an indication of the magnitude of the first effect, the dipole moment of water in dioxane was measured with the same technique as was employed with the pentanediols. The resulting value of 1.91 debyes, like several earlier values (10), was only slightly greater than the vapor value of 1.85 debyes (11). The second effect is more difficult to gauge. The agreement

TABLE III

Dipole moments of diols (debyes) in dioxane

Diol	No. of C atoms between OH groups				Reference
	2	3	4	>4	
1,5-Pentane				2.37±0.03	This work
1,4-Pentane			2.51±0.03		
2,4-Pentane		2.71±0.03			
1,2-Pentane	2.24±0.02				
2,3-Pentane	2.13+0.05				
1,2-Ethane	2.27 (20°)				7
1,3-Propane		2.46 (20°)			7
1,2-Propane	2.25				8
1,4-Butane			2.47 (20°)		7
1,5-Pentane				2.39 (20°)	7
1,6-Hexane				2.48	8
2-Methyl-2,4-pentane		2.9			9
1,9-Nonane				2.45 (20°)	7
1,10-Decane				2.52	8

NOTE: Temperatures 25°, unless otherwise stated.

between the moment of 1,2-ethanediol in dioxane (2.29 debyes) and in the vapor (2.25 debyes) (12*a*) suggests that it is not great for the vicinal diols. The effect may well be greater for diols less completely internally hydrogen bonded than the vicinal ones.

The dipole moment of 1,5-pentanediol is very nearly $\sqrt{2}$ times as large as that typical of monohydroxyl alcohols (1.66 debyes). This suggests that there is, on the average, no net correlation between the directions of the two COH dipoles and that no appreciable internal hydrogen bonding exists. With increasing proximity of the OH groups in the pentanediols the moments increase, until, for the vicinal diols, they fall to their lowest values. As shown by the other moments in Table III, this trend is general for diols.

Calculation of the resultant moment of the internally hydrogen-bonded molecules is in general prevented by a lack of knowledge of the geometry of the rings formed. The presence of a linear hydrogen bond between two OH groups generally results in a higher moment than that to be expected for unbonded configurations, but the constraints imposed by the comparably inflexible valence-bond angles are likely to lead to considerable bending of the O—H- -O bond in small rings. A certain amount of bending increases the moment beyond its value for a linear bond and values of about 3 debyes are to be expected for angles of the order of 135°. This is consistent with the observed moments of 1,4- and 2,4-pentanediol if the extent of *intra*molecular hydrogen bonding is not greatly less in dioxane than in carbon tetrachloride (compare Table II).

For much larger angles of bend of the hydrogen bond a fall in the resultant moment is predicted. This is the case for the *vic*-diols, which, as considered in more detail in the Appendix, appear to consist substantially of internally hydrogen-bonded forms in which the two CO bonds are not far from gauche in their relative orientation about the connecting C—C bond. Part, at least, of the reduction in "strength" of the hydrogen bonds with decreasing separation of the OH groups in the molecule may be attributed to their increasing departure from linearity.

There is some evidence that the extent of internal hydrogen bonding increases with alkyl-group substitution on the carbon atoms bearing the OH groups, as is to be expected from steric considerations. Thus there is a pronounced increase of moment in the

series 1,3-propanediol, 2,4-pentanediol, 2-methyl-2,4-pentanediol (Table III). It appears possible for a highly substituted 1,5-pentanediol to be appreciably internally hydrogen bonded (13).

Static Dielectric Constants

Values of ϵ_0 for the pentanediols in the liquid state are plotted versus $1/T$ in Fig. 2.

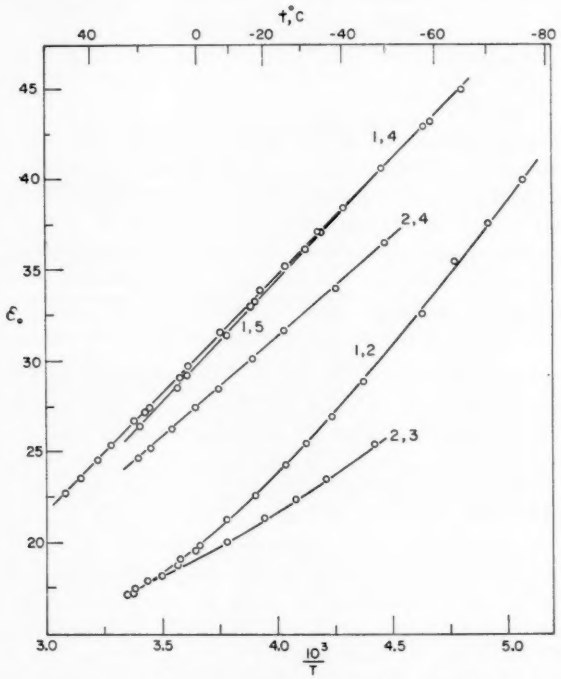

FIG. 2. Temperature dependence of the static dielectric constants of liquid pentanediols.

For three of the diols these values may be represented by a linear function of $1/T$ over the experimental temperature range. The static dielectric constants of the vicinal diols increase more rapidly at low temperatures and are given by

$$\epsilon_0 = a+b/(T-T_c)$$

for which the empirical constants have the values listed in Table IV.*

TABLE IV

Parameters for temperature dependence of ϵ_0

Pentanediol	Temp. range	a	$b\times10^{-3}$	T_c	Av. deviation (%)
1,5	−35 to 25°	−19.54	13.50	0	±0.2
1,4	−65 to 52°	−16.88$_5$	12.89	0	0.3
2,4	−50 to 25°	−12.51	10.96	0	0.2
1,2	−70 to 25°	− 1.13	3.244	120	0.6
2,3	−50 to 25°	+ 4.04	2.487	110	0.2

**Other reported dielectric constants of 1,5-pentanediol (with the values computed from the equation in parentheses) are: −20°, 33.5 (33.8); 0°, 30.0 (29.9); 25°, 26.3 (25.7) (14); and 20°, 26.2 (26.5) (7).*

The dielectric constants of 1,5- and 1,4-pentanediol suggest that the individual OH groups have almost as much freedom to associate with other molecules as has the single OH group in simple alcohols. Thus, each of these diols at 20° has a dielectric constant of which the part arising from the orientation of dipoles (ca. 27–3) is twice that of *n*-pentanol (15–3), a liquid with about half as many OH groups per unit volume. In the case of 1,4-pentanediol, it is likely that a reduced extent of *inter*molecular association is offset by the increased average moment resulting from some *intra*molecular hydrogen bonding. In 2,4-pentanediol the former effect predominates.

The lower dielectric constants of the vicinal diols reflect a high degree of internal hydrogen bonding. Formal calculation of the Kirkwood correlation factors from the observed dielectric constants give values somewhat greater than 2 at room temperature and progressively increasing values at lower temperatures. Although such values cannot be directly compared with those of simple alcohols, for which similar values are obtained (15), they are sufficiently high to suggest the presence of extensive hydrogen-bonded chains. The structure is complicated by the possibility of cross-linking of the chains of hydrogen bonds at some molecules which are not internally hydrogen bonded, a process which should result in higher dielectric constants and which may be responsible for the high values found, particularly for the 1,2-diol, at low temperatures.

Most of the pentanediols remained liquid at temperatures lower than those at which the dielectric dispersion–absorption effects (next section) occurred at audio frequencies.* However, the 1,5-diol froze rapidly when cooled below −30°, even when as much as 5% water was added. Examination of its dielectric constant in the solid revealed no anomalies at temperatures down to −190°. The dielectric constant remained almost invariant at about 2.7 as the sample was heated from this temperature until it started to rise a few degrees below the melting point (−16°).

Dielectric Relaxation

A typical absorption–dispersion locus for each pentanediol is illustrated in Fig. 3.

Since 1,5-pentanediol could not be sufficiently supercooled to bring the dispersion effects into the frequency range of bridge measurements, Q-meter and RX-meter measurements were made at higher frequencies. As shown in the plot of Fig. 3 for the 1,5-diol at −30°, the Q-meter results show considerable scatter, a large part of which may be attributed to changes in lead capacitance brought about by connecting and disconnecting the low potential lead to the cell. In the hope that these effects would show a random scatter, a large number of measurements were made. The RX-meter measurements, for which the height of the liquid between the coaxial electrodes was varied to eliminate fixed capacitance, were more reproducible, but were complicated by inductance effects at high frequencies. The data were not sufficiently accurate to distinguish between a semicircular locus with additional high-frequency dispersion regions, as in the simple alcohols, and a slightly skewed locus (with β of the order of 0.9). From measurements over a very extensive frequency range, Mme. Moriamez-Boullet reported (14) the presence of at least two distinct dispersion regions, of which the principal (low-frequency) one was semicircular. In view of the evidence already given for the ability of each OH group in 1,5-pentanediol to freely associate with other molecules, relaxation behavior similar to that of the simple monohydroxyl alcohols might well be expected.

For the other four pentanediols studied, as is evident from the extent of the agreement between the experimental and calculated points (Fig. 3), the skewed-arc locus provides

*One sample of 2,4-diol slowly froze after being maintained for several days at −45°.

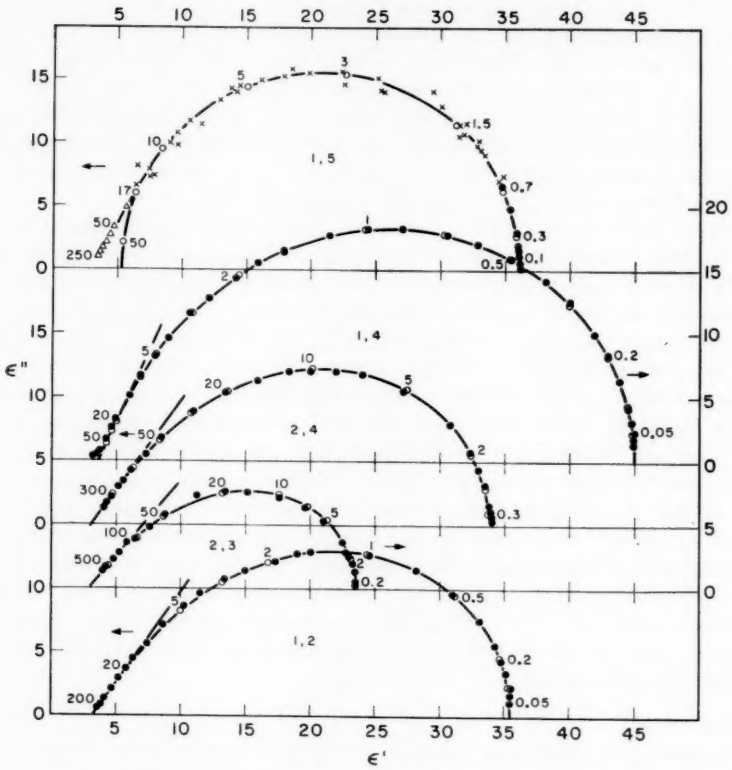

FIG. 3. Complex dielectric constant loci of the pentanediols: ● bridge, × Q-meter, and △ RX-meter measurements; ○ values calculated from the parameters starred in Table V. Numbers on loci are frequencies in Mc/sec for 1,5-pentanediol, in kc/sec for the others.

an accurate description of the dispersion effects (except at relatively high frequencies). Values of β tend to become smaller with the approach of the two OH groups to one another.

Values of the parameters used in the calculation of the absorption–dispersion loci of Fig. 3 are given in Table V, together with the corresponding skewed-arc parameters at several other temperatures.

Relaxation Times

The variation of the relaxation times with temperature is shown in Fig. 4.

The τ_0 values for 1,5-pentanediol are based on three types of measurement, as indicated in the caption of the figure. Debye behavior has been assumed. Bridge measurements of ϵ'' were made at frequencies on the low-frequency side of the absorption region and the relaxation times were calculated from the slope of a plot of ϵ'' vs. frequency, according to

$$\epsilon'' = 2\pi(\epsilon_0 - \epsilon_1)\beta\tau_0 f, \qquad [1]$$

with, in this case, $\beta = 1$. The experimental ϵ'' values were corrected for the contributions

TABLE V

Typical dispersion parameters of the pentanediols

Pentanediol	T (°K)	ϵ_0	ϵ_1	β	τ_0 (sec)
1,5	293.5	26.49		(1)	1.53×10^{-9}
	257.2	33.08		(1)	1.33×10^{-8}
	243.2	36.10*	(5.25)†	(1)	4.60×10^{-8}*
1,4	317.8	23.55			
	295.7	26.74			
	266.5	31.59	(3.48)	(0.77)	3.44×10^{-8}
	233.1	38.53	3.50	0.75	1.87×10^{-6}
	207.8	44.95*	3.64*	0.760*	2.23×10^{-4}*
	193.2	49.7	3.71	0.71	2.0×10^{-2}
1,2	296.8	17.31			
	264.5	21.32	(3.20)	(0.65)	1.70×10^{-8}
	228.5	28.86	3.25	0.64	2.27×10^{-6}
	209.5	35.51*	3.26*	0.629*	1.84×10^{-4}*
	197.2	40.0	3.30	0.63_5	1.07×10^{-2}
2,4	294.5	24.69			
	267.1	28.50	(3.00)	(0.68)	3.9×10^{-8}
	234.9	33.86*	3.08*	0.620*	2.49×10^{-5}*
	223.7	36.5	3.17	0.59	7.58×10^{-4}
2,3	296.9	17.37	(2.61)	(0.60)	4.0×10^{-9}
	253.8	21.39	(2.81)	(0.56)	5.0×10^{-7}
	237.8	23.52*	2.83*	0.545*	1.77×10^{-5}*

*Denotes values used for the computed loci of Fig. 3.
†Values in parentheses are values assumed in order to calculate τ_0.

from d-c. conductance. Relaxation times by this method were considered less accurate than those derived from the frequencies of maximum loss given by the Q-meter and RX-meter measurements, and were assigned half the weight in fitting the temperature dependence of the relaxation times by least squares.

Values of τ_0 of the other pentanediols were obtained from bridge measurements alone. Relaxation times of less than 3×10^{-7} second made use of values of β estimated by extrapolation from lower temperatures, and at the high end of the temperature range equation [1] was employed.

From Fig. 4 it is apparent that, with the possible exception of the 1,5-diol, the relaxation times do not follow an equation of the form

$$\log_{10}\tau_0 = A'+B'/T. \qquad [2]$$

They may, however, be represented over most of the temperature range of the measurements by

$$\log_{10}\tau_0 = A+B/(T-T_\infty), \qquad [3]$$

as in the case of a number of other alcohols (15, 16, 17) and alkyl halides (18). It was found that the values of B, as determined by least-squares best fit of equation [3] to the data, were very nearly the same for the four pentanediols. In fact, for the values of A and T_∞ of Table VI, a plot of the product $(\log_{10}\tau_0-A)(T-T_\infty) = B$ yields values of B which are, within experimental error, equal to 985 over most of the temperature range. (See inset of Fig. 5.) Moreover, the less accurate and extensive data for 1,5-pentanediol can be represented by the same B, with A and T_∞ given in Table VI, slightly better (average deviation between experimental and computed relaxation times of 6.7%) than by equation [2] with A' and B' evaluated by least squares (average deviation 7.7%). It is to be noted (Fig. 5) that, although the data for the 1,5- and 1,4-diols show no departures from equation [3] with $B = 985$ up to room temperature, those for the

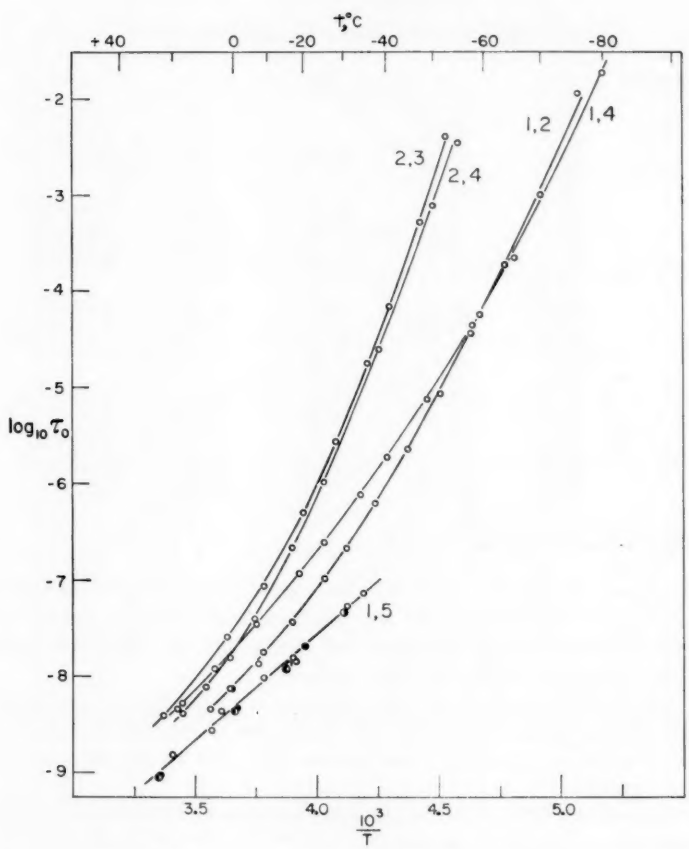

FIG. 4. Arrhenius plots of the relaxation times of the pentanediols: ○ bridge, ◑ Q-meter, ◐ RX-meter measurements; ● from reference 14.

TABLE VI

Parameters of equation [3] for the pentanediols. B = 985

Diol	T_∞ (°K)	A	Temp. range (°C)	No. of points	Av. deviation (%)
1,5	92	−13.814	−35, +25	13	6.7
1,4	111	−13.804	−80, +20	13	2.4
2,4	143	−15.327	−55, +3*	7	3.5
1,2	118.5	−14.595	−75, −15*	10	2.5
2,3	144	−15.279	−73, −10*	7	4.0

*Departures from equation [3] occur at higher temperatures.

2,4- and particularly for the vicinal diols show consistent departures at the high temperature end (Fig. 4) in the sense of greater relaxation times than predicted by equation [3]. It may be significant that the greater the degree of *inter*molecular hydrogen bonding the higher the upper temperature limit of validity of the equation.

Published values of the constant B of equation [3] as it has been applied to other

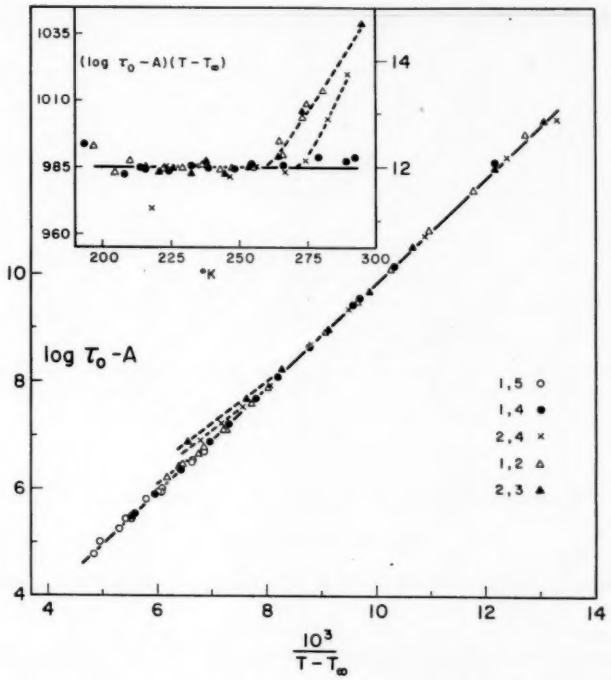

FIG. 5. Dependence of log $\tau_0 - A$ on $1/(T - T_\infty)$ for the values of A and T_∞ listed in Table VI. Inset: temperature variation of (log $\tau_0 - A)(T - T_\infty)$.

hydroxyl-containing liquids (16) are considerably smaller than 985, but this value is approached in the case of highly associated glycerol, for which $B = 957$ has been reported. It is now believed that the available data indicate a common value of B (≈ 985) for liquids at low temperatures. The lower values of B that have been reported probably arise from the inclusion in the data treated of relaxation times obtained at temperatures beyond the range of the common low-temperature behavior.

The case of *n*-propanol may be particularly mentioned. By a combination of bridge and transient techniques, relaxation times between 10^{-8} and 10^{3} seconds have been measured for this liquid. Published (19) parameters for equation [3] (including $B = 477$) describe the experimental relaxation times between 210 and 130° K (that is, up to ca. 10^{-4} second) but not those obtained at lower temperatures. With $B = 985$, together with $A = -14.354$ and $T_\infty = 44°$, on the other hand, the relaxation times in the range 10^{-5} to 10^{3} seconds may be accurately described. Deviations similar to those shown by the vicinal pentanediols become evident at temperatures above 150° K.

The similarity between the temperature dependence of dielectric relaxation times, viscosities, and d-c. conductivities at low temperatures is a matter of common observation, as is also their tendency to depart from such common behavior as the temperature is raised (16, 20, 2). In the case of the pentanediols the conductivities (Fig. 6) vary with temperature very much as do the relaxation times. It was not possible to follow the temperature dependence of conductivity with the same accuracy as for the relaxation

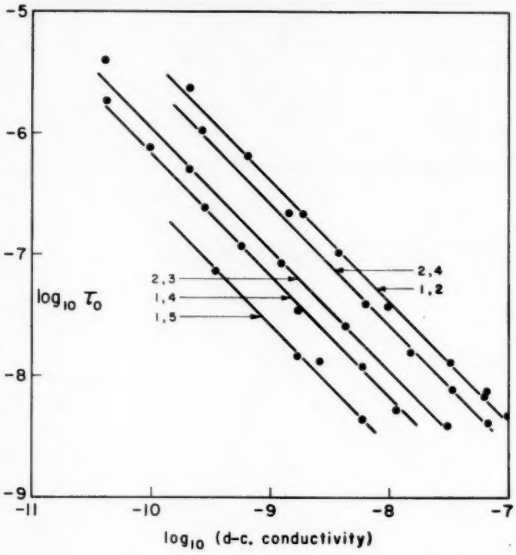

FIG. 6. Plot showing the proportionality between the relaxation times and d-c. conductivities of the pentanediols.

times, since it changed not only from sample to sample, but also slowly with time after the cell had been filled.

The evidence suggests that physical rate processes of many liquids at low temperatures may be represented by equation [3] with a common value of B and a value of T_∞ characteristic of the liquid. For a given liquid only A changes with the rate process being measured. It is planned to examine elsewhere the question of the general validity of equation [3] as a characteristic feature of what may be called "structural relaxation" of liquids.

It is apparent that the present representation of structural relaxation has much in common with Ferry's method of expressing mechanical relaxation times of polymers in terms of their values at an arbitrary standard temperature (21). When put into the form of equation [3], his expression corresponds to a value of B some 10% lower than the one employed here.

Dispersion at High Frequencies

If the principal dispersion region in 1,5-pentanediol is taken to be of the simple Debye type, our data (cf. Fig. 3) show the presence of an additional dispersion region at relatively high frequencies. They are consistent with the results of Mme Moriamez-Boullet (14), who reports at $-20°$ a second dispersion region which is a circular arc defined by $\epsilon_1 = 5.4 \pm 0.2$, $\epsilon_2 = 2.9 \pm 0.2$, $\alpha = 0.11 \pm 0.02$, and a most probable relaxation time some 80 times smaller than the single relaxation time of the primary dispersion.

The other pentanediols, like other liquids exhibiting skewed-arc behavior (1), show additional dispersion–absorption effects at frequencies of the order of several hundred times as great as that which corresponds to τ_0. The nature of these departures from the limiting straight line predicted by the skewed-arc locus for high frequencies is illustrated in the ϵ'' vs. ϵ' plots of Fig. 7.

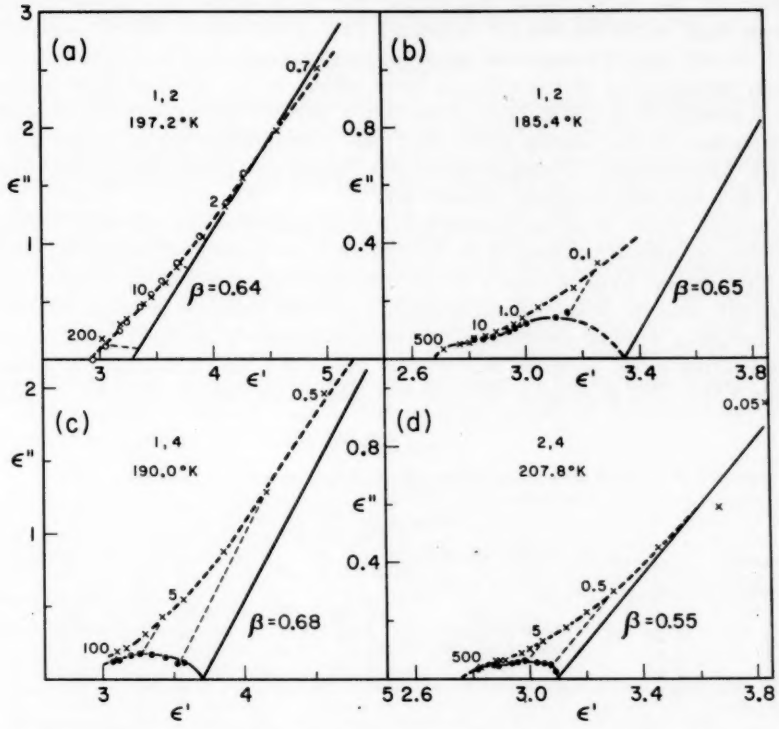

FIG. 7. Departures at relatively high frequencies of pentanediols from skewed-arc behavior: × experimental points; ○ Glarum locus with $a_0 = 4$, $\tau_0 = 1.07\times10^{-2}$ sec; ● points obtained by subtraction from experimental points of skewed-arc loci with values of τ_0 of (*b*) 6.4, (*c*) 3.2×10^{-2}, (*d*) 1.6 sec.

In order to explore the possibility that these effects may arise from the superposition of the skewed-arc locus and some physically distinct relaxation mechanism occurring at relatively high frequencies, attempts have been made to subtract the contribution of the skewed-arc locus to the experimental results. This procedure is more approximate than was the case of, for example, *n*-propanol (16, 19) since the skewed-arc locus makes much larger contributions at high frequencies and requires one more parameter (β) for its representation than does the Debye semicircle. As shown in Fig. 6(*b*, *c*, *d*), it is possible to obtain, by this somewhat laborious procedure, a residual absorption which resembles two overlapping circular arcs, much like those reported for *n*-propanol. It should be pointed out that the only justification for this arbitrary method of treating the data lies in the similarity between the resulting residues and those obtained for simple alcohols. Moreover, slight changes in the skewed-arc parameters lead to either overlap of the residual locus with the high-frequency end of the skewed-arc locus or to negative residual absorption at some frequencies. To get residues of the type shown, it is necessary to assign values of τ_0 which are somewhat larger than predicted by the linear relationship (see above) between $\log \tau_0$ and $1/(T-T_\infty)$.

The Glarum model (22) of relaxation leads to an expression which differs appreciably from that of the skewed arc only at high frequencies. The Glarum equation is capable

of representing the experimental results for the pentanediols to considerably higher frequencies than is the skewed-arc equation. This is illustrated for 1,2-pentanediol in Fig. 6(*a*). At still higher frequencies (or lower temperatures, Fig. 6(*b*)) the experimental absorption exceeds that of the Glarum locus which, in the limit of high frequencies, becomes a straight line which approaches the ϵ' axis at 45°. It is interesting to note that subtraction of the Glarum locus from the experimental one now leaves a single arc, which approximately corresponds to the higher-frequency arc of the pair that resulted from subtraction of the skewed arc.

In all events, there is an extremely broad loss spectrum at very high frequencies, which, if not completely accounted for by the diffusion-controlled relaxation process of Glarum, does appear to arise from a mechanism different from the co-operative orientation of locally ordered molecules responsible (1) for the behavior at lower frequencies.

The values of ϵ_1, whether determined by the high-frequency intercept of the skewed-arc or of the Glarum locus, decrease in the order 1,5-, 1,4-, 1,2-, 2,4-, and 2,3-pentanediol (see Table VII). This is roughly the order in which the relative number of weak and

TABLE VII

Variation of ϵ_1 and β with temperature (based on data between ca. −80 and −20° C)

Pentanediol	Skewed arc				Glarum,
	$\epsilon_1(-60°\text{ C})$	$d\epsilon_1/d(10^3/T)$	$\beta(-60°\text{ C})$	$d\beta/d(10^3/T)$	$\epsilon_1(-60°\text{ C})$
1,5	(5.2_5) (−30° C)		(1)		(5.2_5) (−30° C)
1,4	3.61	+0.020	0.73	−0.10	3.2_1
1,2	3.29	0.014	0.64	−0.03	2.9_8
2,4	3.17	0.012	0.55_5	−0.15	2.8_4
2,3	2.92	0.004	0.52_5	−0.03	2.6_9

broken hydrogen bonds increases, so that the magnitude of ϵ_1 cannot be directly related to the orientation of free or weakly hydrogen-bonded OH groups. At very high frequencies the absorption approaches zero at values of ϵ' of the order of 2.6 to 2.7, somewhat in excess of likely values of the square of the refractive indices, but similar to the dielectric constant observed for solid 1,5-pentanediol at comparable temperatures.

Temperature Dependence of the Dispersion

As may be seen from Table VII, the value of β in the skewed-arc representation tends to decrease with decreasing temperature. Although the values of $d\beta/d(1/T)$ tabulated are only approximate, they seem to show no systematic dependence on β. Moreover, the variation of β with temperature cannot be related to a model which assumes that the distribution of relaxation times arises from the presence of a temperature-independent distribution of barrier heights to rotation, such as may approximately account for the broadening of the dispersion exhibited by some solids with decreasing temperature (23).

In the Glarum representation (22), the shape of the dispersion–absorption locus depends on a_0 alone. As the temperature gets lower, the value of a_0 decreases, that is, the contribution of the diffusion-controlled relaxation becomes greater. Since $a_0 = l^2/D\tau_0$, this may be naively accounted for if the average defect diffusion relaxation time (l^2/D) increases less with decreasing temperature than does relaxation time for co-operative molecular rotation (τ_0) and the values of the two "relaxation times" therefore approach one another.

No extensive results are yet available for liquids at temperatures corresponding to β

less than 0.5 ($a_0 < 1$) where the Glarum theory makes the interesting prediction of behavior intermediate between that of the skewed arc and circular arc.

CONCLUSIONS

It may be concluded that departures of this type of asymmetric locus from the Debye semicircle arise from the presence of disordered regions in the liquid.

The increased asymmetry of the loss spectrum which results from increased interference with *inter*molecular hydrogen bonding as the OH groups move in from the ends of the pentane chain, in the sequence 1,5-, 1,4-, 1,2-, 2,4-, and 2,3-pentanediol, is accompanied at low temperatures by a large increase in the most probable relaxation time τ_0.* This type of relaxation is therefore not made easier by structural irregularity, within the present limits, but rather takes place most readily for liquids with the highest degree of local order. It is apparent that regularity of structure is somehow important in the activation process. This co-operative relaxation process may involve the sharing among many molecules of an accumulation of energy obtained at the expense of the vibrational energy of the quasi-crystalline lattice. The common nature of the variation of τ_0 with temperature is consistent with this picture.

REFERENCES

1. D. W. DAVIDSON. Can. J. Chem. **39**, 571 (1961).
2. D. W. DAVIDSON. Can. J. Chem. **35**, 458 (1957).
3. R. WALKER and D. W. DAVIDSON. Can. J. Chem. **37**, 492 (1959).
4. L. P. KUHN. J. Am. Chem. Soc. **74**, 2492 (1952).
5. V. I. MALYSHEV and V. N. MURZIN. Izvest. Akad. Nauk S.S.S.R. Ser. Fiz. **22**, 1107 (1958).
6. L. P. KUHN. J. Am. Chem. Soc. **80**, 5950 (1958).
7. J. A. A. KETELAAR and N. VAN NEURS. Rec. trav. chim. **76**, 437 (1957).
8. C. P. SMYTH and W. S. WALLS. J. Am. Chem. Soc. **53**, 2115 (1931).
9. A. H. WHITE and S. O. MORGAN. Physics, **2**, 313 (1932).
10. L. G. WESSON. Tables of electric dipole moments. The Technology Press, Cambridge, Mass. 1948.
11. A. A. MARYOTT and F. BUCKLEY. Tables of dielectric constants and electric dipole moments of substances in the gaseous state. Natl. Bur. Standards (U.S.) Circ. No. 537. 1953.
12. C. P. SMYTH. Dielectric behavior and structure. McGraw-Hill Book Co., Inc., New York. 1955. (*a*) p. 370; (*b*) p. 244.
13. K. KULKA, J. A. ROGERS, JR., O. HANSEN, and R. J. EISERLE. J. Org. Chem. In press.
14. C. MORIAMEZ-BOULLET. Compt. rend. **246**, 2364 (1958).
15. W. DANNHAUSER and R. H. COLE. J. Chem. Phys. **23**, 1762 (1955).
16. D. W. DAVIDSON and R. H. COLE. J. Chem. Phys. **19**, 1484 (1951).
17. F. X. HASSION and R. H. COLE. J. Chem. Phys. **23**, 1756 (1955).
18. R. H. COLE. Izvest. Akad. Nauk S.S.S.R. Ser. Fiz. **24**, 4 (1960).
19. D. W. DAVIDSON and J. WHEELER. J. Chem. Phys. **30**, 1357 (1959).
20. D. J. DENNEY. J. Chem. Phys. **30**, 159 (1959).
21. M. L. WILLIAMS, R. F. LANDEL, and J. D. FERRY. J. Am. Chem. Soc. **77**, 3701 (1955).
22. S. H. GLARUM. J. Chem. Phys. **33**, 639 (1960).
23. D. W. DAVIDSON. Can. J. Chem. **39**, 1321 (1961).
24. R. G. BENNETT. Compte rendu du 9e Colloque Ampere, Geneva, 1960. p. 62.

APPENDIX

Calculation of the Dipole Moment of Vicinal Diols

In Table VIII are listed values of dipole moments for assumed models of vicinal diols. The OH and OC bond moments have been taken to be 1.51 (12*b*) and 1.10 debyes, respectively, with all angles assumed, for simplicity, to be tetrahedral. Since the small CH moments have not been taken explicitly into account, their effects are approximately included in the value taken for the OC moment.

Forms (*c*) to (*g*) are internally hydrogen bonded. In (*d*) the free OH group is rotated

**A similar steric effect is noticed in the recent results of Bennett (24), who finds that 1-phenyl-propanol ($\beta = 0.7$) exhibits much higher relaxation times at low temperatures than do 3-phenyl-propanol and 2-phenyl-ethanol ($\beta = 1$).*

TABLE VIII

Calculated dipole moments of vicinal diols

Model	Dipole moment (debyes)
(*a*) Free rot. about all bonds	2.07
(*b*) Free rot. about trans CO bonds	2.01
(*c*) CO bonds cis, all atoms coplanar	2.91
(*d*) CO bonds cis, e.o. in plane	2.52
(*e*) CO bonds gauche, r_{O---H} min, r_{H---H} max	2.64
(*f*) CO bonds gauche, first e.o. in plane of CO, O---H	2.48
(*g*) CO bonds gauche, second e.o. in plane of CO, O---H	2.10

about its CO bond through 120° from the planar case (*c*) so as to bring the direction of maximum electron density of either of the lone pair electron orbitals (e.o.) into the plane of the rest of the molecule.

In the three gauche forms, (*e*) to (*g*), the length of the hydrogen bond is made a minimum by rotation of the bonded OH group about its CO bond. Form (*e*) results from rotation of the free OH group about the CO bond until its H atom is as far as possible from the H atom in the bond. In (*f*) and (*g*) one or the other of the e.o.'s on the O atom is brought by this rotation as near as possible to the H atom in the bond.

The O---H and O---O distances are 1.84 and 2.49 Å, respectively, for the cis forms, and 2.33 and 2.82 Å for the gauche forms, with the following bond lengths assumed: OH 0.97, OC 1.42, C—C 1.54 Å. The O—H---O angles, measured within the ring, are 122° (cis) and 111° (gauche).

Most of the calculated dipole moments of the internally hydrogen-bonded forms are higher than the experimental moments of Table III. Form (*g*) fits the data best, but, since there is no good reason for preferring it to (*f*), the r.m.s. value of the moments of these two forms should be taken. This value (2.31 debyes) is sufficiently close to the experimental moments to suggest that the predominant hydrogen-bonded species are approximately gauche forms in which the orbitals of the lone pair electrons of the O atom in the hydrogen bond tend to be oriented toward the H atom. It is likely that the energy of the hydrogen bond is too small to produce much of a rotation from the normal gauche toward the cis configuration. Although there is no evidence for an appreciable population of trans forms in CCl_4 (compare Table II), it is possible that such forms may be promoted in dioxane by hydrogen bonding to the solvent.

The approximate nature of the calculations should be borne in mind. Thus, the values of the OH and OC bond moments (1.55 and 1.30 debyes) required to give agreement with the experimental moment of 1.66 debyes for monohydroxyl alcohols are considerably larger than the ones assumed here, and result in calculated moments which are larger by some 0.2 debyes than those given in Table VIII. If the O angle is taken to be 105° instead of tetrahedral, the bond moments and the resultant moments are somewhat reduced.

SOLVOLYSIS IN HYDROGEN AND DEUTERIUM OXIDE

IV. HALIDES WITH NEIGHBORING GROUPS[1]

P. M. LAUGHTON[2] AND R. E. ROBERTSON

ABSTRACT

Rate data for the hydrolysis of a series of halohydrins and related compounds in light and heavy water are reported. The solvent isotope effects (k_{D_2O}/k_{H_2O}) from these measurements fall into three groups compared with those of simple halides. Thus the presence of a hydroxyl group in proximity to the seat of reaction may lead to increased, decreased, or normal solvent isotope ratios. The abnormal ratios can be interpreted in terms of the effect of anchimeric assistance on the solvation shell in the activation process.

In previous papers of this series, the solvent isotope effect (k_{D_2O}/k_{H_2O}) was shown to be remarkably insensitive to the structure of the alkyl group (1, 2, 3). This insensitivity appeared to rule out significant changing contributions from secondary isotope effects arising from variation in nucleophilic interaction (4, 5) and led to an explanation of the observed solvent isotope effect in terms of the relative stability of the initial state solvation shell. In the present paper we extend this hypothesis to include a series of compounds where apparent exceptions to the above generalization are found, and we are led to re-examine the hypothesis that transition state differences such as varying nucleophilic interaction may be neglected.

Specifically, we examine the solvent isotope effect for a series of halohydrins and analogous compounds substituted with alkoxyl or halide in positions where in certain cases other evidence leads to the expectation of anchimeric assistance in hydrolysis.

Rate data for the compounds studied in H_2O and D_2O were determined by a conductance method described in an earlier paper (6). It is generally recognized that this method gives the most accurate rate measurements available for this type of reaction, a fact of particular importance where questions relating to differences in rate ratios are involved. Since in this work we report a large number of kinetic data for a series of interesting compounds which, with few exceptions, had not previously been studied in water, it was considered desirable to publish now, even though only a qualitative interpretation is warranted at this time. Rate data for hydrolysis in D_2O and H_2O with corresponding temperatures are given in Table I. The sources of the compounds studied are included in the section on experimental detail, following the discussion.

CORRELATION OF SOLVENT ISOTOPE EFFECTS

In earlier papers we showed that whereas there was a marked difference between the solvent isotope effect for sulphonates and halides, the differences between corresponding halides—chlorides, bromides, and iodides—were much smaller, and these could be further reduced if due allowance was made for the effect of temperature on this ratio (3). We

[1]*Manuscript received June 6, 1961.*
Contribution from the Division of Pure Chemistry, National Research Council, and the Department of Chemistry, Carleton University, Ottawa. Part of this work was assisted by a grant in aid of research from the National Research Council to one of us (P.M.L.). This work was presented in part at the Toronto Meeting of the Chemical Institute of Canada, May 27, 1958.
Issued as N.R.C. No. 6508.
[2]*Department of Chemistry, Carleton University, Ottawa.*

TABLE I

Solvolytic rate constants for the reaction in light and heavy water of some halides with neighboring groups

Code	Halide	Temp., °C	k_{D_2O}, $\times 10^5$ sec^{-1}	k_{H_2O}, $\times 10^5$ sec^{-1}	k_{D_2O}/k_{H_2O}
I	$HO\text{-}CH_2CH_2\text{-}Cl$	90.1_7	0.164 ± 0.0007	0.210 ± 0.0006	0.78
II	$HO\text{-}(CH_2)_3\text{-}Cl$	100.00	$2.15\ \pm0.03$	$2.66\ \pm0.008$	0.81
III	$HO\text{-}(CH_2)_4\text{-}Cl$	80.99	$148.4\ \pm0.2$	$171.0\ \pm0.1$	0.86
IV	$MeO\text{-}(CH_2)_4\text{-}Cl$	80.02	$52.9\ \pm0.1$	$59.5\ \pm0.1$	0.89
V	$HO\text{-}CH_2CH_2Br$	80.15	0.846 ± 0.009	1.082 ± 0.005	0.78
VI	$HO\text{-}(CH_2)_3\text{-}Br$	80.15	$5.87\ \pm0.01$	$7.03\ \pm0.01$	0.83_5
VII	$Br\text{-}(CH_2)_4\text{-}Br$	80.15	$20.4\ \pm0.02$	$24.9\ \pm0.03$	0.82
VIII	$MeO\text{-}(CH_2)_4\text{-}Br$	50.00	$36.98\ \pm0.04$	$44.09\ \pm0.08$	0.84
IX	$HO\text{-}CH_2CH_2\text{-}I$	80.15	0.325 ± 0.002	0.429 ± 0.003	0.76
X	$HO\text{-}(CH_2)_3\text{-}I$*	100.01	$12.1_5\ \pm0.1$	$15.9_5\ \pm0.07$	0.76
XI	$MeO\text{-}(CH_2)_3\text{-}I$*	100.01	$15.0_1\ \pm0.06$	$18.6_6\ \pm0.06$	0.80
XII	$HO\text{-}CMe_2CH_2\text{-}Cl$	90.00	0.940 ± 0.004	1.338 ± 0.009	0.70
XIII	$HO\text{-}CMe_2CH_2\text{-}Br$	80.15	$6.30\ \pm0.03$	$9.70\ \pm0.01$	0.65
XIV	$HO\text{-}CMe_2CHMe\text{-}Cl$	80.16	$17.0\ \pm0.1$	$23.4\ \pm0.1$	0.73
XV	$HO\text{-}CMe_2CHMe\text{-}Br$	51.10	$16.3\ \pm0.2$	$23.9\ \pm0.2$	0.68
XVI	$MeO\text{-}CMe_2CHMe\text{-}Br$*	70.01	$63.9_5\ \pm0.01$	$74.6\ \pm0.2$	0.86
XVII	$HO\text{-}CMe_2CMe_2\text{-}Cl$	29.46	$104.6\ \pm0.0$	$141.4\ \pm0.4$	0.74
XVIII	$I\text{-}CH_2CMe_2\text{-}Cl$	5.09	$50.5\ \pm0\ 1$	$71.5\ \pm0.3$	0.71
XIX	$MeO\text{-}CH_2CMe_2\text{-}Cl$	40.00_5	$59.7_1\ \pm0.2$	$76.2_9\ \pm0.18$	0.78
XX	*trans* 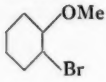	89.99	$12.16\ \pm0.04$	$14.62\ \pm0.03$	0.83
XXI	*trans*	89.68	$22.8\ \pm0.1$	$31.1\ \pm0.2$	0.74
XXII	$MeO\text{-}CMe_2CH_2\text{-}Br$	100.01	$12.12\ \pm\ .05$	$13.64\ \pm0.01$	0.86
XXIII	$Br\text{-}CHMeCMe_2\text{-}Br$	70.00	$1.76_7\ \pm0.008$	1.400 ± 0.007	0.80

*Rates for these compounds were determined by L. E. Hakka, summer research assistant, 1961.

have recently shown (5) that the temperature dependence of the solvent isotope effect for isopropyl bromide can be expressed by the equation

$$[1] \qquad \log_{10} k_{D_2O}/k_{H_2O} = (-693.7073/T) - 4.4867 \log_{10} T + 13.2935$$

and from this we may determine average values of k_{D_2O}/k_{H_2O} to be expected for halides* over the experimental range.

The solid curve in Fig. 1 is a plot of log k_{D_2O}/k_{H_2O} versus $1/T$ for isopropyl bromide. This is shown to parallel the individual values for the k_{D_2O}/k_{H_2O} ratio for a wide range of halides supporting the above generalization.

It will be apparent from this plot that the ratios given in Table I for compounds having a hydroxyl or methoxyl so placed as to provide for a possibility of anchimeric assistance, may be divided with respect to this chosen norm into three groups. A number coincide within a few per cent with the reference curve based on equation [1]. These include the three ethylene halohydrins (I, V, and IX), pinacol chlorohydrin (XVII), and the strongly anchimeric tertiary chloride (XVIII) with a rate enhancement (in 80% ethanol) of 740 (7). Several other values of k_{D_2O}/k_{H_2O} from our earlier work are included in the plot as further evidence of the common trend with temperature in the value of the k_{D_2O}/k_{H_2O} ratio for the halides.

**Actually, because the value of k_{D_2O}/k_{H_2O} for isopropyl bromide is lower than for many halides, the true average would probably lie 1 to 2 per cent higher than given by equation [1].*

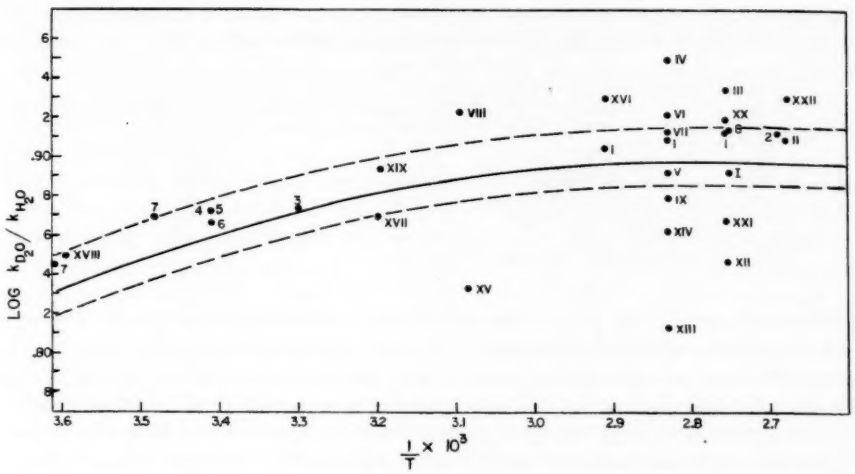

FIG. 1. The temperature dependence of solvent isotope effect for a series of halides, illustrating exceptional cases. Compounds from Table I are identified by Roman numerals. The remaining ratios are taken from paper III in this series (ref. 3): 1, MeBr; 2, EtBr; 3, *p*-$MeC_6H_4CH_2Cl$; 4, *p*-$MeC_6H_4CH_2Br$; 5, *o*-$MeC_6H_4CH_2Br$; 6, $PhCH_2Br$; 7, *t*-BuCl; 8, *t*-BuF. The solid line represents the data for *i*-PrBr from ref. 5.

The five compounds in the second group have ratios which lie below this arbitrary norm (Table II). These are the isobutylene and trimethylethylene halohydrins (XII, XIII, XIV, and XV) and the *trans*-cyclohexene bromohydrin (XXI). In the first four cases there appears to be anchimeric assistance, judging from the higher rates observed compared with the hydroxyl-free analogues and taking into consideration the fact that the normal inductive effect of β-hydroxyl would be reduction of the rate by a factor of 20 to 100 (8).

TABLE II

Rate ratios k_{D_2O}/k_{H_2O} for neighboring group halides showing lower than normal ratios

Code	Halide	k_{D_2O}/k_{H_2O} obs.	k_{D_2O}/k_{H_2O} normal*
XII	$HOCMe_2CH_2Cl$	0.70	0.789
XIII	$HOCMe_2CH_2Br$	0.65	0.788
XIV	$HOCMe_2CHMeCl$	0.73	0.788
XV	$HOCMe_2CHMeBr$	0.68	0.774
XXI	*trans*	0.74	0.789

*Value calculated for *i*-PrBr at the same temperature.

The third group (Table III) displays somewhat higher values of the k_{D_2O}/k_{H_2O} ratio than normal and includes the three fast-reacting tetramethylene derivatives (III, IV, and VIII) and the isobutylene and trimethylethylene methoxybromides (XXII and XVI).

TABLE III

Rate ratios k_{D_2O}/k_{H_2O} for neighboring group halides showing higher than normal ratios

Code	Halide	k_{D_2O}/k_{H_2O} obs.	k_{D_2O}/k_{H_2O} normal*
III	$HO(CH_2)_4Cl$	0.86	0.789
IV	$MeO(CH_2)_4Cl$	0.89	0.789
VIII	$MeO(CH_2)_4Br$	0.84	0.772
XVI	$MeOCMe_2CHMeBr$	0.86	0.787
XXII	$MeOCMe_2CH_2Br$	0.86	0.786

*Value calculated for *i*-PrBr at the same temperature.

Thus it is apparent that an oxygen-containing β-substituent may raise, lower, or leave unchanged the solvent isotope effect. We now propose to show how these varying results can be fitted into the general explanation, based on the relative stability of the initial state solvation shell combined in certain cases (group 2, 3) with the influence of unusual reorganization arising in consequence of anchimeric assistance. It will be obvious that in the case of the halohydrins in D_2O, the OH will rapidly exchange with the medium to give OD, but it does not appear that secondary deuterium isotope effects from this source can provide a sufficient basis for the observed differences between the three groups. At any rate, another effect must dominate since this secondary isotope effect should result in shifting the ratios of all of the anchimerically assisted halohydrins in the same direction.

Evidence for Anchimeric Assistance in Hydrolysis

Because water is a fair nucleophile as well as a good ionizing medium, the probability of anchimeric interaction assisting solvolysis is less here than in the case with acetic acid as solvent (8), but it is not eliminated. With this reservation, evidence of such assistance follows the structural conditions noted in the less nucleophilic solvent. Thus ethylene halohydrins of Cl (I), Br (V), and I (IX) react at .043, .04, and .028 of the rate of the corresponding unsubstituted compounds, and a β-methoxyl introduces a rate reduction of 0.033 in the primary ethyl bromide (est. 5.1×10^{-5} sec^{-1} at 100°) (9), pointing to an absence of anchimeric effects. Methylation of the β- or hydroxyl-carbon leads to increased evidence for anchimeric assistance. For example, isobutylene chlorohydrin (XII) and bromohydrin (XIII) solvolyse more rapidly than ethylene chlorohydrin (I) and bromohydrin (V), as noted earlier by Nilsson and Smith (10) for reaction with alkali, thus differing sharply from the unsubstituted ethyl and isobutyl halides. Although the data are not available to calculate σ^* in the Taft equation ($\log k/k_0 = \rho\sigma^*$ (11)), for substrates isobutylene chlorohydrin (XII) and bromohydrin (XIII), it is plain that there must be substantial anchimeric assistance in these cases. Reasons for this substitution effect have been given by Thorpe *et al.* (12) and Schleyer (13). Tetramethylene chlorohydrin (III) reacts some 60 times more rapidly than *n*-propyl chloride, while trimethylene (II) and ethylene chlorohydrin (I) react successively more slowly. The difference in rate of hydrolysis between the tetramethylene methoxychloride (IV) and III is small. A similar trend is evident in the related bromides V, VI, VII, and VIII in Table I, the tetramethylene bromohydrin proving too reactive to obtain in a pure state. These data confirm the activating influence of a hydroxyl or other basic substituent in a 5-member ring-forming position, as noted by many workers, for example, Heine (14), and recently studied by Winstein *et al.* for solvolysis of methoxyalkyl brosylates (15).

Group 1. Normal k_{D_2O}/k_{H_2O} Values

These compounds in Table I which have normal values of k_{D_2O}/k_{H_2O} include without exception the halohydrins and corresponding methoxyhalides which give no evidence of anchimeric assistance. It would appear that the dihalides give "normal" values of k_{D_2O}/k_{H_2O} whether involving anchimeric assistance, XVIII, or not, XXIII. Tetramethylene dibromide (VII) is apparently a borderline case with the slightly higher than normal ratio of 0.818.

From our study of the temperature dependence of the solvent isotope effect for isopropyl bromide we concluded that the presence of the alkyl halide increased the structural stability of the initial state solvation shell relative to bulk water by about 20%. The very similar values of k_{D_2O}/k_{H_2O} found for the "normal" substrates in Table I suggest that the neighboring OH or MeO have not changed the degree of solvent reorganization about the anionic portion of the molecules in going from the initial to the transition state. Now it is very probable that the hydroxyl group is hydrogen bonded to the adjacent water structure, as is indicated by the large increase in solubility caused by its presence. In the absence of anchimeric assistance there is no reason to believe that this interaction is disturbed in the activation process, and hence there is no significant change in the energy required to reorganize the solvent in the activation process, from that required for the unsubstituted halide. It follows that normal k_{D_2O}/k_{H_2O} ratios are observed.

Group 2. Low k_{D_2O}/k_{H_2O} Values (Table II)

All of the compounds in this group are halohydrins; it is noteworthy that the corresponding methoxy compounds fall in group 3.

Following our earlier explanation of the solvent isotope effect, either the substrates with unusually low k_{D_2O}/k_{H_2O} ratios have a more stable solvent structure in the initial state or a more drastic reorganization occurs in the activation process. The first alternative is ruled out by the results of group 1 halohydrins, and since group 2 compounds all show anchimeric assistance, the second suggestion would seem more plausible. However, a further assumption is necessary since the third group with k_{D_2O}/k_{H_2O} values higher than "normal" also gives evidence of anchimeric assistance.

Judging from enhanced solubility compared with that of unsubstituted halides it may be inferred that the OH groups of those compounds giving abnormal k_{D_2O}/k_{H_2O} values must, like the normal compounds, interact, through hydrogen bonding, with the water in the initial state. It is noteworthy that the corresponding methoxy compounds fall into group 3.

Evidence of anchimeric assistance implies that, in contrast to group 1 compounds, this hydrogen bonding is more or less disrupted in the activation process. The phrase "more or less" is purposely vague for we do not yet possess sufficiently detailed knowledge to correlate the variation from the "normal" values of k_{D_2O}/k_{H_2O} with the degree of anchimeric assistance. To account for the abnormal k_{D_2O}/k_{H_2O} values it is sufficient to assume that the hydroxyl group will be pulled out of its initial state position in the water structure and bent laterally to form the transitory ethyleneoxonium ions. This more extensive rearrangement will, of course, accentuate the effects of structural differences between D_2O and H_2O as observed.

It is notable that as the seat of reaction changes successively from primary (XII, XIII) to secondary (XIV, XV) to tertiary (XVII) there is a trend toward more normal k_{D_2O}/k_{H_2O} ratios. This trend parallels the expected decrease in the importance of anchimeric assistance in these compounds.

While this rationalization is admittedly *ad hoc*, our proposed explanation has certain implications concerning accompanying changes in entropy, enthalpy, and heat capacity which are open to experimental verification and these are currently under investigation.

Group 3. High k_{D_2O}/k_{H_2O} Values (Table III)

There are a number of hydroxyl- and methoxyl-substituted halides which show varying degrees of anchimeric assistance and yet have solvent isotope ratios (k_{D_2O}/k_{H_2O}) closer to unity than "normal". These include the tetramethylene chlorohydrin (III), methoxychloride (IV), and methoxybromide (VIII); trimethylene bromohydrin (VI); and isobutylene (XXII), trimethylethylene (XVI), and *trans*-cyclohexene methoxybromides (XX), which are to be contrasted with the corresponding bromohydrins (XIII, XV, and XXI). To these may be added isobutyl and neopentyl bromide, which gave indications of "higher" than normal solvent isotope ratios (3). The solvent isotope effects here deviate less from the normal than those found for group 2, and it is by no means certain that these deviations arise from the same cause in every case.

In an earlier paper (1) we discounted the isotope effect arising from varying nucleophilic interaction, yet it was difficult to imagine that the degree of reorganization which occurs about the cation would have no solvent isotope effect at all. It was more reasonable to equate at least part of the scatter apparent among the unsubstituted halides (normal solvent isotope effect) to this source. Both when the substituent group in the initial state blocks the rear side of the carbon undergoing displacement, and particularly when, as in the anchimerically assisted cases, it also serves as the displacing nucleophile, a lesser degree than normal of solvent reorganization will take place. This should lead to ratios nearer unity.

While the differentiation between groups 2 and 3 has a strong *ad hoc* flavor, it does have the advantage of explaining the quite different behavior of the tetramethylene chlorides (III) and (IV), both of which are group 3 compounds, while the pairs of compounds (XIII) and (XXII), (XV) and (XVI), and (XX) and (XXI) split between groups 2 and 3. In the latter cases the lateral displacements of the intramolecular nucleophiles require, for (XIII), (XV), and (XXI), the removal of the hydroxyl group *from* the water shell, and for (XIII), (XVI), and (XX), the movement of methoxyl *within* the solvent shell. The former leads to extensive reorganization and lower isotopic ratios; the latter leads to higher ratios because the displacement leads to relatively less reorganization than the abstraction of one water molecule from the solvent shell to serve as nucleophilic reagent. In the case of (III) and (IV), on the other hand, the intramolecular nucleophile must lie properly oriented behind the carbon–halogen bond early in the activation process, hence little reorganization is required.

At first we found it troublesome to understand why the iodochloride (XVIII) did not have as high a ratio as the isobutylene methoxybromide (XXII). Inspection of models shows that the iodine atom is so large that it is already almost touching the backside of the tertiary carbon undergoing displacement in XVIII, while the methoxyl group in XXII has to move an appreciable distance. However, the iodine is not hydrogen bonded to water in the initial state but presumably interacts as an exposed iodonium ion in the transition state. The methoxyl oxygen, on the other hand, is protected from solvation in the transition state by the alkyl group.

The case of compounds (XX) and (XXI) is being further investigated because their thermodynamic parameters of activation (24) indicate no noticeable anchimeric rate enhancement, although they clearly split between groups 2 and 3. A more detailed

analysis may show whether an anchimeric reaction may be proceeding through an unfavorable diaxial conformation, thus offsetting the rate enhancement.

EXPERIMENTAL DETAIL

The sources of the compounds and the available physical constants are summarized in Table IV. Commercially available compounds were either recrystallized or fractionally distilled under reduced pressure. In all cases linear pseudo first-order plots were obtained and this was considered to be the best critique of purity for the present purpose. Those compounds not otherwise available were synthesized* by the methods referenced in Table IV.

TABLE IV

Summary of sources and characteristics of halides solvolysed

Code	Halide	Boiling point	n_D^{25}	Source
I	2-Chloroethanol	56° (40 mm)	1.4260	Comm.
II	3-Chloro-1-propanol	56° (10 mm)	1.4415	"
III	4-Chloro-1-butanol	86° (20 mm)	1.4513 (23°)	"
IV	4-Chloro-1-methoxybutane	48–53° (20 mm)	1.4290	*a*
V	2-Bromoethanol	51–52° (14 mm)	1.4880 (26°)	Comm.
VI	3-Bromo-1-propanol		1.4861 (26°)	"
VII	1,4-Dibromobutane		1.5161	"
VIII	4-Bromo-1-methoxybutane	46–49° (12 mm)	1.4479	16
IX	2-Iodoethanol	88° (30 mm)	1.5625	*b*
X	3-Iodo-1-propanol	88–90° (7 mm)	1.5768 (24°)	17
XI	3-Iodo-1-methoxypropane	155–158°	1.4873 (27°)	*c*
XII	1-Chloro-2-methyl-2-propanol	56° (40 mm)	1.4260	*d*
XIII	1-Bromo-2-methyl-2-propanol	45° (15 mm)	1.4704	19
XIV	3-Chloro-2-methyl-2-butanol		1.4415	18
XV	3-Bromo-2-methyl-2-butanol	48–49.5° (10 mm)	1.4719	19
XVI	3-Bromo-2-methoxy-2-methyl-butane	56–57° (24 mm)	1.4551	19
XVII	3-Chloro-2,3-dimethyl-2-butanol	45–50° (15 mm)	m. 63.5–64.5°	20
XVIII	2-Chloro-1-iodo-2-methylpropane	54.5–55.2° (25 mm)	(Colored)	8
XIX	2-Chloro-1-methoxy-2-methylpropane	88–90°	1.4039 (24°)	*e*
XX	*trans*-2-Bromo-1-methoxy-cyclohexane		1.4890	22
XXI	*trans*-2-Bromocyclohexanol	73–75° (5 mm)	1.5184	*f*
XXII	1-Bromo-2-methoxy-2-methylpropane		1.4575	*g*
XXIII	2,3-Dibromo-2-methyl-butane	45–49° (10 mm)	1.5030	23

a. Prepared by method of (16) applied to tetramethylene chloride. The material isolated by fractionation was further purified on a Perkin–Elmer V.P.C. column.

b. Finckelstein reaction on ethylene chlorohydrin.

c. Finckelstein reaction on 3-bromo-1-methoxypropane, b. 129°, n_D^{26} 1.4448, prepared as for compound VIII.

d. Method of Smith and Skyle (18) applied to isobutylene using a dry ice reflux condenser.

e. Prepared from the alcohol (21) by Dr. K. T. Leffek.

f. Kindly supplied by Dr. R. A. B. Bannard; m.p. 27°, but supercools readily.

g. Prepared by the method used for compound XVI, applied to isobutylene, and purified by fractional freezing.

ACKNOWLEDGMENT

We wish to acknowledge the assistance of Mr. S. Sugamori in determining many of the rate data on which this paper is based.

**The following Carleton University students contributed to these preparations: H. G. Dodds, L. E. Hakka, C. A. McDonell, W. J. Meath, A. D. Relf, R. D. Sully, and R. Wardle.*

REFERENCES

1. P. M. LAUGHTON and R. E. ROBERTSON. Can. J. Chem. **34**, 1714 (1956).
2. R. E. ROBERTSON and P. M. LAUGHTON. Can. J. Chem. **35**, 1319 (1957).
3. P. M. LAUGHTON and R. E. ROBERTSON. Can. J. Chem. **37**, 1491 (1959).
4. J. A. LLEWELLYN, R. E. ROBERTSON, and J. M. W. SCOTT. Can. J. Chem. **38**, 222 (1960).
5. R. L. HEPPOLETTE and R. E. ROBERTSON. J. Am. Chem. Soc. **83**, 1834 (1961).
6. R. E. ROBERTSON. Can. J. Chem. **33**, 1536 (1955).
7. A. STREITWIESER, JR. J. Am. Chem. Soc. **78**, 4935 (1956).
8. S. WINSTEIN and E. GRUNWALD. J. Am. Chem. Soc. **70**, 828 (1948).
9. M. J. BLANDAMER. Private communication.
10. H. NILSSON and L. SMITH. Z. physik. Chem. (Leipzig), A, **166**, 136 (1933).
11. R. W. TAFT, JR. J. Am. Chem. Soc. **75**, 4231 (1953).
12. R. M. BEESLEY, C. K. INGOLD, and J. F. THORPE. J. Chem. Soc. **107**, 1080 (1915).
13. P. VON R. SCHLEYER. J. Am. Chem. Soc. **83**, 1368 (1961).
14. H. W. HEINE, A. B. MILLER, W. H. BARTON, and R. W. GREINER. J. Am. Chem. Soc. **75**, 4778 (1953).
15. S. WINSTEIN, E. ALLRED, R. HECK, and R. GLICK. Tetrahedron, **3**, 1 (1958).
16. A. KIRRMANN and N. HAMAIDE. Bull. soc. chim. France, 789 (1957).
17. L. HENRY. Bull. classe sci. Acad. roy. Belg. **33** (3), 407 (1897).
18. L. SMITH and S. SKYLE. Acta Chem. Scand. **5**, 1415 (1951).
19. S. WINSTEIN and L. L. INGRAHAM. J. Am. Chem. Soc. **74**, 1163 (1952).
20. F. BÄYER AND CO. DRP 317, 635 (1916). Fortschritte der Teerfarben-fabrikation und Verwandter Industriezweige **13**, 73 (1916–21).
21. M. H. PALOMAA. Ann. Acad. Sci. Fennicae, Ser. A, **10**, No. 17 (1918).
22. S. WINSTEIN and R. R. HENDERSON. J. Am. Chem. Soc. **65**, 2196 (1943).
23. A. H. BLATT. Organic syntheses. Coll. Vol. II. John Wiley and Sons, Inc., New York. 1943. p. 408.
24. M. J. BLANDAMER and R. E. ROBERTSON. Unpublished data.

RADIATION CHEMISTRY OF CYCLOHEXANE

III. EFFECT OF BENZENE AND IODINE ON THE ISOTOPIC COMPOSITION OF RADIOLYTIC HYDROGEN FROM C_6D_{12}–C_6H_{12} MIXTURES[1]

P. J. Dyne and W. M. Jenkinson

ABSTRACT

The isotopic composition of hydrogen evolved in the radiolysis of C_6D_{12}–C_6H_{12} mixtures has been measured in the presence of various amounts of benzene and iodine. The yield of the unimolecular decomposition and the specific yield of the bimolecular reaction are reduced in approximately the same proportion as the yield of total hydrogen. It is concluded that (i) iodine and benzene interact to a comparable extent with both unimolecular and bimolecular decomposition modes, (ii) it is probable that neither of these additives act by scavenging, and (iii) it is probable that they act by quenching a common precursor of the two decomposition modes.

INTRODUCTION

We have shown from measurements of the isotopic composition of hydrogen produced in the radiolysis of C_6D_{12}–C_6H_{12} mixtures (1) that part of the hydrogen is formed in a bimolecular process

$$C_6H_{12} \text{ —}\sim\sim\rightarrow X_H + P \qquad \text{yield } G_2(H) \qquad [1]$$

$$X_H + C_6H_{12} \rightarrow H_2 + P \qquad [2]$$

where the atoms in the H_2 molecule come from two different cyclohexane molecules, and part is formed in a unimolecular process

$$C_6H_{12} \text{ —}\sim\sim\rightarrow H_2 + P \qquad \text{yield } G_1(H) \qquad [3]$$

where both hydrogen atoms come from the same cyclohexane molecule. The symbol P represents any product or residue and X_H is the reactive intermediate in the bimolecular process.

The specific yield of the decomposition

$$C_6D_{12} \text{ —}\sim\sim\rightarrow D_2 + P \qquad \text{yield } G_1(D) \qquad [4]$$

in a large excess of C_6H_{12} was shown to be 0.25 molecules/100 ev absorbed in the C_6D_{12}. However, the yield of reaction [3] in pure C_6H_{12} may amount to between 25% (2) and nearly 50% (3) of the total yield. It is conceivable that this large "isotope effect" expresses variations in $G_1(D)$ and $G_1(H)$ with the isotopic composition of the solvent due to some type of energy transfer or charge transfer effect. In the experiments described in this paper we used the yield of D_2 from C_6D_{12} as an "indicator" of the efficiency of unimolecular processes in benzene and iodine solutions in cyclohexane.

We also showed (1) that $G_1(D)$, the yield of reaction [4], was reduced by biphenyl, and slightly reduced by iodine. We concluded that biphenyl could act as a quenching agent[2] on the excited precursors involved in the unimolecular decomposition.

In this paper we describe a series of measurements of the isotopic composition of hydrogen evolved in the radiolysis of C_6D_{12}–C_6H_{12} mixtures in the presence of varying amounts of benzene and iodine. We find that, for both these substances, $G_1(D)$ is reduced in approximately the same proportion as the total hydrogen yield, and we infer that the unimolecular and bimolecular decompositions are quenched to approximately the same extent by these substances. Burton and Chang (4) have studied the change in isotopic

[1]*Manuscript received June 22, 1961.*
Contribution from the Research Chemistry Branch, Atomic Energy of Canada Limited, Chalk River, Ontario. Issued as A.E.C.L. No. 1340.

[2]*In this paper 'quenching' refers to any process (energy transfer, charge transfer), other than radical scavenging, which inhibits decomposition or reduces a yield.*

composition of hydrogen evolved from mixtures containing roughly equimolar amounts of C_6H_{12} and C_6D_{12} and have discussed their results in terms of the function

$$f = \frac{[HD]^2}{[H_2][D_2]}.$$

The addition of benzene, iodine, methyl iodide, and cyclohexene to a given mixture of C_6D_{12} and C_6H_{12} changes f very little, even though G(hydrogen) may be reduced by as much as 80%.

Our work is, in the main, in agreement with their results and conclusions.[3] It differs in the following respects: we studied solutions containing less than 10 mole% C_6D_{12}, and discuss our results in terms of changes in G_1(D) and G(HD) rather than in f. At these concentrations of C_6D_{12} we observed small changes in f on the addition of benzene and iodine to a C_6D_{12}–C_6H_{12} mixture.

EXPERIMENTAL

The salient experimental details have been given in ref. 1. In the present experiments, however, the 2-ml samples were irradiated for 2 hours at a dose rate of $\sim 2.2 \times 10^{22}$ ev/lt hr. The total dose is about one-third that given in the earlier experiments and the experimental values of G(hydrogen) are, consequently, higher.

Solutions of four concentrations of C_6D_{12}, viz. 2.43, 4.78, 6.98, and 9.09 mole% were studied at four concentrations of benzene and three of iodine. These results are shown in Table I.

TABLE I

Isotopic composition of radiolytic hydrogen evolved from C_6D_{12}–C_6H_{12} mixtures

Mole% C_6D_{12}	Concn. of additive	G(hydrogen)	% H_2	% HD	% D_2	$f = \frac{[HD]^2}{[H_2][D_2]}$
2.43 = *a*			98.01	1.84	0.15	0.230
4.78 = *b*	0	5.34	96.11	3.59	0.30	0.446
6.98 = *c*			94.33	5.21	0.46	0.625
9.09 = *d*			92.53	6.83	0.64	0.787
a			97.91	1.94	0.15	0.256
b	C_6H_6	4.80	95.92	3.75	0.33	0.444
c	0.25 mole%		93.93	5.58	0.49	0.676
d			92.03	7.27	0.70	0.820
a			97.86	1.99	0.15	0.269
b	C_6H_6	4.66	96.21	3.51	0.28	0.457
c	0.608 mole%		93.86	5.64	0.50	0.673
d			91.89	7.42	0.69	0.868
a			97.74	2.10	0.16	0.282
b	C_6H_6	4.03	95.61	4.06	0.33	0.522
c	1.22 mole%		93.67	5.83	0.50	0.722
d			91.62	7.67	0.71	0.903
a			97.50	2.31	0.19	0.288
b	C_6H_6	2.70	95.12	4.52	0.36	0.596
c	6.02 mole%		92.86	6.60	0.54	0.869
d			90.54	8.69	0.77	1.083
a			97.78	2.04	0.18	0.236
b	I_2	3.85	95.68	3.95	0.37	0.440
c	1×10^{-2} *M*		93.58	5.82	0.60	0.603
d			91.53	7.61	0.86	0.735
a			97.77	2.07	0.16	0.273
b	I_2	3.45	95.48	4.11	0.41	0.431
c	3×10^{-2} *M*		93.37	5.99	0.64	0.600
d			91.34	7.78	0.88	0.752
a			97.71	2.10	0.19	0.237
b	I_2	3.31	95.38	4.21	0.41	0.453
c	5×10^{-2} *M*		93.24	6.11	0.65	0.615
d			91.23	7.86	0.91	0.744

[3]*We are indebted to Professor Burton and Dr. Chang for their courtesy in sending us preprints of papers describing their work.*

Values of $G_1(D)$, the unimolecular yield, were obtained using the graphical extrapolation described in (1). Values of $g(HD)$,[4] the yield of HD per unit mole fraction of C_6D_{12}, were obtained from the slope of the linear plot of $G(HD)$ vs. mole fraction C_6D_{12}. These derived values, together with values normalized to the mixture containing neither benzene nor iodine, are given in Table II.

TABLE II
Values of absolute and normalized yields

Concn. of additive	G(hyd) ±0.08	Norm.	G_1(D) ±0.02	Norm.	g(HD) ±0.1	Norm.
None	5.34	1.00	0.32_2	1.00	3.59	1.00
0.25% C_6H_6	4.80	0.89_7	0.28	0.87_0	3.49	0.97_0
0.62% C_6H_6	4.66	0.87_1	0.25	0.77_7	3.27	0.90_9
1.22% C_6H_6	4.03	0.75_3	0.25	0.77_7	3.07	0.85_3
6.02% C_6H_6	2.70	0.50_4	0.19	0.59_0	2.37	0.65_8
1×10^{-2} M I_2	3.85	0.71_9	0.26	0.80_8	2.92	0.81_1
3×10^{-2} M I_2	3.45	0.64_5	0.25	0.77_7	2.68	0.74_5
5×10^{-2} M I_2	3.31	0.61_8	0.23	0.71_8	2.60	0.72_2

The error given in the value of G(hyd) in Table II covers the range of the experimental values. The errors in $G_1(D)$ and $g(HD)$ were obtained from the extreme values of the intercepts and slopes which could be derived from the experimental points and contain errors from both G(hydrogen) and from the isotopic analysis. Uncertainties in % D_2 at the lowest concentration of C_6D_{12} amount to ±10% and to ±2% at the highest.

The value of $G_1(D)$ in the absence of additives, 0.32 ± 0.02, is greater than the value of 0.25 previously reported. This is because the present experiments were carried out at lower total doses. The newer value is more precise and compares well with the value of 0.35 obtained by Burton and Chang in similar experiments.

THE KINETIC ANALYSIS

The complete mechanism used for the interpretation of these results is:

$C_H \longrightarrow C_H^*$	yield $G_1(H)$
$C_H^* \rightarrow H_2 + P$	
$C_D \longrightarrow C_D^*$	yield $G_1(D)$
$C_D^* \rightarrow D_2 + P$	
$C_H \longrightarrow C_H^{**}$	yield $G_2(H)$
$C_H^{**} \rightarrow X_H + P$	
$C_D \longrightarrow C_D^{**}$	yield $G_2(D)$
$C_D^{**} \rightarrow X_D + P$	
$X_H + C_H \rightarrow H_2 + P$	rate constant k_1
$X_D + C_H \rightarrow HD + P$	k_2
$X_H + C_D \rightarrow HD + P$	k_3
$X_D + C_D \rightarrow D_2 + P$	k_4

where $C_H = C_6H_{12}$, $C_D = C_6D_{12}$. P and X_H have been defined in the introduction.

We have shown (1) that, in mixtures containing C_D moles of C_6D_{12} and C_H moles of C_6H_{12},

$$G(D_2) = G_2(D)\times k_4/k_2\times(C_D/C_H)^2+G_1(D)\times C_D/C_H \qquad [1]$$

when $CH \gg C_D$.

[4] *g(HD) is precisely defined in the discussion.*

A similar steady state argument gives

$$G(\mathrm{HD}) = \mathrm{C_D}/\mathrm{C_H}\,[(k_3/k_1)\times G_2(\mathrm{H})+G_2(\mathrm{D})] \qquad [2]$$

when $\mathrm{C_H} \gg \mathrm{C_D}$. We define $g(\mathrm{HD}) = (k_3/k_1)\times G_2(\mathrm{H})+G_2(\mathrm{D})$.

The above analysis identifies the unimolecular yield $G_1(\mathrm{D})$ as that fraction of the yield of $\mathrm{D_2}$ which is first order with respect to $\mathrm{C_D}$ and resolves the term $g(\mathrm{HD})$ into the sum of two terms, the weighted yields of the intermediates $\mathrm{X_H}$ and $\mathrm{X_D}$ in the bimolecular reactions. The terms $G_1(\mathrm{D})$, $G_2(\mathrm{D})$ and $G_1(\mathrm{H})$, $G_2(\mathrm{H})$ contribute to the total yields in proportion to the mole fractions of $\mathrm{C_6D_{12}}$ and $\mathrm{C_6H_{12}}$.

DISCUSSION: IMMEDIATE CONCLUSIONS

An additive may interfere with and reduce either or both of the two decomposition mechanisms. Consider an additive which quenches the unimolecular mechanism and leaves the bimolecular mechanism unchanged. The yield $G_1(\mathrm{D})$, measured in these experiments, will decrease, and should decrease more rapidly than the total yield of hydrogen if the effects on $G_1(\mathrm{D})$ and $G_1(\mathrm{H})$ are comparable. Further, in experiments where essentially all the observed $\mathrm{D_2}$ comes from the unimolecular decomposition (as in the present case), the percentage of $\mathrm{D_2}$ must decrease. Since, by hypothesis, $g(\mathrm{HD})$ is unchanged and G(hydrogen) is reduced, then the % HD must increase.

The changes in % $\mathrm{D_2}$ and % HD will depend on the relative contributions of the unimolecular and bimolecular yields. If, for instance, the bimolecular yield is a large fraction of the total, then the change in % $\mathrm{D_2}$ will be of the same order as the percentage change in total hydrogen. If the bimolecular yield is small the change in % $\mathrm{D_2}$ will be large compared with the change in total hydrogen.

The possible changes in $G_1(\mathrm{D})$, $g(\mathrm{HD})$, and percentage composition are summarized below:

	$G_1(\mathrm{D})$	$g(\mathrm{HD})$	% $\mathrm{D_2}$	% HD
Unimolecular mechanism quenched	Decreased more rapidly than total hydrogen	Unchanged	Decreased	Increased
Bimolecular mechanism quenched or scavenged	Unchanged	Decreased more rapidly than total hydrogen	Increased	Decreased
Both mechanisms quenched/ scavenged	Decreased	Decreased	Small changes +ve or −ve	Small changes +ve or −ve

In the case where both mechanisms are quenched the magnitude of the decreases in $G_1(\mathrm{D})$ and $g(\mathrm{HD})$ relative to the decrease in G(hydrogen) will depend on several factors: the relative yields of the two mechanisms, the sensitivity of the precursors $\mathrm{C_H}^*$, $\mathrm{C_H}^{**}$, or $\mathrm{X_H}$ to the additive, and isotope effects in the reactivity of $\mathrm{C_H}^*$ and $\mathrm{C_D}^*$ or $\mathrm{X_H}$ and $\mathrm{X_D}$ with the additive.

Qualitatively the results in Tables I and II and Fig. 1 fall into the third category, and it follows that both the unimolecular and bimolecular yields of hydrogen are quenched/scavenged by benzene and by iodine to a comparable extent.

It can be argued, from these results, firstly, that the action of these additives is the quenching of both mechanisms, and secondly, that both mechanisms have a common precursor, i.e. $\mathrm{C_H}^* \equiv \mathrm{C_H}^{**}$. These arguments proceed as follows. If the bimolecular mechanism is reduced by scavenging then the scavenging reaction,

$$\mathrm{M} + \mathrm{X_H} \rightarrow \text{products}, \qquad [a]$$

has a comparable efficiency to the quenching of the unimolecular mechanism,

$$\mathrm{C_H}^* + \mathrm{M} \rightarrow \mathrm{C_H} + \mathrm{M}^*. \qquad [b]$$

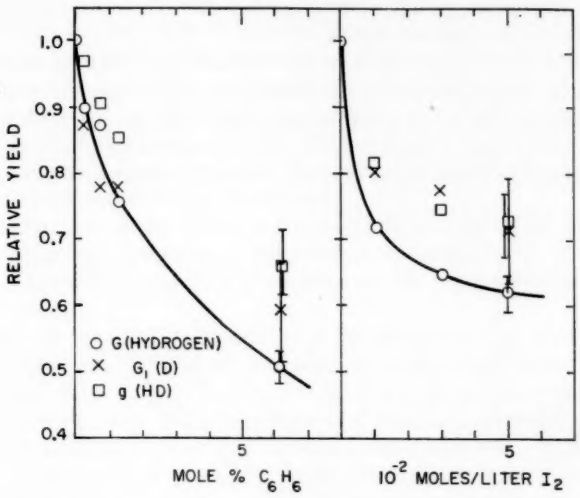

FIG. 1. Relative values of G(hydrogen), G_1(D), and g(HD) as a function of (*a*) benzene and (*b*) iodine concentrations. The precise numerical data may be found in Table II. The bars at the highest concentrations give the limits of error on the values.

These are different physical processes; one involves the rearrangement of chemical bonds, the other does not. It is consequently improbable that they would have rate constants which are within about 30% of one another, as implied by our data, and even more improbable that this would be so for both benzene and iodine. The mode of interaction is therefore *quenching* of both mechanisms, i.e. by [*b*] and

$$C_H^{**} + M \rightarrow C_H + M^*. \qquad [c]$$

It can also be argued that it is improbable that there are two quenching reactions [*b*] and [*c*] having comparable rates for both additives. The simplest explanation is that the precursors C_H^* and C_H^{**} are identical. The reaction scheme is therefore

$$C_H \rightsquigarrow C_H^*$$

$$C_H^* \begin{cases} \nearrow X_H + P \\ \searrow H_2 + P \end{cases}$$

$$C_H^* + M \rightarrow C_H + M^*.$$

This last conclusion would be inescapable if the isotopic composition were precisely unaltered by the addition of benzene or iodine.

However, as can be seen from an inspection of Table I, some changes in isotopic composition are observed. Further significant differences can be observed from the behavior of the function

$$f = [HD]^2/[H_2]\,[D_2].$$

If hydrogen were produced exclusively by a bimolecular mechanism which proceeded statistically with no isotopic discrimination, then $f = 4$.

From the kinetic scheme given above it can be shown that

$$f = 4\frac{k_2 k_3}{k_1 k_4}$$

and a consideration of the isotope effects in hydrogen and deuterium abstraction reactions shows that f will be always greater than 4.

As, experimentally, f is always less than 4 it follows that other processes forming H_2 and D_2 are operative: this is prima facie evidence that the contribution of the unimolecular processes is appreciable (2, 3) (or that the species X_H are not hydrogen atoms and the ratios k_1/k_2, k_3/k_4 are quite different from the estimates). In Fig. 2 we present a plot of f vs. mole% C_6D_{12}. The addition of benzene raises the value of f significantly; iodine lowers it slightly.

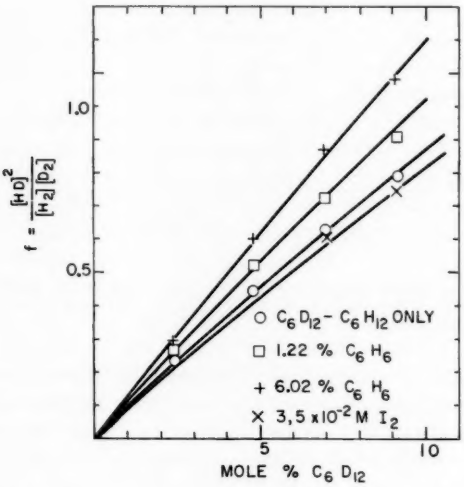

FIG. 2. Variation of f as a function of the concentrations of C_6D_{12} in the presence of varying amounts of benzene and iodine. The precise numerical data may be found in Table I.

These effects of benzene and iodine on f make it appear that, in effect, benzene quenches the unimolecular processes (giving H_2 and D_2) slightly more efficiently than the bimolecular processes. Iodine reacts conversely. The same conclusion can be reached from Fig. 1. For benzene, for instance, the curve for $G_1(D)$ lies below the curve for $g(HD)$. Such an effect could be produced by an isotopic effect in the efficiency of quenching C_H^* and C_D^*. If C_D^* were more efficiently quenched than C_H^*, then $G_1(D)$ would fall more rapidly than $g(HD)$, which is, in effect, the sum of the net yields of C_H^{**} and C_D^{**}.

In summary we conclude that (i) iodine and benzene interact to a comparable extent with both unimolecular and bimolecular decomposition modes, and (ii) it is probable that neither of these additives act by scavenging, and (iii) it is probable that they act by quenching a common precursor of the two decomposition modes. The first conclusion is clear; the second and third are debatable.

FURTHER IMPLICATIONS

The effects of benzene, iodine, and other additives on $G(H_2)$ from cyclohexane have been studied by many workers. (See, for instance, refs. 5–8.) In general the curve of $G(H_2)$ vs. additive concentration consists of two segments: an initial rapid decrease in

the concentration range 0–5% and a much slower decrease at higher concentrations. The yield curve cannot be described by simple kinetic schemes involving the quenching or scavenging of one precursor. The existence of two precursors is frequently postulated; one of these is readily quenched (or scavenged) at low concentrations, the other is only quenched (or scavenged) at high concentrations. As the additives are often supposed to be very reactive radical scavengers, the efficient reaction may be identified as radical scavenging and the less efficient reaction identified as the quenching of a non-scavengeable reaction, e.g. the unimolecular decomposition.

In this paper we have shown that benzene and iodine reduce the bimolecular (scavengeable) and unimolecular (unscavengeable) yields concurrently in the low concentration region, and it follows that the interpretations of the type outlined above are, at best, only partially true.

In the absence of chemical identification of the products of scavenging this discrepancy turns on two points, the validity of the kinetic analysis which distinguishes between the two processes and the assumption that the additive acts as a scavenger.

The kinetic analysis is generally performed on transformed versions of the yield curve involving functions of the reciprocal of the yield: these versions give linear plots. It should be noted that a reciprocal of a smooth curve (such as the yield curve) will always give an approximate straight line.[5] Consequently the linearity of these plots, if based on a limited region of the yield curve, is as significant or trivial as, for instance, the linearity of a logarithmic plot. (See for instance ref. 11.) A kinetic analysis which leads to the conclusion that two processes are occurring only demonstrates rigorously that one process in a simple scheme *cannot* account for the data.

It is well known that many reactive radical scavengers are potentially efficient energy sinks or charge acceptors. Our ignorance of the mechanism of energy and charge transfer in irradiated liquid systems is so profound that it is unwise to identify a substance, *a priori*, as a radical scavenger and assume that it cannot react otherwise.

For benzene there is chemical evidence that it does not act as a conventional scavenger, since G(-benzene) is small at these concentrations (9). This does not preclude the possibility (7, 10), that benzene acts as a "catalyst" by a series of reactions such as

$$C_6H_6 + H \rightarrow C_6H_7$$

$$C_6H_7 + C_6H_{11} \rightarrow C_6H_6 + C_6H_{12}.$$

For iodine it is known that HI is found in the initial stage of the radiolysis in an amount which is equivalent to the concurrent reduction in hydrogen yield, and which is also consistent with the 'hydrogen atom yield' derived from kinetic analysis. If the unimolecular decomposition of cyclohexane is a significant fraction of the total, then we would be forced to conclude, in spite of the strong arguments to the contrary advanced by Forrestal and Hamill (11), that HI is formed by some reaction other than hydrogen atom scavenging by molecular iodine.

ACKNOWLEDGMENTS

It is a pleasure to acknowledge both the detailed correspondence we have had with Professor Milton Burton and the helpful discussions we had with Dr. R. H. Betts.

[5]*The sceptical reader might test this with synthetic, freehand yield curves. We are obliged to Dr. J. W. Otvos for pointing out to us this property of numbers.*

REFERENCES

1. P. J. DYNE and W. M. JENKINSON. Can. J. Chem. **38**, 539 (1960).
2. T. D. NEVITT and L. P. REMSBERG. J. Phys. Chem. **64**, 969 (1960).
3. M. BURTON and J. CHANG. Private communication.
4. M. BURTON and J. CHANG. 137th Meeting of American Chemical Society, Cleveland, Ohio. 1960. Abstract 109, Section R.
5. M. BURTON, J. CHANG, S. LIPSKY, and M. P. REDDY. Radiation Research, **8**, 203 (1958).
6. G. E. ADAMS, J. H. BAXENDALE, and R. D. SEDGWICK. J. Phys. Chem. **63**, 854 (1959).
7. G. R. FREEMAN. J. Chem. Phys. **33**, 71 (1960).
8. T. J. HARDWICK. J. Phys. Chem. **65**, 101 (1961).
9. P. J. DYNE and J. A. STONE. Unpublished work.
10. P. J. DYNE, J. W. FLETCHER, and W. M. JENKINSON. A.E.C.L. Report CRC-941. July, 1960.
11. L. J. FORRESTAL and W. H. HAMILL. J. Am. Chem. Soc. **83**, 1535 (1961).

THE VIBRATIONAL SPECTRA OF SULPHURYL AND THIONYL HALIDES[1]

R. J. GILLESPIE AND E. A. ROBINSON[2]

ABSTRACT

New assignments are proposed for the fundamental frequencies of SOF_2, $SOCl_2$, SO_2Cl_2, SO_2F_2, and SO_2FBr, based on new measurements of the Raman spectrum of SO_2Cl_2 and previous measurements of the infrared and Raman spectra of these molecules. The fundamental frequencies of these molecules are found to be related to each other and to those of similar molecules when the normal modes are described in terms of characteristic vibrations of the SO, SO_2, S(Hal), and $S(Hal)_2$ groups.

INTRODUCTION

The purpose of this paper is to give a consistent assignment of the observed vibrational frequencies of the thionyl and sulphuryl halides to the various modes of vibration of these molecules. This work was undertaken as a necessary preliminary to the interpretation of the vibrational spectra of a number of more complicated polysulphuryl compounds (1). Although both the infrared and Raman spectra of several of these molecules have each been examined a number of times, no complete agreement has been reached concerning the assignments of the observed frequencies (e.g. references 2, 3, and 4). We have found, by comparing the spectra of these molecules and certain others containing SO, SO_2, S(Hal), and $S(Hal)_2$ groups, that a consistent and satisfactory set of assignments can be given for all the sulphuryl and thionyl halides that have been studied.

Of the spectra discussed, only the Raman spectrum of SO_2Cl_2 has been re-examined in the present work. The spectrum is shown in Fig. 1. The vibrational frequencies for

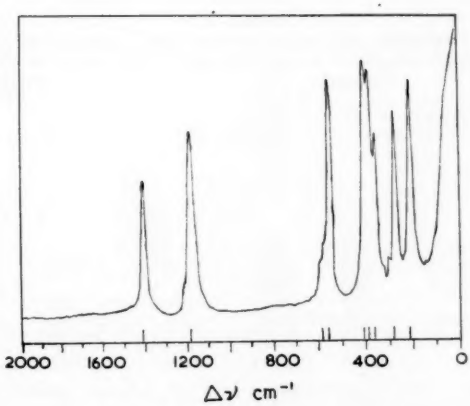

FIG. 1. The Raman spectrum of sulphuryl chloride.

sulphuryl chloride and for the other sulphuryl and thionyl halides obtained in the present and previous work are given in Tables I–V.

[1]*Manuscript received May 15, 1961.*
Contribution from the Department of Chemistry, McMaster University, Hamilton, Ontario.
[2]*Present address: Department of Chemistry, University of Toronto, Toronto, Ontario.*

TABLE I

Observed frequencies and assignments for SO_2F_2 (frequencies in cm^{-1})

Raman	Infrared	Assignment	
(*a*)	(*b*)	(*c*)	(*b*)
	274	Impurity	$\nu_4(a_1)$
388 dp	386	$\nu_9(b_2)$	$\nu_9(b_2)$
	539	$\nu_7(b_1)$	$\nu_7(b_1)$
547 dp	544	$\nu_4(a_1)$	$2\nu_4(A_1) = 548$
	553	$\nu_3(a_1)$	$\nu_3(a_1)$
	668	$\nu_6-\nu_2(B_1) = 656$	$\nu_4+\nu_9(B_2) = 660$
	720	$2\nu_5(A_1)$	$2\nu_5(A_1)$
	769	$2\nu_9(A_1) = 772$	$2\nu_9(A_1) = 772$
846 p	848	$\nu_2(a_1)$	$\nu_2(a_1)$
887	885	$\nu_8(b_2)$	$\nu_8(b_2)$
	925	$\nu_4+\nu_9(B_2) = 930$	$2\nu_4+\nu_9(B_2) = 930$
	954	$\nu_6-\nu_3(B_1) = 949$	$\nu_6-\nu_3(B_1) = 949$
	1077	$2\nu_7(A_1) = 1078$	$2\nu_7(A_1) = 1078$
	1092	$2\nu_4(A_1) = 1088$	$\nu_3+\nu_7(B_1) = 1092$
	1103	$\nu_3+\nu_4(A_1) = 1097$	$2\nu_3(A_1) = 1106$
	1118	$2\nu_3(A_1) = 1106$	$\nu_2+\nu_4(A_1) = 1122$
1270 p	1269	$\nu_1(a_1)$	$\nu_1(a_1)$
	1389	$\nu_2+\nu_7(B_1) = 1387$	$\nu_2+\nu_7(B_1) = 1387$
1502 dp	1502	$\nu_6(b_1)$	$\nu_6(b_1)$
	1698	$2\nu_2(A_1) = 1696$	$2\nu_2(A_1) = 1696$
	1772	$\nu_2+\nu_8(B_2) = 1733$	$\nu_2+\nu_8(B_2) = 1733$
	1820	$\nu_1+\nu_3(A_1) = 1822$	$\nu_1+\nu_3(A_1) = 1822$
	1889	?	?
	2052	$\nu_3+\nu_6(B_1) = 2055$	$\nu_3+\nu_6(B_1) = 2055$
	2115	$\nu_1+\nu_2(A_1) = 2117$	$\nu_1+\nu_2(A_1) = 2117$
	2355	$\nu_2+\nu_6(B_1) = 2350$	$\nu_2+\nu_6(B_1) = 2350$
	2536	$2\nu_1(A_1) = 2538$	$2\nu_1(A_1) = 2538$
	2760	$\nu_1+\nu_6(B_1) = 2771$	$\nu_1+\nu_6(B_1) = 2771$
	2995	$2\nu_6(A_1) = 3004$	$2\nu_6(A_1) = 3004$

NOTE: (*a*) Bender and Wood (21); (*b*) Hunt and Wilson (2); (*c*) this paper.

TABLE II

Observed frequencies and assignments for SO_2Cl_2 (frequencies in cm^{-1})

Raman		Infrared			Assignment	
(*a*)	(*b*)	(*c*)	(*d*)	(*e*)	(*f*)	(*d*)
218 p	209				$\nu_4(a_1)$	$\nu_4(a_1)$
282 dp	280				$\nu_7(b_1)$	$\nu_8(a_2)$
362 dp	363				$\nu_9(b_2)$	$\nu_7(b_1)$
388 dp	388				$\nu_8(a_2)$	$\nu_9(b_2)$
408 p	403				$\nu_3(a_1)$	$\nu_3(a_1)$
560 p	556		577	(557)	$\nu_2(a_1)$	$\nu_8(b_2)$
	563		586	(566)	$2\nu_7(B_1) = 564$	$\nu_2(a_1)$
580 dp	578		595	(575)	$\nu_6(b_1)$	$\nu_4+\nu_7(B_1) = 580$
			611	(591)	$\nu_4+\nu_9(B_2) = 580$	$\nu_4+\nu_9(B_2) = 606$
			619	(599)	$\nu_3+\nu_4(A_1) = 626$	$\nu_3+\nu_4(A_1) = 623$
			714	(694)	$\nu_3+\nu_7(B_1) = 690$	$2\nu_7(A_1) = 724$
			793	(773)	$\nu_2+\nu_4(A_1) = 778$	$\nu_2+\nu_4(A_1) = 784$; $\nu_4+\nu_9(B_1) = 775$
			946	(926)	$\nu_2+\nu_9(B_2) = 922$	$\nu_2+\nu_7(B_1) = 928$
			996	(976)	$\nu_2+\nu_8(B_2) = 988$	$\nu_3+\nu_9(B_2) = 962$; $\nu_2+\nu_3(A_1) = 971$
		1160	1171	(1151)	$2\nu_5(A_1) = 1160$	$2\nu_2(A_1) = 1132$; $\nu_2+\nu_9(B_1) = 1123$
1182 p	1186	1196	1205	(1185)	$\nu_1(a_1)$	$\nu_1(a_1)$
1414 dp	1411	1419	1434	(1414)	$\nu_6(b_1)$	$\nu_6(b_1)$
			2004	(1984)	$\nu_2+\nu_6(B_1) = 1974$	$\nu_2+\nu_6(B_1) = 1974$; $\nu_1+\nu_2+\nu_4(A_1) = 1961$
			2398	(2378)	$2\nu_1(A_1) = 2364$	$2\nu_1(A_1) = 2364$
			2632	(2612)	$\nu_1+\nu_6(B_1) = 2596$	$\nu_1+\nu_6(B_1) = 2596$
			2869	(2849)	$2\nu_6(A_1) = 2828$	$2\nu_6(A_1) = 2828$

NOTE: (*a*) Present work; (*b*) Vogel-Högler (19); (*c*) Schreiber (33); (*d*) Martz and Lagemann (18); (*e*) Infrared frequencies corrected to allow for discrepancy with Raman results (column (*d*) minus 20 cm^{-1}); (*f*) this paper.

TABLE III

Observed frequencies and assignments for SOF_2 (frequencies in cm^{-1})

Raman		Infrared	Assignment	
(*a*)	(*b*)	(*c*)	(*d*)	(*c*)
	326		$\nu_4(a')$	
393 dp	395	390	$\nu_6(a'')$	$\nu_6(a'')$
		(410)		$\nu_4(a')$
526 p	529	530	$\nu_3(a')$	$\nu_3(a')$
721 dp	720	748	$\nu_5(a'')$	$\nu_5(a'')$
801 p	795	806	$\nu_2(a')$	$\nu_2(a')$
		920	$\nu_3+\nu_6(A'') = 920$	$\nu_3+\nu_6(A'') = 920$
		940	$\nu_1-\nu_6(A'') = 943$	$\nu_3+\nu_4(A') = 940$
		1136	$\nu_2+\nu_4(A') = 1132$	$\nu_5+\nu_6(A') = 1138$
				$\nu_5+\nu_4(A'') = 1158$
			$\nu_1(a')$	$\nu_1(a')$
1308 p	1312	1333	$\nu_2+\nu_3(A') = 1336$	$\nu_2+\nu_3(A') = 1336$
		1480	$2\nu_5(A') = 1496$	$2\nu_5(A') = 1496$
		1546	$\nu_2+\nu_5(A'') = 1554$	$\nu_2+\nu_5(A'') = 1554$
		1612	$2\nu_2(A') = 1612$	$2\nu_2(A') = 1612$
		1718	$\nu_1+\nu_6(A'') = 1723$	$\nu_1+\nu_6(A'') = 1723$
			$\nu_1+\nu_4(A') = 1743$	$\nu_1+\nu_4(A') = 1743$
		2144	$\nu_1+\nu_2(A') = 2139$	$\nu_1+\nu_2(A') = 2139$
		2652	$2\nu_1(A') = 2666$	$2\nu_1(A') = 2666$

NOTE: (*a*) Bender and Wood (21); (*b*) Yost (5); (*c*) O'Loane and Wilson (20); (*d*) this paper.

TABLE IV

Observed frequencies and assignments for $SOCl_2$ (frequencies in cm^{-1})

Raman	Infrared		Assignment
(*a*)	(*b*)	(*c*)	(*d*)
194 p			$\nu_4(a')$
284 dp			$\nu_6(a'')$
344 p			$\nu_3(a')$
443 dp		455	$\nu_5(a'')$
490 p		492	$\nu_2(a')$
		735	$\nu_5+\nu_6(A') = 739$
		778	$\nu_2+\nu_6(A'') = 776$
		800	$\nu_3+\nu_5(A'') = 799$
		833	$\nu_2+\nu_3(A') = 836$
		950	$\nu_2+\nu_5(A'') = 947$
	1140		
	1200		
	1238	1251	$\nu_1(a')$
	1350	1360	SO_2 impurity
		2506	$2\nu_1(a') = 2502$

NOTE: (*a*) Vogel-Högler (19), McDowell (34); (*b*) Schreiber (33); (*c*) Martz and Lagemann (18); (*d*) this paper and Martz and Lagemann (18).

The sulphuryl halides, SO_2X_2, have C_{2v} symmetry and they therefore have nine fundamental vibrations, four of which are totally symmetric. To a first approximation, at least, three of the vibrations can be associated with valency deformations of the SO_2 group (symmetric and asymmetric stretches and a bend) and three similar vibrations with the SX_2 group. The remaining normal modes can be described as a torsion (inactive in the infrared) and as SO_2 and SX_2 rocking modes.

The thionyl halides, SOX_2, have pyramidal structures with C_s symmetry and six fundamental vibrations which may be approximately described as an SX_2 symmetric and asymmetric stretch, an SX_2 rock, an SO stretch, and an SO wag (or OSX_2 deformation).

TABLE V

Observed frequencies and assignments for SO_2FBr
(frequencies in cm^{-1})

Infrared	Assignment	
(*a*)	(*b*)	(*a*)
270	$\nu_6(a')$	$\nu_6(a')$
320	$\nu_9(a'')$	$\nu_9(a'')$
353	$2\nu_9(A')$	
450	$\nu_9+\nu_6(A'') = 446$	$\nu_5(A')$
461	$\nu_8(a'')$	$\nu_4(a')$
497	$\nu_4(a')$	$\nu_3(a')$
551	$2\nu_6(A') = 540$	
608	$\nu_3(a')$	$\nu_2(a')$
650	$2\nu_5(A') = 640$	
720	$2\nu_6+\nu_9(A'') = 716$	
728	$\nu_6+\nu_8(A'') = 731$	
814	$\nu_2(a')$	$\nu_8(a'')$
873	$\nu_3+\nu_6(A') = 878$	
930	$\nu_5+\nu_3(A') = 928$	
948	$\nu_4+\nu_8(A'') = 958$	
984	$\nu_2+\nu_9(A'') = 990$	
1069	$\nu_3+\nu_8(A'') = 1069$	
1080	$\nu_2+\nu_6(A') = 1084$	
1140	$\nu_7-\nu_6(A'') = 1140$	
1228	$\nu_1(a')$	$\nu_1(a')$
1305	$\nu_2+\nu_4(A') = 1311$	
1460	$\nu_7(a'')$	$\nu_7(a'')$
1511	$\nu_1+\nu_6(A') = 1498$	
1622	$2\nu_5(A') = 1624$	
1713	$\nu_7+\nu_6(A'') = 1730$	
1763	$\nu_5+\nu_7(A'') = 1780$	
2035	$\nu_1+\nu_5(A') = 2042$	
2265	$\nu_7+\nu_2(A'') = 2274$	
2440	$2\nu_1(A') = 2456$	
2650	$\nu_1+\nu_7(A'') = 2688$	
2890	$2\nu_7(A') = 2920$	

NOTE: (*a*) Crow and Lagemann (29); (*b*) this paper.

DISCUSSION

Thionyl Fluoride and Thionyl Chloride

All six normal vibrations have been observed for thionyl chloride, and, as expected, four of the lines in the Raman spectrum are polarized (Table IV). Only five fundamentals, three of which are polarized, have been observed with certainty for thionyl fluoride, although Yost (5) has claimed a line in the Raman spectrum at 326 cm^{-1}, in addition to the five lines reported by other workers.

Frequencies can readily be assigned to the SO stretch, the SX_2 stretches, and the SX_2 bend in both SOF_2 and $SOCl_2$ by comparison with the frequencies of these vibrations in similar molecules, as shown in Table VI. The polarized line at 344 cm^{-1} in the spectrum of $SOCl_2$ must then be assigned to the totally symmetric SO wag and the remaining line at 284 cm^{-1} (depolarized) to the SCl_2 rocking mode. Similarly in the spectrum of SO_2F_2 the depolarized line at 393 cm^{-1} must be assigned to the SF_2 rocking mode and the remaining line at 326 cm^{-1} to the SO wag. Although the degree of polarization of this line is not known, it seems reasonable to suppose that it is polarized, since only three of the other lines have been found to be polarized. Our assignment for $SOCl_2$ agrees with that given by Martz and Lagemann (18). Assignments for the spectra of selenium oxychloride (17) and selenium oxyfluoride (16) can readily be made by comparison with the

TABLE VI

Summary of assignments for the thionyl, sulphuryl, and selenyl halides (frequencies in cm^{-1})

	SOF_2	$SOCl_2$	SO_2F_2	SO_2Cl_2	SO_2FBr	Related molecules	$SeOF_2$	$SeOCl_2$
SO stretch*	1308	1229				SO, 1124 (6); R_2SO, 1040–1060 (7)	1012	955
SO_2 stretch, s			1269	1182	1228	R_2SO_2, 1130–1160, 1310–1335 (22, 23)		
SO_2 stretch, a			1502	1414	1460	CH_3SO_2Cl, 1175, 1370 (25); CH_3SO_2F, 1210, 1401 (26)		
SF_2 stretch, s	801		848			SF_6, 775, 644 (8); SF_4, 889, 867, 728 (9)	664	
SF_2 stretch, a	721		885			$XOSO_2F$, 820–850 (10, 11)	605	
SF stretch					814			
SCl_2 stretch, s		490		405		SCl_2, 514, 535 (12); S_2Cl_2, 447 (13)		388
SCl_2 stretch, a		443		362				347
SBr stretch					270			
SO_2 bend			545	560	608	SO_2, 525 (24); CH_3SO_2Cl, 538 (25); CH_3SO_2F, 531 (26)		
SF_2 bend	526		545			SF_6, 524 (8); SF_4, 557 (9); SOF_4, 567 (14); PF_3, 531, 486 (15)	373	
SCl_2 bend		194		218		SCl_2, 208 (12); PCl_3, 257, 190 (27)		279
SO_2 rock			545	580	497			
SF_2 rock	393		388				308	
SCl_2 rock		284		282				255
SO wag	326	344					278	279
SF wag					320			
SBr wag					176			
Torsion			360	388	461			

*Or SeO stretch etc., as appropriate.

spectra of the corresponding thionyl compounds. Our assignments for these molecules are given in Table VI.

Sulphuryl Chloride and Sulphuryl Fluoride

In the Raman spectrum of sulphuryl chloride eight of the expected nine lines are observed as distinctly resolved peaks. The ninth appears as a shoulder at approximately 580 cm^{-1} on the 560 cm^{-1} peak. Vogel-Högler (19) reported three lines at 556, 563, and 578 cm^{-1} in the infrared in this region. Martz and Lagemann (18) also reported three lines in the infrared, but at frequencies of 577, 586, and 595 cm^{-1}, of which the first two were intense and assigned as fundamentals while the third was rather weak and assigned as a combination band. We will assume that there are only two fundamentals in this region of the spectrum with frequencies of approximately 560 cm^{-1} and 580 cm^{-1}. Raman frequencies for the liquid appear to be consistently lower than the corresponding infrared frequencies for the gas. To facilitate comparison with the Raman data, infrared frequencies that have been reduced by 20 cm^{-1} are listed in addition to the observed values.

In the case of sulphuryl fluoride, three lines at 539, 544, and 553 cm^{-1} have been reported (2, 20) in the infrared spectrum but only one at 547 cm^{-1} in the Raman spectrum (4, 21). It seems likely that there are indeed three lines that are not resolved from each other in the Raman spectrum; accordingly three vibrations are each assigned a frequency of 545 cm^{-1}.

Frequencies can readily be assigned to the SO_2 stretches, the SO_2 bend, the SX_2 stretches, the SX_2 bends, and the SX_2 rocking mode by comparison with the frequencies of these vibrations in the thionyl halides or other similar molecules, as shown in Table VI. The only vibrations to which frequencies cannot be easily assigned in this way are the SO_2 rocking mode and the torsion, which is inactive in the infrared. In the spectrum of sulphuryl chloride we have unassigned lines at 388 cm^{-1} (R) and at 580 cm^{-1} (R and I.R.) and in the spectrum of sulphuryl fluoride at 274 cm^{-1} and at 545 cm^{-1} (the third of three lines with approximately this frequency). The torsion must therefore be assigned at 388 cm^{-1} in SO_2Cl_2. It is reasonable that no line of approximately this frequency is observed in the Raman spectrum of SO_2F_2, as it would probably not be resolved from the rather broad band at 388 cm^{-1}, which has been assigned as the SF_2 rocking mode. Hunt and Wilson (2) have indeed assigned this vibration at a frequency of 360 cm^{-1} in sulphuryl fluoride on the ground of the observation of a line at 720 cm^{-1} in the infrared, which they interpret as the first overtone of 360 cm^{-1}. This leaves a line at approximately 545 cm^{-1} in SO_2F_2 and the line at 580 cm^{-1} in SO_2Cl_2 to be attributed to the SO_2 rock in these molecules.

Hunt and Wilson (2) have assigned a frequency of 274 cm^{-1}, which they observed in the infrared spectrum of SO_2F_2, to the SF_2 bending mode by comparison with a frequency of 235 cm^{-1} in the spectrum of sulphur tetrafluoride, which has been assigned as an SF bending mode (9). It seems to us more probable that this low frequency of 235 cm^{-1} in the Raman spectrum of liquid SF_4 is due to some polymeric species formed by fluorine bridging between SF_4 molecules in the same way that antimony pentafluoride is associated by fluorine-bridge bonds (28). The line at 274 cm^{-1} reported by these authors is difficult to understand as its frequency seems to be too low for it to be due to any vibration of SO_2F_2. A possible explanation is that it is due to either SO_2Br_2 or SO_2FBr formed by attack on the bromide windows of the cell and, indeed, a frequency of 270 cm^{-1} has been observed in the spectrum of SO_2FBr (29). All the overtone bands that have been observed in the infrared spectra of SO_2F_2, SO_2Cl_2, $SOCl_2$, and SOF_2 can be satisfactorily accounted for as allowed combinations of the fundamentals, as shown in Tables I–IV.

Sulphuryl Bromofluoride

The infrared spectrum of sulphuryl bromofluoride, SO_2BrF, has been reported by Crow and Lagemann (29), who have given an assignment of the observed frequencies in terms of characteristic vibrations of the SO_2 and SFBr groups. We prefer, however, to treat the vibrations of the S—F and S—Br bonds separately and to describe the nine fundamental vibrations as an SO_2 symmetric and asymmetric stretch, an SO_2 bend and an SO_2 rock, an SF stretch and an SF wag, an SBr stretch and an SBr wag, and a torsion. On this basis we have been able to assign frequencies to all except one of the fundamental vibrations in a manner which is quite consistent with the assignments which have been proposed above for SO_2Cl_2 and SO_2F_2, as shown in Table VI. The justification for the majority of these assignments is obvious from the data given in this table. The frequency of the S—Br stretch would be expected to fall in the range 250–320 cm^{-1} from the following data for the P—Hal symmetric stretches: POF_3, 873 cm^{-1}; $POCl_3$, 486 cm^{-1}; $POBr_3$, 340 cm^{-1} (30, 31); and for the S—Hal stretches: SO_2F_2, 848 cm^{-1}; SO_2Cl_2, 405 cm^{-1}. Therefore, one of the frequencies 320 cm^{-1} or 270 cm^{-1} must be assigned to this vibration. The S—F wag might be expected to have a frequency somewhere near that of the S=O wag in SOF_2 (326 cm^{-1}), since the SF_2 bend and the SO_2 bend in SO_2F_2 have similar frequencies of approximately 545 cm^{-1}. Thus it seems reasonable to assign 320 cm^{-1} to this vibration, which leaves 270 cm^{-1} as the S—Br stretch. The S—Br wag would be expected to have a very low frequency, certainly lower than the S—Br stretch. P—Br bending modes have been assigned frequencies of 162 and 173 cm^{-1} in PBr_3 (32) and 173 cm^{-1} in $POBr_3$ (31), for which the stretching modes have been assigned at 380 and 340 cm^{-1}, respectively. We conclude therefore that the S—Br wag has a frequency less than 200 cm^{-1} and has not been observed. A detailed examination of the infrared spectrum leads to the conclusion that the infrared band at 353 cm^{-1} is best interpreted as the first overtone of the S—Br wag so that a frequency of 176 cm^{-1} can be assigned to this vibration. This assignment enables certain other overtone bands in the infrared to be assigned in a satisfactory manner (Table V). The remaining frequency of 461 cm^{-1} is assigned to the torsion. The complete infrared spectrum of SO_2BrF can be satisfactorily accounted for on the basis of the present assignment of the fundamental vibrations (Table V).

EXPERIMENTAL

Sulphuryl chloride was purified by double distillation of the commercial product, which had been dried over phosphoric oxide. The fraction boiling at 69° was collected. The Raman apparatus and the method used for obtaining depolarization factors are described in the following paper (1).

ACKNOWLEDGMENTS

The National Research Council and the Ontario Research Foundation are thanked for financial assistance.

REFERENCES

1. R. J. GILLESPIE and E. A. ROBINSON. Can. J. Chem. This issue. p. 2179.
2. E. R. HUNT and M. K. WILSON. Spectrochim. Acta, **16**, 570 (1960).
3. H. STAMMREICH, K. KAWAI, and Y. TAVARES. Spectrochim. Acta, **15**, 438 (1959).
4. H. SIEBERT. Z. anorg. Chem. **275**, 210 (1954).
5. D. M. YOST. Proc. Indian Acad. Sci. **8**, 333 (1938).
6. D. N. READ. Phys. Rev. **46**, 571 (1934).
7. L. J. BELLAMY. The Infra-red Spectra of Complex Molecules. 2nd ed. Methuen, London. 1958. p. 350.
8. R. T. LAGEMANN and E. A. JONES. J. Phys. Chem. **19**, 534 (1951).
9. R. E. DODD, L. A. WOODWARD, and H. L. ROBERTS. Trans. Faraday Soc. **52**, 1052 (1956).

10. F. B. DUDLEY, G. H. CADY, and D. F. EGGERS. J. Am. Chem. Soc. **78**, 290 (1956).
11. F. B. DUDLEY and G. H. CADY. J. Am. Chem. Soc. **79**, 513 (1957).
12. H. STAMMREICH, R. FORNERIS, and K. SORET. J. Chem. Phys. **23**, 972 (1955).
13. Y. MORINO and S. MIZUSHIMA. Sci. Papers Inst. Phys. Chem. Research (Tokyo), **32**, 220 (1937).
14. F. B. DUDLEY, G. H. CADY, and D. F. EGGERS. J. Am. Chem. Soc. **78**, 1553 (1956).
15. H. S. GUTOWSKY and A. D. LIEHR. J. Chem. Phys. **20**, 1653 (1952).
16. J. A. ROLFE and L. A. WOODWARD. Trans. Faraday Soc. **51**, 778 (1955).
17. H. GERDING, P. SMITS, and R. WESTRICK. Rec. trav. chim. **61**, 513 (1941).
18. D. E. MARTZ and R. T. LAGEMANN. J. Chem. Phys. **22**, 1193 (1954).
19. R. VOGEL-HÖGLER. Acta. Phys. Austriaca, **1**, 323 (1948).
20. J. K. O'LOANE and M. K. WILSON. J. Chem. Phys. **23**, 1313 (1955).
21. P. BENDER and J. M. WOOD. J. Chem. Phys. **23**, 1313 (1955).
22. E. A. ROBINSON. Can. J. Chem. **39**, 247 (1961).
23. L. J. BELLAMY and R. J. WILLIAMS. J. Chem. Soc. 863 (1957).
24. H. GERDING and W. J. NIJVOLD. Nature, **137**, 1070 (1936).
25. R. N. HASZELDINE and J. M. KIDD. J. Chem. Soc. 2901 (1955).
26. N. S. HAM and A. N. HAMBLY. Australian J. Chem. **6**, 33 (1953).
27. A. BRAUNE and G. ENGELBRECHT. Z. physik. Chem. (Leipzig), B, **19**, 303 (1932).
28. C. J. HOFFMAN, B. E. HOLDER, and W. L. JOLLY. J. Phys. Chem. **62**, 364 (1958).
29. T. T. CROW and R. T. LAGEMANN. Spectrochim Acta, **12**, 143 (1958).
30. M. L. DEWAULLE and M. F. FRANCOIS. Compt. rend. **226**, 894 (1948).
31. M. L. DEWAULLE and M. F. FRANCOIS. Compt. rend. **220**, 817 (1945).
32. M. L. DEWAULLE. Compt. rend. **222**, 1391 (1946).
33. K. C. SCHREIBER. Anal. Chem. **21**, 1168 (1949).
34. C. A. MCDOWELL. Trans. Faraday Soc. **49**, 371 (1953).

THE RAMAN SPECTRA OF SOME POLYSULPHURYL CHLORIDES AND FLUORIDES[1]

R. J. GILLESPIE AND E. A. ROBINSON[2]

ABSTRACT

The Raman spectrum of disulphuryl chloride, $S_2O_5Cl_2$, has been reinvestigated and the Raman spectra of $S_2O_5F_2$, S_2O_5ClF, $S_3O_8Cl_2$, $S_3O_8F_2$, and the new compound S_3O_8ClF are reported for the first time. The vibrational spectra of these polysulphuryl halides are interpreted in terms of characteristic group frequencies by comparison with the vibrational spectra of simple sulphuryl compounds. The spectra are consistent with acyclic structures for the polysulphuryl halides.

The Raman spectrum of disulphuryl chloride, $S_2O_5Cl_2$, has been investigated previously by Gerding and Linden (1), and the infrared spectrum of disulphuryl fluoride, $S_2O_5F_2$, has been obtained over a limited frequency range (2). We have measured the Raman spectra of both of these compounds and also of disulphuryl chlorofluoride, S_2O_5ClF; trisulphuryl chloride, $S_3O_8Cl_2$; trisulphuryl fluoride, $S_3O_8F_2$; and the new compound trisulphuryl chlorofluoride, S_3O_8ClF. The spectra are given in Tables I, II, and III and Fig. 1.

It has generally been assumed that these substances have the acyclic configurations I and II, although no direct experimental evidence for these structures has been obtained. The fluorine n.m.r. spectrum of $S_2O_5F_2$ has been found to consist of a single line (3), and in the present work we have found that the n.m.r. spectrum of $S_3O_8F_2$ also consists of

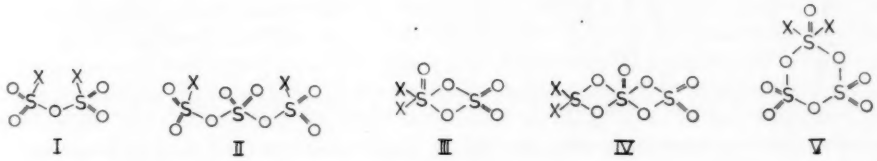

I II III IV V

a single line, showing that the fluorine atoms are structurally equivalent; this is consistent with structures I and II. Other formally possible formulations such as III, IV, and V contain improbable four-membered rings and five-co-ordinated sulphur. It has been shown, moreover, that $S_2O_5Cl_2$ is not just a molecular "addition compound" of SO_2Cl_2 and SO_3 since it is not formed in mixtures of these substances at room temperature or on being refluxed at 60°. Similarly $S_3O_8F_2$ is not formed from $S_2O_5F_2$ and SO_3 (4). Hydrolysis of $S_2O_5Cl_2$ and $S_2O_5F_2$ gives 2 moles of the corresponding halogenosulphuric acid and not sulphuric acid and the sulphuryl halide, as would be expected for structure III. Thus the acyclic structures I and II seem very probable, and it is shown in this paper that the Raman spectra are also consistent with these structures.

[1]*Manuscript received May 15, 1961.*
Contribution from the Department of Chemistry, McMaster University, Hamilton, Ontario. Presented in part at the 43rd Annual Conference of the Chemical Institute of Canada, Ottawa, Ontario, June 13–15, 1960.
[2]*Present address: Department of Chemistry, University of Toronto, Toronto, Ontario.*

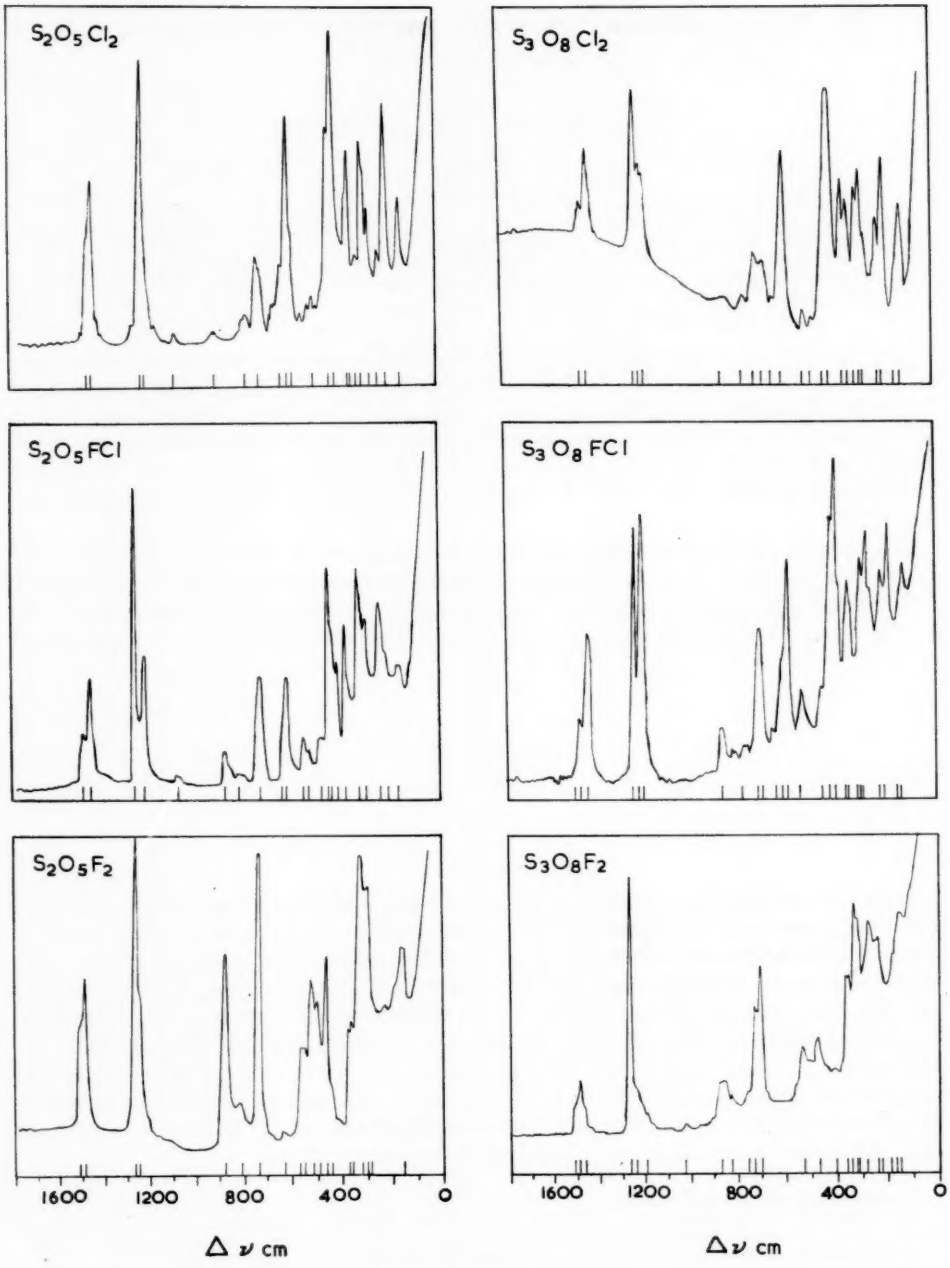

FIG. 1. Raman spectra.

DISULPHURYL HALIDES

If the disulphuryl halides have the acyclic structure I they should have 21 normal modes of vibration. Gerding and Linden (1) assumed that $S_2O_5Cl_2$ had the conformation VI and C_{2v} symmetry. In this case all 21 normal modes are active in the Raman effect

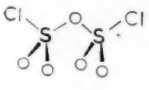

VI

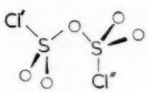

VII

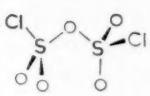

VIII

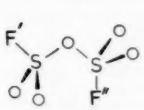

IX

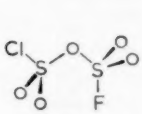

X

and 7 of the Raman lines should be polarized. It seems more likely, however, that the molecule will have a staggered conformation, either VII, in which the halogen atoms are trans to each other (C_s symmetry), or VIII, in which the halogen atoms are in the "*gauche*" position and which has no symmetry elements. For VII, 13 of the 21 Raman lines should be polarized. We find at least nine of the Raman lines of $S_2O_5Cl_2$ to be polarized, which supports a staggered configuration such as VII or VIII rather than the cis conformation VI. Similarly $S_2O_5F_2$ and S_2O_5ClF would be expected to have the conformations IX and X respectively.

It is convenient to describe the normal modes of vibration in terms of the group frequencies that have been used previously for the simple sulphuryl compounds (5). This description can only be a rather crude approximation, but, as we shall show, it does enable a very reasonable assignment to be made for the majority of the Raman shifts of the polysulphuryl halides.

Seven vibrations may be ascribed to the SO_2X group: SO_2 symmetric and asymmetric stretches, an SO_2 bend, an SO_2 rock, an S—X stretch, an S—X wag, and a torsion. Each of these gives rise to two lines in the spectrum. These may be regarded as arising from coupling between the two halves of the molecule, and they may be conveniently described as in-phase and out-of-phase motions of the two SO_2X groups. In the staggered conformations VII and VIII the two SO_2X groups are not equivalent to each other, so slightly different frequencies for each group would be expected even if there were no coupling between them. In addition, the SO_2 rocking vibrations and the S—X wags can each occur parallel to, or perpendicular to, the plane containing the SOS group. Finally, three vibrations may be assigned to the SOS bridging group: a symmetric stretch, an asymmetric stretch, and a bend.

Frequencies can be readily assigned to the SO_2 stretches, the SO_2 bends, and the SF and SCl stretching modes, as shown in Tables I and II, by comparison with the frequencies observed for these vibrations in the simple sulphuryl halides (5). The SO_2 stretching frequencies are consistent with the linear relationship that has been shown to hold between the frequencies of the symmetric and asymmetric SO_2 stretches (6). The mean SO_2 symmetric and asymmetric frequencies in $S_2O_5F_2$ are both slightly lower than the corresponding frequencies in SO_2F_2, which is consistent with the replacement of fluorine by the slightly less electronegative SO_3F group. On the other hand, in $S_2O_5Cl_2$ these frequencies are both slightly higher than the corresponding frequencies in SO_2Cl_2; this is consistent with the replacement of chlorine by the more electronegative SO_3Cl group (6). In S_2O_5ClF, one of the SO_2 symmetric stretches, one of the asymmetric

TABLE I

Raman spectra of $S_2O_5Cl_2$

Present work			Gerding and Linden (1)		
Frequencies (cm^{-1})	Assignment	Species (C_s symmetry)	Frequencies (cm^{-1})	Assignment	Species (C_2 symmetry)
147 p	SOS bend	a'	143 p	SCl wag	a_1
200	SCl wag	a''	202	SCl wag	a_2, b_2
235	SCl wag	a'	234	SCl wag	
273	Torsion	a''	264 p	SCl wag	b_1
298 p	SOS stretch, s	a'	293	Torsion	a_2, b_2
326	SCl wag				
353 p	SCl wag	a'	350	SO_2 rock	a_2, b_2
370	Torsion	a''			
412 p	SCl stretch, i	a'	412 p	SCl stretch	a_1
427 p	SCl stretch, o	a'	434	SCl stretch	b_1
490	SO_2 rock, $\parallel$, i	a'	486 p	SOS bend	a_1
560	SO_2 rock, $\perp$, i	a''	545 p	SO_2 rock	a_1, b_1
593 p	SO_2 bend, i	a'	592 p	SO_2 bend	a_1, b_1
607 p	SO_2 bend, o	a'			
621	SO_2 rock, $\perp$, o	a''			
716	SO_2 rock, $\parallel$, o	a'	716 p	SOS stretch, s	a_1
760	SOS stretch, a	a''	773	SOS stretch, a	b_1
(885)	?				
(1090)	?				
1189	SO_2 stretch, s, o	a'			
1209 p	SO_2 stretch, s, i	a'	1221 p	SO_2 stretch, s	a_1
1442	SO_2 stretch, a, o	a''	1446	SO_2 stretch, a	a_1, b_2
1462	SO_2 stretch, a, i	a''			

NOTE: p, polarized line; s, symmetric vibration; a, asymmetric vibration; i, in-phase vibration; o, out-of-phase vibration; $\parallel$, parallel to SOS plane; $\perp$, perpendicular to SOS plane. Frequencies in parentheses indicate extremely weak lines.

TABLE II

Raman spectra of $S_2O_5F_2$ and S_2O_5ClF

$S_2O_5F_2$			S_2O_5ClF	
Frequencies (cm^{-1})				
Raman	I.R. (2)	Assignment	Frequencies (cm^{-1})	Assignment
157 p		SOS bend	154 p	SOS bend
290		Torsion	204	SCl wag
301		SF wag	231	SCl wag
323 p		SOS stretch, s	284	Torsion
350		SF wag	313 p	SOS stretch, s
366		Torsion	360	Torsion
435		SF wag	397 p	SF wag
455 p		SF wag	419	SF wag
487		SO_2 rock, $\parallel$, i	432 p	SCl stretch
518 p		SO_2 bend, i	458	SO_2 rock, $\parallel$, i
540		SO_2 bend, o	515	SO_2 bend
560		SO_2 rock, $\perp$, i	535	SO_2 rock, $\perp$, i
630		SO_2 rock, $\perp$, o	602 p	SO_2 bend
733 p	735	SO_2 rock, $\parallel$, o	616	SO_2 rock, $\perp$, o
814	824	SOS stretch, a	715	SO_2 rock, $\parallel$, o
872 p	872	SF stretch	802	SOS stretch, a
1249 p	1248	SO_2 stretch, s, o	860 p	SF stretch
1264 p		SO_2 stretch, s, i	(1068)	?
1490		SO_2 stretch, a, i	1205 p	SO_2 stretch, s, o
1511	1513	SO_2 stretch, a, i	1248 p	SO_2 stretch, s, i
			1453	SO_2 stretch, a, o
			1487	SO_2 stretch, a, i

NOTE: p, polarized line; s, symmetrical vibration; a, asymmetric vibration; i, in-phase vibration; o, out-of-phase vibration; $\parallel$, parallel to SOS plane; $\perp$, perpendicular to SOS plane. Frequencies in parentheses indicate extremely weak lines.

stretches, and one of the SO_2 bends have frequencies close to those in $S_2O_5F_2$, while the other frequencies for these vibrations are close to those in $S_2O_5Cl_2$.

SOS Skeletal Vibrations

An important feature of the spectra of $S_2O_5F_2$, S_2O_5ClF, and $S_2O_5Cl_2$ is the occurrence of rather broad, moderately strong, polarized lines at 157, 154, and 147 cm^{-1}, respectively. No lines at such a low frequency are observed in the spectra of the simple sulphuryl halides and they can therefore only be reasonably attributed to an SOS skeletal vibration; since the SOS bending mode would be expected to have the lowest frequency of the three skeletal vibrations, they are assigned to this vibration. The similar frequencies of this vibration in the three molecules suggest that the corresponding SOS symmetric stretches might also have rather similar frequencies. An examination of the frequency of the symmetric stretch in a number of simple nonlinear triatomic molecules shows that this is generally approximately twice that of the bend (7). Thus the relatively strong polarized lines at 323, 313, and 298 cm^{-1}, are assigned as the SOS symmetric stretch in $S_2O_5F_2$, S_2O_5ClF, and $S_2O_5Cl_2$, respectively. The asymmetric SOS stretch is more difficult to assign. It is expected to have a considerably higher frequency than the symmetric stretch since it is largely the vibration of an oxygen atom between the two relatively heavy SO_2X groups. A weak depolarized line, which cannot be attributed to any of the group vibrations which are observed in the simple sulphuryl halides, occurs in all three spectra at approximately 800 cm^{-1}. Therefore the lines at 814, 802, and 760 cm^{-1} in the spectra of $S_2O_5F_2$, S_2O_5ClF, and $S_2O_5Cl_2$, respectively, are assigned to the asymmetric SOS stretch.

Our assignment for these skeletal vibrations is consistent with the assignment recently given by Kriegsmann (8) for the Si—O—Si vibrations in some siloxanes. For example, for hexamethyldisiloxane he gives the Si—O—Si bend at 180 cm^{-1}, the symmetric Si—O—Si stretch at 519 cm^{-1}, and the asymmetric stretch at 1055 cm^{-1}.

SO_2 Rocking Modes

The SO_2 rock has been assigned frequencies of 580 and 545 cm^{-1} in SO_2Cl_2 and SO_2F_2 respectively (5). It is apparent from a model that for structure VII there is considerable interaction between one SO_2 group and the halogen atom on the other sulphur atom. This would be expected to lead to a considerable difference in the frequencies of the two SO_2 parallel rocking modes. The out-of-phase mode, in which the two SO_2 groups move towards each other, would be expected to have the higher frequency. A rather strong, polarized line is observed at 733, 715, and 716 cm^{-1} in the spectra of $S_2O_5F_2$, S_2O_5ClF, and $S_2O_5Cl_2$, respectively, and this is assigned to the out-of-phase SO_2 parallel rock. In the spectrum of $S_2O_5Cl_2$ there are three lines between 716 cm^{-1} and the lines due to the S—Cl stretching modes at 427 and 412 cm^{-1}. These lines, at 621, 560, and 490 cm^{-1}, are tentatively assigned to the three remaining SO_2 rocking modes, possibly the perpendicular out-of-phase, the perpendicular in-phase, and the parallel in-phase, respectively. Similarly in $S_2O_5F_2$ and in S_2O_5ClF these vibrations are assigned frequencies of 630, 560, and 487 cm^{-1} and of 616, 535, and 458 cm^{-1} respectively.

SX Wagging Modes

The SCl wag has been assigned a frequency of 200 cm^{-1} in chlorosulphuric acid and 220 cm^{-1} in the chlorosulphate ion (9), and it is a rather similar vibration to the SCl_2 bend, which is at 218 cm^{-1} in SO_2Cl_2 and 194 cm^{-1} in $SOCl_2$. Therefore the pair of frequencies at 200 and 235 cm^{-1} in the spectrum of $S_2O_5Cl_2$ can be reasonably assigned as the SCl′ wags. The higher frequencies of 326 and 353 cm^{-1} are assigned to the SCl″ wags,

as the motions of the Cl″ atom are restricted by the proximity of the SO_2 group to which it is not directly bonded. This assignment receives some confirmation from the fact that lines at 204 and 231 cm^{-1}, which must also presumably be assigned as SCl wags, are found in the spectrum of S_2O_5ClF.

In SO_2FBr and CH_3SO_2F the SF wag has been assigned frequencies of 320 and 326 cm^{-1} respectively (5, 10); thus the two lines at 301 and 350 cm^{-1} in the spectrum of $S_2O_5F_2$ may be reasonably assigned as SF′ wagging modes and the pair of lines at 435 and 455 cm^{-1}, which are analogous to the pair at 326 and 353 cm^{-1} in the spectrum of $S_2O_5Cl_2$, are assigned to the SF″ wagging modes. The conformation of S_2O_5ClF is expected to be X in which the chlorine atom resembles the Cl′ in $S_2O_5Cl_2$ and the F atom resembles the F″ in $S_2O_5F_2$. Thus the S—Cl wags should correspond to the low-frequency pair in $S_2O_5Cl_2$ and the SF wags should correspond to the high-frequency pair in $S_2O_5F_2$. The latter may therefore be assigned to the pair of lines at 397 and 419 cm^{-1}.

Torsional Modes

In sulphuryl chloride and sulphuryl fluoride the torsional mode has a frequency of approximately 360 cm^{-1} (5). It seems reasonable, therefore, to attribute the as-yet-unassigned lines at 366 cm^{-1} for $S_2O_5F_2$, 370 cm^{-1} for $S_2O_5Cl_2$, and 360 cm^{-1} for S_2O_5ClF to one of the torsional modes in these molecules.

There is another moderately strong line, as yet unassigned, which occurs at a very similar frequency for each of the species, i.e. $S_2O_5F_2$, 290 cm^{-1}; S_2O_5ClF, 284 cm^{-1}; $S_2O_5Cl_2$, 273 cm^{-1}, in the spectrum of each of the disulphuryl halides. This line we also assign to a torsion on the grounds that the frequency is relatively independent of the nature of the halogen atoms involved, as is the case for the torsional modes in SO_2Cl_2 and SO_2F_2.

Although a number of the assignments made above are somewhat tentative, it is clear that others are quite certain, e.g. the SO_2 and S(Hal) stretching modes, and the SOS bend and symmetric stretch, which are characteristic of the disulphuryl group. The strong polarized line at approximately 700 cm^{-1}, which is very probably the SO_2 parallel rocking vibration, and the vibration in the region of 270 to 290 cm^{-1}, which we have assigned as a torsion, also appear to be diagnostic of the disulphuryl group. Use is made of these assignments in identifying disulphuryl compounds in other systems, e.g. disulphuric acid and fluoro- and chloro-disulphuric acids, as will be discussed in following papers.

A number of rather weak or ill-defined shoulders on various peaks in the spectra have not been assigned. It seems probable that at least some of these may be due to conformational isomers arising from hindered rotation around the 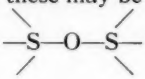 bonds.

Comparison with Previous Work

A number of our assignments for $S_2O_5Cl_2$ differ from those given previously by Gerding and Linden (1). For example, these authors assign the polarized line at 147 cm^{-1} as an S—Cl wag whereas we have assigned it as the SOS bend. The earlier assignment is not consistent with the fact that an obviously similar line is found at 157 cm^{-1} in the spectrum of $S_2O_5F_2$ since S—F wags are expected, and are generally found, to have appreciably higher frequencies than the corresponding S—Cl vibrations. Gerding and Linden assign to the SOS bend a frequency of 486 cm^{-1}: this is presumably the line we find at 490 cm^{-1}, which does not appear to be polarized and which we have assigned as an SO_2 rock. These authors assign to the SOS symmetric stretch the frequency of 716 cm^{-1}, which seems very

high in view of the total mass of the atoms attached to each sulphur atom, and which is, moreover, not consistent with our assignment for the SOS bend. For both of these reasons our assignment of the polarized line at 298 cm^{-1} to the SOS symmetric stretch seems more reasonable.

TRISULPHURYL HALIDES

The trisulphuryl halides presumably have one of several possible staggered conformations with C_s symmetry such as II. They have 33 normal modes of vibration, all of which should be active in the Raman effect. In terms of the description we have used for the disulphuryl halides there will be three symmetric and three asymmetric SO_2 stretching modes, three parallel and three perpendicular SO_2 rocking modes, three SO_2 bending

TABLE III

Raman spectra of $S_3O_8Cl_2$, $S_3O_8F_2$, and S_3O_8ClF

Frequency (cm^{-1})	Assignment	Frequency (cm^{-1})	Assignment
$S_3O_8Cl_2$			
136 p	Skeletal bends	512	SO_2 rock
169 p		595 p	SO_2 bend
200	SCl wag	650	SO_2 rock
226	SCl wag	686	SO_2 rock
275	Torsion	723 p	SO_2 rock
291	Skeletal stretches	770	Skeletal stretches
308		870	
342	SCl wag or torsion	1193	SO_2 stretches, s
362	Torsion	1208	
415 p	SCl stretch	1220	
440	SCl stretch	1450	SO_2 stretches, a
485	SO_2 rock	1480	
$S_3O_8F_2$			
145 p	Skeletal bends	699 p	SO_2 rock
165		724 p	SO_2 rock
195		761	Skeletal stretches
226		835	
245		876 p	SF stretch
288	Torsion	(1029)	
318	Skeletal stretches	1198	SO_2 stretches, s
324		1198	
350	SF wag and torsion	1241 p	
359		1268	
403	SF wag	1468	SO_2 stretches, a
468	SF wag	1490	
528	SO_2 bend	1515	
S_3O_8ClF			
150 p	Skeletal bends	580	SO_2 bend
158 p		598 p	SO_2 bend
204	SCl wag	620	SO_2 rock
235	SCl wag	658	SO_2 rock
274	Skeletal bend	700	SO_2 rock
290	Torsion	715 p	SO_2 rock
301	Skeletal stretches	778	Skeletal stretch
318		865 p	SF stretch and skeletal stretch
353	Torsion and/or SF wag	1210 p	SO_2 stretches, s
366		1222 p	
398	SF wag	1257 p	
418 p	SCl stretch	1453	SO_2 stretches, a
435	SCl stretch	1462	
468	SO_2 rock	1499	
549	SO_2 bend		

modes, and three torsions. In addition there will be two SX stretches and four SX wags for $S_2O_5X_2$ molecules, or an SX stretch, an SY stretch, two SX wags, and two SY wags for S_3O_8XY molecules, and nine skeletal, or SOSOS, vibrations.

By comparing the spectra of the trisulphuryl halides with each other and with the spectra of the disulphuryl halides it was possible to make reasonable assignments for all the observed lines, as shown in Table III. There are several features that distinguish the spectra of trisulphuryl compounds from those of disulphuryl compounds. An important characteristic of the spectra of the trisulphuryl halides is the occurrence of two high-frequency SO_2 rocks in the region of 700 cm^{-1}, as compared to the occurrence of a single line in this region in the spectra of disulphuryl compounds. A similar "splitting" of a frequency in this region of the spectra has been previously claimed as diagnostic of the change in structure in going from a diphosphate to a triphosphate (11). In the infrared spectra of diphosphates an absorption band near 730 cm^{-1} is replaced by two bands near 680 and 730 cm^{-1} in triphosphates. Another distinct difference between the spectra of disulphuryl and trisulphuryl compounds is that the symmetric stretch near 300 cm^{-1} in disulphuryl compounds is replaced by two skeletal stretches in the same region of the spectrum in trisulphuryl compounds and that the SOS asymmetric stretch, which occurs near 800 cm^{-1} in the spectrum of disulphuryl halides, is replaced by two skeletal stretches of similar frequencies in trisulphuryl compounds.

In addition to the four stretching modes the SOSOS skeleton also has five bending modes. These are thought to give rise to the low-frequency lines at 145, 165, 195, 226, and 241 cm^{-1} in the spectrum of $S_3O_8F_2$. Fewer than five lines that can be attributed to these bending modes are observed in the spectra of $S_3O_8Cl_2$ and S_3O_8ClF; this is probably because they coincide with the very strong lines due to the SCl wags which also occur in this region of the spectrum.

EXPERIMENTAL

Disulphuryl Fluoride

This compound was prepared by the reaction between antimony pentafluoride and liquid sulphur trioxide, according to the method of Hayek and Koller (12). The components were heated under gentle reflux for 2 hours and the resulting $S_2O_5F_2$ was distilled off. The product was washed with 100% sulphuric acid to remove sulphur trioxide and redistilled, b.p. 51–52°.

Disulphuryl Chloride

This compound was made by the reaction of 2 moles of sulphur trioxide and 1 mole of carbon tetrachloride at 40 to 45° for several hours. The mixture was then distilled and the fraction boiling above 140° collected. It was washed with 100% sulphuric acid and redistilled. The fraction boiling at 151 to 153° at atmospheric pressure was collected. Redetermination of the boiling point gave 152°.

Disulphuryl Chlorofluoride

This compound was prepared by fluorinating $S_2O_5Cl_2$ with AgF_2. Contrary to a previous report (13) this was found to be a satisfactory method. Disulphuryl chloride was added slowly from a dropping funnel to AgF_2 in a flask equipped with a reflux condenser. Two moles of $S_2O_5Cl_2$ were used per mole of AgF_2. After the vigorous reaction had subsided the product was distilled and the fraction boiling above 95° collected. Redistillation through an efficient column gave a fraction of b.p. 100–101°. The material had a fluorine n.m.r. spectrum consisting of a single peak. The % F was determined by comparing the

areas of the fluorine n.m.r. peaks in a mixture of the compound with $S_2O_5F_2$ (found, 9.5%; calculated for S_2O_5ClF, 9.57%).

Trisulphuryl Fluoride

This compound was prepared by the method of Lehmann and Kolditz (14) by bubbling BF_3 gas through liquid sulphur trioxide until a dense, solid white mass resulted. Sulphuric acid, previously cooled in ice, was then added to the mixture, and two liquid layers were obtained, a lower layer of sulphuric acid and an upper layer containing $S_3O_8F_2$. (It made little difference whether the decomposition was carried out with 70% sulphuric acid, as recommended by Lehmann, or with 100% acid.) The trisulphuryl fluoride layer was separated and washed several times with sulphuric acid to remove sulphur trioxide. It was then washed with water and dried over phosphoric oxide. The fraction of b.p. 29–31° at a pressure of 2 to 4 mm Hg was collected. Redetermination of the boiling point at atmospheric pressure gave a value of 121.5° (Lehmann and Kolditz reported a value of 120°), but slow decomposition takes place under these conditions. The material had a fluorine n.m.r. spectrum consisting of a single peak. The % F was determined by comparing the areas of the two fluorine n.m.r. peaks in a mixture of the compound with $S_2O_5F_2$ (found, 15.0%; calculated for $S_3O_8F_2$, 14.87%).

Trisulphuryl Chloride

This compound was prepared by the method of Lehmann and Ladwig (15) by heating 4 moles of sulphur trioxide and 1 mole of carbon tetrachloride under reflux for 4 hours during which time the temperature was raised to 85°:

$$CCl_4 + 3SO_3 = S_3O_8Cl_2 + COCl_2.$$

The mixture was distilled under reduced pressure and gave $S_3O_8Cl_2$, b.p. 55–65° at 2 to 3 mm Hg pressure, and a small amount of $S_2O_5Cl_2$. The product was washed with sulphuric acid and redistilled. The fraction b.p. 60–65° at 2.5 to 3 mm Hg was collected.

Trisulphuryl Chlorofluoride

This compound was prepared by fluorination of $S_3O_8Cl_2$ with AgF_2, using 2 moles of $S_3O_8Cl_2$ to 1 mole of AgF_2. In contrast to the violent reaction of $S_2O_5Cl_2$ with AgF_2 the reaction was slow, as indicated by the conversion of the fluoride to silver chloride, and it was necessary to heat the reaction mixture to 100° for 12 hours. The product was separated from silver chloride and distilled under reduced pressure. Redistillation at 15 to 20 mm of Hg pressure gave S_3O_8ClF, b.p. 40–45°. At atmospheric pressure the substance boils with decomposition at approximately 145°. The material had a fluorine n.m.r. spectrum consisting of a single peak. The % F was determined by comparing the areas of the two fluorine n.m.r. peaks in a mixture of the compound with $S_3O_8F_2$ (found, 6.8%; calculated for 6.82%).

Apparatus

The apparatus consisted of a Hilger E612 Raman spectrometer with glass prisms, used in conjunction with a water-cooled mercury-arc lamp. After the spiral of the lamp had been preheated with infrared lamps, and the mercury pool electrodes with nichrome heaters, the arc was easily struck by using the discharge from a "tesla" coil. The power supply was 250 volts d-c. and an operating current of 12 amp was used.

Liquid samples from 5 to 40 ml were contained in Pyrex glass cells mounted vertically and surrounded by a jacket containing saturated sodium nitrite solution as an optical filter. The filter solution was cooled and circulated through the jacket.

A prism was used to reflect the Raman radiation through 90° and a two-lens system ensured that most of the light scattered from the sample was collected. Spectra were recorded on Kodak 103*a*O, 2*a*O, or 3*a*O spectroscopic plates and the positions of the lines were measured by means of a Leeds and Northrup microphotometer, using an iron arc for calibration. Raman shifts could be measured to ± 3 cm^{-1} directly from the chart paper. When a qualitative comparison of the intensities of lines from different samples was required the spectra were compared on the same photographic plate. When fast plates (103*a*O or 2*a*O) were used, exposures of a few minutes gave excellent spectra with little background and tolerable broadening of the 4358 Å exciting line, so that Raman shifts as small as 150 cm^{-1} were easily resolved from the exciting line.

Polarization measurements were carried out using polaroid cylinders polarized parallel to and perpendicular to the plane of the incident light. A system of baffles was used to ensure that the incident light was perpendicular to the plane of the polaroid, which was situated inside the filter jacket surrounding the sample tube. Such polarization measurements are only qualitative.

CONCLUSIONS

Our Raman spectra provide strong support for the acyclic structures I and II for the di- and tri-sulphuryl halides.

The general consistency of the assignments of group vibrational frequencies for all the molecules we have discussed show that our approximate description of the normal modes is useful for at least some of the vibrations, and that characteristic spectral features due to —SO_2—, —S_2O_5—, and S_3O_8— groups can be recognized. Use is made of these conclusions in following papers to obtain structural information on some related compounds.

The close similarities between the spectra of S_3O_8ClF and those of $S_3O_8F_2$ and $S_3O_8Cl_2$, and also the expected relationship to the spectrum of S_2O_5ClF, appear to adequately establish its structure; additional evidence will be presented in a following paper.

ACKNOWLEDGMENTS

Mr. A. W. Richardson and Mr. R. C. Dixon are thanked for the preparation of disulphuryl chlorofluoride and for help with the measurement of its Raman spectrum.

Our thanks are also due to Professor H. L. Welsh of the Department of Physics, University of Toronto, for assistance with the construction of the "Toronto" mercury-arc lamp.

The National Research Council, the Defence Research Board, and the Allied Chemical Company are thanked for financial assistance.

REFERENCES

1. H. Gerding and A. C. Linden. Rec. trav. chim. **61**, 735 (1942).
2. H. C. Clark and H. J. Emeleus. J. Chem. Soc. 190 (1958).
3. E. L. Muetterties and D. D. Coffman. J. Am. Chem. Soc. **80**, 5914 (1958).
4. R. J. Gillespie and E. A. Robinson. Can. J. Chem. This issue. p. 2189.
5. R. J. Gillespie and E. A. Robinson. Can. J. Chem. This issue. p. 2171.
6. E. A. Robinson. Can. J. Chem. **39**, 247 (1961).
7. G. Herzberg. Molecular spectra and molecular structure. Vol. 2. D. van Nostrand Inc., New York. 1945. p. 167.
8. H. Kriegsmann. Z. Electrochem. **61**, 1088 (1957); Z. anorg. Chem. **299**, 78 (1959).
9. R. J. Gillespie and E. A. Robinson. To be published.
10. N. S. Ham, A. N. Hambly, and R. H. Laby. Australian J. Chem. **4**, 443 (1960).
11. D. E. C. Corbridge and E. J. Lowe. J. Chem. Soc. 493 (1954).
12. E. Hayek and W. Koller. Monatsh. **82**, 942 (1951).
13. A. Engelbrecht. Z. anorg. Chem. **273**, 269 (1953).
14. H. A. Lehmann and L. Kolditz. Z. anorg. Chem. **272**, 76 (1953).
15. H. A. Lehmann and G. Ladwig. Z. anorg. Chem. **284**, 1 (1956).

THE RAMAN SPECTRA OF LIQUID SULPHUR TRIOXIDE AND SOLUTIONS OF SULPHUR TRIOXIDE IN INERT SOLVENTS[1]

R. J. GILLESPIE AND E. A. ROBINSON[2]

ABSTRACT

The Raman spectra of liquid sulphur trioxide and of sulphur trioxide dissolved in a number of "inert" solvents have been investigated. A detailed analysis of the spectrum of liquid sulphur trioxide supports the earlier suggestion of Gerding and Nijveld that the main polymeric species in liquid sulphur trioxide is the cyclic trimer. Frequencies are assigned for all the Raman active vibrations of the cyclic trimer. These assignments differ substantially from those given previously by Gerding and Nijveld.

The spectra of dilute solutions of sulphur trioxide in sulphur dioxide, sulphuryl chloride, carbon tetrachloride, tetrachlorethylene, and trichlorfluormethane (Freon 11) show that the sulphur trioxide is present mainly in the monomeric form at low concentrations while at higher concentrations a polymeric form, which is very probably the trimer, is also present.

The chemistry of sulphur trioxide is complex due to the ease with which it polymerizes. In the solid state, three principal forms are recognized: the γ or ice-like form, the β or low-melting asbestos form, and the α or high-melting asbestos form. Liquid sulphur trioxide is stable under anhydrous conditions but in the presence of a trace of water, high-molecular-weight polymers are formed and a solid phase separates. The structures of the solid forms and of liquid sulphur trioxide have been examined previously by Raman spectroscopy and by X-ray diffraction (1, p. 351; 2–9).

Only one strong line at 1069 cm^{-1} has been found in the Raman spectrum of sulphur trioxide gas at a pressure of 11 atm (2). Vapor pressure measurements have shown (5) that sulphur trioxide is monomeric in the gas phase, so this line can be assigned to the monomer. Other vibration frequencies for the monomer have been obtained from the spectra of mixtures of sulphur trioxide and sulphur dioxide at 60° (7, 8). The SO_3 molecule is planar (10) and therefore has four fundamental vibrations one of which is inactive in the Raman and one inactive in the infrared (Table I). The present measurements on

TABLE I

The vibrational frequencies of sulphur trioxide monomer

Assignment	cm^{-1}	
ν_1'	1069*	Forbidden in infrared
ν_2'	652	Forbidden in Raman
ν_3'	1390	
ν_4'	532	

*Sharp, strong, and diagnostic.

liquid sulphur trioxide and on solutions of sulphur trioxide dissolved in various solvents support these assignments. The Raman spectrum of sulphur trioxide monomer is therefore well established and the strong, sharp line at 1069 cm^{-1} is diagnostic of this species.

LIQUID SULPHUR TRIOXIDE

The most extensive previous study of the Raman spectrum of liquid sulphur trioxide is due to Gerding and Nijveld (9), who also summarized the earlier work of Bhavagantam

[1]*Manuscript received May 15, 1961.*
Contribution from the Department of Chemistry, McMaster University, Hamilton, Ontario.
[2]*Present address: Department of Chemistry, University of Toronto, Toronto, Ontario.*

(3) and Venkateswaren (4). Gerding and Nijveld found 17 Raman lines, 5 of which were definitely polarized, in addition to those of the monomer. In the present work, 25 Raman shifts were observed, 5 of which were found to be definitely polarized and 1 possibly weakly polarized (Table II and Figs. 1 and 2). Liquid sulphur trioxide, obtained by

TABLE II

The Raman spectrum of sulphur trioxide (frequencies in cm^{-1})

				Solid		
	Liquid		Gas	γ-SO_3	β-SO_3	α-SO_3
(*a*)	(*b*)	(*c*)	(*d*)	(*e*)	(*f*)	(*g*)
147	166(1)					
(243)*		255			254(1/2)	
290	290(6)	289		292(1)	286(0)	
322	319(1)	319			328(1)	327(1/2)
(337)						
368 p†	370(7) p	369 p		371(1d)		
407	408(1)	408			425(0)?	
480	483(1)	483			458(0)	
534	531(3)	531 p	530	525(0)		
560					566(0)	
(600)	597(1/2)	597				
657 p	650(2) p	651 p		662(1/2)	652(1)	650(1/2)
665 p	668(3) p	664				
698 p	699(3) p	697 p		698(1/2)		689(0)
(773)	775(0)	775				
844	840(1)	840				
860	866(1/2)	866				
(1018)						
1073 p	1068(5) p	1068 p	1069	1074(1/2)		1076(0+)
(1162)						
1231	1229(1)	1231				
1270 p	1271(6) p	1271 p		1273(2)	1258(1−)	1260(1/2)
1390	1390(1)	1390	1390			
1489	1490(2)	1487				
1515	1516(1) p?	1515				

NOTE: (*a*) This investigation at approximately 25°; (*b*) collected results from Hibben (2); (*c*) Gerding and Nijveld (9); (*d*) Gerding, Nijveld, and Muller (6); (*e*), (*f*), and (*g*) Gerding and Moerman (7).
*Frequencies in brackets are lines of very weak intensity.
†p indicates a polarized line.

distillation from 65% oleum, and "Sulfan B" (stabilized liquid sulphur trioxide) gave exactly the same Raman lines although the relative intensity of the monomer lines was slightly greater in the "Sulfan B" than in the freshly distilled material.

Sulphur trioxide can presumably polymerize to give either rings or long chains, e.g. structures I, II, III, and IV. The dimer I, which involves a four-membered ring, and other possible higher polymers involving the same ring are rather improbable because of the high degree of strain that would be present, particularly at the oxygen atoms. The corresponding dimetaphosphate ion V, for example, is not known (11). In the trimer II, tetramer III, similar larger cyclic polymers, and long chains such as IV, the configuration around sulphur is tetrahedral and the structures are expected to be non-planar. Gerding and Nijveld (9) have calculated the number of fundamental vibrations of both the planar and the more probable non-planar forms of the dimer, trimer, and tetramer (Table III). Although their evidence was by no means conclusive these authors suggested that liquid sulphur trioxide consists mainly of a mixture of the cyclic trimer II and the monomer. When the temperature is raised extensive depolymerization apparently takes

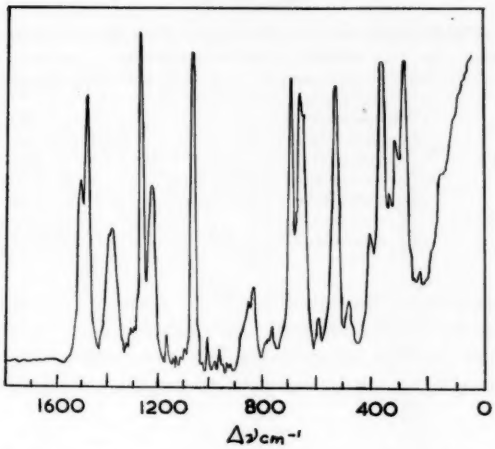

FIG. 1. The Raman spectrum of liquid sulphur trioxide.

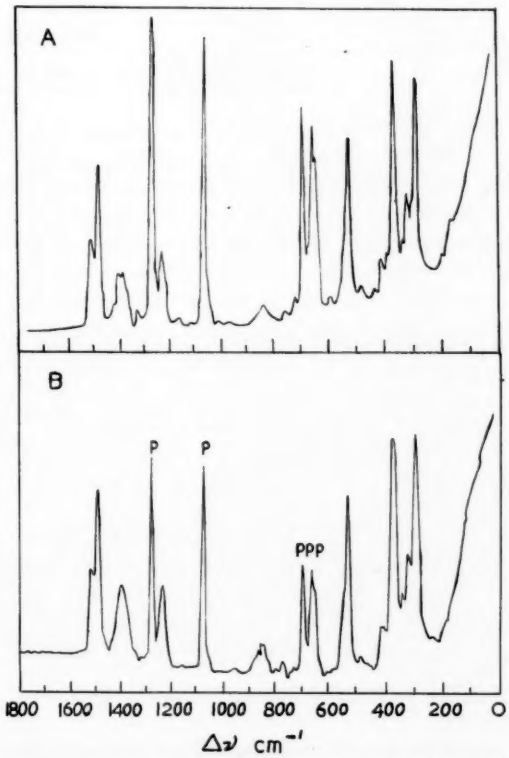

FIG. 2. Polarization measurements on liquid sulphur trioxide: (A) incident light polarized in a vertical plane; (B) incident light polarized in a horizontal plane (polarized lines denoted by P are of reduced intensity).

TABLE III

Raman active vibrations for sulphur trioxide polymers

Polymer	Symmetry	Number of vibrations
S_2O_6	D_{2h} (planar)	9 (4p, 5dp)
	C_{2v} (non-planar)	18 (7p, 11dp)
S_3O_9 ring	D_{3h} (planar)	14 (4p, 10dp)
	C_{3v} (non-planar), "chair form"	17 (7p, 10dp)
	C_s (non-planar), "boat form"	30 (17p, 13dp)
S_4O_{12} ring	D_{4h} (planar)	15 (4p, 11dp)
	C_{4v} (non-planar)	29 (7p, 22dp)

place, as the Raman spectrum of the liquid at 100° (7) shows only those vibration frequencies which have been assigned to the monomer. Open chains IV, of varying lengths, may also be present in the liquid at room temperature but presumably only in small amounts as they require end groups Y, which would have to originate from impurities.

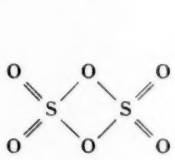

I

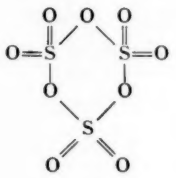

II

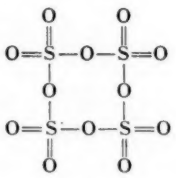

III

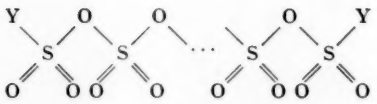

IV

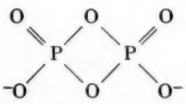

V

Further support for the suggestion that liquid sulphur trioxide consists of the trimer in equilibrium with the monomer can be obtained by a comparison of the spectrum of the liquid with the spectra of the solid α, β, and γ forms. The lines of the γ form all occur quite strongly in the spectrum of the liquid, and this form has been shown by X-ray crystallography to have a structure consisting of trimeric rings (III) in the "chair" form with C_{3v} symmetry. The solid β form on the other hand consists of SO_4 tetrahedra linked together to form long spiral chains (12, 13).

If it is assumed that the trimer is the main species present in the liquid and that the trimer is, at least mainly, in the chair form, frequencies can be assigned to this molecule as shown in Table IV. There are 20 normal vibrations of which the three A_2 vibrations are inactive in the Raman. Seven of the vibrations, 3 of which are polarized, can be assigned to the ring and the other 10, 4 of which should be polarized, involve the atoms of the SO_2 groups (9) (Fig. 3).

Sulphuryl Group Vibrations

Sulphuryl group vibrations would be expected to have frequencies close to those observed in simple molecules such as sulphuric acid and sulphuryl fluoride and would be expected therefore to occur at approximately the following frequencies: symmetric

TABLE IV

Assignment of fundamental frequencies for the *chair* conformation of trimeric sulphur trioxide

Species	Vibration	Assignment (cm^{-1}) (*a*)	(*b*)	
A_1	ν_1	1270	1271	Polarized
	ν_2	534*	657	Polarized
	ν_3	368	664	Polarized
	ν_4	665 or 657	698	Polarized
	ν_5	1515	1489	Polarized
	ν_6	698	775	Polarized
	ν_7	665 or 657	369	Polarized
A_2	ν_8	—	597	Forbidden
	ν_9	—	319	Forbidden
	ν_{10}	—	1515	Forbidden
E	ν_{11}	1231	1271	
	ν_{12}	480	657	
	ν_{13}	560	319	
	ν_{14}	407	408	
	ν_{15}	860	1231	
	ν_{16}	840	840	
	ν_{17}	1489	1489	
	ν_{18}	680	775	
	ν_{19}	322	597	
	ν_{20}	290	289	

NOTE: (*a*) This investigation; (*b*) Gerding and Nijveld (9).
*Coincident with the analogous vibration of the monomer.

stretches, 1100–1300 cm^{-1}; asymmetric stretches, 1300–1500 cm^{-1}; symmetric deformations, 500–600 cm^{-1}; rocking and torsional vibrations, 300–600 cm^{-1} (14).

The five lines observed at frequencies greater than 1200 cm^{-1} can only be reasonably assigned as SO_2 stretching vibrations. One of these, at 1390 cm^{-1}, is due to the monomer and the other four may be assigned in pairs as the in-phase symmetric and asymmetric stretch ν_1 and ν_5 at 1270 cm^{-1} and 1515 cm^{-1}, respectively, and the out-of-phase symmetric and asymmetric stretch ν_{11} and ν_{17} at 1231 and 1489 cm^{-1}, respectively (Table II). The in-phase vibrations are of species A_1 and should therefore be polarized. The vibration at 1270 cm^{-1} is definitely polarized and that at 1515 cm^{-1} was reported to be weakly so by Venkateswaren (4). The frequencies of both pairs of lines are consistent with the linear relationship that has been found between the SO_2 symmetric and asymmetric stretching frequencies (15, 16). The relatively high values of the SO_2 vibrational frequencies imply that the S—O bonds exterior to the ring have substantial double-bond character. This is consistent with the bond length of 1.4 Å and the large OSO angle of 122° (17). It appears reasonable to assign the in-phase vibrations at higher frequencies than the out-of-phase vibrations since in the former, but not in the latter, distortion of the ring occurs. Gerding and Nijveld (9) assumed that coupling between the SO_2 groups is very weak and that the in-phase and out-of-phase vibrations of the SO_2 group are degenerate. They assigned the line at 1270 cm^{-1} to the symmetric stretch and the line at 1489 cm^{-1} to the asymmetric stretch. These authors attributed the 1515 cm^{-1} frequency to the forbidden ring vibration ν_{10} and the line at 1230 cm^{-1} to the ring vibration ν_{15}.

In simple sulphuryl compounds such as sulphuric acid, the SO_2 bend is in the range 500–600 cm^{-1}, and in the sulphur trioxide monomer the similar vibration is at 532 cm^{-1}. In liquid sulphur trioxide there is a line at 534 cm^{-1} which is relatively strong and is

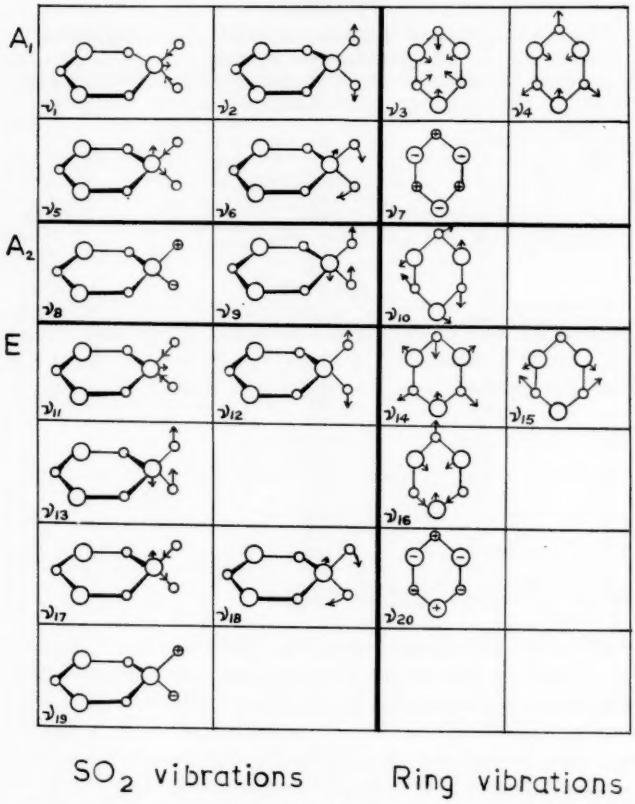

FIG. 3. Approximate atomic motions in the normal modes of S_3O_9. In the A_1 and A_2 vibrations the motions of the three SO_2 groups are in-phase while in the E vibrations the motions of the SO_2 groups are out-of-phase.

probably polarized and this we assign to the in-phase bend of the trimer ν_2, as well as to the monomer, since it is much stronger in the liquid than would be expected for the amount of monomer implied by the intensity of the 1070 cm^{-1} Raman shift in the liquid.

The out-of-phase SO_2 bend, ν_{12}, may be tentatively assigned as the rather weak line at 480 cm^{-1}. Gerding and Nijveld assigned the polarized line at 651 cm^{-1} to the SO_2 bend, but although a large number of compounds have been investigated the SO_2 bend has never been found at such a high frequency and it very rarely occurs at a frequency higher than 600 cm^{-1} (14).

Rocking and torsional modes of the sulphuryl group have frequencies in the range 300–600 cm^{-1} in simple sulphuryl compounds (14). In trimeric sulphur trioxide there is a total of six vibrations of these types: four rocking modes ν_6, ν_9, ν_{13}, and ν_{18} and two torsional modes ν_8 and ν_{19}, of which ν_8 and ν_9 are forbidden in the spectrum for a molecule with C_{3v} symmetry. Vibration ν_6 is of species A_1 and should therefore be polarized. There are four polarized lines as yet unassigned at 368, 657, 665, and 698 cm^{-1}. A model of the chair form of sulphur trioxide trimer shows that the axial oxygens of the SO_2 groups are close together and there will be considerable interaction between these oxygen atoms

in vibration ν_6; this would be expected to increase its frequency above the range of 500–600 cm^{-1} found for simple sulphuryl compounds, and therefore one of the lines at 657, 665, or 698 cm^{-1} must be assigned to this vibration. Tentatively we choose the 698 cm^{-1} line as it has been found in the di- and tri-sulphuryl halides, where similar interaction between an SO_2 group and a halogen occurs in an SO_2 rocking mode, that the frequency can be raised as high as 730 cm^{-1} (18). The frequency of ν_{18} would be expected to be fairly close to that of ν_6. There is no obvious depolarized line in this region of the spectrum and it must be assumed that it is of low intensity and is hidden under the broad, incompletely resolved band between 657 and 698 cm^{-1}. The remaining SO_2 rocking mode, ν_{13}, would be expected to be of lower frequency and the only possibility seems to be to assign it to the shoulder of the 534 cm^{-1} line at approximately 560 cm^{-1}. As ν_{13} would give a depolarized line, this provides an explanation for the difficulty of observing the expected polarization of the 534 cm^{-1} line. Torsional modes have frequencies in the range 270–370 cm^{-1} in mono-, di-, and tri-sulphuryl chlorides and fluorides (14, 18) and therefore it seems reasonable to assign the line observed at 322 cm^{-1} to ν_{19}. Gerding and Nijveld assigned the very weak line at 600 cm^{-1} to this vibration, but in none of the simple sulphuryl, or polysulphuryl, compounds has a torsional mode been found to have such a high frequency.

Ring Vibrations

The three vibrations ν_3, ν_4, and ν_7 should give rise to polarized lines; they must therefore be assigned to the three lines at 368, 657, and 665 cm^{-1}. The symmetric breathing vibration would be expected to have the lowest frequency and can therefore be assigned to the 368 cm^{-1} line. This vibration is, moreover, rather similar to the symmetric SOS skeletal stretch of the disulphuryl halides which have been assigned at 298, 313, and 323 cm^{-1} for $S_2O_5Cl_2$, S_2O_5ClF, and $S_2O_5F_2$ respectively.

The remaining unassigned lines, other than very weak lines and some very low frequency lines, are at 860, 840, 407, and 290 cm^{-1}. If we assume that the order of the frequencies of the ring vibrations of species E will be the same as for the analogous vibrations of the benzene ring, then these may be assigned as ν_{15}, ν_{16}, ν_{14}, and ν_{20} respectively. The analogous vibrations of the benzene molecule have frequencies of 1585, 1478, 606, and 404 cm^{-1} respectively (19). The assignment of these ring vibrations agrees with that given by Gerding and Nijveld except that they assigned ν_{15} to the 1231 cm^{-1} line which we have assigned as ν_{11}. Gerding and Nijveld did not assign the 860 cm^{-1} line and they assumed that ν_{11} had the same frequency as ν_1, i.e. 1270 cm^{-1}.

Weak Lines

Of the 25 lines observed with certainty in the Raman spectrum of liquid sulphur trioxide, 18 have been assigned to the chair form of the trimer together with the monomer, 16 to the trimer, and 3 to the monomer with one coincidence. This assignment accounts for all except seven very weak lines at 150, 243, 327, 600, 773, 1018, and 1162 cm^{-1} and some very indefinite shoulders on the side of the exciting line at frequencies of less than 150 cm^{-1}. Some of these lines could be overtone or combination bands but perhaps the most likely explanation for most of them is the presence of small amounts of the "boat" form of the trimer. Other possible species that may be present in small quantities are the tetramer and higher cyclic polymers, together with acyclic polymers, presumably of fairly high molecular weight. The line at 150 cm^{-1} could be due to acyclic polymers since the SOS skeletal bending mode has been assigned frequencies of approximately 150 cm^{-1} in the di- and tri-sulphuryl halides (18).

Conclusion

The Raman spectrum of liquid sulphur trioxide can be reasonably satisfactorily accounted for in terms of an equilibrium between the monomer and the "chair" form of the cyclic trimer. All except the very weakest lines in the spectrum can be accounted for in this way. The additional lines are probably due to small concentrations of the "boat" form of the trimer and higher cyclic or acyclic polymers.

SOLUTIONS OF SULPHUR TRIOXIDE

Solutions of sulphur trioxide in sulphur dioxide, sulphuryl chloride, disulphuryl chloride, disulphuryl fluoride, carbon tetrachloride, tetrachlorethylene, and trichlorfluormethane (Freon 11) were investigated. In most cases, the spectra show only lines due to sulphur trioxide and the solvent, although in a few cases there are additional lines which can be attributed to small amounts of polysulphuryl halides. An estimate of the proportions of monomeric and trimeric sulphur trioxide can be made from the relative intensities of the line at approximately 1069 cm^{-1}, characteristic of the monomer, and the strongest line of the trimer at 1270 cm^{-1}.

Solutions in Sulphur Dioxide

The spectra of three solutions of composition approximately 10, 20, and 40% sulphur trioxide by weight were investigated at approximately −10°. All the spectra (Fig. 3 and Table V) clearly show that sulphur trioxide in sulphur dioxide is present mainly

TABLE V

Raman spectra of solutions of sulphur trioxide in liquid sulphur dioxide (frequencies in cm^{-1})

Mole fraction of SO_3:			
0.088	0.170	0.370	Assignment
530 (mw)	530 (mw)	530 (mw)	ν_2'
1071 (s)	1071 (s)	1071 (s)	ν_1'
—	—	1270 (vw)	ν_1
1400 (vw)	1400 (w)	1390 (vw)	ν_3'
—	—	1405 (vw)	

Solvent: 530 (mw); 1139 (vs); 1330 (w).

as the monomer. Only in the 40% solution did the 1270 cm^{-1} line characteristic of S_3O_9 appear. The spectra of the solutions are just a superposition of the components and no new substances appear to be formed. Previous workers (1, p. 358) have claimed the occurrence of an unstable volatile liquid with the composition $2SO_3.SO_2$ but no evidence for such a compound is given by our Raman spectra.

Solutions in Sulphuryl Halides

The Raman spectra of these solutions show that there is no reaction between sulphur trioxide and sulphuryl chloride (Fig. 2) at room temperature, although higher polysulphuryl halides could, in principle, have been formed, e.g. $S_2O_5Cl_2 + SO_3 = S_3O_8Cl_2$. For solutions of sulphur trioxide in disulphuryl chloride and in disulphuryl fluoride similar results were obtained. In the case of sulphuryl chloride this conclusion has also been reached by other workers (20, 21), who refluxed sulphur trioxide with various proportions of sulphuryl chloride for periods up to 24 hours and obtained only the pure components on distillation. The compound $2SO_2Cl_2.SO_3$ has been claimed at low temperatures but is reported as being unstable above the melting point (22).

The Raman spectra show that at low concentrations, sulphur trioxide is almost entirely in the form of the monomer while solutions containing more sulphur trioxide than 0.2 mole fraction contain increasing concentrations of the trimer (Table VI).

TABLE VI
Raman spectra of solutions of sulphur trioxide in sulphuryl chloride (frequencies in cm^{-1})

Mole fraction of SO_3:				
0.106	0.309	0.420	0.549	Assignment
—	—	—	478 (vw)	ν_{14}
530 (w)	525 (w)	528 (w)	528 (m)	ν_2' and ν_2
—	—	—	650 (w)	ν_3
—	—	—	667 (w)	ν_7 or ν_{15}
—	—	—	694 (w)	ν_4 or ν_7
—	—	—	848 (vw)	ν_{16}
—	—	—	1009 (vw)	?
1073 (m)	1068 (s)	1073 (s)	1072 (vs)	ν_1'
—	—	—	1163 (w)	ν_{16}
—	—	—	1226 (w)	ν_{11}
1270 (vw)	1270 (w)	1265 (m)	1265 (s)	ν_1
—*	—*	1405 (m)	1375 (mw)	ν_3'
—	1485 (w)	1480 (w)	1488 (w)	ν_{13}
—	1515 (w)	1510 (w)	1510 (w)	ν_5

Solvent: 218 (s); 282 (s); 362 (s); 388 (vs); 408 (vs); 560 (vs); 600 (w); 1180 (s); 1414 (s).
*1390 cm^{-1} of monomeric sulphur trioxide obscured by solvent line at 1414 cm^{-1}.

Solutions in Halogen-substituted Hydrocarbons

The spectra of solutions of sulphur trioxide in carbon tetrachloride, tetrachlorethylene, and trichlorfluormethane are shown in Tables VII–IX and in Fig. 4. Except for the

TABLE VII
Raman spectra of solutions of sulphur trioxide in carbon tetrachloride (frequencies in cm^{-1})

Mole fraction of SO_3:			
0.129	0.306	0.461	Assignment
—	—	136 (w)	$S_2O_5Cl_2$
—	188 (vw)	188 (w)	$S_2O_5Cl_2$
256 (vw)	261 (vw)	257 (w)	?
—	286 (vw)	290 (s)	ν_{20}
—	345 (vw)	345 (m)	ν_9
358 (vw)	364 (w)	367 (m)	ν_6
—	—	388 (w)	$S_2O_5Cl_2$?
415 (vw)	408 (vw)	408 (w)	ν_{18}
528 (w)	530 (w)	528 (ms)	ν_2'
—	543 (vw)	543 (w)	ν_2
—	576 (vw)	573 (w)	$S_2O_5Cl_2$
605 (vw)	605 (w)	602 (m)	$S_2O_5Cl_2$
—	660 (vw)	665 (m)	ν_7 or ν_4
—	693 (w)	693 (m)	ν_4 or ν_7
—	—	717 (w)	$S_2O_5Cl_2$
—	833 (vw)	815 (w)	?
—	873 (w)	873 (w)	ν_{15}
1068 (m)	1068 (s)	1068 (s)	ν_1'
1200 (w)	1200 (w)	1197 (m)	$S_2O_5Cl_2$
1250 (vw)	1245 (w)	1245 (m)	ν_{11}
1267 (w)	1267 (m)	1267 (m)	ν_1
1380 (vw)	1380 (vw)	1394 (w)	ν_3'
—	1488 (vw)	1482 (w)	ν_{17}

Solvent: 217 (s); 315 (s); 459 (s); 760 (m); 790 (m); 1537 (w).

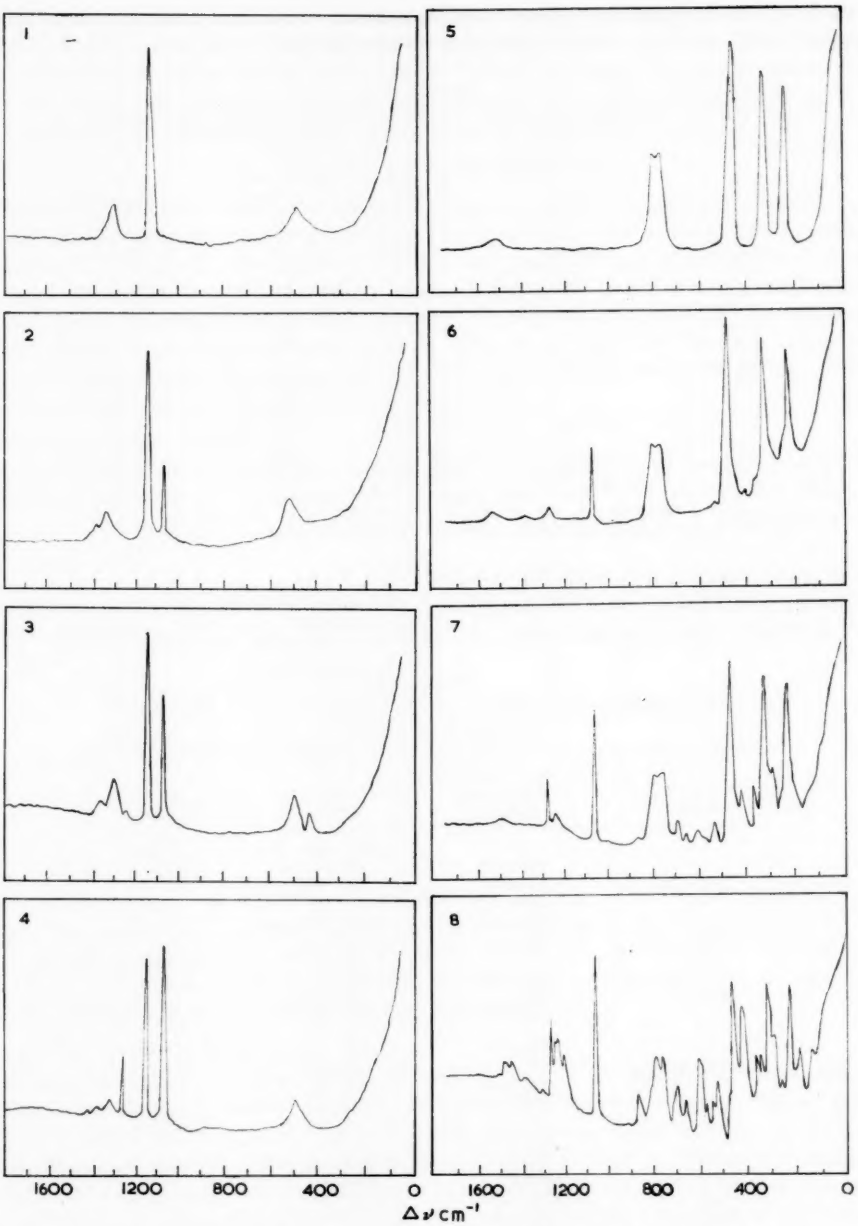

FIG. 4. Raman spectra of solutions of sulphur trioxide in liquid sulphur dioxide and in carbon tetrachloride: (1) liquid sulphur dioxide; (2, 3, 4) solutions of sulphur trioxide in liquid sulphur dioxide, N_{SO_3} = 0.088, 0.170, and 0.370; (5) carbon tetrachloride; (6, 7, 8) solutions of sulphur trioxide in carbon tetrachloride, N_{SO_3} = 0.129, 0.306, and 0.461.

TABLE VIII

Raman spectra of solutions of sulphur trioxide in tetrachlorethylene (frequencies in cm^{-1})

Mole fraction of SO_3:			
0.194	0.368	0.678	Assignment
290 (w)	290 (m)	281 (m)	ν_{20}
—	—	381 (w)	ν_{13}
—	369 (m)	370 (w)	ν_6
398 (w)	398 (w)	398 (w)	ν_{18}
530 (vw)	527 (w)	530 (mw)	ν_2' and ν_2
650 (vw)	646 (w)	650 (m)	ν_3
668 (vw)	662 (w)	665 (m)	ν_7 or ν_4
698 (vw)	698 (w)	698 (m)	ν_4 or ν_7
—	—	849 (w)	ν_{16}
1068 (m)	1068 (s)	1068 (vs)	ν_1'
—	—	1225 (w)	ν_{11}
—	—	1247 (w)	?
1270 (w)	1267 (m)	1270 (vs)	ν_1
—	1385 (vw)	1385 (w)	ν_3'
—	1488 (w)	1490 (m)	ν_{17}
—	1520 (vw)	1517 (w)	ν_5

Solvent: 133 (vw); 183 (w); 241 (s); 322 (w); 350 (m); 395 (w); 450 (vs); 466 (w); 515 (m); 580 (w); 725 (vw); 780 (vw); 1005 (vw); 1028 (w); 1572 (s); 1820 (w); 2000 (w); 2020 (vw).

TABLE IX

Raman spectra of solutions of sulphur trioxide in trichlorfluormethane (Freon 11) (frequencies in cm^{-1})

Mole fraction of SO_3:		
0.245	0.427	Assignment
—	322 (vw)	?
—	368 (m)	ν_6
369 (w)	375 (m)	ν_6
—	650 (w)	ν_3
668 (w)	666 (m)	ν_7 or ν_4
698 (w)	695 (m)	ν_4 or ν_7
—	865 (w)	ν_{15}
1072 (m)	1068 (s)*	ν_1'
—	1245 (vw)	ν_{11}
1270 (m)	1265 (s)	ν_1
1390 (vw)	1390 (w)	ν_3'
1485 (vw)	1491 (w)	ν_{17}
1520 (vw)	1520 (w)	ν_5

Solvent: 146 (vw); 192 (vw); 247 (s); 298 (w);† 355 (s); 402 (s); 478 (w); 540 (s);† 785 (w); 835 (s); 1073 (m broad);* 1660 (w); 1680 (vw).

*Coincidence between solvent line and the S—O symmetric stretch of monomeric SO_3 but latter is sharp and strong.

†Coincidence with SO_3 line.

carbon tetrachloride solutions the observed lines can be attributed to the solvent or to SO_3 monomer or trimer.

Sulphur trioxide is known to react with carbon tetrachloride under reflux (22) to give polysulphuryl halides according to the equation

$$CCl_4 + nSO_3 = SO_2(SO_3)_{n-1}Cl_2 + COCl_2.$$

The Raman spectra show that this reaction appears to proceed slowly even at room temperature, as additional lines, which can reasonably be attributed to $S_2O_5Cl_2$, appear

in the spectra of the carbon tetrachloride solutions. The amounts of polysulphuryl halides formed in a few hours are however quite small and carbon tetrachloride is for many purposes a useful solvent for sulphur trioxide.

In all the solutions studied, monomer and trimer are in equilibrium. At low concentrations the equilibrium favors the monomer but the actual position of the equilibrium for a given concentration of sulphur trioxide depends on the solvent. Thus in solutions of a given concentration in the following solvents, the monomer–trimer equilibrium shifts progressively in favor of the trimer in the order sulphur dioxide, sulphuryl chloride, halogenated hydrocarbons.

EXPERIMENTAL

The Raman spectrometer has been described previously (18). When necessary, for example for sulphur dioxide solutions, an additional jacket was provided between the sample tube and the filter jacket through which cold alcohol could be passed to cool the sample.

Sulphur trioxide was obtained by distillation from 65% oleum from which sulphur dioxide had been removed by oxidation with potassium persulphate. "Sulfan B" was obtained from the Allied Chemical Company. The solvents used were dried over phosphoric oxide and purified by distillation except for sulphur dioxide, which was obtained from a cylinder and purified by trap-to-trap distillation. Sulphuryl chloride was stored in the absence of light. The preparation of disulphuryl chloride and disulphuryl fluoride has been described previously (18, 23).

ACKNOWLEDGMENTS

We thank the National Research Council, the Ontario Research Foundation, and the Allied Chemical Company for financial assistance.

REFERENCES

1. GMELINS HANBUCH DER ANORGANISCHEN CHEMIE. No. 9, B1. Verlag Chemie, Weinheim. 1953.
2. J. H. HIBBEN. The Raman effect and its chemical applications. Reinhold, New York. 1939.
3. S. BHAVAGANTAM. Indian J. Phys. **5**, 1, 49 (1930).
4. S. VENKATESWAREN. Phil. Mag. **15**, 263 (1933).
5. A. SMITS and N. F. MOERMAN. Nature, **134**, 698 (1934).
6. H. GERDING, W. J. NIJVELD, and G. J. MULLER. Z. physik. Chem. B, **35**, 193 (1937); Nature, **137**, 1033 (1936).
7. H. GERDING and N. F. MOERMAN. Z. physik. Chem. B, **35**, 216 (1937).
8. H. GERDING and J. LECOMTE. Physica, **6**, 737 (1939).
9. H. GERDING and W. J. NIJVELD. Rec. trav. chim. **59**, 1209 (1940).
10. W. G. PALMER. J. Am. Chem. Soc. **60**, 2360 (1950).
11. J. R. VAN WAZER. Phosphorus and its compounds. Vol I. Chemistry. Interscience Publishers Inc., New York. 1958.
12. R. WESTRICK and C. H. MACGILLAVRAY. Rec. trav. chim. **60**, 794 (1941).
13. R. WESTRICK and C. H. MACGILLAVRAY. Acta Cryst. **7**, 764 (1954).
14. R. J. GILLESPIE and E. A. ROBINSON. Can. J. Chem. This issue. p. 2171.
15. L. J. BELLAMY and R. L. WILLIAMS. J. Chem. Soc. 863 (1957).
16. E. A. ROBINSON. Can. J. Chem. **39**, 247 (1961).
17. L. E. SUTTON (*Editor*). Tables of interatomic distances. Chem. Soc. (London), Spec. Publ. No. 11 (1958).
18. R. J. GILLESPIE and E. A. ROBINSON. Can. J. Chem. This issue. p. 2179.
19. G. HERZBERG. Infrared and Raman spectra of polyatomic molecules. D. van Nostrand Co., Inc., New York. 1945. p. 367.
20. A. PICTET and G. KARL. Bull. soc. chim. France, **3**, 1114 (1908).
21. E. HAYEK and K. HINTERAUER. Monatsh. **82**, 205 (1951).
22. G. P. LUCHINSKII and A. I. LIKHACHEVA. J. Gen. Chem. (U.S.S.R.), **7**, 405 (1937).
23. E. HAYEK and W. KOLLER. Monatsh. **82**, 942 (1951).

SOME STEREOCHEMICAL STUDIES ON α,β-UNSATURATED KETONES USING RAMAN SPECTROPHOTOMETRY[1]

K. NOACK[2] AND R. NORMAN JONES

ABSTRACT

The Raman spectra of 12 α,β-unsaturated open-chain and cyclic ketones have been measured in the region of the C=O and C=C stretching vibrations, and the band positions and intensities have been compared with the corresponding bands in the infrared spectra. If due allowance is made for solvent effects, the infrared and Raman bands are observed at the same positions, but the relative intensities of the C=O and C=C bands are different; in particular, the Raman C=O stretching bands of the ketones in the *s*-trans configuration are from 5 to 10 times more intense than the Raman bands for the *s*-cis isomers. The cyclic *s*-trans ketones with a hydrogen atom on the α-carbon atom exhibit a solvent-sensitive doubling of the carbonyl maximum similar to that noted previously for certain α,β-unsaturated lactones, unsaturated acid anhydrides, and Δ^2-cyclopentenone derivatives. These doublet carbonyl maxima are observed also in the infrared spectra. The C=C frequency is not similarly perturbed and the effect is distinct from the doubling of both the C=O and the C=C bands exhibited by some open-chain α,β-unsaturated ketones that exist in the liquid phase as equilibrium mixtures of *s*-cis and *s*-trans isomers.

INTRODUCTION

The use of Raman spectroscopy by organic chemists for the characterization of natural products has been limited by the intrinsic weakness of the Raman effect and the need to employ large samples of material. Recent instrumental developments make it practical to record Raman spectra photoelectrically, using liquid samples excited in capillary tubes. Complete spectra can be measured over the range 150–4000 cm^{-1} using 25- to 200-mg samples, and the more intense bands, such as those associated with C=C and C≡C stretching modes, can be recorded with 10-mg samples in carbon disulphide solution.

In the absence of steric hindrance, a system of two conjugated double bonds will favor a planar conformation, for which *s*-cis (I) and *s*-trans (II) structures are possible. In cyclic ketones (III, IV) these configurations are fixed. In open-chain structures one

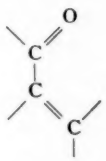

I

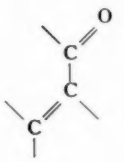

II

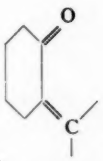

III

IV

of the conformations will commonly be preferred to the virtual exclusion of the other; occasions do arise, however, where the energy differences are small and both forms are present in significant concentration in the liquid or vapor phase.

Mecke and Noack (1, 2) have shown that, for α,β-unsaturated ketones, such conformational isomers can be distinguished by the positions and intensities of the C=O and C=C stretching bands in the infrared spectrum, and additional examples have been cited by Erskine and Waight (3) and by Timmons (4). The Raman spectra of some of

[1]*Manuscript received June 21, 1961.*
Contribution from the Division of Pure Chemistry, National Research Council of Canada, Ottawa, Canada. Issued as N.R.C. No. 6513.
[2]*National Research Council of Canada Postdoctorate Fellow.*

these compounds have now been measured. The Raman frequencies of the C═O and C═C stretching bands agree with the infrared frequencies if allowances are made for solvent effects; these effects are particularly significant for the C═O stretching band of the *s*-trans isomers. The relative intensities of the C═O and the C═C Raman and infrared bands differ, but the Raman spectra confirm the conformational assignments proposed by Noack and Mecke for the open-chain compounds on the basis of infrared measurements. Some of the cyclic *s*-trans ketones exhibit solvent-sensitive doublet carbonyl peaks in the Raman spectra, and on reinvestigation the same effects are noted in the infrared spectra. Doublet C═O and C═C bands also occur in some open-chain ketones, but, in these cases, conformational equilibria are involved. Ketones exhibiting conformational equilibria of this type are dealt with in a separate paper in which effects of temperature change are also examined (5).

EXPERIMENTAL

The ketones employed in this investigation (V–XVI) were obtained from a collection prepared by Mecke and Noack for the infrared studies, and their chemical characterization

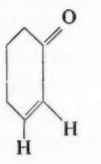
V

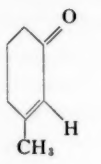
VI

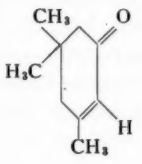
VII

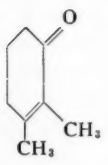
VIII

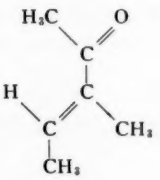
IX

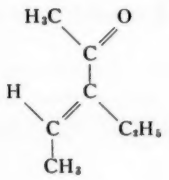
X

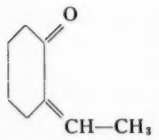
XI

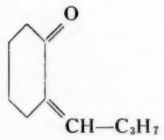
XII

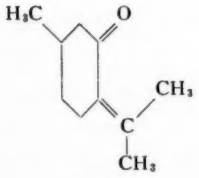
XIII

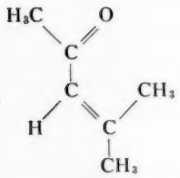
XIV

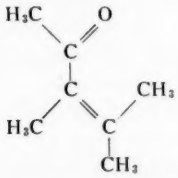
XV

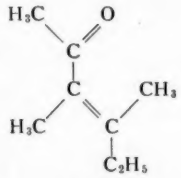
XVI

has already been described (2). The Raman spectra were measured on a Cary Model 81 spectrophotometer using a micro sample tube of 2-mm external diameter and 200-microliter volume. After quantitative dilution with carbon tetrachloride, as described below, the freshly distilled ketone was introduced into the Raman tube by means of a narrow, flexible metal capillary tube attached to a hypodermic syringe mounted vertically on a stand. Ketone mole ratios of approximately 0.4 were normally employed, and 120–150 mg of the ketone was needed to fill the cell. The spectra were measured at a spectral slit width of 5 cm^{-1} and the estimated uncertainty in the positions of the band maxima is ± 2 cm^{-1}. A scanning rate of 15 cm^{-1} per minute was normally used.

The Toronto-type arc lamp was constructed of Corning 1720 glass, and the Hg 4358 Å exciting line was isolated with aqueous potassium nitrite and aqueous Rhodamine GDN extra filter solutions in separate annular jackets with a common dividing wall. The potassium nitrite solution in the outer jacket was circulated through a cooling system; the Rhodamine solution was not circulated and was stabilized by the addition of hydrochloric acid. A cylindrical Polaroid polarizer with the direction of polarization perpendicular to the axis of the Raman tube was inserted between the filter system and the Raman tube to eliminate effects of oblique illumination.

Intensity Measurements

The peak heights of the Raman bands were measured relative to the 459 cm^{-1} band of carbon tetrachloride, which was taken as 100 units. The accurate evaluation of this intensity involves several instrumental and theoretical factors (6–9). The unit employed here, and in other contemporary papers from this laboratory, does not take into account all the variables that may affect the accuracy of the measurements; it has been devised to meet immediate needs, and to cope with technical problems associated with the use of the capillary sample tube.

The determination of the Raman band intensities involves comparison with an internal or external standard (8). If an external standard is used the emission intensity of the measured Raman band is compared with the standard band as observed with a matched sample tube under the same experimental conditions. This assumes that the illumination of the Raman tube, and its alignment with respect to the spectrometer optics, are reproducible. These conditions are usually not critical, but the external-standard method also suffers from the serious defect that the sample spectrum and the standard spectrum are usually obtained from media of different refractive index. The refractive index influences the intrinsic intensity of the Raman radiation through a solvent field effect and it also determines the fraction of the total Raman radiation that enters the spectrometer. Using wide tubes, where wall effects can be neglected, Woodward and George (9) have shown that the instrumental effect is inversely proportional to the square of the refractive index of the medium. Rea (7) has analyzed the problem for narrower tubes where wall effects become significant, though his initial treatment was not complete, and the application of an additional empirical correction was later required (10). When the Raman radiation is generated within a capillary tube, the energy entering the spectrometer from a Pyrex capillary is found to increase by a factor of five with increase in the refractive index from 1.35 to 1.65. It would appear that under these conditions, the wall effect becomes dominant, the radiation probably suffering multiple reflection before reaching the entrance slit; a considerable proportion is accordingly lost through the walls of the tube en route.

The difficulties associated with the intensity measurement can be largely circumvented

by the addition of the standard calibrating liquid to the sample in known proportion. The standard band is then measured in a medium of the same refractive index as the sample band. The internal-standard technique can only be used where the overlap of the two spectra is not significant, but using the 459 cm^{-1} carbon tetrachloride band as standard, this problem caused no difficulty for the ketones considered in this paper. The use of the internal standard also avoids the need to determine the density of the liquid, which is otherwise required if the intensities are to be expressed on a molar basis. The intrinsic intensity of the standard may be modified by intermolecular interactions but this can be checked to some extent by use of a series of measurements at different concentrations, or by cross checking with different secondary standard bands; significant variations may be involved here (11) but more extensive experimental and theoretical study is needed if these effects are to be properly interpreted. In our investigations the concentrations were so adjusted that the peak height of the 459 cm^{-1} carbon tetrachloride band was comparable with the C=O and C=C bands, and, for this, mole fractions of about 0.4 ketone and 0.6 carbon tetrachloride were required.

On the basis of these considerations, the Raman intensity coefficient was expressed as

$$[1] \qquad k_A^{\nu} = \frac{I_A^{\nu}}{I_{CCl_4}^{459}} \cdot \frac{N_{CCl_4}}{N_A} \cdot 100,$$

where k_A^{ν} = the Raman intensity coefficient at ν cm^{-1} displacement from the exciting line for substance A;

I_A^{ν} = the emission intensity at ν cm^{-1} displacement from the exciting line, measured in arbitrary units;

$I_{CCl_4}^{459}$ = the emission intensity at the 459 cm^{-1} peak of carbon tetrachloride measured in the same units as I_A^{ν};

N_A = the mole fraction of A;

N_{CCl_4} = the mole fraction of carbon tetrachloride.

No correction was applied for the change in the spectral sensitivity of the spectrophotometer since this did not vary by more than 3% over the measured wavenumber range.

The insertion of the cyclindrical polarizer influences the intensity considerably, as the 459 cm^{-1} carbon tetrachloride band is highly polarized, and the convergence errors are large if the measured band has a different depolarization ratio from the standard band. Comparisons made with and without the Polaroid filter (oriented to transmit radiation with the electric vector perpendicular to the tube axis) consistently gave values for these ketones that were 30% lower when the polarizer was in place. The Raman C=O bands of compounds VII and XIV have also been measured by Michel and Duyckaerts (8) with no polarizer in their spectrometer. Their measurements were some 30% greater than the values we obtain when the polarizer is used. The constancy of this systematic intensity difference is attributed to the fact that all the C=O bands in these ketones have similar depolarization ratios close to 0.4.

The measurement of band height against a sloping background invariably introduces uncertainty in the location of the baseline. Where feasible, the line was drawn tangentially to the curve, usually at about three half band widths on either side of the band center. In some cases the location of the line was rather arbitrary; this accounts for the major uncertainty in the measured intensity coefficients and largely invalidates any attempts to apply corrections for smaller physical variables affecting the accuracy of the measurements.

Band Area Measurements

The area beneath the Raman band was not measured directly, but a quantity approximately proportional to it was calculated. This quantity, which we call the *band area coefficient* (L), is defined as

$$[2] \qquad L_A^{\nu_{max}} = k_A^{\nu_{max}} \cdot \frac{\Delta\nu_{\frac{1}{2}}^{A}}{\Delta\nu_{\frac{1}{2}}^{CCl_4}},$$

where $L_A^{\nu_{max}}$ = the band area coefficient for the band of substance A;
$\Delta\nu_{\frac{1}{2}}^{A}$ = the band width at half maximal intensity, measured on the spectral chart in arbitrary units;
$\Delta\nu_{\frac{1}{2}}^{CCl_4}$ = the band width at half maximal intensity of the 459 cm^{-1} band of carbon tetrachloride measured under the same conditions as $\Delta\nu_{\frac{1}{2}}^{A}$.

The band area coefficient is, therefore, equal to 100 times the ratio of the sample band area to that of the (internal) standard band. The ratio L can be derived directly from the measured spectrum without resort to arithmetical integration, and it is adequate for the comparison of gross differences between Raman bands of varying types. More refined measurements are not justified in view of the large errors associated with contemporary microtechniques.

RESULTS

The positions and intensities of the C=O and C=C stretching bands in the Raman and infrared spectra of ketones V–XVI are listed in Table I.

Band Positions

Though the two fundamental absorption bands of α,β-unsaturated ketones in the 1750–1600 cm^{-1} range are coupled, it is customary (and convenient) to identify the band at higher wavenumber with a localized "C=O stretching" vibration and the band at lower wavenumber with a "C=C stretching" mode.*

Comparison of ν_{max} for the infrared and Raman bands listed in Table I indicates that the bands fall into the same frequency ranges in both the infrared and the Raman spectra. The *s*-cis and *s*-trans structures can therefore be distinguished from the Raman band positions as well as from the infrared, and the conformational assignments for the open-chain ketones made by Mecke and Noack from the infrared data are confirmed by the Raman measurements. For both the cyclic and open-chain *s*-cis compounds the Raman and infrared C=O and C=C band frequencies agree within the precision of the experimental data (± 3 cm^{-1}) and this holds also for the C=C bands of the cyclic and open-chain *s*-trans ketones. For the cyclic and open-chain *s*-trans ketones, however, the Raman C=O frequencies given in Table I are uniformly 4–8 cm^{-1} lower than the corresponding infrared values. Whereas the Raman spectra were measured at high concentrations in carbon tetrachloride, the infrared spectra were initially obtained at much lower concentrations in tetrachloroethylene. When the infrared spectra were remeasured on capillary films in carbon tetrachloride at the same concentrations as were used for the Raman spectra, the band positions listed in Table II were obtained. This table demonstrates clearly that the significant differences between the infrared and Raman C=O peak positions are due to solvent effects. The infrared band positions in dilute solutions of

**The tacit assumption that the "C=O" band invariably lies above the "C=C" band may not be justified, and Cook has recently suggested that the sequence may be inverted for 2,6-dimethyl-4-pyrone (12).*

TABLE I

Positions and intensities of the C=O and C=C stretching bands in the Raman and infrared spectra of α,β-unsaturated ketones*

Compound	Raman spectrum* †						Infrared spectrum‡ §					
	ν_{C-O}			ν_{C-C}			ν_{C-O}			$\nu_{C=C}$		
	ν_{max}	L	k	ν_{max}	L	k	ν_{max}	$E\times10^{-2}$		ν_{max}	$E\times10^{-2}$	
s-Trans configuration												
V. Δ^2-Cyclohexen-1-one	1686 1677	155	71	1617	51	81	1689 1675	110	(8.9)	1621	0.3	(0.03)
VI. 3-Methyl-Δ^2-cyclohexen-1-one	1664 (1676)	135	76	1632	81	67	1680 1672	117	(9.45)	1635	18	(1.53)
VII. 3,5,5-Trimethyl-Δ^2-cyclohexen-1-one	1668	165	120	1635	118	127	1674	110	(9.0)	1637	18	(1.52)
VIII. 2,3-Dimethyl-Δ^2-cyclohexen-1-one	1666	151	106	1635	167	155	1673	103	(8.5)	1635	22	(1.87)
IX. *trans*-3-Methyl-Δ^2-penten-2-one	1669	262	215	1646	290	309	1675	81	(6.64)	1646	17	(1.44)
X. *trans*-3-Ethyl-Δ^2-penten-2-one	1667	177	146	1640	223	258	1675	74	(6.06)	1642	16	(1.34)
s-Cis configuration												
XI. 2-Ethylidene cyclohexanone	1692	17	13	1621	148	103	1693	55	(4.4)	1622	46	(4.08)
XII. 2-(*n*-Butylidene) cyclohexanone	1690	21	21	1617	185	134	1692	56	(4.51)	1620	46	(4.04)
XIII. 5-Methyl-2-isopropylidene-cyclohexanone	1684	28	14	1610	223	50	1685	61	(4.98)	1611	40	(3.51)
XIV. 4-Methyl-Δ^3-penten-2-one	1692	22	19	(1630) 1623	261	127	1693	48	(3.88)	(1636) 1622	72	(6.28)
XV. 3,4-Dimethyl-Δ^3-penten-2-one	1686	38	22	1622	130	42	1689	61	(4.98)	1622	31	(2.66)
XVI. *trans*-3,4-Dimethyl-Δ^2-hexene-2-one	1686	46	11	1623	81	41	1690	60	(4.87)	1625	31	(2.65)

*Inflections are indicated in parentheses in the wavenumber columns.

†For a mole ratio of 0.4 ketone in carbon tetrachloride, approximately equivalent to 3 M.

‡For approximately 0.02 M solutions in tetrachloroethylene. These data are taken from the paper of Mecke and Noack (2).

§The infrared band intensities are recorded in the "practical unit" defined by the Commission on Molecular Structure and Spectroscopy of IUPAC (19). This unit is given by $E_{\nu_1}^{\nu_2}=\int_{\nu_1}^{\nu_2}\epsilon_\nu d\nu$, where $\epsilon_\nu = 1/bc \log_{10}(I_0/I)_\nu$ in which b is the cell length in cm, c is the concentration in moles per liter, and $\log_{10}(I_0/I)$ is the absorbance.

Mecke and Noack employed an intensity unit based on a wavelength abscissa, and their values ($A_{(M)}$) are given in parentheses in the infrared band intensity columns of the table. The IUPAC "practical unit" E and the Mecke unit $A_{(M)}$ are related, in close approximation, by the equation $E = 0.434 A_{(M)} \nu^2_{max}.10^{-4}$.

TABLE II

Solvent effects on the C=O and C=C band positions for *s*-trans ketones*

	Concn. (*M*)	Solvent	Compound V	VI	VII	VIII
C=O band						
Raman	3	CCl_4	1686±2	1664±2	1668±2	1666±2
Infrared	3	CCl_4	1686±1	1666±1	1670±1	1665±1
Infrared	0.02	CCl_4	1689	1680 1672	1674	1670
Infrared	0.02	C_2Cl_4	1689	1680	1674	1673
Infrared	0.02	$CHCl_3$	1687 1669	1662	1665	1656
C=C band						
Raman	3	CCl_4	1617±2	1632±2	1635±2	1635±2
Infrared	3	CCl_4	1618±1	1634±1	1634±1	1633±1
Infrared	0.02	CCl_4	n.m.	1635	1634	1635
Infrared	0.02	C_2Cl_4	1621	1635	1637	1635
Infrared	0.02	$CHCl_3$	n.m.	1633	1635	1632

*Positions of band maxima in cm^{-1}.

NOTE: n.m. = weak band, position not measured.

carbon tetrachloride agree with the measurements on dilute solutions in tetrachloroethylene and the considerable displacements between the infrared and Raman C=O frequencies of the *s*-trans ketones are due more to the concentration difference than to the specific nature of the solvent.

The open-chain *s*-trans ketones IX and X, and 2,3-dimethyl-Δ^2-cyclohexen-1-one (VIII) give Raman C=O bands of normal contour. The C=O bands of the cyclic *s*-trans compounds V–VII, however, exhibit asymmetry of varying degree (Figs. 1–3). This is most apparent for the Raman spectrum of cyclohexenone (Fig. 1), which exhibits a main peak at 1686 cm^{-1} and a shoulder at 1677 cm^{-1} in carbon tetrachloride solution. In chloroform, the relative intensities of these peaks are reversed. On re-examination, the

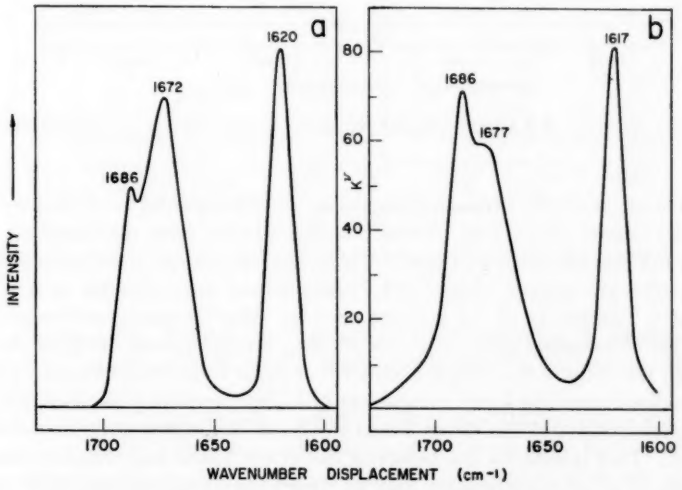

FIG. 1. Raman spectrum of Δ^2-cyclohexen-1-one (V): *a*, in chloroform; *b*, in carbon tetrachloride.

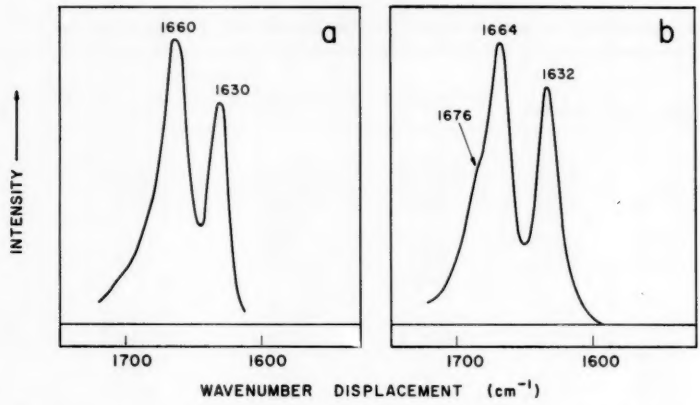

FIG. 2. Raman spectrum of 3-methyl-Δ^2-cyclohexen-1-one (VI): *a*, in chloroform; *b*, in carbon tetrachloride.

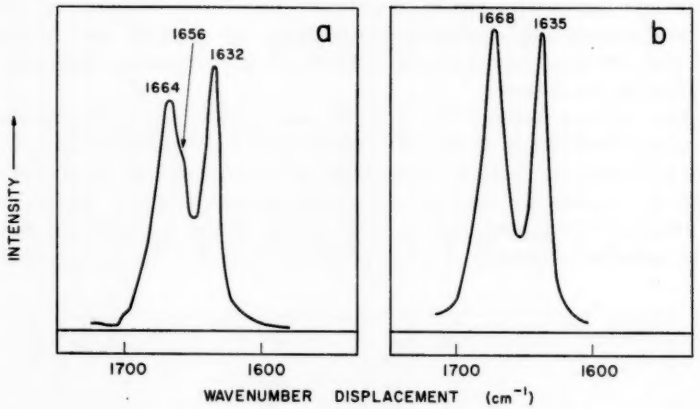

FIG. 3. Raman spectrum of 3,5,5-trimethyl-Δ^2-cyclohexen-1-one (VII): *a*, in chloroform; *b*, in carbon tetrachloride.

infrared spectra of the cyclic *s*-trans ketones demonstrated similar C=O band asymmetry in an enhanced degree (Figs. 4–6). These infrared spectra were measured on a Perkin–Elmer Model 112 spectrometer at a spectral slit width of 1.5 cm^{-1} and were subsequently checked on a nitrogen-purged Model 221 Perkin–Elmer spectrometer at a spectrai slit width of 1 cm^{-1}. The purity of the ketones used for these measurements was established by vapor phase chromatography, and, for all four samples, over 99% of the material passed through the column in a single symmetrical peak. In both the Raman and infrared spectra of cyclohexenone the band component of higher frequency augments in intensity in carbon tetrachloride and the lower frequency band intensifies in chloroform solution. (Figs. 1 and 4). This resembles the behavior noted by Yates and collaborators (13, 14) for derivatives of Δ^2-cyclopentenone and by Jones and collaborators (15) for α,β-unsaturated lactones and cyclic unsaturated acid anhydrides. The asymmetry of VI follows

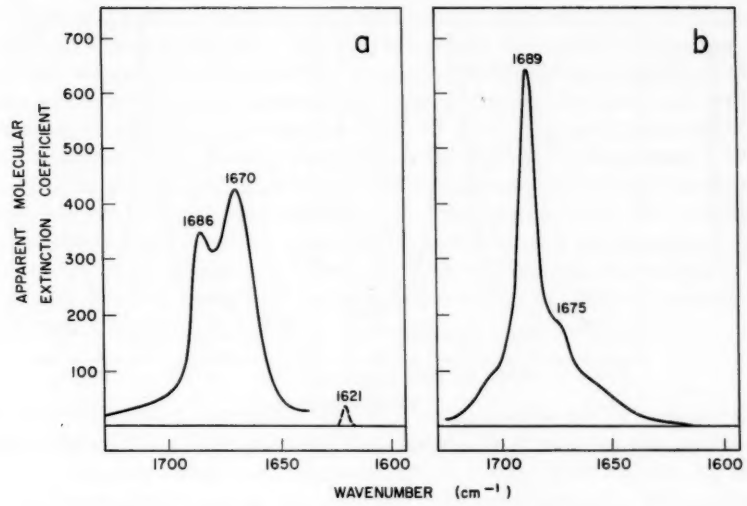

FIG. 4. Infrared spectrum of Δ^2-cyclohexen-1-one (V) (C=C band measured on liquid film): *a*, in chloroform; *b*, in carbon tetrachloride.

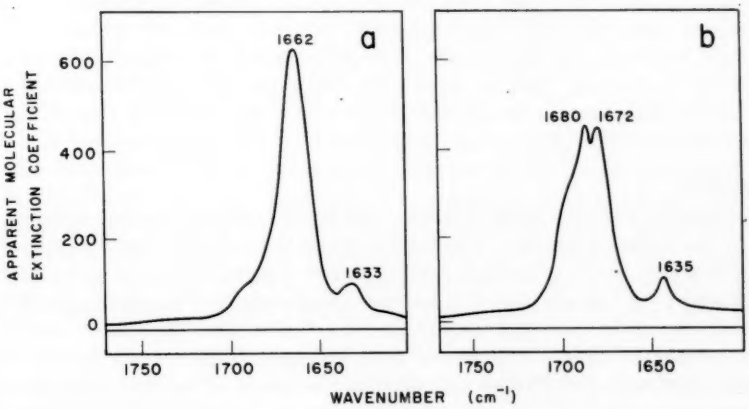

FIG. 5. Infrared spectrum of 3-methyl-Δ^2-cyclohexen-1-one (VI): *a*, in chloroform; *b*, in carbon tetrachloride.

the same pattern as V, though the high-frequency component is weaker. The spectra of VII differ in that the asymmetry is more pronounced in chloroform than in carbon tetrachloride.

The failure to observe any C=O band asymmetry for VIII supports the view that the partial structure XVII, with a free α-hydrogen atom, is required for this effect, and it is commonly presumed that this solvent-sensitive C=O band splitting is caused by a Fermi resonance with the overtone of the α-C—H out-of-plane deformation vibration.

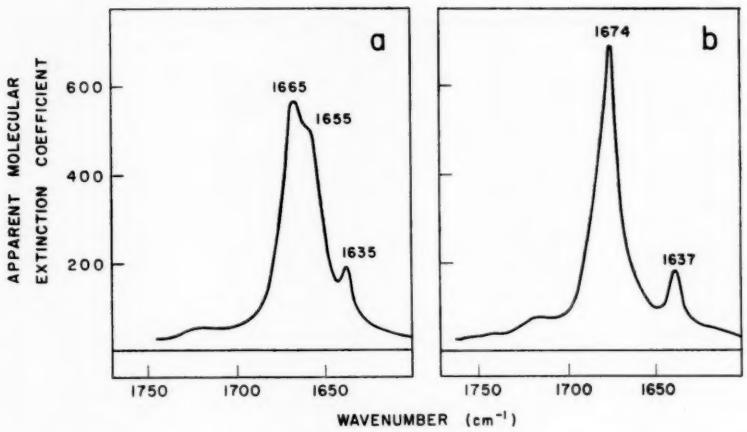

FIG. 6. Infrared spectrum of 3,5,5-trimethyl-Δ^2-cyclohexen-1-one (VII): *a*, in chloroform; *b*, in carbon tetrachloride.

The absence of the carbonyl doublet from the spectra of the *s*-cis cyclic ketones XI and XII is in conformity with the failure to observe it for exocyclic unsaturated lactones, such as XVIII, which have been studied in the infrared by Brügel (16).

XVII

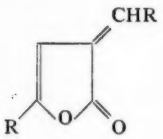

XVIII

Band Intensities

The relationships between band intensity and steric configuration are different for the Raman and the infrared spectra. The intensities of the infrared C=O bands of all the conjugated ketones lie in a comparatively narrow range. The *s*-cis compounds have weaker infrared C=O bands than the *s*-trans compounds, but no significant differences are noted between cyclic *s*-cis and open-chain *s*-cis compounds. The cyclic *s*-trans ketones have more intense infrared C=O bands than the open-chain *s*-trans ketones but this may be associated with the doublet character of the bands of the cyclic compounds.

The intensities of the infrared C=C stretching bands are more variable and the bands for the *s*-cis compounds are significantly stronger than for the *s*-trans. The extreme weakness of the infrared C=C band in Δ^2-cyclohexenone is particularly remarkable.

In the Raman spectra the band area coefficients of the C=C bands vary from 51 units for V to 290 units for IX but the variations do not fall into any distinguishable classes in terms of conformation or cyclization. The Raman C=O band intensities, on the contrary, show marked stereochemical specificity, and the *s*-trans C=O bands (135–263 units) are from 5 to 10 times more intense than the *s*-cis bands (17.5–46 units). In terms of peak heights, the relationships are similar, though the band area measurements for the doublet carbonyl bands of V–VII group more closely with VIII–X than do the peak height measurements.

These Raman band intensities can be compared with data in the literature for C=O and C=C groups in non-conjugated systems. An extensive study of the Raman C=C stretching bands of mono-olefins by Rea (10) has shown that alkyl substitution has little effect and the integrated intensities fall in the range 30–50 when converted to units that are comparable with ours.* Conjugation with the ketone therefore raises the Raman C=C stretching band intensity by a factor of 5 to 10. According to Michel and Duyckaerts (8) the peak heights of the Raman C=O bands for saturated ketones fall in the range 10–13 in our units, reducing to approximately 8–10 units when corrected for polarization convergence effects. In the *s*-cis configuration, conjugation with the ethylene bond enhances the C=O band intensity slightly, and in the *s*-trans configuration it is raised by a factor of about 10. Mecke and Noack (2) have pointed out previously that for the infrared spectra the C=O intensity for *s*-cis ketones may actually be weaker than for comparable non-conjugated systems.

DISCUSSION

The four distinguishing features of the *s*-cis configuration are (*a*) greater frequency separation between the C=O and the C=C stretching bands in comparison with the *s*-trans; (*b*) the greatly diminished intensity of the Raman C=O band; (*c*) the lesser, but still significant diminution in the infrared C=O band intensity; (*d*) the increase in the infrared C=C band intensity. It is difficult to account for all these effects by any simple and self-consistent mechanism.

In both the *s*-cis and the *s*-trans configurations, the C=O and the C=C band frequencies are displaced downwards from their positions in non-conjugated systems carrying comparable substituents. Assuming, for the time being, that the two frequencies are not vibrationally coupled, it follows that both the C=O and the C=C bonds have reduced force constants in the conjugated system, presumably because of the mesomeric effect. This in turn must lead to charge displacements on the terminal atoms, and the polarized *s*-cis structure XIX will then be further stabilized by a direct field interaction between the ends of the conjugated system. This could lead to an additional lowering of both the C=O and the C=C frequencies in comparison with the *s*-trans frequencies. If it is assumed that change in bond polarization with bond length increases in systems where the bond is more highly polarized in the equilibrium position, both the *s*-cis C=O and the *s*-cis C=C infrared bands should be intensified by this field effect. This is consistent with the observed changes for the C=C band, but not for the C=O band.

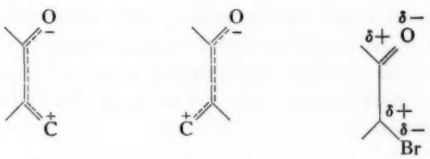

XIX XX XXI

The closer proximity of the terminal charges for XIX in comparison with XX may also induce mutual perturbations of the C=O and C=C bond polarizations of a more direct type, and these are considered by Erskine and Waight (3) to have the major effect

**Rea's intensities are based on the use of an external standard and a wider Raman tube. One of his intensity units is approximately equivalent to one hundred of ours (10).*

in influencing the C=O and C=C band intensities. Such direct field effects can be quite large, as is well recognized in systems such as XXI where the C—Br dipole induces an upward displacement of 20 cm^{-1} in the C=O frequency, and also diminishes the intensity (17). Regarded from this point of view, the dipole interaction in XIX should produce an opposite effect on the C=O band than does the C—Br group, since the direction of the dipole is reversed. On this basis we would also expect both the C=O and the C=C infrared bands to be intensified and displaced to lower frequency in the *s*-cis configuration. It is therefore difficult in these terms to account for the diminished intensity and upward frequency displacement of the *s*-cis C=O infrared band.

The Raman band intensities, being dependent on the change in the bond polarizability during the vibration, might be expected to vary with the electron density in the bond and should, therefore, be increased by factors that increase the degree of double-bond character. The very low intensity of the Raman C=O band in the *s*-cis configuration would then indicate a high charge displacement at the equilibrium bond length. However, Michel and Duyckaerts (8) have shown that in general the Raman and infrared C=O band intensities vary in the same sense, and not inversely, and more extensive investigations are obviously needed to clarify the relationships between bond polarization and bond polarizability in conjugated systems.

These difficulties may in part be due to the fact that the C=O and C=C stretching bands should not be regarded as localized vibrations. Since the separation between the two bands is less in the *s*-trans than the *s*-cis form, the vibrational coupling will be greater for *s*-trans isomers. As the unperturbed C=O and C=C frequencies approach the same value, the character of the vibrations will change from localized double-bond stretching modes to in-phase and out-of-phase coupled modes extending through the conjugated system. In the limit the bands will become analogues of the doublet C=O band systems of acid anhydrides and peroxides. The over-all pseudosymmetry of the conjugated system may then become an important factor in determining the relative intensity of the two bands, as Bellamy and collaborators have suggested for the anhydride and peroxide systems (18). There may be a minimum separation distance between the observed "C=O" and "C=C" frequencies below which the coupling becomes strong enough to force the frequencies apart again. It is not suggested that these are the *dominant* factors in the conjugated systems considered here, and the fact that the band at higher frequency is much more sensitive to solvent effects (particularly in the trans configuration) is a good indication that this band is predominantly carbonylic while the band at lower frequency is predominantly ethylenic (Table II). Nevertheless, considerations of this kind must be kept in mind when one is dealing with vibrational modes of conjugated systems. Analogies with substitutional effects in non-conjugated carbonylic and olefinic systems, must be made with caution, particularly when attempts are made to consider the substitution effects quantitatively, as, for example, by correlating them with Taft or Hammett sigma parameters.

ACKNOWLEDGMENTS

We wish to thank the Cyanamid European Research Institute for providing facilities for vapor phase chromatography and for the use of the Model 221 spectrophotometer. We are also grateful to Mrs. M. A. MacKenzie and Dr. J. W. Elliott for measuring four Raman and infrared spectra at Ottawa.

REFERENCES

1. R. MECKE and K. NOACK. Spectrochim. Acta, **12**, 391 (1958).
2. R. MECKE and K. NOACK. Chem. Ber. **93**, 210 (1960).
3. R. L. ERSKINE and E. S. WAIGHT. J. Chem. Soc. 3425 (1960).
4. C. J. TIMMONS. Proceedings of the IVth International Meeting of the European Molecular Spectroscopy Group, Bologna, Italy. 1959. In press.
5. K. NOACK and R. N. JONES. Can. J. Chem. This issue. p. 2225.
6. H. J. BERNSTEIN and G. ALLEN. J. Opt. Soc. Am. **45**, 237 (1955).
7. D. G. REA. J. Opt. Soc. Am. **49**, 90 (1959).
8. G. MICHEL and G. DUYCKAERTS. Spectrochim. Acta, **10**, 259 (1958).
9. L. A. WOODWARD and J. H. B. GEORGE. Nature, **167**, 193 (1951).
10. D. G. REA. Anal. Chem. **32**, 1638 (1960).
11. D. G. REA. J. Mol. Spectroscopy, **4**, 507 (1960).
12. D. COOK. Can. J. Chem. **39**, 1184 (1961).
13. P. YATES, N. YODA, W. BROWN, and B. MANN. J. Am. Chem. Soc. **80**, 202 (1958).
14. P. YATES, and L. L. WILLIAMS. J. Am. Chem. Soc. **80**, 5896 (1958).
15. R. N. JONES, C. L. ANGELL, T. ITO, and R. J. D. SMITH. Can. J. Chem. **37**, 2007 (1959).
16. W. BRÜGEL, K. DURY, G. STENGEL, and H. SUTER. Angew. Chem. **68**, 440 (1956).
17. R. N. JONES, D. A. RAMSAY, F. HERLING, and K. DOBRINER. J. Am. Chem. Soc. **74**, 2828 (1952).
18. L. J. BELLAMY, B. R. CONNELLY, A. R. PHILPOTTS, and R. L. WILLIAMS. Z. Elektrochem. **64**, 563 (1960).
19. International Union of Pure and Applied Chemistry, Comptes Rendus de la Vingtième Conférence. Vol. 20. Butterworths Scientific Publications, London. 1959. p. 187.

CONFORMATIONAL EQUILIBRIA IN DIETHYL KETONE[1]

R. NORMAN JONES AND K. NOACK[2]

ABSTRACT

A variable-thickness, variable-temperature absorption cell, modified from the design of Holden, Taylor, and Johnston, has been used to compare the infrared spectrum of diethyl ketone at −75° and +25° C. The Raman spectrum of diethyl ketone has also been measured at +6°, +25°, and +85° C, and the proton magnetic resonance spectrum over the range −61° to 104° C.

Both the infrared and Raman spectra exhibit pronounced temperature sensitivity, which is attributed to the presence of at least two conformational isomers in the liquid phase. Possible structures for these isomers are considered. Small but significant chemical shifts are noted in the proton magnetic resonance spectrum.

The vibrational spectra of large molecules are particularly difficult to interpret when the substance exists as a mixture of conformational isomers in the liquid state; to analyze such spectra it is first necessary to recognize the presence of the equilibria and to sort out the bands belonging to the different forms. This may sometimes be done by comparison with the spectrum of the crystalline solid, since only one conformational form will normally be present in the crystal lattice. The solid phase spectra, however, may be perturbed by intermolecular force fields and hydrogen bonding. In the liquid phase the equilibrium between the conformational isomers is usually temperature sensitive and the spectra of the isomers can be differentiated by noting the relative changes in the band intensities with temperature.

Cells suitable for such measurements tend to become complicated, particularly if it is desired to control the temperature with some accuracy, and to make measurements at temperatures that depart appreciably from those obtainable with simple cryostatic systems. In this paper we describe a cell suitable for the measurement of infrared spectra over a wide range of temperature, and discuss its use to investigate conformational equilibria in diethyl ketone.

EXPERIMENTAL

The variable-temperature infrared absorption cell is illustrated in Figs. 1 and 2. It is based on the excellent design of Holden, Taylor, and Johnston (1), but is intended only for use above −190°; this permits a simplification of the cell proper and of the gear mechanism and controls for varying the sample thickness without breaking the vacuum. The apparatus is portable and the cell fits conveniently into the 14-cm working space of the Perkin–Elmer Model 21 and Model 112 spectrometers.

The cell proper consists of a pair of silver chloride windows (2.5-cm diameter) sealed by Teflon washers and separated by one convolution of a soft bronze bellows, which is soldered to fixed and moveable units of the cell body. Motion is provided by means of a worm drive attached through a universal joint to the control shaft, which passes out through the top of the vacuum chamber through a vacuum seal. The maximum cell window separation is about 1 mm. The cell assembly is held vacuum tight by a steel spring and three set screws, as shown in the exploded section of the diagram in Fig. 2. A copper–constantan thermocouple is inserted in a hole in one of the silver chloride

[1]*Manuscript received June 21, 1961.*
Contribution from the Division of Pure Chemistry, National Research Council, Ottawa, Canada.
Issued as N.R.C. No. 6514.
[2]*National Research Council of Canada Postdoctorate Fellow.*

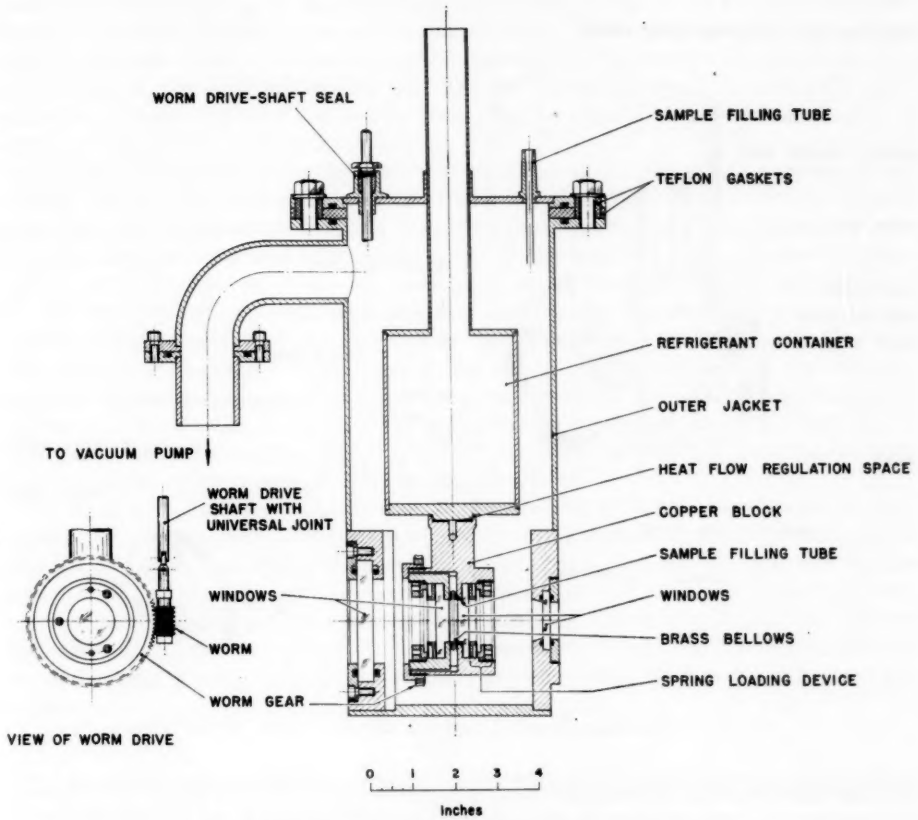

FIG. 1. Variable-temperature infrared cell. General diagram.

windows, with the leads passing out through the top of the cell. The cell unit is attached by a heavy copper bar to the coolant chamber. As in the design of Holden, Taylor, and Johnston, a transverse slot is milled into the neck of the copper bar, and provision is made for the slot to be filled with hydrogen to raise the heat conduction; alternatively the slot cavity can be evacuated for maximal thermal insulation of the cell unit. A 100-watt heating coil is wrapped around the cell proper so that temperatures above the cryostatic control temperature can be maintained.

The cell unit is mounted in an outer container which can be evacuated with an oil diffusion pump. This pump, not shown in the diagram, is welded directly to the wide vacuum connection tube of the lower component of the outer jacket. The apparatus is demountable, the inner cell unit being attached to the upper portion of the outer container through which pass all access tubes and controls except the evacuation outlet. The upper unit is bolted to the lower unit by a flange. The two sections of this flange are separated by a Teflon ring to improve the thermal insulation. The inner cell unit is constructed of copper and the outer vessel of brass, while stainless steel is used for all metal sections in which heat transfer is to be avoided. A mechanical backing pump, a

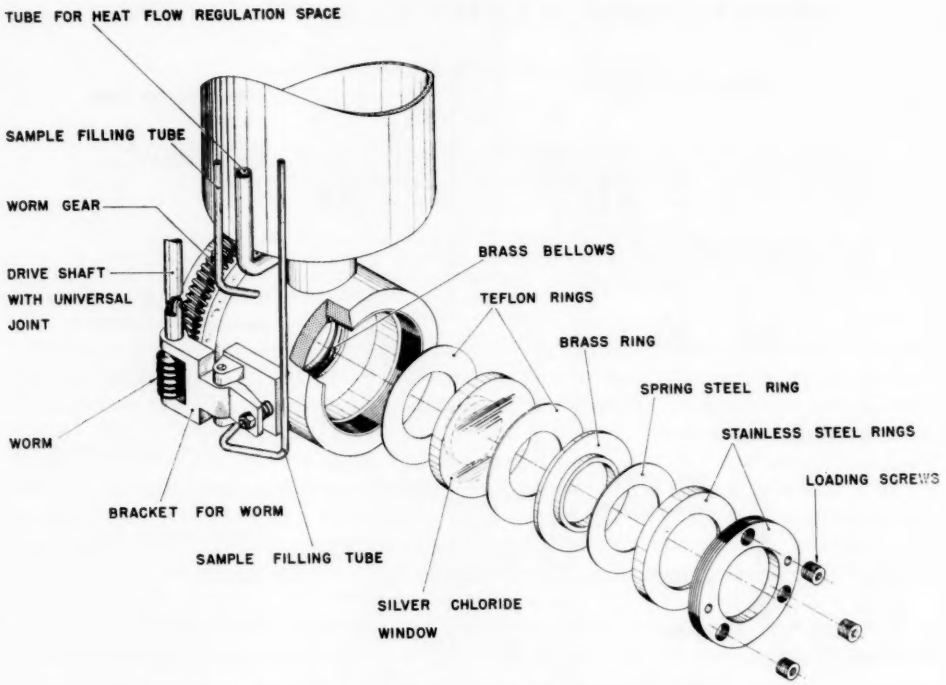

FIG. 2. Variable-temperature infrared cell. Details of inner cell structure.

Phillips vacuum gauge, a potentiometer, and a control Variac for adjusting and monitoring the temperature and pressure in the cell are mounted separately on a portable carriage which permits the cell to be used conveniently with different spectrometers.

For low-temperature measurements in solution, carbon disulphide can be used to $-100°$. For the range 1500–1300 cm^{-1}, where carbon disulphide is opaque, a ternary mixture of carbon tetrachloride, chloroform, and tetrachloroethylene in proportions of 58:36:6 by volume can be used to $-80°$, and a binary mixture of carbon tetrachloride and tetrachloroethylene (70:30), to $-58°$. The latter solvent mixture has superior transparency, particularly near 1450 cm^{-1}.

In precision low-temperature infrared spectrophotometry there are several sources of systematic error that need to be considered. Allowance must be made for the change in concentration due to the increase in the density of the cooled solution, and a small additional error, of opposite sign, may be introduced by the linear contraction of the cell thickness. In these investigations the density of the solvent was measured at $-75°$ and the extinction coefficients were adjusted proportionately; it was assumed that the densities of the solutions and the solvent did not differ significantly. No correction was applied for the cell-length contraction.

In the Perkin–Elmer Model 112 spectrometer, the beam chopper is located between the cell and the detector. Under these conditions rotation of the chopper may induce a

pulsed temperature change at the tuned amplifier frequency due to the fact that when the chopper interrupts the beam, the thermocouple "sees" black-body radiation at a temperature different from that radiated by the cooled cell. This would manifest itself as a displacement of the zero-transmission line. For the region between 1500 and 1350 cm^{-1} this source of error has been checked by observing the apparent transmission through a 1-mm path length of carbon disulphide at $+25°$ and $-75°$ C. In this wavenumber range carbon disulphide is almost totally absorbing and can be used as a temperature-variable shutter. The displacement of the zero-transmission curve with cooling did not exceed 2%, and the photometric errors due to this cause were considered negligible though they could become appreciable in other regions of the spectrum and at lower temperatures. It was also observed that with 1-mm path length of cooled carbon disulphide in the cell the zero-transmission line was not significantly displaced when an opaque shutter, at room temperature, was placed either between the cell and the entrance slit of the spectrometer, or between the source and the cell.* In the discussion of the infrared spectrum of diethyl ketone which follows we are concerned only with relative changes in the intensities of neighboring bands, but the factors considered above will have to be investigated more thoroughly before attempts are made to evaluate absolute infrared band intensities at depressed or elevated temperatures.

The Raman spectra were measured on a Cary Model 81 spectrophotometer. Room-temperature spectra were obtained with an internal carbon tetrachloride standard, using the technique described previously (2) except that a 5-ml Raman tube was used in place of the capillary tube and the convergent errors were not corrected with a polarizer. Depolarization ratios were measured by the method of Edsall and Wilson (3) and are also uncorrected for convergence. Raman spectra at $+6°$ and $+85°$ were obtained by surrounding the Raman tube with a jacket through which cooled or heated water was circulated.

RESULTS

The positions and intensities of both the infrared and Raman spectra, measured at room temperature, are summarized in Table I.

At room temperature, diethyl ketone exhibits a series of six infrared bands at 1461, 1454, 1414, 1379, 1355, and 1327 cm^{-1} (bands A–F of Fig. 3). These were investigated in carbon tetrachloride solution by Nolin and Jones (4), and from a comparative study of the spectra of selectively deuterated derivatives it was established that bands A, B, and D involve methyl group vibrations while C and E are associated with methylene groups. These investigators did not discuss the weak band F at 1320 cm^{-1} but it is evident from their published spectra that this also is a methylene band. The infrared spectrum of diethyl ketone in the ternary solvent mixture at $+25°$ and $-70°$ is shown in Fig. 3. The spectra of the pure liquid at room temperature and of the solid at $-75°$, measured under slightly lower resolution, are compared in Fig. 4, and the Raman spectrum in the presence of 9% by weight of carbon tetrachloride, measured at $+25°$, is shown in Fig. 5.

With falling temperature, most of the bands sharpen because of thermal solvent effects, and caution is necessary to distinguish this from the more fundamental effects of temperature on the molecular structure of the solute. Band C at 1414 cm^{-1} splits into a doublet in the cooled solution (Fig. 3) and it is clear from the shape of the band envelope that this is a real change and not merely a consequence of the band sharpening. The other

*We wish to thank Dr. R. Ripley for making these measurements.

TABLE I

Infrared and Raman spectra of diethyl ketone at room temperature

Infrared spectrum*		Raman spectrum†		
ν_{max} (cm^{-1})	ϵ_{max}*	ν_{max} (cm^{-1})	k_{max}	$\rho_{apparent}$
n.m.	—	216	0.3	0.65
310	12	307	0.3	0.75
408	2.8	406	8.2	0.44
—	—	468	0.2	—
525	2.4	526	0.4	0.5
—	—	580	0.1	—
620	3.5	621	0.5	0.74
—	—	748	4.3	0.27
784	4	784	5.1	0.31
810	21	(812)	0.4	—
939	20	944	1.2	0.87
955	31	960	1.5	0.90
1008	12	—	—	—
(1014)	—	1017	4.0	0.61
1094	19	1097	9.3	0.27
1120	63	(1121)	0.7	—
1167	18	1174	0.2	—
1240	4	1238	2.0	0.86
1327	3	1329	0.5	0.50
1358	60	—	—	—
1380	83	(1384)	0.7	—
1414	56	1421	8.8	0.83
1455	23	—	—	—
1461	109	1463	10.3	0.90
1718	206	1717	9.4	0.45
—	—	2788	2.7	—
(2883)	40	(2890)	18	—
2902	45	2908	47	0.33
2936	65	2945	65	0.29
2977	95	2984	30	0.72

NOTE: n.m. = region not measured.

*The infrared spectra were measured in carbon tetrachloride (3000–1300 cm^{-1}), carbon disulphide (1300–650 cm^{-1}), and *n*-hexane (650–300 cm^{-1}) using a Perkin–Elmer Model 112 single-beam spectrometer with CaF_2, NaCl, and CsBr prisms, under the standard operating conditions of the laboratory (9).

†See experimental section.

pair of methylene bands also shows significant changes. The peak at 1355 cm^{-1} shifts to 1362 cm^{-1} with a shoulder remaining at 1355 cm^{-1}, and the absorption at 1325 cm^{-1} intensifies. Comparison with the changes in the solid phase spectrum (Fig. 4) also suggests that real structural changes in the molecule are involved. The changes in the methyl bands are more difficult to assess. The intensification of band D without frequency displacement is probably only a thermal effect. Bands A and B are both more clearly resolved in the low-temperature spectrum, but the ratio of the peak intensities is not significantly altered. In the spectrum of the solid the most notable change is the complete disappearance of the 1355 cm^{-1} band, the development of the 1333 cm^{-1} maximum, and the profound change in the methyl absorption between 1475 and 1440 cm^{-1}.

The Raman spectrum, shown in Fig. 5, is less informative in the 1500–1300 cm^{-1} region, as the bands are less well resolved. The absence of the 1375 cm^{-1} band is in accord with the well-established fact that the symmetrical C—H bending mode of the methyl group is Raman inactive in aliphatic hydrocarbons.

Spectra in Other Regions

Apart from noting their complexity, Nolin and Jones did not discuss the spectra of the

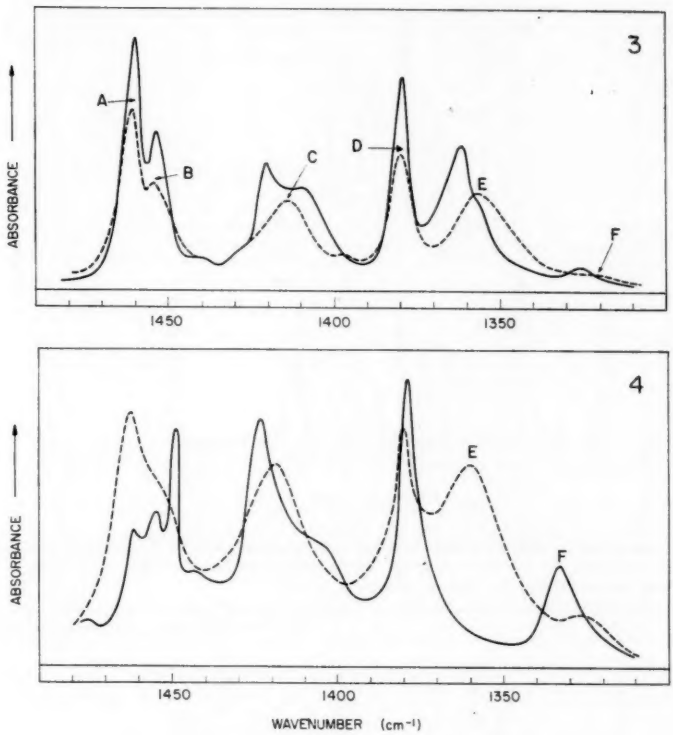

FIG. 3. Infrared spectrum of diethyl ketone. The effect of temperature on 1500–1300 cm^{-1} region in $CCl_4/C_2Cl_4/CHCl_3$ solution at 0.3 *M* concentration. —— −70° C; - - - +25° C.

FIG. 4. Infrared spectrum of diethyl ketone. Comparison of spectra in liquid and solid phases over the range 1500–1300 cm^{-1}. —— solid at −75° C; - - - liquid at +25° C.

deuterated diethyl ketones below 1300 cm^{-1}. The infrared and Raman spectra shown in Figs. 5–7 exhibit a number of temperature-sensitive bands; particularly notable is the highly polarized pair of Raman bands at 784 and 748 cm^{-1}, which reverse in relative intensity at +85°. The most significant temperature effect in the infrared spectrum is the weakening of the 1167 cm^{-1} and the 939 cm^{-1} bands in the cooled solution, and the disappearance of these bands from the spectrum of the solid.

The carbonyl stretching band, measured in the ternary solvent mixture at 0.3 *M* concentration, is symmetrical, with a maximum at 1761 cm^{-1} at 25° C. When the solution is cooled to −75° the maximum shifts to 1710 cm^{-1} with no significant change in the band shape. Such a solvent–temperature shift is normal to a monomolecular species and discounts dimolecular association as an explanation for the behavior of the other temperature-sensitive bands. The band is at 1710 cm^{-1} for the solid at room temperature. In the C—H stretching region both the infrared and the Raman spectra exhibit the four bands that have been discussed previously and none show significant temperature sensitivity.

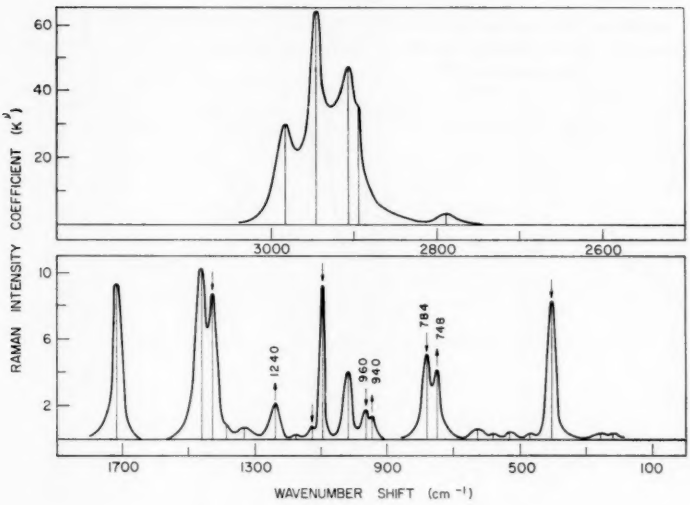

FIG. 5. Raman spectrum of diethyl ketone at room temperature (+25° C). The measured band positions and intensities are indicated by the vertical lines. The band contours are diagrammatic only. Bands which intensify on heating are indicated by upward pointing arrows.

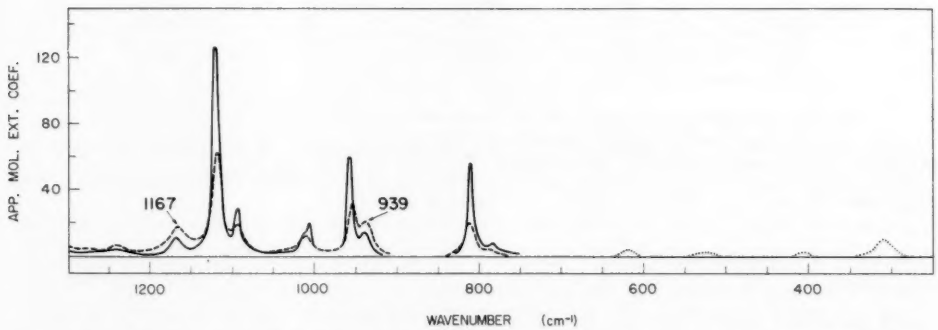

FIG. 6. Infrared spectrum of diethyl ketone in the range 1300–280 cm^{-1}. —— CS_2 solution, −75° C, 0.35 *M*; - - - CS_2 solution, +25° C, 0.35 *M*; . . . *n*-C_6H_{14} solution, +25° C, 0.78 *M*.

DISCUSSION

The flexibility of the diethyl ketone molecule permits great freedom for conformational variation, and any attempt to relate these spectral changes to the molecular structure must, of necessity, be speculative. Assuming restricted rotation about the CO—CH_2 bonds, but free rotation about the C—CH_3 bonds, the four conformational structures I–IV can be written for diethyl ketone. They all possess either a plane of symmetry, a twofold axis of symmetry, or both. There are, in addition, innumerable forms with C_s symmetry which may be visualized as derived from I by the synchronous rotation of the C—Et bonds in the same direction; after rotation through 180°, structure IV is

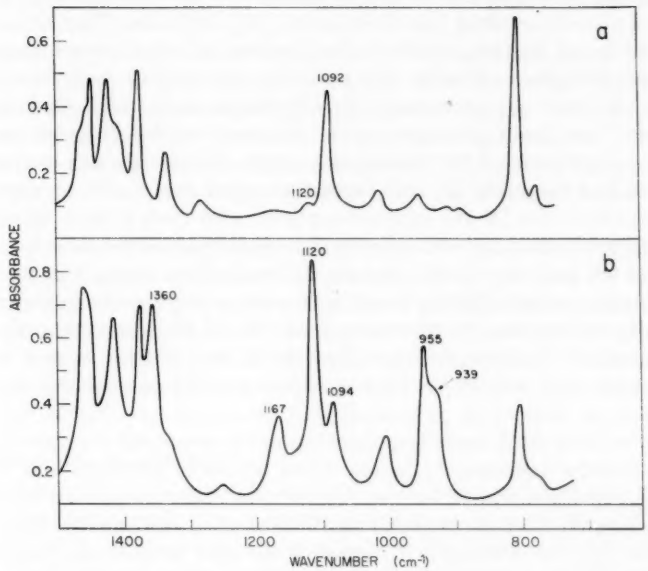

FIG. 7. Infrared spectrum of diethyl ketone. Comparison of the spectra in the solid (*a*, −75° C) and liquid (*b*, +25° C) phases over the range 1500–700 cm^{-1}.

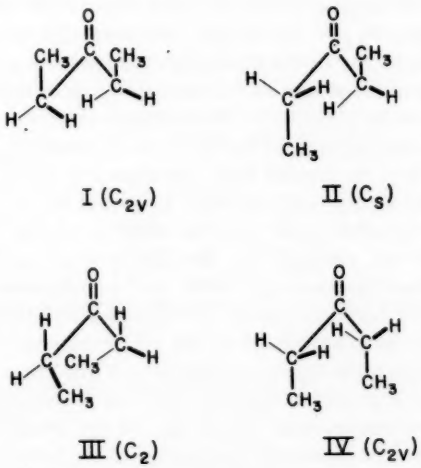

reached. If the C—Et bonds of I are synchronously rotated in opposite directions an infinite set of C_2 structures is obtained, a 120° rotation corresponding to III while an 180° rotation again produces IV. Unequal rotation of the C—Et bonds in either direction will produce skew structures with no symmetry elements save identity.

Sirkar and Bishui (5) consider that the presence of a totally depolarized Raman

band with a depolarization ratio close to the theoretical maximum of 0.857 is acceptable as evidence for a plane or twofold axis of symmetry in a molecule. They noted such bands in the spectra of liquid acetone, methyl ethyl ketone, and di-*n*-propyl ketone, but not in diethyl ketone. We observed bands in the Raman spectrum of diethyl ketone at 1463, 1238, 960, and 944 cm^{-1} with measured depolarization ratios of 0.90, 0.86, 0.90, and 0.87 respectively, but the significance to be attached to these figures depends very critically on the magnitude of the convergence error. When this was evaluated by the method of Rank and Kagarise (6), our correction curve was found to slope much less steeply than that reported by the original authors, who used a lamp of different geometrical form. In particular, our correction was negligibly small for measured depolarization ratios above 0.8 and large (>0.2) for strongly polarized bands. Our measurements, therefore, lead us to conclude that at least four bands in the Raman spectrum of diethyl ketone are totally depolarized. Furthermore, it is difficult to believe that diethyl ketone would exist exclusively in skew conformations while such closely related molecules as methyl ethyl ketone and di-*n*-propyl ketone possess a plane of symmetry, or a twofold axis of symmetry, or both.

In the present state of our knowledge, caution must be exercised in attaching structural significance to "totally depolarized" bands. More accurate techniques for the absolute measurement of depolarization ratios are needed, and experience must be acquired in interpreting their significance in connection with the normal vibrations of large molecules.

This discussion will be developed in terms of the four structures illustrated above which, from symmetry considerations, must approximate closely to conformations of minimum or maximum energy. Displacements may occur to minimize the non-bonded hydrogen–hydrogen and hydrogen–oxygen interactions but unless the molecule is thermally excited these should be small; they are more likely to be symmetrical than skew.

The spectrographic data do not distinguish unequivocally among the structures I–IV, but there are no features of the liquid phase spectra that are inconsistent with a simple equilibrium between two of these species. Structure IV can be rejected on thermodynamic grounds, because of the close packing of the hydrogen atoms of the methyl groups. The non-bonded interaction energies will undoubtedly be minimal for III, in which the methyl groups project forward and backward from the plane of the C—CO—C skeletal unit. Structure III would accordingly seem strongly preferred in the liquid phase. Structural significance is undoubtedly associated with the splitting of the 1415 cm^{-1} band into the 1420, 1410 cm^{-1} doublet on cooling. The displacement of this α-methylene scissoring band from its unperturbed position near 1467 cm^{-1} in aliphatic hydrocarbons depends on its steric relation to the carbonyl group. The appearance of the two peaks at low temperature favors II for the form stabilized at low temperature in the liquid phase, as this is the only structure in which the steric environment of the two methylene groups differs. The 1410 cm^{-1} frequency approaches closely to the low α-methylene scissoring frequency of 1406 cm^{-1} in cyclopentanone, with which one of the α-methylene groups of II has configurational similarity. The increased complexity of the methylene wagging absorption at 1362, 1355, and 1327 cm^{-1} in the cooled solution is also consistent with this structure. Splitting of the α-methylene scissoring band could come about through an in-phase and out-of-phase coupling between the scissoring modes of the two methylene groups provided they are suitably located relative to one another. This might be realized in I, but this structure is not preferred in the liquid phase because there will be appreciable non-bonded repulsion between the eclipsed hydrogens of the two methylene groups which occupy

1,3 positions (7); there will also be repulsion between the methyl groups and the oxygen atom.

In so far as the solid is concerned, it is unfortunate that no X-ray diffraction measurements have yet been made, and recent attempts to prepare single crystals suitable for such analysis have been unsuccessful (8). The planar zig-zag structure (I) would pack more conveniently into a lattice and this entropy factor could favor I for the crystal in spite of the objections in the preceding paragraph. Its higher C_{2v} symmetry is also in accord with the much simpler infrared spectrum of the solid in comparison with the cooled liquid (Fig. 5).*

In summary, these spectrographic measurements indicate that diethyl ketone exists as an equilibrium mixture of at least two conformational forms in the liquid state. It is not possible to identify the particular structures involved, and the flexibility of the molecule would permit innumerable skew structures of low symmetry. Certain aspects of the spectra are most simply reconciled with the requirements of conformational stability by an equilibrium between structures II and III in which II predominates at low temperatures. The ketone may crystallize as II or possibly as I.

Proton Magnetic Resonance Spectrum

The n.m.r. spectrum of diethyl ketone has also been measured at a concentration of 5 mole% in cyclopentane over a temperature range from −61° to 104° C, using tetramethylsilane as an internal frequency standard. The spectrum exhibits the quartet and triplet band systems characteristic of the methylene and methyl groups. The band contours exhibit no significant changes with temperature but the centers of the band systems are displaced, the methylene signals moving to higher field and the methyl signals to lower field with increasing temperature (Table II). Though the shifts are not directly

TABLE II

Temperature effects on the proton magnetic resonance spectrum of diethyl ketone

Temperature (°C)	Proton chemical shift*		
	Methylene	Methyl	Difference
−61	139.5	57.0	82.5
+28	137.0	59.0	78.0
+60	138.0	60.0	78.0
+104	134.5	60.0	74.5

*Measured in cycles per second at 60 Mc/sec relative to tetramethylsilane at 5 mole% concentration in cyclopentane.

interpretable in terms of molecular structure, they are not inconsistent with the changes in the vibrational spectra.

ACKNOWLEDGMENTS

We wish to thank Mr. J. R. Nicholson for measuring the n.m.r. spectrum and to acknowledge our appreciation to Dr. W. G. Schneider and Dr. A. W. Hanson for helpful discussion in connection with n.m.r. and X-ray spectroscopy.

**The band at 1120 cm^{-1} calls for comment. This appears to intensify on cooling of the solution (Fig. 6) but virtually disappears from the infrared spectrum of the cooled solid (Fig. 7).*

REFERENCES

1. R. B. HOLDEN, W. J. TAYLOR, and H. L. JOHNSTON. J. Opt. Soc. Am. **40**, 757 (1950).
2. K. NOACK and R. N. JONES. Can. J. Chem. This issue. p. 2201.
3. J. T. EDSALL and E. B. WILSON. J. Chem. Phys. **6**, 124 (1938).
4. B. NOLIN and R. N. JONES. J. Am. Chem. Soc. **75**, 5626 (1953).
5. S. C. SIRKAR and B. M. BISHUI. Indian J. Phys. **20**, 35 (1946).
6. D. H. RANK and R. E. KAGARISE. J. Opt. Soc. Am. **40**, 89 (1950).
7. D. H. R. BARTON and R. C. COOKSON. Quart Revs. (London), **10**, 44 (1956).
8. A. W. HANSON. Personal communication.
9. R. N. JONES. Spectrochim. Acta, **9**, 235 (1957).

CONFORMATIONAL EQUILIBRIA IN OPEN-CHAIN α,β-UNSATURATED KETONES[1]

K. NOACK[2] AND R. NORMAN JONES

ABSTRACT

The infrared and Raman spectra of *trans*-Δ^3-penten-2-one have been measured over the temperature range +30° to −75° and +85° to +5° respectively. The temperature-dependent changes observed in the spectra indicate that this ketone exists as an equilibrium mixture of *s*-cis and *s*-trans conformational isomers in the liquid state. The *s*-trans form is the more stable and is present exclusively in the crystalline solid.

Similar measurements have been carried out on Δ^3-buten-2-one. The infrared and Raman spectra of this ketone also exhibit temperature effects that can be explained by a similar equilibrium, though the evidence is not as conclusive as for *trans*-Δ^3-penten-2-one.

The influence of alkyl substitution at the α- and β-carbon atoms on the relative stability of the *s*-cis and *s*-trans forms of α,β-unsaturated ketones is discussed.

INTRODUCTION

The *s*-cis (I) and *s*-trans (II) conformations of open-chain α,β-unsaturated ketones can be distinguished from the positions and intensities of the C=O and C=C stretching

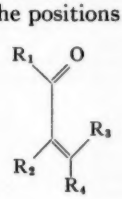

I

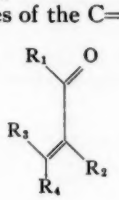

II

bands in the infrared (1–4) and Raman (5) spectra. In the liquid state most conjugated ketones exist predominantly or perhaps exclusively in one or other of the two conformations, but Mecke and Noack (2) have observed that the infrared spectrum of *trans*-Δ^3-penten-2-one (III*a*) and related compounds (III*b*–III*d*) exhibit two carbonyl bands near 1700 cm^{-1} and 1680 cm^{-1} in tetrachloroethylene solution. The positions of these bands

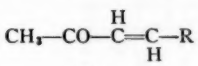

III

(*a*) R = $-CH_3$
(*b*) R = $-CH_2-CH_3$
(*c*) R = $-CH_2-CH_2-CH_3$
(*d*) R = $-CH(CH_3)_2$

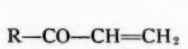

IV

(*a*) R = $-CH_3$
(*b*) R = $-CH_2-CH_3$

suggested an equilibrium between the *s*-cis and *s*-trans isomers. Similar doublet carbonyl bands were noted by Mecke and Noack for ketones of structure IV*a*–IV*b*. Timmons and collaborators (4) have commented similarly on the spectrum of *trans*-Δ^3-penten-2-one, and other examples of this behavior have been cited by Erskine and Waight (3).

In the present investigation the effects of temperature on the infrared and Raman spectra of *trans*-Δ^3-penten-2-one and Δ^3-buten-2-one have been examined in an attempt to confirm the existence of these equilibrium systems.

[1]*Manuscript received June 21, 1961.*
Contribution from the Division of Pure Chemistry, National Research Council of Canada, Ottawa, Canada. Issued as N.R.C. No. 6515.
[2]*National Research Council of Canada Postdoctorate Fellow.*

EXPERIMENTAL METHODS AND RESULTS

The preparation and purification of the ketones have been described by Mecke and Noack (2). The infrared spectra were measured on Perkin–Elmer Model 21 and Model 112 spectrometers using the low-temperature technique described previously (6). The Raman spectra were obtained with a Cary Model 81 spectrometer (5). The spectra are illustrated in Figs. 1–8 and the numerical data are summarized in Tables I–III.

TABLE I

Band positions and intensities in the infrared and Raman spectra of trans-Δ^3-penten-2-one

Raman spectrum*		Infrared spectrum†		Raman spectrum*		Infrared spectrum†	
Wavenumber‡ (cm^{-1})	k^{max}	Wavenumber‡ (cm^{-1})	ϵ_{max}	Wavenumber‡ (cm^{-1})	k^{max}	Wavenumber‡ (cm^{-1})	ϵ_{max}
377§	4.5	381	4	1303	14.0	(1300)	—
—	—	418	4	—	—	1310	25
501	12.0	498	6	(1360)	—	1359	98
543	2.6	543	31	1377	14.9	1378	72
557	1.3	(560)	—	—	—	1425	52
603§	3.7	604	27	—	—	(1435)	—
620§	1.9	(622)	—	1443	26.4	1441	97
799	11.6	798	11	(1619)	30	(1615)	60
861	1.0	860‖¶	10	1631	59§	1630‖¶	196
943	2.5	943	35	1644	47	1645	72
(967)	—	971	146	1673	90	1674	400
992	12.7	(993)	—	(1697)	—	1693‖¶	144
—	—	1018	17	2856	10.5		—
1042	3.6	1040	6	2881	9.0		—
1065	2.4	—	—	2918	78		
1105	5.0	—	—	2944	26	n.m.	
1175	v.w.	1177‖¶	70	2974	18		
1252	17.7	1250	168	(3008)	—		
—	—	1270	46	3020	23		
(1291)§	4.9	1289‖¶	25				

NOTE: v.w. = resolved but very weak band; n.m. = region not measured.

*Intensities are measured relative to the 459 cm^{-1} band of CCl_4 ($k^{459}_{CCl_4} = 100$). Measured in the presence of 9% by weight of CCl_4 at +5° C.

†Measured at +30° C. For experimental details see references 6 and 9.

Wavenumber range (cm^{-1})	Solvent	Concentration (M)
1750–1320	$CHCl_3/CCl_4/C_2Cl_4$	0.24
1320–700	CS_2	0.36
700–300	n-C_6H_{14}	0.7

‡Inflections are indicated in parentheses.
§The Raman band intensifies at higher temperature.
‖The infrared band weakens at higher temperature.
¶The band is absent from the infrared spectrum of the solid.

Spectra of trans-Δ^3-Penten-2-one

The infrared spectrum of *trans*-Δ^3-penten-2-one, measured in a eutectic mixture of carbon tetrachloride, tetrachloroethylene, and chloroform (6) in the region of the C=O and C=C stretching bands is shown in Fig. 1. At room temperature, four well-resolved bands (A–D) are observed at 1693, 1674, 1645, and 1630 cm^{-1} with a weaker shoulder (E) at 1615 cm^{-1}. In the Raman spectrum, measured at +5° in the presence of 9% by weight of carbon tetrachloride, the bands occur near the same positions (Fig. 2), but the relative intensities are different; band A, in particular, is reduced to a weak inflection. From comparison with the spectra of other α,β-unsaturated ketones (2, 5), bands A and D can be assigned to the *s*-cis isomer and bands B and C to the *s*-trans form. The weak

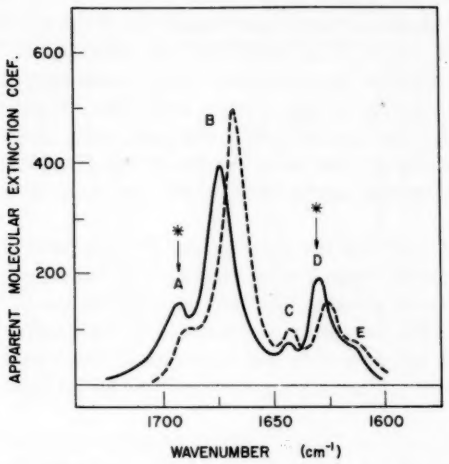

FIG. 1. Infrared spectrum of *trans*-Δ³-penten-2-one in $CHCl_3/CCl_4/C_2Cl_4$ solvent. Bands indicated by arrows and asterisks weaken in the cooled solution and are absent from the spectrum of the solid. —— +30° C; - - - −75° C.

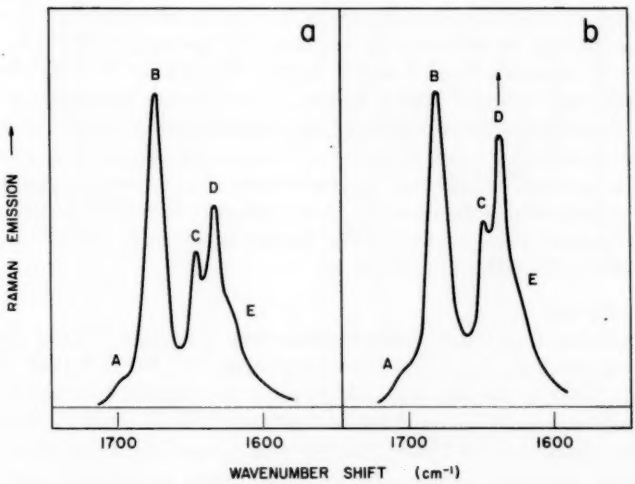

FIG. 2. Raman spectrum of *trans*-Δ²-penten-2-one measured in the presence of 9% by weight of carbon tetrachloride: *a*, +6° C; *b*, +85° C. The intensity scale is arbitrarily adjusted so that band B is of equal height in both spectra.

band E is probably an overtone or combination band; its weakness in the Raman spectrum is an argument against attributing it to a C=C vibration of an impurity.

In the infrared spectrum at −75° (Fig. 1) bands B and C are more intense than at room temperature while bands A and D are weaker, indicating the greater thermodynamic stability of the *s*-trans form. Bands A and D are absent from the spectrum of the solid

at $-100°$, suggesting that the ketone crystallizes exclusively in the *s*-trans form. The Raman spectrum at $+85°$ shows a relative intensification of the *s*-cis bands. The intensity ratio k_B/k_D is 1.38 at $+5°$ and 1.17 at $+85°$ and the ratio k_D/k_C is 1.28 and 1.47 respectively at the lower and higher temperatures. While these figures indicate an intensification of the *s*-cis band relative to the *s*-trans with rising temperature, they are not necessarily proportional to the concentration changes, since the bands broaden with rising temperature. Unfortunately the band overlap is too great to permit evaluation of the areas beneath the component peaks from which the relative concentrations of the isomers might be derived.

The fact that both the C=O and the C=C bands are temperature sensitive indicates that the band splitting is not due to a Fermi resonance of the type associated with C=O band splitting in cyclic *s*-trans ketones (5). It is also significant in this connection that the room-temperature spectra for dilute solutions in carbon tetrachloride, chloroform, and tetrachloroethylene closely resemble the spectrum of the liquid ketone; only minor changes in band position and intensity are noted, such as would be expected from normal solvent effects.

Other regions of the infrared and Raman spectra of *trans*-Δ^3-penten-2-one are shown in Figs. 3 and 4. Infrared bands of liquids and solutions usually become narrower and sharper with diminishing temperature, and it is difficult to distinguish an increase in band height due to this solvent–solute effect from band intensification due to an increase in the relative concentration of a conformational isomer. The inverse effect, viz. the weakening of a band at lower temperature due to the fall in concentration of a less-stable isomer is more convincing as evidence for a change in isomer equilibrium, and in the infrared spectrum of *trans*-Δ^3-penten-2-one in carbon disulphide at $-65°$ the bands at 1289, 1177, and 860 cm^{-1} weaken in this fashion. Furthermore the bands at 1289 cm^{-1} and 860 cm^{-1} are absent from the spectrum of the solid ketone at $-100°$, while the band at 1177 cm^{-1} persists only as a broad residuum. These bands can all be attributed to the *s*-cis form. For the spectra at elevated temperatures, the converse argument applies, and the bands that intensify on heating are most plausibly indentified with a change in the equilibrium in favor of the *s*-cis form. In the Raman spectrum at $+85°$ this is observed for the bands at 1291, 620, 603, and 377 cm^{-1}.

Spectra of Δ^3*-Buten-2-one*

The infrared spectrum of Δ^3-buten-2-one, measured on a capillary film of the undiluted ketone, exhibits two bands in the C=O stretching region at 1701 and 1683 cm^{-1} (bands A and B of Fig. 5). Cooling the film to $-65°$ changes the relative intensities; the ratios of the maximal absorbances (B/A) are 1.64 at $+30°$ and 2.08 at $-65°$. The positions are consistent with the assignment of band A to the *s*-cis isomer and band B to the *s*-trans form. In the infrared spectrum of the solid at $-100°$ there is no band near 1700 cm^{-1} but there is a doublet at 1680 and 1673 cm^{-1} (Fig. 5). It seems reasonable to interpret this as a splitting of band B, and the disappearance of band A. The splitting introduces a complication in the interpretation of the structure of the solid; it could be due to combination with a lattice vibration or to the packing of two molecules in a slightly different environment in the unit cell. The latter explanation is supported by the similar close splitting of the C=C band, also shown in Fig. 5. In the Raman spectrum at $+5°$ the 1700 cm^{-1} component appears only as a weak inflection on the high-frequency side of the strong band at 1677 cm^{-1} and there is no measurable change at higher temperature. The weakness of this Raman band is consistent with the *s*-cis assignment (5).

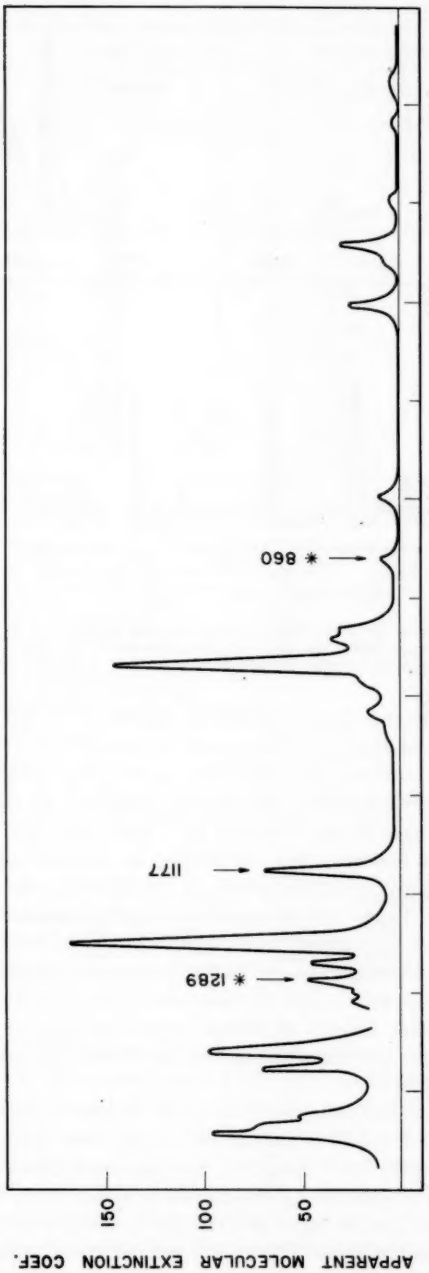

FIG. 3. Infrared spectrum of *trans*-Δ^3-penten-2-one. For conditions see footnote † of Table I and footnote to Fig. 1.

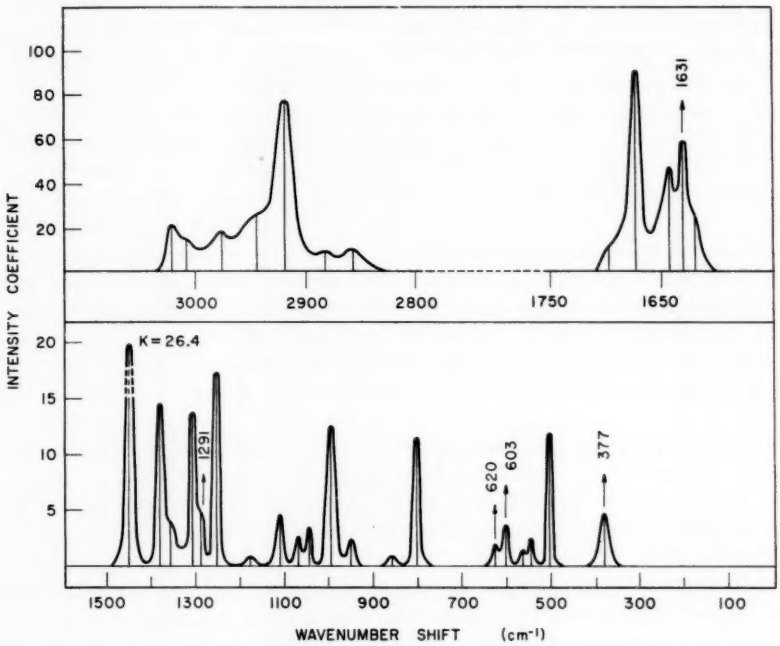

FIG. 4. Raman spectrum of *trans*-Δ^3-penten-2-one measured in the presence of 9% by weight of carbon tetrachloride. The carbon tetrachloride bands at 459, 314, and 218 cm^{-1} are omitted. The band contours are diagrammatic only. Upward pointing arrows designate bands that intensify on heating.

Δ^3-Buten-2-one exhibits only one C=C stretching maximum in both the infrared and the Raman spectra, and if the two carbonyl bands are to be attributed to a conformational equilibrium it is necessary to assume that the C=C stretching bands for both the *s*-cis and the *s*-trans forms overlap each other and are not resolved. In the case of *trans*-Δ^3-penten-2-one the parallel changes in the A/D and B/C band pairs are a strong argument in support of the equilibrium system, and the failure to observe similar behavior for Δ^3-buten-2-one adds considerably to the difficulty in interpreting the other temperature changes in this spectrum. In Table III the positions and intensities of the C=O and C=C bands of Δ^3-buten-2-one in carbon tetrachloride and chloroform are compared. The ratios of the C=O band intensities in the two solvents are not very different and do not suggest that we are dealing with a Fermi resonance type of carbonyl band splitting (5, 7). The change in the relative heights of several bands distributed through the 1400–900 cm^{-1} region of the spectrum are described below, and these also are inconsistent with the Fermi resonance explanation.

The infrared spectrum of Δ^3-buten-2-one from 1750 to 280 cm^{-1} is shown in Fig. 6, and the temperature-sensitive bands are illustrated in the three infrared spectra shown in Fig. 7, covering the 1400–900 cm^{-1} range at temperatures extending from −65 to +85°. Changes are particularly notable for the bands at 1360, 1248, 991, and 954 cm^{-1}, which intensify on cooling, and for the band at 1180 cm^{-1}, which weakens on cooling and is absent from the spectrum of the solid. These changes are most readily reconciled with

TABLE II

Band positions and intensities in the infrared and Raman spectra of Δ^3-buten-2-one

Raman spectrum*		Infrared spectrum†		Raman spectrum*		Infrared spectrum†	
Wavenumber‡ (cm^{-1})	k_{max}	Wavenumber‡ (cm^{-1})	ϵ_{max}	Wavenumber‡ (cm^{-1})	k_{max}	Wavenumber‡ (cm^{-1})	ϵ_{max}
278	4.6	—	—	—	—	1063	11
298	4.4	300	4	1183	0.8	1180§‖	73
426	1.6	427	4	—	—	1216	19
487	1.5	485	14	1247	7.0	1246	86.5
527	2.1	523	4	1280	15.6	1274	16
600	1.6	603	7	1293	10.4	—	—
—	—	669		1357	0.8	1360	88
686	1.0	685		—	—	1400	106
760	12.1	758	6	1408	16.8	—	—
773	7.3	773	4	—	—	1423	49
—	—	824	2	(1430)	—	—	—
—	—	(940)		1616	54	1616	65.5
946	6.1	951	103	1677	70	1687	376
963	4.7	(963)		(1700)	—	1706§‖	141
—	—	982	54	2926	53		
997	0.4	992	57	2987	25	n.m.	n.m.
—	—	1020	23	3026	72		
1054	10.9	—	—	3103	26.4		

NOTE: n.m. = region not measured.

*Intensities are measured relative to the 459 cm^{-1} band of CCl_4 ($k^{459}_{CCl_4} = 100$). Measured in the presence of 9% by weight of CCl_4 at +5° C.

†

Wavenumber range (cm^{-1})	Solvent	Concentration (M)
1750–1600	CCl_4	0.16
1500–1300	CCl_4	0.6
1300–650	CS_2	0.6
650–280	n-C_6H_{14}	0.7

‡Inflections are indicated in parentheses.

§The infrared band weakens at higher temperature.

‖The band is absent from the infrared spectrum of the solid.

TABLE III

Solvent effects of the C=O and C=C infrared bands of Δ^3-buten-2-one*

	A		B			C	
	Position (cm^{-1})	Intensity	Position (cm^{-1})	Intensity	B/A	Position (cm^{-1})	Intensity
Carbon tetrachloride	1700	(140)	1687	(375)	2.68	1616	(66)
Chloroform	1700	(115)	1680	(340)	2.94	1616	(75)

*Concentration, 0.02 M.

the *s*-cis ⇌ *s*-trans equilibrium though they mainly involve intensification on cooling. It may be significant that a band near 1180 cm^{-1} appears to be associated with the *s*-cis forms of both Δ^3-buten-2-one and *trans*-Δ^3-penten-2-one. The Raman spectrum of Δ^3-buten-2-one measured at +5° is shown in Fig. 8; raising of the temperature to +70° causes the bands at 1247, 1054, 686, and 527 cm^{-1} to diminish in peak height by about 30% while the remaining bands retain 90–100% of their intensity at +5°.

In summary we infer from these experiments that *trans*-Δ^3-penten-2-one exists as a mixture of *s*-cis and *s*-trans isomers. For Δ^3-buten-2-one, the failure to observe two C=C

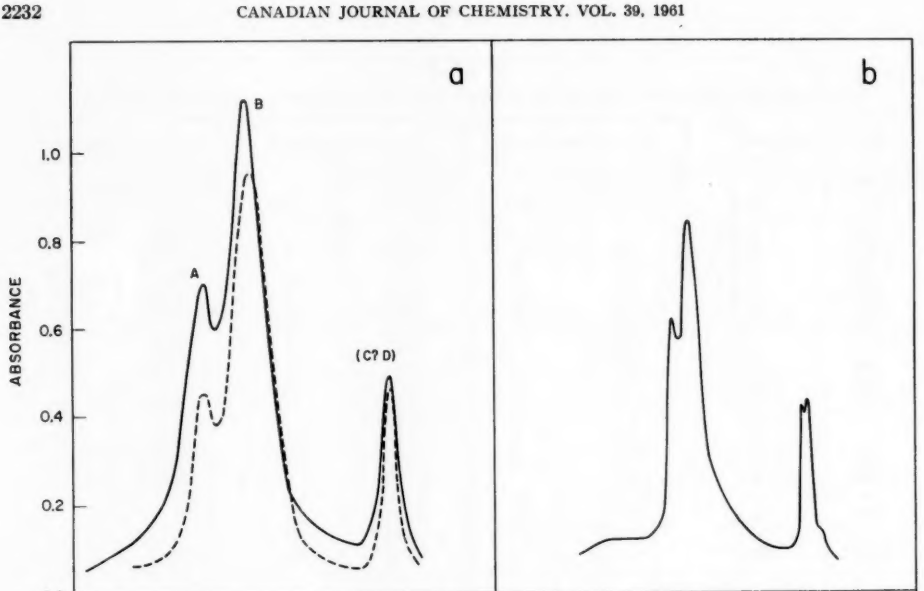

FIG. 5. Infrared spectrum of Δ^3-buten-2-one, measured on the undiluted liquid ketone: *a*, liquid film, —— $+30°$ C, - - - $-65°$ C; *b*, solid film, $-100°$ C.

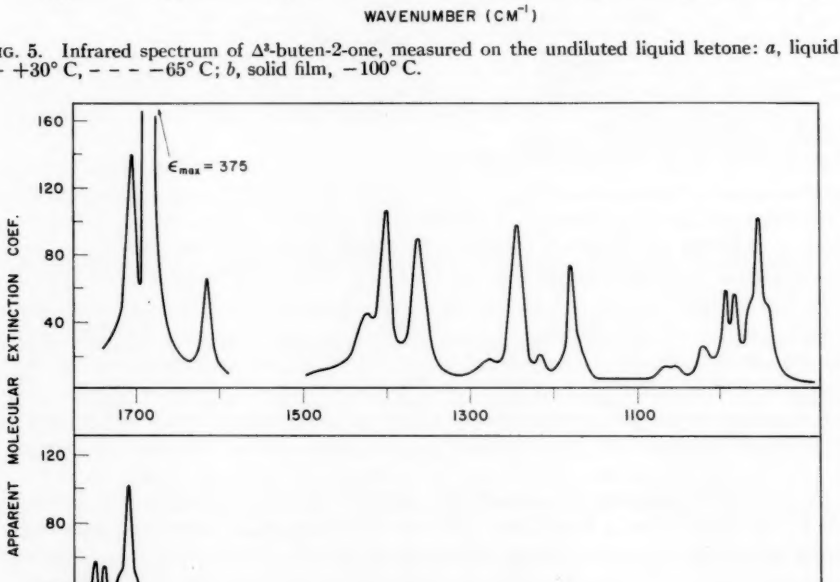

FIG. 6. Infrared spectrum of Δ^3-buten-2-one. For conditions see footnote † of Table II.

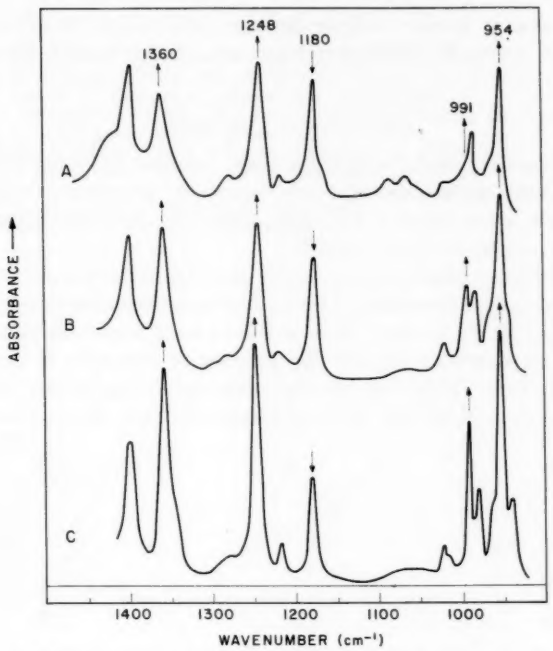

FIG. 7. Effects of temperature on the infrared spectrum of Δ^3-buten-2-one. For curve A (+85° C) the solvent is tetrachloroethylene and for curves B (+30° C) and C (−65° C), carbon disulphide. Upward pointing arrows designate bands that intensify on cooling.

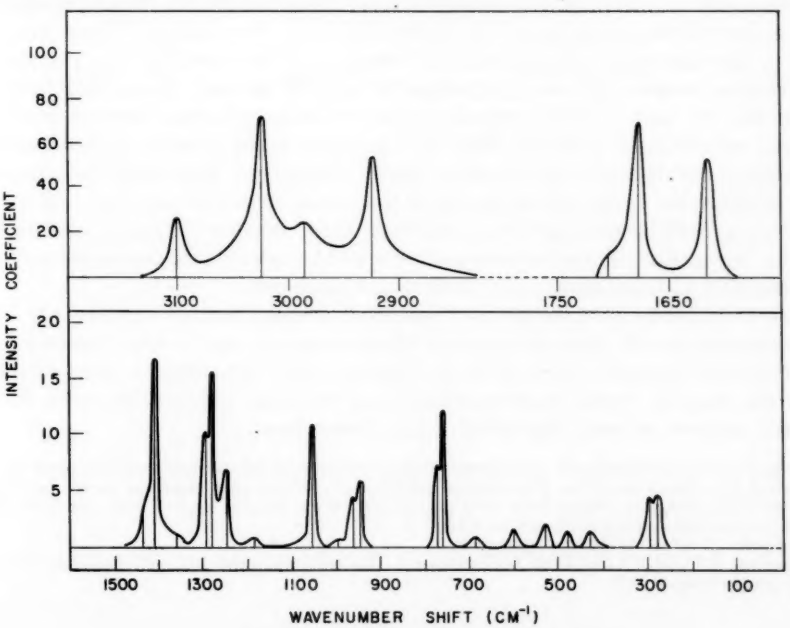

FIG. 8. Raman spectrum of Δ^3-buten-2-one.

stretching bands makes it unwise to draw definite conclusions, though the temperature changes through the remainder of the spectrum are consistent with the presence of the equilibrium system.

CONCLUDING REMARKS

The α,β-unsaturated ketones for which equilibria between *s*-cis and *s*-trans forms have been observed or postulated possess common structural features. It appears necessary that (*a*) the α-carbon atom carry a hydrogen atom, (*b*) the *s*-trans form be sterically unhindered (viz. R_2 and R_3 = H in I and II).

If the hydrogen at R_2 is replaced by alkyl, only the *s*-trans form is obtained, presumably because the *s*-cis structure is destabilized by repulsion between the non-bonded hydrogen atoms on R_1 and R_2.* If R_3 is alkyl there will be strong repulsion in the *s*-trans form between the hydrogen atoms on R_1 and R_3; ketones of structure V therefore exist exclusively in the *s*-cis form. This remains the preferred configuration even when alkyl groups are present at R_2 and R_4 (VI, VII), although, as noted above, there is some steric

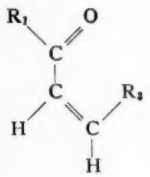

V

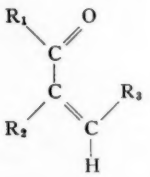

VI

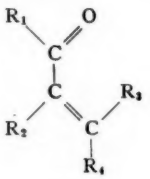

VII

strain between R_1 and R_2 in these structures. In VI and VII the conditions are favorable for non-planar forms, but the three ketones of these types included in these investigations show no abnormal displacements of the C=O and C=C frequencies. These would be expected if the molecules were significantly non-planar. It is notable that the infrared C=C stretching bands of ketones of structure VI and VII are very broad, their half band widths are 20.5, 36, and 17.5 cm^{-1} respectively in tetrachloroethylene solution, compared with normal values in the range 8.5–16.5 cm^{-1} for other types of open-chain α,β-unsaturated ketones;† the Raman spectra show similar behavior.‡ This band broadening is probably attributable to the destabilization of the planar structure, resulting in a shallow potential-energy well for rotation about the center C—C bond of the conjugated system. As a result, the torsionally excited energy levels will be more highly populated and these will be associated with decreased C=C stretching frequencies.

It is also to be noted that the ketones that exist predominantly or exclusively in the *s*-cis conformation readily undergo a partial isomerization to the β,γ-unsaturated ketones in the presence of iodine or other catalysts. Ketones with unhindered *s*-trans structures are much less reactive under these conditions and isomerize only to the (*s*-cis) cis α,β-unsaturated ketones without migration of the double bond.

**Equilibrium systems containing the s-cis isomer might be expected for the converse structure where R_1 = H and R_2 = alkyl, i.e. α-methylacrolein. The infrared spectrum of this aldehyde, measured on the pure liquid, shows no significant change on cooling from +30 to −65° (8); it has normal singlet C=O and C=C bands (2, 7) and is presumably entirely in the s-trans form.*

†See compounds 43–45 in the table in reference 2.

‡See compounds XV and XVI in Table I of reference 5. The half band widths are not reported in this paper but they are proportional to L/k.

REFERENCES

1. R. MECKE and K. NOACK. Spectrochim. Acta. **12**, 391 (1958).
2. R. MECKE and K. NOACK. Chem. Ber. **93**, 210 (1960).
3. R. L. ERSKINE and E. S. WAIGHT. J. Chem. Soc. 3425 (1960).
4. C. J. TIMMONS. Proceedings of the IVth International Meeting of the European Molecular Spectroscopy Group, Bologna, Italy. In press.
5. K. NOACK and R. N. JONES. Can. J. Chem. This issue. p. 2201.
6. R. N. JONES and K. NOACK. Can. J. Chem. This issue. p. 2214.
7. R. N. JONES, C. L. ANGELL, T. ITO, and R. J. D. SMITH. Can. J. Chem. **37**, 2007 (1959).
8. K. NOACK and R. N. JONES. Unpublished observation.
9. R. N. JONES. Spectrochim. Acta, **9**, 235 (1957).

POLAROGRAPHIC DETERMINATION OF THE DISSOCIATION CONSTANT OF THE SULPHYDRYL GROUP AND DIFFUSION COEFFICIENT MEASUREMENTS OF THIOMALIC ACID[1]

R. C. KAPOOR, O. P. AGRAWAL, AND T. D. SETH

ABSTRACT

Polarographic study of thiomalic acid has been made in the pH range 1–12.5 using Britton–Robinson buffer at 30°. The half-wave potential ($E_{\frac{1}{2}}$) values have been used to determine the pK_3 (SH) value of the acid (pK_3 = 10.55).

The diffusion current obtained in these experiments has been utilized to calculate the diffusion coefficients of the different charged species of thiomalic acid. The values thus obtained for the respective species are $H_3A = 1.20\times10^{-5}$ cm²/sec; $H_2A^- = 1.16\times10^{-5}$ cm²/sec; $HA^{--} = 1.08\times10^{-5}$ cm²/sec; and $A^{---} = 7.67\times10^{-6}$ cm²/sec.

The standard potential of the reaction

$$TSH + Hg = TSHg + H^+ + e^-$$

has been calculated as +0.266 volt vs. N.H.E.

Thiomalic acid or mercaptosuccinic acid has been recently used in a number of studies with metal complexes such as copper (1), zinc, cobalt, and nickel (2), and some other metals (3). Polarographic behavior of this compound has been systematically investigated (4, 5, 6) in these laboratories.

Cheney, Fernando, and Freiser (2) have reported the acid dissociation constants of thiomalic acid as calculated from potentiometric titration data.

Thiomalic acid has three replaceable hydrogen ions as indicated in the formula below.

$$\begin{array}{l} {}^{III}HSCHCOOH^{I} \\ \quad\quad\quad\quad | \\ \quad\quad\quad CH_2COOH^{II} \end{array}$$

If we represent the acid as H_3A the equilibria involved are

$$H_3A \rightleftharpoons H_2A^- + H^+, \qquad [1]$$

$$H_2A^- \rightleftharpoons HA^{--} + H^+, \qquad [2]$$

$$HA^{--} \rightleftharpoons A^{---} + H^+, \qquad [3]$$

which correspond to the three dissociation constants K_1, K_2, and K_3. K_1 and K_2 correspond to the two carboxylic hydrogen atoms while K_3 corresponds to the hydrogen atom linked to the sulphur atom. The three values reported by Cheney *et al.* (2) at 25° are pK_1 = 3.30; pK_2 = 4.94; pK_3 (SH) = 10.64.

The authors have used polarographic data in calculating the pK_3 value of thiomalic acid. The different charged species of thiomalic acid have been shown to have different diffusion properties. The diffusion coefficient values of these species have also been calculated.

MATERIAL

Thiomalic acid was obtained as a gift from Evans Chemetics Incorporated, New York. The material was 99% pure and was used as such. Stock solutions were prepared in doubly distilled water, and only freshly prepared solutions were used. All other chemicals used were of AnalaR or chemically pure grade. The mercury used in the dropping mercury

[1]*Manuscript received June 19, 1961.*
Contribution from the Chemistry Department, University of Allahabad, Allahabad, Uttar Pradesh, India.

electrode was first purified chemically by treatment with nitric acid and subsequently distilled twice.

EXPERIMENTAL

Automatic polarograms were taken with a Leeds and Northrup Electro-Chemograph, Type E. Current–voltage curves in all cases were also taken manually with a circuit described by Lingane and Kolthoff (7).

Current–voltage curves were taken at 30°. All potentials were measured against the saturated calomel electrode (S.C.E.). An atmosphere of purified nitrogen was maintained throughout all investigations.

The characteristics of the capillary used are $m = 1.357$ mg/sec; $t = 3.37$ sec; $m^{2/3}/t^{1/6} = 1.501$ $mg^{2/3}sec^{-1/2}$.

The pH measurements were made with a Leeds and Northrup pH meter (Cat. 7666).

RESULTS AND DISCUSSION

Dissociation Constant of the Sulphydryl Group

Polarograms of 5×10^{-4} M thiomalic acid were taken at different pH values using Britton–Robinson buffer. Fig. 1 shows the current–voltage curves of 5×10^{-4} M thiomalic acid at different pH values.

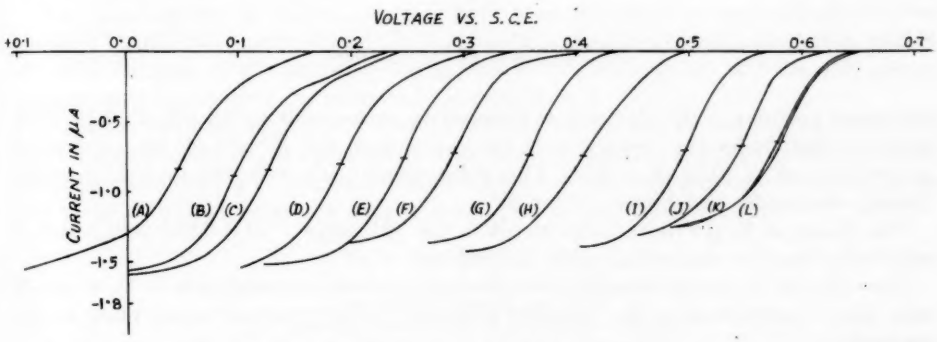

FIG. 1. Anodic waves of 5×10^{-4} M thiomalic acid in B–R buffer at different pH values. The pH and $E_{\frac{1}{2}}$ values are given respectively as (A) 1.15, −0.045 v; (B) 2.0, −0.095 v; (C) 2.5, 0.125 v; (D) 3.7, −0.190 v; (E) 4.6, −0.246 v; (F) 5.6, −0.291 v; (G) 6.6, -0.357_5 v; (H) 7.7, −0.405 v; (I) 9.0, −0.495 v; (J) 10.0, −0.545 v; (K) 11.35, -0.577_5 v; (L) 11.7, -0.582_5 v.

Thiomalic acid gives a prewave at low pH values up to 3.7. Such prewaves are often given by sulphur compounds such as glutathione, thioglycollic acid, and 2,3-dimercaptopropanol (8, p. 470). These prewaves have adsorption character and occur at more negative potential than the main anodic wave. The half-wave potentials of the main waves have been marked after separation of the prewaves. However, the total current is diffusion-controlled and corresponds to a one-electron change in all the polarograms.

The characteristics of the anodic wave of thiomalic acid have already been established (4, 5, 6). It has been shown that the anodic wave is not due to formation of a dimer but due to the formation of a mercury compound as indicated below:

$$TSH + Hg = TSHg + H^+ + e^-.$$

A plot of $E_{\frac{1}{2}}$ values against pH is given in Fig. 2. It can be easily seen that there are

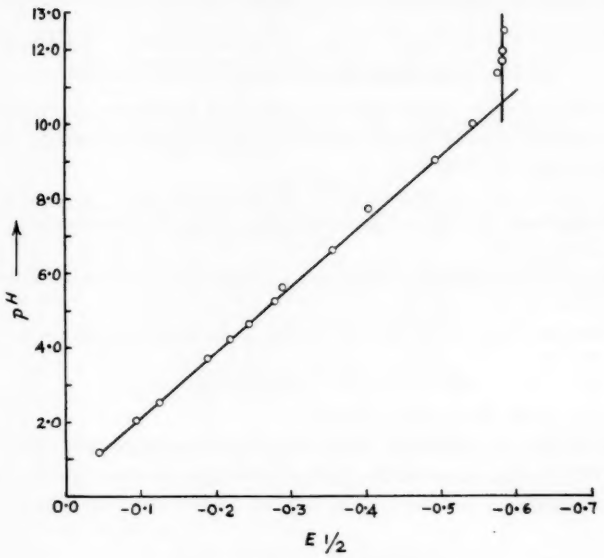

FIG. 2. Plot of $E_{\frac{1}{2}}$ and pH values.

two linear portions in the plot, whose intersection corresponds to the pH of 10.55. This indicates that under the conditions of the experiment the H^+ ion of the sulphydryl group has a pK of 10.55 (8, p. 472). This value agrees fairly well with that obtained by Cheney, Fernando, and Freiser (2) at 25°.

The change of $E_{\frac{1}{2}}$ per unit change of pH in the pH range 1–10 is 0.057 volt, which is sufficiently near the theoretical value of 0.060 volt at 30°.

The value of $E_{\frac{1}{2}}$, extrapolated to zero pH (hydrogen ion concentration = 1), is +0.02 volt, which corresponds to the standard potential of the reaction taking place at the electrode:

$$TSH + Hg = TSHg + H^+ + e^-.$$

The value thus calculated is +0.266 volt vs. N.H.E.

Diffusion Coefficients of Different Charged Species of Thiomalic Acid

Measurements of diffusion currents of thiomalic acid have been made in the pH range 1.15 to 12.50. Table I includes the values of the diffusion coefficient constants calculated according to the Ilkovič equation. The value of the diffusion current decreases on increasing the pH.

Thiomalic acid, as indicated earlier, exists in solution in four different species. The percentage of the different species can be calculated by the three pK values of this acid. The variation of the acid constants with temperature can be estimated from the apparent heats of ionization ($\Delta H'$) for the two carboxyl groups by applying the van't Hoff's equation and assuming that $\Delta H'$ is independent of temperature over the range of measurement.

The $\Delta H'$ for the two acid dissociation constants, K_1 and K_2, of succinic acid have been reported as +710 cal/mole and −340 cal/mole respectively (9). These same values of

TABLE I

pH	i_d (μa)	$D\times10^5$ (cm²/sec)	$E_{\frac{1}{2}}$(v)
1.15	−1.48	1.20	−0.045
2.0	−1.38	1.20	−0.095
2.5	−1.50	1.23	−0.125
3.7	−1.43	1.13	−0.190
4.2	−1.545	1.15	−0.220
4.6	−1.55	1.16	−0.246
5.2	−1.505	1.09	−0.280
5.6	−1.45	1.01	−0.291
6.6	−1.455	1.03	-0.375_5
7.7	−1.50	1.08	−0.405
9.0	−1.43	0.980	−0.495
10.0	−1.365	0.894	−0.545
11.35	−1.30	0.810	-0.577_5
11.7	−1.285	0.795	-0.582_5
11.95	−1.29	0.801	-0.582_5
12.5	−1.26	0.767	-0.587_5

$\Delta H'$ were used for the two carboxyl groups of thiomalic acid to give calculated pK values at 30° of $pK_1 = 3.29$ and $pK_2 = 4.94$.

pK_3 as determined by our experiments from the $E_{\frac{1}{2}}$ values is 10.55 at 30°.

The percentage of different species of thiomalic acid can be calculated on the basis of the above pK values.

The concentration of different species have been calculated on such a basis that we see that at pH 1.15 practically all the acid exists in the form of uncharged H_3A species. At pH 7.7 almost all the acid is in the form of HA^{--}, while at pH 12.5 the only species present in the solution is the completely ionized form A^{---}.

Thus the diffusion currents at these three pH values can be used to calculate the diffusion coefficients of the above-mentioned three species. The diffusion coefficient of the remaining species, H_2A^-, can be calculated from the intermediate measurements in the pH range 3.70–5.60 using the already calculated D values of H_3A and HA^{--} species.

TABLE II

Diffusion coefficient values of different species of thiomalic acid at 30°

Species	$D\times10^5$ (cm²/sec)	pH
H_3A	1.20	1.15
HA^{--}	1.08	7.7
A^{---}	0.767	12.5
H_2A^-	1.16	4.2
H_2A^-	1.19	4.6
H_2A^-	1.14	5.2

The average value of the species H_2A has been taken as 1.16×10^{-5} cm²/sec.

REFERENCES

1. I. M. Klotz, G. H. Czerlinski, and H. A. Fiess. J. Am. Chem. Soc. **80**, 2920 (1958).
2. G. E. Cheney, Q. Fernando, and H. Freiser. J. Phys. Chem. **63**, 2055 (1959).
3. R. N. Sen Sarma. Science and Culture, **23**, 434 (1958).
4. R. C. Kapoor and S. K. Tiwari. Proc. Natl. Acad. Sci. (India), A, **28**, 52 (1959).
5. S. K. Tiwari and R. C. Kapoor. Proc. Natl. Acad. Sci. (India), A, **28**, 272 (1959).
6. S. K. Tiwari and R. C. Kapoor. Proc. Natl. Acad. Sci. (India), A, **28**, 278 (1959).
7. J. J. Lingane and I. M. Kolthoff. Chem. Revs. **24**, 1 (1939).
8. M. Brezina and P. Zuman. Polarography in medicine, biochemistry and pharmacy. Interscience Publishers, Inc., New York. 1958. p. 470.
9. E. J. Cohn and J. T. Edsall. Proteins, amino acids and peptides. Reinhold Publishing Corporation, New York. 1943. p. 82.

ASSOCIATION IN THE BINARY LIQUID SYSTEM DIMETHYL SULPHOXIDE - WATER[1]

J. M. G. Cowie and P. M. Toporowski

ABSTRACT

The viscosities and densities of several mixtures of dimethyl sulphoxide and water have been measured at 25°, 45°, and 65° C. Heats of mixing and refractive indices at 25° C are also reported. The results indicate there is strong association of the two liquids which may be attributed to hydrogen bonding.

INTRODUCTION

The widespread application of dimethyl sulphoxide (DMSO) as a solvent, plasticizer, and chemical intermediate has led to its large-scale production in recent years. In spite of the increased use of this compound its physical properties do not appear to have been studied extensively.

DMSO is a colorless, non-toxic liquid which boils at 189° C and freezes at 18.5° C. It is completely miscible with water and is strongly hygroscopic, but little has been reported about the behavior of DMSO–H_2O mixtures (1). During the course of a recent investigation on the solution properties of amylose dissolved in DMSO, it was found that water alters the viscosity of amylose–DMSO solutions in such a manner as to suggest a strong interaction between DMSO and H_2O.

Many binary liquid systems exhibit non-linear viscosity isotherms which pass through a minimum. However, a smaller group possess a maximum, indicating some form of liquid–liquid interaction, and the DMSO–H_2O system was found to belong to this latter class.

Viscosities and densities of 14 mixtures have been measured at 25°, 45°, and 65° C while refractive indices and heats of mixing have been determined at 25° C.

EXPERIMENTAL

Solvents

DMSO, supplied by Crown Zellerbach Corporation, was carefully dried by refluxing for 24 hours over CaO. It was left in contact with this drying agent for about 10 days with occasional shaking and then fractionally distilled under reduced pressure. The middle fraction, with boiling point approximately 68° C at 6–7 mm pressure, was collected and used in all physical measurements. The purity of this fraction was determined by analysis for water using two independent methods.

LeBel and Goring (1) have suggested a method using infrared spectroscopy in which the height of the OH absorption peak at 3500 cm^{-1} is measured and can be related to the water concentration in the sample. The method was calibrated using mixtures up to 0.5% water but no peak was detected in the distilled DMSO used in this investigation.

Analysis for water by the Karl Fischer (2) technique indicated that there was less than 0.01% water present in the DMSO.

Viscosity

The viscometer used was a Cannon-Ubbelohde model designed to have negligible

[1]*Manuscript received July 10, 1961.*
Contribution from the Division of Applied Chemistry, National Research Council, Ottawa, Canada.
Issued as N.R.C. No. 6510.

kinetic energy correction (3). Absolute viscosities, measured in centipoise, could be obtained from the flow time of the liquid, its density, and a calibration constant supplied by the manufacturer. The viscometer was reproducibly positioned in the thermostat baths by a three-point suspension system. Thermostat temperatures were maintained at 25°, 45°, and 65°±0.01° C.

Density

The liquid densities were determined at 25°, 45°, and 65° C using a Sprengel Ostwald pycnometer with a capacity of about 21 ml.

Refractive Index

Refractive indices were measured on an Abbé refractometer at 25° C using the sodium D line (λ = 5893 Å).

Calorimetry

The heats of mixing of several mixtures of water and DMSO were measured in a Dewar calorimeter similar to the one described by Vold (4). The liquids were kept separate in the calorimeter before being mixed by means of a hollow glass cylinder resting on a pool of mercury. Rapid mixing was obtained by raising the cylinder and stirring one liquid into the other. The final liquid volume was always about 150 ml, which kept the vapor space above the mixtures at a minimum. Recorded temperature rises varied from 7° to 25° C. The heat capacity of the calorimeter and its contents was determined after each measurement by passing a specific amount of electric current through the heater and measuring the temperature rise produced.

RESULTS

Table I lists the viscosities, densities, and refractive indices of several DMSO–H_2O mixtures. The results all show a positive deviation from ideality, which strongly suggests

TABLE I

Viscosity, density, and refractive index values for the system DMSO–H_2O

Mole fraction water	25° C			45° C		65° C	
	Viscosity (centipoise)	Density (g/ml)	Refractive index	Viscosity (centipoise)	Density (g/ml)	Viscosity (centipoise)	Density (g/ml)
0.000	2.003	1.0956	1.4765	1.394	1.0756	1.038	1.0556
0.047	2.054	1.0961	1.4754	1.423	1.0762	1.055	1.0564
0.089	2.118	1.0965	1.4741	1.457	1.0768	1.073	1.0570
0.186	2.298	1.0976	1.4710	1.553	1.0781	1.126	1.0582
0.335	2.708	1.0990	1.4648	1.758	1.0799	1.233	1.0604
0.522	3.449	1.0983	1.4525	2.083	1.0802	1.378	1.0612
0.590	3.676	1.0964	1.4460	2.164	1.0787	1.402	1.0603
0.651	3.764	1.0927	1.4385	2.172	1.0756	1.389	1.0574
0.702	3.674	1.0881	1.4308	2.102	1.0715	1.340	1.0538
0.743	3.467	1.0826	1.4232	1.985	1.0667	1.273	1.0495
0.812	2.854	1.0693	1.4075	1.672	1.0548	1.088	1.0391
0.867	2.232	1.0537	1.3911	1.346	1.0411	0.897	1.0268
0.910	1.748	1.0388	1.3757	1.086	1.0280	0.743	1.0150
0.945	1.382	1.0238	1.3607	0.880	1.0146	0.615	1.0032
0.975	1.110	1.0102	1.3461	0.724	1.0024	0.516	0.9920
1.000	0.898	0.9971	1.3330	0.599	0.9902	0.435	0.9806

that there is association of the liquids through hydrogen bonding. This is illustrated in Fig. 1, where the solution viscosity is plotted against the mole fraction of water. In the

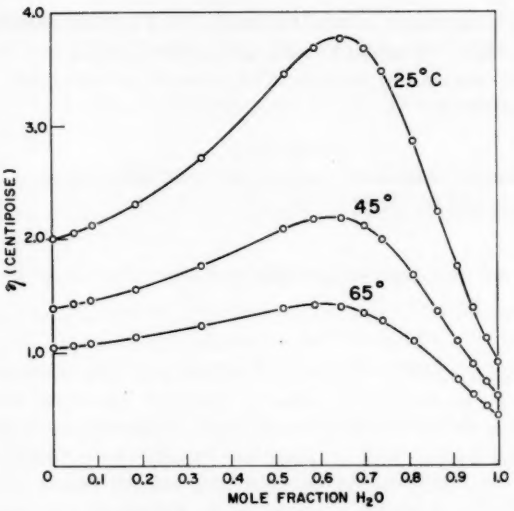

FIG. 1. The viscosities of DMSO–H_2O mixtures at 25°, 45°, and 65° C as a function of mole fraction of water.

region of 0.65 mole fraction of water, each isotherm exhibits a maximum which decreases with increase in temperature, and shifts slightly towards a lower water concentration. A maximum is also observed in the density measurements at 0.40 mole fraction of water which shifts towards higher water concentration with increase in temperature.

It has been suggested by Geddes (5) that such maxima have no real meaning and that it is the point of greatest deviation from linearity which is related to the composition of any complex formed on mixing. On this basis both viscosiy and density measurements have maximum deviations at a ratio of 2 moles water to 1 mole DMSO.

Heats of mixing are listed in Table II. These are negative over the whole range of compositions examined, which is again indicative of a strong interaction between the

TABLE II

Heats of mixing of DMSO and water

Mole fraction water	ΔH (calories per mole solution)	ΔH (calories per mole water)
0.183	−258	−1408
0.307	−412	−1338
0.436	−575	−1321
0.558	−604	−1083
0.675	−611	− 905
0.725	−600	− 828
0.792	−574	− 724
0.897	−348	− 388

two liquids. A graph of the heat of mixing expressed in calories/mole solution plotted against mole fraction water passes through a flat maximum at 0.63 mole fraction water and $\Delta H = -620$ calories.

DISCUSSION

Aqueous solutions of non-electrolytes are the most difficult class of binary liquid systems to understand, and as a result no theory has been developed which can describe their thermodynamic properties adequately. An attempt has been made by Rowlinson (6) to classify these systems in terms of increasing numbers of solute–water hydrogen bonds, ranging from weakly interacting substances such as ketones to the strongly bonded hydrogen peroxide – water system.

The results obtained here indicate that there is a greater degree of association in water–DMSO mixtures than in water alone, which may be explained in terms of the polar sulphoxide group. The DMSO molecule can be represented (7) by the forms I and II,

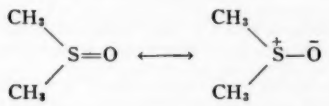

I II

in which the negatively charged oxygen should form hydrogen bonds with the water molecules. This hypothesis is substantiated by the considerable volume contraction on mixing, the large negative heat of mixing, and the positive maxima in the viscosity isotherms.

Thus it is probable that a DMSO hydrate is formed, although it cannot be stated definitely from the above data that a stable compound exists at the temperatures investigated. The fact that the maximum in the viscosity isotherm decreases with increasing temperature suggests that any association complex formed is thermally labile and could only be expected to exist in a completely undissociated state at low temperatures. Further investigation would be necessary to establish its existence and composition.

CONCLUSIONS

The system DMSO–H_2O belongs to the class of solutions possessing numerous solute–water bonds which are stronger than the hydrogen bonds between water molecules. Evidence is presented for the existence of a 2:1 association complex between water and DMSO, but this cannot be proved on the basis of the data presented. Finally it should be stressed that DMSO must be carefully dried before being used as a solvent in physical measurements, especially viscosity determinations, if meaningful results are to be obtained.

ACKNOWLEDGMENTS

The authors wish to thank Dr. D. A. I. Goring for allowing them access to his manuscript prior to publication, Mr. R. Ironside for carrying out the water analyses, and Dr. S. Bywater for his interest in the work.

REFERENCES

1. R. G. LeBel and D. A. I. Goring. J. Chem. Eng. Data. In press.
2. J. Mitchell and D. M. Smith. Aquametry. Interscience Publishers Inc., 1948.
3. M. R. Cannon, R. E. Manning, and J. D. Bell. Anal. Chem. **32**, 355 (1960).
4. R. D. Vold. J. Am. Chem. Soc. **59**, 1515 (1937).
5. J. A. Geddes. J. Am. Chem. Soc. **55**, 4832 (1933).
6. J. S. Rowlinson. Hydrogen bonding. Proc. Conf. I.U.P.A.C. Ljubljana, Yugoslavia. 1957. p. 423.
7. W. A. Waters. Physical aspects of organic chemistry. Routledge and Kegan Paul Ltd., London. 1953.

THE DECOMPOSITION OF CARBON DIOXIDE BY Hg $6(^3P_1)$ AND Hg $6(^3P_0)$ ATOMS[1]

OTTO P. STRAUSZ AND HARRY E. GUNNING

ABSTRACT

Carbon dioxide has been shown to decompose into carbon monoxide and oxygen atoms, when exposed to radiation at 2537 Å, in the presence of mercury vapor. The rate rises steeply with decreasing substrate pressure, and varies directly with the 1.8 ± 0.1 power of the light intensity. The proposed mechanism attributes reaction to the collision of electronically excited CO_2 molecules with Hg $6(^3P_1)$ atoms. The suppression of reaction at higher substrate pressures is readily explained in terms of collisional deactivation of the excited CO_2 species. Nitrogen was found to increase the rate of CO formation; the maximum effect was obtained for a mixture of 7.4 mm nitrogen and 3.74 mm carbon dioxide, in which case the rate was 1.58 times that for pure substrate. It is shown that nitrogen serves to generate metastable Hg $6(^3P_0)$ atoms, which can sensitize the decomposition. The reaction might serve as a chemical method for monitoring Hg $6(^3P_0)$ atoms. For CO_2–N_2 mixtures, the rate was found to rise when the reacting system was exposed to radiation at 4047 Å. This is taken as direct evidence of sensitization by higher states of mercury, generated by stepwise excitation, since radiation at 4047 Å converts Hg $6(^3P_0)$ to Hg $7(^3S_1)$.

INTRODUCTION

Several studies (1–4) have been made of the photolysis of carbon dioxide in the vacuum ultraviolet. With a xenon source, Groth (2) found the quantum yield of CO formation, Φ_{CO}, to be 0.96, and he suggested that atomic oxygen is formed in the primary process. However, Jucker and Rideal (3), for the 1470-Å line of xenon, obtained 1.9 ± 0.2 for Φ_{CO}. They proposed a mechanism involving the initial formation of an excited molecule which, upon collision with the substrate, formed $2CO + O_2$. Recently Mahan (4) has studied the photolysis, at both 1236 Å and 1470 Å. In agreement with Groth (2), he found Φ_{CO} to have values near unity at both wavelengths and he presented convincing arguments for a primary process leading to the formation of excited (^1D) oxygen atoms.

The first mercury-photosensitized decomposition of carbon dioxide was carried out by Herschfinkel (5), although the role of mercury was not recognized until later by Coehn and May (6). In a more detailed study, Cline and Forbes (7) showed that the decomposition was specifically initiated by Hg $6(^1P_1)$ atoms, arising by absorption by mercury of its resonance radiation at 1849 Å; they found no evidence for a reaction of carbon dioxide with Hg $6(^3P_1)$ atoms.

The present study arose from the observation that carbon dioxide, in the presence of mercury vapor, undergoes a slow decomposition when exposed to 2537-Å radiation, contrary to previous findings (7). The dissociation of CO_2 into $CO + O$ requires at least 126.7 kcal/mole, whereas only 112.2 kcal/mole are available from a simple collision of the second kind with Hg $6(^3P_1)$ atoms. The additional energy needed for the reaction to proceed could be supplied either from the primary formation of HgO, or from reactions involving energy accumulation, such as the formation of excited carbon dioxide molecules. In the present study, emphasis has been placed on the nature of the primary reactions involved in the decomposition. The investigation forms part of a general program on primary processes in mercury photosensitization.

[1]*Manuscript received July 5, 1961.*
Contribution from the Department of Chemistry, University of Alberta, Edmonton, Alberta.

EXPERIMENTAL

The reaction was studied under static conditions. For the reaction cell, a cylindrical tube of Vycor 7900 glass was used, 120 mm in length and 26 mm in diameter, with flat windows of Vycor 7910 glass at each end. The side arm connecting the cell to the high-vacuum system was placed near one window, in order that the cell could be inserted axially into the coils of a spiral Hanovia SC-2537 mercury resonance source. The lamp-cell assembly was positioned in a water thermostat, maintained at 30°, in such a fashion that the end windows were opposite ports of window glass in the sides of the thermostat. Thus, in addition to the radiation from the spiral lamp, the cell could be independently irradiated at both ends by sources external to the thermostat. For these external sources, Hanovia Biosteritron resonance lamps were employed.

After each exposure, gases non-condensable in liquid nitrogen were transferred to a gas burette, and subsequently analyzed by gas–liquid partition chromatography (G.L.P.C.). Between experiments the cell was cleaned in hot nitric acid, rinsed with distilled water and ethanol, and dried at 200°. A reaction was also performed by using a ^{202}Hg electrodeless discharge source. A Vycor 7910 glass cell attached to a small mercury pump and to a 1-liter bulb was filled with CO_2, sealed off, and irradiated with the above lamp. After the reaction was completed the cell containing the HgO was pumped for 12 hours. Then the HgO was dissolved in very dilute HCl, plated out on copper wire, distilled, and collected *in vacuo* into a small break-seal. Finally the isotopic composition of the recovered mercury was determined by mass spectrometry.

The carbon dioxide used was Matheson 'Bone-Dry' grade, with stated purity of 99.8%. It was subjected, before use, to several low-temperature distillations, after which no impurities could be detected by G.L.P.C. The nitrogen (Canadian Liquid Air 'Purified Grade', with minimum purity of 99.9%) was passed through a quartz furnace containing copper filings at 500°, and several liquid nitrogen traps, before use.

RESULTS

The products of the reaction were carbon monoxide and mercuric oxide. Molecular oxygen was not detected in any of the runs. In Fig. 1, the micromoles of CO formed, as a function of CO_2 pressure, are given for runs of 150 minutes in duration. The percentage conversion at the lowest pressure, 0.6 mm, was 28.7%. At 13.3 mm, only 0.5% of the CO_2 was decomposed.

The absorbed light intensity at 2537 Å, as determined with propane as actinometer (8), was 3.34×10^{-5} einstein/minute. The maximum rate of CO formation occurred at a CO_2 pressure of 0.6 mm; 2.87 μmoles of CO were formed in 150 minutes of exposure. This rate would correspond to a quantum yield of 5.7×10^{-4} moles/einstein. Of course, at a pressure of 0.6 mm, only a small fraction of the excited mercury atoms are quenched. It is estimated that the actual quantum yield of CO formation under these conditions is at least 0.01.

The addition of nitrogen was found to influence markedly the rate of CO formation. The effect is shown in Table I. The runs with and without added nitrogen were carried out under identical conditions. The highest rate increase observed was 58%, in the case of a mixture of 3.74 mm CO_2 and 7.4 mm N_2.

The fact that the rate of CO formation rapidly decreases with increasing substrate pressure, as shown in Fig. 1, would suggest that excited CO_2 molecules are involved in

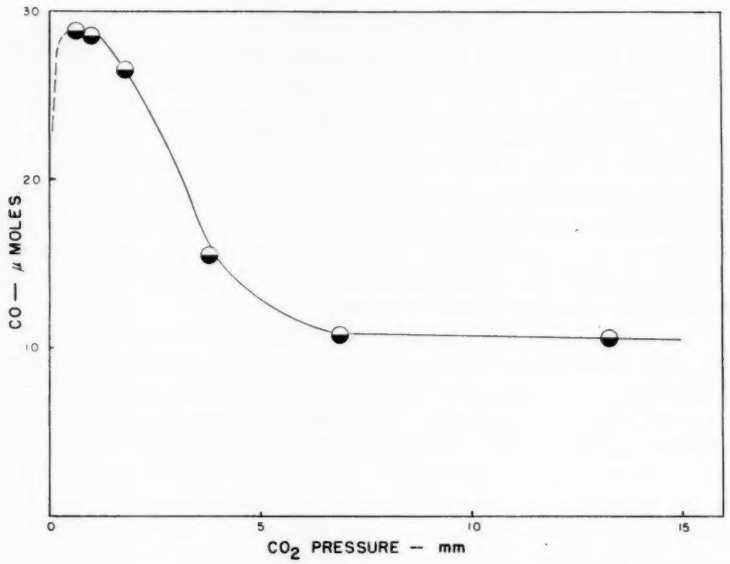

FIG. 1. Micromoles of CO formed for runs of 150 minutes in duration, as a function of substrate pressure.

TABLE I

The effect of nitrogen on the rate of CO formation in the reaction of CO_2 with Hg $6(^3P)$ atoms

P_{CO_2} (mm)	P_{N_2} (mm)	CO formed (μmoles)	Increase in R_{CO} (%)
3.22	—	3.32	41
3.13	6.2	4.69	
3.22	—	7.08	39
3.30	6.2	9.85	
1.02	—	3.30	
1.02	6.5	3.74	13
9.91	—	1.16	
8.24	—	1.11	av. 36
8.88	11.2	1.54	
3.57	—	1.80	58
3.74	7.4	2.85	

the reaction, and that these are suffering progressive collisional deactivation with increasing CO_2 pressure. From Table I, which exhibits the marked effect of nitrogen on the rate of CO formation, the participation of metastable Hg $6(^3P_0)$ atoms is suggested. If the CO product is formed by collisions between excited CO_2 molecules and Hg $6(^3P_1)$ atoms and/or Hg $6(^3P_0)$ atoms, one would expect the rate to depend upon the square of the absorbed light intensity. An alternative or additional process which could be operative is that of stepwise excitation. Mercury resonance lamps are good sources of the 4047-Å line, which is absorbed by Hg $6(^3P_0)$ atoms to form the $7(^3S_1)$ state. Direct collisional deactivation of $7(^3S_1)$ atoms to the ground, $6(^1S_0)$, state would release 7.95 ev, or ca. 183 kcal/mole. For the afore-mentioned reasons, it appeared particularly instructive to

examine the effect of light intensity and 4047-Å radiation on the rate of CO formation.

The dependence of the rate upon light intensity was determined by the use of two bromine filters of different transmission characteristics. Both filters were doughnut types, 110 mm in length, 35 mm I.D., and 60 mm O.D. They were designed to fit axially over the reaction cell and within the coils of the spiral resonance lamp. Both filters were filled with bromine vapor at 170 mm. Their transmission characteristics were determined both spectrophotometrically and by propane actinometry (8). Filter I was made of Vycor 7910 and filter II of Vycor 7900. Their characteristics were as follows: filter I, transmitted 55.7% at 2537 Å, and less than 1% at 4047 Å; filter II, transmitted 17.5% at 2537 Å, and less than 1% at 4047 Å.

In Table II the results are given for six experiments performed with decreased light

TABLE II

The relation between μmoles of CO formed and incident intensity at 2537 Å, for runs of 150 minutes in duration

Filter	P_{CO_2} (mm)	P_{N_2} (mm)	CO formed (μmoles)	Exponent of light intensity
I	1.7	—	0.66	2.1
None	1.6	—	2.33	
I	3.5	6.3	1.12	1.7
None	3.4	6.2	2.96	
I	1.7	—	0.82	2.0
None	1.7	—	2.67	
I	7.4	—	0.40	1.7
None	7.4	—	1.07	
I	7.0	—	0.40	1.7
None	7.0	—	1.07	
II	1.5	—	0.17	1.6
None	1.5	—	2.75	
				Mean = 1.8±0.1

intensities, achieved by inserting the filters as indicated. In each case, the results are compared with those without filter. In the last column is given the order of dependence of the rate on the intensity of the 2537-Å radiation. The mean value of the exponent is 1.8±0.1. It should also be noted from Table II that the near second-order dependence of the rate upon the light intensity also obtains in the presence of added nitrogen.

The effect of 4047-Å radiation on the reaction was studied by placing Biosteritron sources at the ports of the thermostat. By this means the cell could be exposed at both ends to the radiation transmitted through the window glass in the thermostat ports. Only radiation exceeding ca. 3800 Å in wavelength could thereby enter the cell.

In Table III is shown the effect, on the rate of CO formation, of dosing the reaction cell at each end with 4047-Å radiation, while the normal reaction is in progress. It can be seen that the 4047-Å radiation increases the rate by ca. 22% for the optimum CO_2–N_2 mixture, for an incident intensity at 2537 Å of 3.3×10^{-5} einstein/minute. The effect appears to be much larger at lower intensities of the resonance radiation, as shown in the last run listed in the table, where a 53% increase in rate is achieved.

In order to confirm that the reaction was indeed mercury sensitized, one experiment was performed at 5°. Under these conditions there was a drastic decrease in reaction rate, indicating the dependence of the reaction on the presence of mercury vapor.

TABLE III

The effect of 4047-Å radiation on the rate of CO formation in the reaction of CO_2 with Hg $6(^3P)$ atoms

4047 Lamps*	Filter	P_{CO_2} (mm)	P_{N_2} (mm)	CO formed† (μmoles)	Fractional increase
On	—	2.7	7.2	3.94	1.22
Off	—	2.9	6.9	3.22	
On	—	3.3	5.5	3.17	1.09
Off	—	3.3	5.5	2.90	
On	—	1.5	—	2.96	1.06
Off	—	1.5	—	2.80	
On	I	3.1	6.3	2.20	1.53
Off	I	3.1	6.2	1.44	

*It is estimated that the two Biosteritron sources increased the intensity at 4047 Å by a factor of 10.
†For runs of 150 minutes in duration.

Finally, one 30-hour run was made with $P_{CO_2} = 1.82$ mm, using a ^{202}Hg electrodeless discharge source. Mass spectrometric analysis showed that the ^{202}Hg content of the HgO product was 31.6%, compared to the normal abundance of 29.8%.

DISCUSSION

From Fig. 1, it is apparent that the reaction of carbon dioxide with Hg $6(^3P)$ atoms is a remarkable example of collisional deactivation. In the pressure region studied, i.e. 0–15 mm, the rate of CO formation, R_{CO}, falls off rapidly with increasing substrate pressure, despite the fact that the fraction of the incident light energy transferred to the substrate by quenching is simultaneously rising. Combining the foregoing with the near-second-order dependence of R_{CO} on light intensity, as shown in Table II, would suggest strongly a mechanism involving the reaction of excited CO_2 molecules with Hg $6(^3P)$ atoms:

$$Hg + h\nu \rightarrow Hg^* \quad [1]$$

$$Hg^* \rightarrow Hg + h\nu \quad [2]$$

$$Hg^* + CO_2 \rightarrow CO_2^* + Hg \quad [3]$$

$$CO_2^* + CO_2 \rightarrow 2CO_2 \quad [4]$$

$$CO_2^* + Hg^* \rightarrow CO + Hg + O, \quad [5]$$

where $Hg^* = Hg\ 6(^3P_1)$ and CO_2^* represents an energy-rich CO_2 molecule. It is assumed that the CO_2^* which reacts in [5] possesses at least (126.7−112.2) kcal/mole of excess energy.

Since the quantum yield, Φ_{CO}, is very small for the reaction, i.e. less than 0.01, we may reasonably assume that step [5] does not appreciably alter the steady-state concentrations of Hg^*. With this approximation we obtain the following expression for the rate of CO formation:

$$R_{CO} = K\frac{(CO_2)}{A+B(CO_2)+C(CO_2)^2+D(CO_2)^3}, \quad [a]$$

where $K = K_3K_5I_a^2$, $A = K_2K_5I_a$, $B = K_2^2K_4 + K_3K_5I_a$, $C = 2K_2K_3K_4$, $D = K_3^2K_4$, and I_a is the absorbed light intensity at 2537 Å. The mechanism therefore predicts that R_{CO} will (*a*) decrease rapidly with increasing substrate pressure and (*b*) vary nearly

directly with I_a^2, in qualitative accordance with our findings. Alternately step [5] may be replaced by

$$CO_2^* + CO_2^* \rightarrow CO_2 + CO + O. \qquad [5']$$

An approximate solution of the steady-state equations with [5'] replacing [5] yields an expression similar to [a]. Thus both steps [5] and [5'] are qualitatively consistent with the observed kinetics for pure carbon dioxide. In this connection, it should be noted that the absence of molecular oxygen precludes the possibility of O_2 formation in [5'].

At low substrate pressure other processes such as radiative transition and(or) deactivation at the wall may also occur.

The low isotopic enrichment of the HgO formed in the reaction gives additional evidence that the process

$$CO_2 + Hg^* \rightarrow CO + HgO$$

does not occur to an appreciable extent.

The electronic state of the excited carbon dioxide is probably a metastable triplet. Indeed the first known electronic state above the ground state is triplet π, with an excitation energy estimated not to exceed 130 kcal/mole (9, 10). Now for reaction [5] to be energetically possible, CO_2^* must possess 14.5 kcal/mole of excess energy. It is pertinent here to note that Walsh (11, 12) has assigned to CO_2 a $^3B_2$ state at 30–40 kcal/mole above the ground state. For this state to participate in the present reaction, CO would have to be formed by [5] rather than [5'].

The effect of added nitrogen on R_{CO} can readily be explained by the production of metastable Hg $6(^3P_0)$ atoms (Hg^0) and by their subsequent reactions with CO_2:

$$CO_2 + Hg^0 \rightarrow CO_2^* + Hg \qquad [6]$$

$$CO_2^* + Hg^0 \rightarrow CO + Hg + O. \qquad [7]$$

Klumb and Pringsheim (13, 14) have shown that the concentration of Hg^0, in the presence of nitrogen, may be expressed by the relation

$$(Hg^0) = AP/[1+BP+CP^2],$$

where A, B, and C are constants, and P is the nitrogen pressure. The maximum value of (Hg^0) was reported to occur at a nitrogen pressure of 6 mm. We observed a maximum 1.58-fold increase in R_{CO} (Table I) when 7.4 mm N_2 was added to 3.74 mm CO_2, which would correspond to a 2.4-fold increase if we compare it to R_{CO} at a CO_2 pressure equal to the total pressure of CO_2 and N_2 (approx. 11 mm).

Owing to the higher lifetime for the metastable state, the concentration of Hg $6(^3P_0)$ atoms should be about 1 or 2 orders of magnitude higher than the concentration of Hg $6(^3P_1)$ atoms. We may therefore infer that the metastable species show much lower reactivity in the present system than do Hg $6(^3P_1)$ atoms.

In Table III, evidence is presented for a positive contribution of 4047-Å radiation to the rate of decomposition of CO_2–N_2 mixtures. The results with filter I in position are especially interesting. Here the 4047-Å radiation from the spiral source has been reduced to ca. 1% of its original value by the filter. When 4047-Å radiation is then introduced at the ends of the cell, the value of R_{CO} increases by 53%. It would appear unwise at this time to attempt to write a mechanism for this effect. We may note that quenching by CO_2 of Hg $7(^3S_1)$ atoms could result in the mercury being converted to any of the three triplet states, or to the ground state. Certainly the phenomenon merits more detailed study.

CONCLUSIONS

As a result of the present investigation, it may be concluded that carbon dioxide undergoes a slow decomposition when sensitized by either Hg $6(^3P_1)$ or Hg $6(^3P_0)$ atoms. The observed kinetics dictate the participation in the reaction of excited CO_2 molecules, presumably in metastable triplet states. Apart from its inherent interest as an example of a mercury-photosensitized reaction which is second order in the light intensity, the system might serve as a chemical method for monitoring Hg $6(^3P_0)$ atoms. Finally, the present study has provided evidence of reaction associated with higher states of mercury which have been generated *in situ* by stepwise excitation.

ACKNOWLEDGMENTS

The authors are indebted to Dr. Willard F. Allen, Dr. Paul Kebarle, Dr. Roger Klemm, and Mr. Thomas Dingle, all of this laboratory, for many helpful discussions. This investigation has been partially supported by the National Research Council under N.R.C. Grant No. B.T. 74. This assistance is most gratefully acknowledged.

REFERENCES

1. D. L. CHAPMAN, S. CHADWICK, and J. E. RAMSBOTTOM. J. Chem. Soc. **91**, 951 (1907).
2. W. GROTH. Z. phys. Chem. (Leipzig), B, **38**, 366 (1938).
3. H. JUCKER and E. K. RIDEAL. J. Chem. Soc. 1058 (1957).
4. B. H. MAHAN. J. Chem. Phys. **33**, 959 (1960).
5. H. HERSCHFINKEL. Compt. rend. **149**, 395 (1909).
6. A. COEHN and B. W. MAY. Z. phys. Chem. (Leipzig), B, **26**, 117 (1934).
7. J. E. CLINE and G. S. FORBES. J. Am. Chem. Soc. **61**, 716 (1939).
8. S. BYWATER and E. W. R. STEACIE. J. Chem. Phys. **19**, 319 (1951).
9. K. J. LAIDLER. J. Chem. Phys. **17**, 221 (1949).
10. K. J. LAIDLER. The chemical kinetics of excited states. Clarendon Press, Oxford. 1955.
11. A. D. WALSH. J. Chem. Soc. 2266 (1953).
12. A. G. GAYDON. The spectroscopy of flames. Chapman & Hall, London. 1957.
13. H. KLUMB and P. PRINGSHEIM. Z. Physik, **52**, 610 (1928).
14. J. A. BERBERET and K. C. CLARK. Phys. Rev. **100**, 506 (1955).

PRIMARY QUANTUM YIELD DETERMINATION BY INTERMITTENT ILLUMINATION IN THE REACTION OF METHANOL VAPOR WITH Hg $6(^3P_1)$ ATOMS[1]

ARTHUR R. KNIGHT AND HARRY E. GUNNING

ABSTRACT

The decomposition of methanol vapor by Hg $6(^3P_1)$ atoms has been studied under intermittent illumination conditions, in a static system at 25° C. The behavior of the NO-inhibited reaction under intermittent illumination has also been examined.

For the pure substrate at a pressure of 50 mm, the quantum yield of hydrogen formation, $\Phi(H_2)$, was found to rise steadily toward unity with decreasing light period (t_L). The maximum value of $\Phi(H_2)$ at a given t_L could only be obtained if the dark period (t_D) exceeded 100 mseconds. At the shortest t_L studied, 0.156 msecond, $\Phi(H_2)$ was 0.89 compared with the steady illumination value, at zero extent of reaction, of 0.46. A linear relation was found to obtain between $\Phi(H_2)$ and log (t_L) at a given t_D. Extrapolation showed that $\Phi(H_2)$ would be unity at $t_L = 0.040$ msecond.

For a mixture of 4.8 mm of NO and 50 mm of CH_3OH, $\Phi(CH_3ONO)$ was found to rise from its steady illumination value of 0.14 to 0.27 at a sector speed of 300 r.p.m., with a dark/light ratio of 20. At higher speeds the quantum yield decreased again.

From the study it is concluded that the primary process of H atom detachment is at least 89% efficient, and that the primary quantum yield is likely unity. The fact that the quantum yield under steady illumination is only 0.46 is attributed to the consumption of H atoms by radical addition processes of which the most probable is the addition of H to CH_2OH. For the inhibited reaction the low value of $\Phi(CH_3ONO)$ under steady illumination is ascribed to the abstractive attack of CH_3O on NOH.

The kinetic effects of intermittent illumination are discussed, in the light of the results. It is concluded that the technique should be of considerable value in primary process studies in mercury photosensitization.

INTRODUCTION

In a previous study (1) of the reaction of methanol vapor with Hg $6(^3P_1)$ atoms, it was shown that the quantum yield of hydrogen formation, extrapolated to zero exposure duration, $\Phi(H_2)$, was 0.46. The fact that this value is not unity could be due to the reactions:

$$H + H \xrightarrow{M} H_2, \qquad [1]$$

$$H + CH_2OH \rightarrow CH_3OH, \qquad [2]$$

$$H + CH_3O \rightarrow CH_3OH. \qquad [3]$$

Since, at the substrate pressure used (50 mm) in the previous study (1), CH_3O was shown to react almost exclusively with the substrate to form CH_2OH, it is likely that [2] is the most important of the above three steps competing for H atoms with the abstraction reaction:

$$H + CH_3OH \rightarrow H_2 + CH_2OH. \qquad [4]$$

For the reaction inhibited by NO, the steps

$$CH_3O + NOH \rightarrow CH_3OH + NO \qquad [5]$$

and

$$CH_3O + CH_3ONO \rightarrow CH_3OH + CH_2O + NO \qquad [6]$$

have been suggested (1) to explain the fact that $\Phi°(CH_3ONO)$ was found to be less than unity. The rates for reactions [1]–[3] will be proportional to the products of the con-

[1]*Manuscript received July 21, 1961.*
Contribution from the Department of Chemistry, University of Alberta, Edmonton, Alberta.

centrations of the radicals involved. Similarly, for the inhibited reaction, (NOH) will vary with (H), and therefore the rate of step [5] will also depend upon a product of radical concentrations.

Under intermittent illumination, with progressive shortening of the light period (t_L), it should be possible to interrupt the light beam before the radical concentrations have reached their steady-state values. In this region, $\Phi(H_2)$ should rise sharply with decreasing t_L, provided that the radical concentrations are allowed to decay to zero during the dark period (t_D). Hence it is also necessary to study the effect of t_D on $\Phi(H_2)$. With decreasing t_L, $\Phi(H_2)$ should approach unity, if (*a*) the primary reaction between Hg $6(^3P_1)$ and CH_3OH shows perfect efficiency for detachment of H atoms, and (*b*) steps [1]–[3] include the processes responsible for the disappearance of H atoms without concomitant H_2 formation.

In the present communication are reported the results of varying t_L and t_D, on $\Phi(H_2)$ for the decomposition of pure CH_3OH, and on $\Phi(CH_3ONO)$ for the reaction in the presence of NO.

EXPERIMENTAL

The purification and storage of the methanol, the all-quartz high-vacuum system employed, and the analytical techniques have been previously described (1). After the reaction cell had been filled, it was placed in one of the two devices detailed below.

For the runs with pure substrate with t_D = 103 and 67 milliseconds (msec), and for the studies on the inhibited reaction, the sector apparatus consisted of a Hanovia, 87A45, mercury-in-quartz resonance tube, in a cylindrical housing, with a 5-cm diameter window covered with a Vycor 7910 filter. A rotating metal disk with an adjustable sector aperture was interposed between the light source and a shield with a 5-cm diameter opening, directly behind which the cell was placed. The disk was mounted on the shaft of a variable speed motor, of which the speed of rotation could be controlled to ±4%. The r.p.m. of the sector was checked during each run by a stroboscope. The disk consisted of two metal plates from which two 90° sectors had been cut. The sector angle was determined by closing the plates on a steel rod of accurately known diameter, placed at a known distance from the center. One of the two resulting apertures was closed for all runs except those at long t_L.

For the runs with t_D = 80 and 160 msec, the lamp (Engelhard 11639) was placed in a rectangular housing with a 6-cm² opening covered by a Vycor 7910 filter. The light beam was chopped by two overlapping disks mounted between two $\frac{3}{8}$-in. plates, connected by a gear chain, and driven by a constant speed motor. One disk, rotating at 3000 r.p.m., had one sector aperture set accurately as described above. The other sector disk revolved at 375 r.p.m. and had two approximately 30° apertures. The beam was partially collimated by a 6-cm diameter opening, placed between the disks and the cell. The cell was located behind the shield already described. The rotations of the disks were so synchronized that the more slowly rotating sector uncovered the entire cell face as the high speed disk made each exposure. With both 30° sector apertures operative, t_D was 80 msec; by blocking one of the apertures, t_D = 160 msec was obtained.

Light intensities were determined with propane as actinometer (2), using the differential method of Back (3) for obtaining the steady-state value for dH_2/dt.

At the end of each run, the products non-condensable in liquid nitrogen were analyzed by G.L.P.C. on a molecular sieves column. The hydrogen content of this gas was never less than 96 mole%, with the remainder consisting of CO and CH_4. For the runs with

$t_L < 0.5$ msec, the $(CO+CH_4)$ content was less than 0.5 mole%. The analysis for methyl nitrite has been previously described (1).

RESULTS

During the course of the investigation various minor modifications were made in the sector system which resulted in changes in the absorbed light intensity at 2537 Å. For the range of values of the sector parameters reported here, it was found that $\Phi(H_2)$ was independent of exposure duration at least to a total quantum input of 5 microeinsteins. In Fig. 1, $\Phi(H_2)$ is shown as a function of log (t_L) for four series of runs at dark periods of 67, 80, 103, and 160 mseconds. In all cases, the cell was filled with pure CH_3OH at a pressure of 50 mm. For the runs with $t_D = 67$ and 103 mseconds, the single sector was used, with absorbed light intensities of both 0.91 and 1.06 microeinsteins/minute, and net exposure durations of 4.3–5.0 minutes. The series with $t_D = 80$ and 160 msec were performed with the double sector apparatus. Here, absorbed light intensities of 1.25, 2.19, and 3.25 microeinsteins/minute were used, and net exposure durations of 0.43–1.0 minutes.

From the plot of $\Phi(H_2)$ vs. log (t_L) in Fig. 1, it is apparent that $\Phi(H_2)$ rises steadily

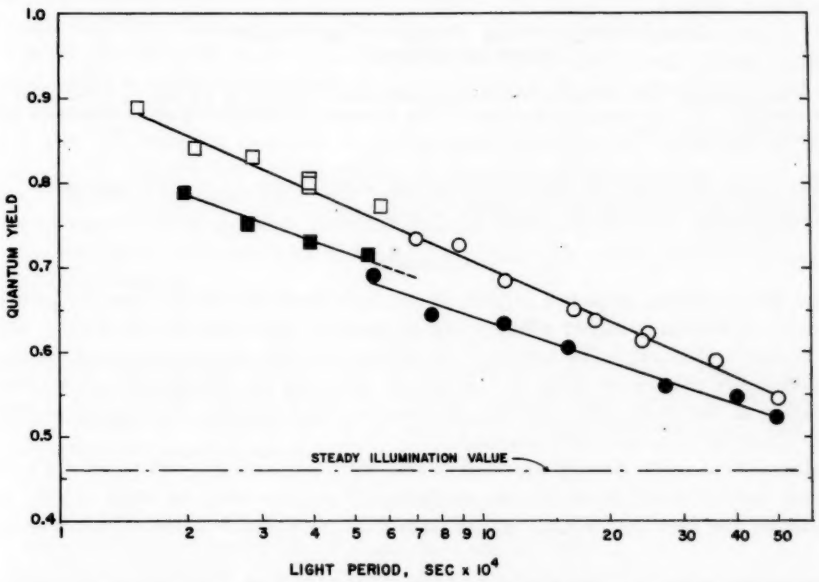

FIG. 1. The quantum yield of hydrogen formation at a methanol pressure of 50 mm, as a function of the logarithm of the light period for dark periods of □ 160, ■ 80, ○ 103, and ● 67 milliseconds.

above its steady illumination value of 0.46 with decreasing t_L, at least for t_L values less than 5 mseconds. Furthermore, from Fig. 1, the effect of t_D on $\Phi(H_2)$ is to be noted. For maximum values of $\Phi(H_2)$ at a given t_L, it is necessary that t_D be at least ca. 100 mseconds. In these runs the maximum value obtained for $\Phi(H_2)$ was 0.89, with $t_L = 0.156$ msecond and $t_D = 160$ mseconds. The absorbed light intensity was 1.25 microeinsteins/minute, and the net exposure duration was 1.00 minute. The t_L value of 0.156 msecond was the

shortest light pulse which could be obtained with the sector equipment used. Since $\Phi(H_2)$ seems to be a linear function of log (t_L), the upper curve in Fig. 1 was linearly extrapolated to $\Phi = 1.00$. The corresponding t_L value was 0.040 msecond.

For the inhibited reaction, a short series of runs was performed with a constant t_D/t_L ratio of 20, in which t_L was varied from 6.50 to 2.79 mseconds. The reaction mixture consisted of 4.8 mm of NO and 50 mm of CH_3OH. The net exposure duration was 4.75 minutes. In Fig. 2, $\Phi(CH_3ONO)$ is shown as a function of the r.p.m. of the sector. The

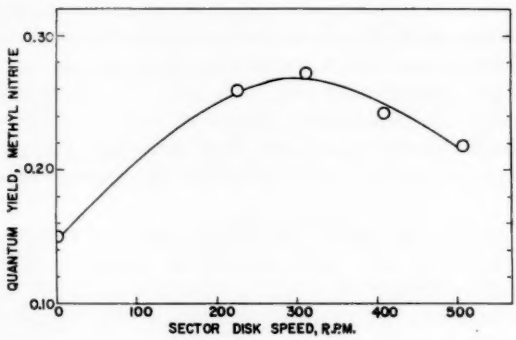

FIG. 2. The quantum yield of methyl nitrite formation for a mixture of 4.8 mm of nitric oxide and 50 mm of methanol, for a net exposure duration of 4.75 minutes, as a function of sector disk speed for a constant dark/light ratio of 20.

maximum value obtained for $\Phi(CH_3ONO)$ was 0.272, with $t_L = 4.61$ mseconds. The steady illumination value for $\Phi(CH_3ONO)$ was 0.140.

DISCUSSION

For the decomposition of pure CH_3OH, the present study has shown that the primary process is of considerably higher efficiency than would be indicated by the $\Phi°(H_2)$ value of 0.46. Since the highest value obtained for $\Phi(H_2)$ was 0.89, the primary process must have an efficiency of at least 89%. Furthermore, assuming the validity of a short linear extrapolation of the upper $\Phi(H_2)$ vs. log (t_L) line in Fig. 1, we may conclude that $\Phi(H_2)$ would be unity for a t_L of 0.040 msecond.

The observed increase toward unity of $\Phi(H_2)$ with decreasing t_L supports the hypothesis that radical addition reactions involving H atoms, such as steps [1]–[3], are responsible for the fact that $\Phi°(H_2)$, under steady illumination, is considerably less than unity.

One surprising result of this study was the relatively long dark period required to achieve the maximum value of $\Phi(H_2)$ at a constant t_L. The data, however, clearly indicate that there must be at least 100 mseconds between light pulses for optimum $\Phi(H_2)$ values to be obtained. If the 100-msecond dark interval does not represent the actual time required for the radical concentrations to decay to negligible values, then an alternate explanation might be that radiation partitioning to reaction products is occurring in the light period, and the dark period serves to allow these products to diffuse away from the reaction zone. From the previous study (1), formaldehyde would be the most reactive primary product present in the reaction zone. The presence of CO would be evidence of the secondary decomposition of this material. However, our analyses show that the

total yields of ($CO+CH_4$) do not exceed 0.5 mole% of the non-condensable gas runs with t_L less than 0.5 msecond. It therefore seems unlikely that product diffusion is a significant factor in determining the magnitude of the optimum dark period. Now at the onset of the dark period, the radicals present in greatest abundance would likely be H and CH_2OH. The H atoms would diffuse much more rapidly than the CH_2OH radicals from the reaction zone, and this diffusive separation would favor reaction [4] over [2], with a resulting increase in $\Phi(H_2)$.

The behavior of $\Phi(CH_3ONO)$ as a function of sector disk speed, as shown in Fig. 2, again illustrates the effects of both t_L and t_D on the radical concentrations. With decreasing t_L, the concentrations of both CH_3O and NOH would be reduced, rendering step [5] less probable, and thus favoring the formation of CH_3ONO. This accounts for the increasing $\Phi(CH_3ONO)$ with r.p.m. of the sector, as shown in Fig. 2. The decline in nitrite yield at high sector speeds is attributable to the decreasing t_D, resulting in a finite radical concentration being present at the beginning of the next light pulse.

CONCLUSIONS

As a result of the present study it can be concluded that the primary process of H atom detachment in the reaction of methanol vapor with Hg $6(^3P_1)$ atoms is at least 89% efficient, and that it is likely that the primary quantum yield is in fact unity. The fact that $\Phi^\circ(H_2)$ is only 0.46 under steady illumination conditions would appear to be due to radical addition reactions involving H atoms, of which the most probable is the addition of H atoms to CH_2OH radicals.

For the NO-inhibited reaction, it is concluded that the low value for $\Phi(CH_3ONO)$ under steady illumination is due mainly to the abstractive attack of CH_3O on NOH.

As a general conclusion from the present study, the rotating sector method should prove of considerable value in primary process studies in mercury photosensitization. Similar studies on the reactions of Hg $6(^3P_1)$ atoms with ethanol and isopropanol will be published shortly.

ACKNOWLEDGMENTS

The authors would like to express their appreciation to Dr. W. F. Allen of this laboratory for valuable assistance and advice. Our program was supported in part by the National Research Council under Term Grant No. NRC T-162 (Gunning). This support is very gratefully acknowledged.

REFERENCES

1. A. R. KNIGHT and H. E. GUNNING. Can. J. Chem. **39**, 1231 (1961).
2. S. BYWATER and E. W. R. STEACIE. J. Chem. Phys. **19**, 319 (1951).
3. R. A. BACK. Can. J. Chem. **37**, 1834 (1959).

THEORETICAL STUDIES ON THE ELECTRONIC SPECTRA OF SUBSTITUTED AROMATIC MOLECULES

PART I. THE INTRAMOLECULAR ELECTRON TRANSFER MODEL[1]

J. E. BLOOR

ABSTRACT

A simple empirical model, based on molecular orbital theory without configuration interaction, is used to interpret the *K* band transitions of substituted aromatic molecules as involving intramolecular electron transfer between substituent and hydrocarbon. For electron-donating substituents, such as amino, methoxyl, chloro, bromo, and iodo, the transfer is from substituent to hydrocarbon, while for electron-attracting substituents, such as nitro, formyl, acetyl, and cyano, the charge transfer is from hydrocarbon to substituent. Such a treatment is successful for "long field molecules" (benzene, diphenyl, terphenyl, styrene, and stilbene), but for "round field" molecules agreement between experiment and theory was achieved only for electron-donating substituents. The theory, like less empirical theories, overestimates the relative effect of a substituent in the 2-position compared with substitution in the 1-position.

In molecular orbital (MO) calculations of the electronic transitions in conjugated molecules the importance of configuration interaction is well recognized (1–4). However, for all but the simplest molecules it has been the custom to restrict, quite arbitrarily (4), the configuration interaction to singly excited configurations and to introduce empirically the values of certain interaction integrals by recourse to experiment (5, 6). Because of this empirical element in self-consistent field calculations and the rather large amount of labor necessary for the carrying out of such calculations it is still of interest to see whether it is possible to interpret the electronic spectra of aromatic molecules containing polar substituents by some simple model without configuration interaction (CI), in which the neglect of CI might be compensated for by empirical adjustment of the parameters of the adopted model. Such a model is that used previously (7–10) to calculate the transition energy of the *K* bands of substituted benzenes as being due to an electron transfer between substituent and benzene. We have found it possible to extend this interpretation to the *K* band spectra of long field molecules (11), substituted in the 4-position by the nitro, the cyano, the acetyl, and the formyl groups and for both long field and round field molecules substituted by the electron-donating amino, methoxyl, bromo, chloro, and iodo groups. Such an interpretation of the *K* band spectra is similar to the qualitative theory of Burawoy (12–14), which, however, assumes that electron transfer in the ground state occurs only by an inductive mechanism.

METHODS AND RESULTS

The details of the method have been described elsewhere (7–10). The substituted hydrocarbon is regarded as being built up from two sets of energy levels, those of the parent hydrocarbon (R—H) and those of the substituent (S—H). The difference between the energy levels of the isolated systems R—H and S—H and the system R—S are calculated by a perturbation method. The energy of the intramolecular charge transfer band (E_1) is then given, for electron-attracting substituents, by the difference in energy between the highest occupied perturbed level of fragment R− and the lowest unoccupied perturbed level of fragment S, eq. [1]. For electron-donating substituents the energy

[1]*Manuscript received July 7, 1961.*
Contribution from the Chemistry Division, British Columbia Research Council, Vancouver 8, B.C.

of the intramolecular charge transfer band is given by the difference (E_2) between the energy of the highest perturbed occupied level of fragment $-$S and the energy of the lowest unoccupied perturbed level of fragment R$-$, eq. [2].

[1] $$E_1 = [(V_S - H_R)^2 + 4C_{V_S}^2 C_{H_R}^2 \beta_{R-S}^2]^{\frac{1}{2}},$$

[2] $$E_2 = [(V_R - H_S)^2 + 4C_{V_R}^2 C_{H_S}^2 \beta_{R-S}^2]^{\frac{1}{2}}.$$

H_R and H_S are the energies of the highest unperturbed occupied molecular orbitals (MO's) of R—H and S—H respectively. V_R and V_S are the energies of the unperturbed unoccupied MO's of R—H and S—H respectively. The atomic orbital (AO) coefficients C_{H_R}, C_{H_S}, C_{V_R}, C_{V_S}, are the values in the MO's of energies H_R, H_S, V_R, V_S at the atoms at which the connecting link between R—S is formed. H_S has previously (7–10) been taken as the ionization potential of either the corresponding methyl derivative (Me—S) or hydrogen derivative (H—S). However, in the hydrocarbon H—S the substituent S is attached to a trigonally hybridized carbon atom which is more electron attracting than either a tetrahedrally hybridized carbon atom or a hydrogen atom, so values of H_S were obtained by fitting eq. [1] to the experimental results for the K bands of benzene derivatives. The values so obtained are given in Table II.

V_S has previously been taken as the difference between the ionization potential and the energy of the R band transition of the corresponding methyl derivative (Me—S) (7). This assumption is open to the objection that both the repulsion forces and the changes in the Hamiltonian on going from the ground state to the excited state are different for R bands than for K bands, since the charge distribution in the excited state is different for the two transitions. Therefore empirical values for V_S were obtained by adjusting its value so that eq. [1] reproduced the experimental values of the K band of benzene derivatives. These values are given in Table II. For the nitro group the value which fitted nitrobenzene ($V_S = -4.4$ ev) gave poor results for the other derivatives so $V_S = -5.1$ ev was adopted as giving the best over-all results.

V_R has previously (7) been taken as the difference between the observed energy of the K band transition of R—H and its ionization potential (H_R), i.e. the K band of the hydrocarbon R—H is assumed to arise from a configuration in which an electron is excited from the highest filled MO to the lowest unoccupied MO. Such an assumption, however, always results in an electron transfer (ET) configuration of higher energy than the parent hydrocarbon K band for all values of H_S consistent with the limitation (necessary to explain the reduction of the ionization potential of R—H on substitution by an electron-donating S) that H_S should be less than H_R. V_R was therefore regarded as an empirical parameter and was obtained by equating E_2, calculated by eq. [2], to the observed K band spectra. The results of Table IV are those obtained by using such average values given in Table I. Such an adjustment of parameters is made very simple by the fact that eq. [2] is a hyperbola of the type $x^2 - b^2 = y^2$ where x is E_2 and y is $(H_S - V_R)$ and the range of values of x in which the transitions under discussion lie are such that a plot of E_2^2 against $(H_S - V_R)^2$ is linear for a given series of substituents with the same value of C_{H_S}. The empirical values of V_R so obtained are in the same relative order as those obtained by using ionization potential and ultraviolet data (Table I).

The AO coefficients C_{H_R} and C_{V_R} were obtained by LCAO calculations. C_{H_S} and C_{V_S} were given values between 0.5 and 1.0 consistent with giving the best fit between experiments and theory, Nagakura's (7–10) values being adopted wherever possible. The values used are given in Tables I and II. The values of E_1 and E_2 calculated by inserting

TABLE I

Parameters for hydrocarbon fragment R

R	$-H_R$, ev*	$-V_R$, ev†	$-V_R$, ev‡	$C_{H_R} = -C_{V_R}$
Benzene	(9.24)	3.04	6.00	0.578
Styrene	(8.86)	3.86	6.30	0.390
Stilbene	8.48	4.40	6.90	0.314
Diphenyl	8.78	3.73	6.24	0.398
Terphenyl	8.62	4.12	6.47	0.297
Naphthalene	(8.68)	4.40	7.1	0.425 (1 pos.) 0.263 (2 pos.)
Anthracene	(8.20)	4.90	8.23	0.440 (9 pos.)

*Experimental ionization potentials in parentheses; the others are obtained from a linear plot of these against the energy in β units (of the highest occupied MO) as calculated by the simple LCAO method.
†Calculated from ionization potential and ultraviolet data.
‡Empirical average values obtained by fitting experimental data to eq. [2].

TABLE II

Parameters for substituents

S	$-V_S$, ev*	$-H_S$, ev*	C_{V_S}*	C_{H_S}*	$-V_S$†	$-H_S$†	C_{V_S}†	C_{H_S}†
Nitro	5.10	—	0.70		5.50		0.70	
Formyl	4.63	—	0.70		5.91		0.89	
Acetyl	4.70	—	0.70		5.46		0.89	
Cyano	4.43	—	0.70					
Amino	—	10.02		1.00		10.52		0.81
Methoxy	—	10.44		1.00		—		—
Chloro	—	10.60		1.00		—		—
Bromo	—	10.58		1.00		—		—
Iodo	—	10.42		1.00		—		—

*Values used in this paper.
†Values used by Nagakura.

the parameters of Tables I and II in eq. [1] and [2] are compared with the available experimental data in Tables III and IV. Table V compares results for nitro compounds with $V_S = -5.5$ ev with those of Nagakura (8) with $V_S = -5.1$ ev. β_{R-S} is given the value 3 ev for all substituents (7–10).

DISCUSSION

The calculated values obtained by using the parameters of Tables I and II in eq. [1] and [2] are compared with experimental data for K band absorption in Tables III, IV, and V. In general, the calculated values are in fairly good agreement with the experimental ones.

For the electron-attracting groups the experimental data are not at the moment extensive enough to carry out a satisfactory statistical test of the validity of the simple charge transfer model. However, it can be seen from Table III that once the appropriate choice of H_R and V_S has been made the difference in K band transition energy of the nitro, acetyl, formyl, and cyano derivatives of benzene and diphenyl is predicted correctly within 0.03 ev (i.e. within 30° A at 3100° A). Using $V_{NO_2} = -5.1$ ev the K band positions of seven nitro compounds have been calculated (Tables IV and V) and these give a correlation coefficient of 0.850 on comparison with the observed values. The agreement would be even better if the experimental results (Table V) for 1-nitro-2-methyl-ethylene and 1-nitro-4-methyl-butadiene were corrected for the bathochromic effect of the methyl group (0.1 ev) and the solvent effect of the ethanol, the results being taken from (8).

TABLE III

Calculated and observed* K band transition energies (in ev) for electron-attracting substituents

	Substituent							
	$-NO_2$		$COCH_3$		CHO		CN	
Hydrocarbon	Calc.	Obs.	Calc.	Obs.	Calc.	Obs.	Calc.	Obs.
Benzene	4.80	4.93	(5.21)	5.21	(5.24)	5.24	(5.38)	5.38
Styrene	4.13	4.11	4.90	—	4.52	—	4.76	4.73
Stilbene	3.63	3.73	4.07	—	4.01	—	4.25	—
Diphenyl	4.04	4.05	4.48	4.49	4.41	4.38	4.66	4.65
Terphenyl	3.74	3.80	4.18	4.20	4.11	—	4.36	4.37
1-Naphthalene	4.06	3.81	4.43		4.36		4.79	—
2-Naphthalene	3.75	4.19	4.19	4.41	4.13	—	4.58	—
9-Anthracene (16)	3.73	3.57	4.02	—	3.96	—	4.20	3.40

*Unless otherwise stated these results have been measured by Burawoy and collaborators (refs. 13, 14, and unpublished work) in hexane solution.

TABLE IV

Calculated and observed* K band transition energies (in ev) for electron-donating substituents

	Substituent									
	NH_2		OMe		Cl		Br		I	
Hydrocarbon	Calc.	Obs.	Calc.	Obs.	Calc.	Obs.	Calc.	Obs.	Calc.	Obs.
Benzene	(5.30)	5.30	5.65	(5.65)	(5.78)	5.78	(5.74)	5.74	5.62	5.39
Styrene	4.53	4.54	4.50	4.85	4.89	4.90	4.88	4.90	4.74	—
Stilbene	3.96	3.92	3.97	4.00	4.15	4.05	4.13	—	3.99	—
Diphenyl	4.45	4.52	4.76	4.85	4.92	4.9	4.942	4.88	(4.81)	4.81
Terphenyl	3.98	4.19	4.36	4.35	4.50	4.45	4.47	4.44	4.33	4.42
1-Naphthalene (17)	3.87	3.98	4.18	4.22	4.33	4.32	4.31	4.29	4.16	4.211
9-Anthracene (16)	3.19	3.18	4.42		3.55	3.54	—	—	—	—

*Unless otherwise stated, these results have been measured by Burawoy and collaborators (refs. 13, 14, and unpublished work) in hexane solution.

TABLE V

Nitro compounds

Parent hydrocarbon R—H	Observed transition energies in ev		Predicted transition energies in ev		Free valence F	$E_{R-H}-E_{R-NO_2}$
	E_{R-NO_2}	E_{R-H}	$V_{NO_2}=-5.1$	$V_{NO_2}=-5.5$		
Ethylene	5.39	−7.6	5.37	5.51	0.731	2.21
Butadiene	4.41	6.0	4.49	4.56	0.391	1.59
Benzene	4.93	6.2	5.10	4.69	0.398	1.27
Styrene	4.11	5.06	4.13	3.74	0.414	0.95
Diphenyl	4.05	5.02	4.04	3.68	0.412	0.97
Terphenyl	3.80	4.51	3.74	3.58	0.412	0.71
Stilbene	3.73	4.25	3.63	3.26	0.418	0.52

The use of $V_{NO_2} = -5.1$ ev can be seen to give better agreement with experiment than the original value of $V_{NO_2} = -5.5$ ev used by Nagakura (8). The theory predicts well the effect of increasing the size of the conjugated system attached to the nitro group. This is shown in Fig. 1 where the experimental and predicted values are plotted against the size of the conjugated system. The results of Table V also give a theoretical basis to the empirical rule of Burawoy (14) that the larger the conjugated system (a good measure of the length of the conjugation is the K band transition energy of the hydrocarbon) the

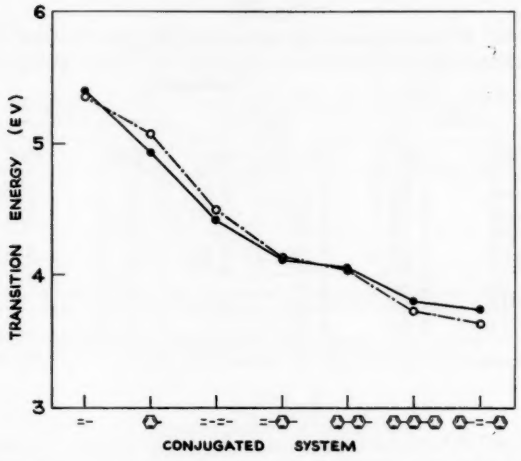

FIG. 1. Comparison between calculated (-·-o-·-) and observed (-●-) K band transition energies of conjugated nitro compounds.

smaller the effect of a given substituent. Thus the magnitude of the transition energy change brought about by the nitro group grows smaller as we descend Table V from ethylene (where the change on substitution is 2.03 ev) to stilbene (where it is only 0.52 ev).

The free valence (15) has often been taken as a measure of the conjugating power of a hydrocarbon with a substituent and either this or the proportional quantity, the self-polarizability (18), is related to the K band transition energy change on substitution. The values of the free valence and the observed transition energy change recorded in Table V show that this is only a very rough approximation. In particular the free valence predicts that the conjugating power of diphenyl and terphenyl in the para position should be the same and that stilbene should have a conjugating power greater than benzene when in fact the nitro group has the least effect on the K band transition energy of stilbene as is predicted on the "charge transfer" model.

In the case of the round field molecules, naphthalene and anthracene, it can be seen from Table III that agreement between experiment and theory is poor. Whereas it is always found experimentally that substitution in the 1-position of naphthalene produces a bigger bathochromic shift of the K band than substitution in the 2-position, the simple charge transfer theory predicts the opposite for both electron-attracting and electron-donating substituents. No explanation for this breakdown can be offered but it should be pointed out that even the most sophisticated calculations carried out to date (19), which include limited configuration interaction, overestimate the effect of the effect of the substituent in the 2-position of naphthalene. It is possible that calculations using self-consistent field ground state orbitals may remove this deficiency.

For electron-donating substituents which may be regarded as monatomic substituents the available experimental data is much more plentiful than for electron-attracting substituents. For the K bands of long field molecules the band maxima of both the parent hydrocarbon and the substituted compound are quite sharp and the band envelopes are, with the exception of benzene and halogeno-benzenes, fairly symmetrical. This means

that the changes in transition energy can be measured to within 50–100 cm^{-1} (i.e. to within less than 0.1 ev) whereas for round field molecules the K band is much broader and often contains fine structure which is altered on substitution (19, 20).

In Table III are recorded 29 comparisons between experimental and theoretical transition energies. The relationship between calculated and observed transition energies gives a correlation coefficient of 0.951 (this includes the particularly bad result for 4-methoxy-stilbene but omits the results for 2-substituted naphthalenes since, as has been discussed above, it is known the theory is incorrect in its predictions for these latter compounds).

This high correlation coefficient is most unexpected for such a crude theory which neglects completely the interaction between the highest occupied level of the parent hydrocarbon and the corresponding level in the substituent. This interaction on the LCAO model is regarded as the main effect of the substituent (21). It seems likely that the empirical element introduced into the theory by the adjustment of the parameters to fit experimental data and the neglect of configuration interaction may compensate for this neglect.

Both the charge transfer and the LCAO methods involve a transfer of electrons from the electron-donating substituent to the parent hydrocarbon; however, comparison of similar calculations show that the LCAO method consistently predicts a greater charge transfer in the ground state than the charge transfer method when the parameters are chosen to give agreement with experiment. It may therefore be possible to decide which is the better model by comparison between theoretical calculations and experiments on ground state properties (heats of combustion, n.m.r. chemical shifts, and infrared stretching frequencies and intensities). It has recently been reported (22) that the charge transfer method gives a satisfactory model for the interpretation of the infrared intensities of substituted benzonitriles; similar calculations using the LCAO method are not yet available.

The author is indebted to the ICI Fellowship Committee of the University of Manchester, England, and the National Research Council of Canada for financial support.

REFERENCES

1. W. Moffitt. J. Chem. Phys. **22**, 320, 1820 (1954).
2. J. Jacobs. Proc. Phys. Soc. (London), A, **62**, 710 (1948).
3. H. C. Longuet-Higgins. Advances in chemical physics. Vol. 1. Interscience Publishers, Inc., New York. 1958. p. 239.
4. R. Pariser and R. G. Parr. J. Chem. Phys. **21**, 466 (1953).
5. L. Goodman and H. Shull. J. Chem. Phys. **27**, 1388 (1957).
6. E. G. McRae and L. Goodman. J. Mol. Spectroscopy, **2**, 464 (1958).
7. S. Nagakura and J. Tanaka. J. Chem. Phys. **22**, 236 (1954).
8. S. Nagakura. J. Chem. Phys. **23**, 1441 (1955).
9. J. Tanaka, S. Nagakura, and M. Kobayshi. J. Chem. Phys. **24**, 311 (1956).
10. J. Tanaka and S. Nagakura. J. Chem. Phys. **24**, 1274 (1956).
11. J. R. Platt. J. Chem. Phys. **17**, 484 (1949).
12. A. Burawoy. Tetrahedron, **2**, 122 (1958).
13. A. Burawoy and P. Critchley. Tetrahedron, **5**, 340 (1959).
14. A. Burawoy, P. Brocklehurst, R. S. Berry, and A. R. Thompson. Tetrahedron, **10**, 102, 109 (1960).
15. B. Pullman and A. Pullman. Progress in organic chemistry. Vol. 4. *Edited by* J. W. Cook. Butterworths Scientific Publications, London. 1958. p. 31.
16. R. N. Jones. Chem. Revs. **41**, 353 (1947).
17. H. G. de Laszlo. Proc. Roy. Soc. (London), A, **111**, 355 (1926).
18. G. M. Badger and R. G. Battery. J. Chem. Soc. 2156 (1953).
19. H. Baba and S. Suzuki. Bull. Chem. Soc. Japan, **34**, 82 1961.
20. American Petroleum Institute. Research project 44. Ultraviolet spectral data sheets.
21. Y. I'Haya. J. Am. Chem. Soc. **81**, 6120 (1959).
22. T. L. Brown. J. Phys. Chem. **64**, 1798 (1960).

SOME ASPECTS OF THE NUCLEAR MAGNETIC RESONANCE SPECTRA OF COMPOUNDS CONTAINING C-METHYL GROUPS[1]

F. A. L. Anet

ABSTRACT

The N.M.R. spectra of compounds containing various types of C-methyl groups are discussed with special reference to the effects of spin coupling. Particular attention is given to compounds containing the $CHCH_3$ group in saturated systems. It is pointed out that the observed splitting of the methyl band is not always equal to the coupling constant between the methyl protons and the adjacent proton, even when the chemical shift between the two groups of protons is large.

The detection and differentiation of C-methyl groups in organic compounds is of importance, particularly in natural product chemistry. The standard (Kuhn–Roth) method of estimating C-methyl groups consists of oxidizing the compound with chromic acid and determining the acetic acid (and(or) higher homologue(s)) produced. By suitable modifications (1) it is possible to analyze for each acid separately and so to find out whether the group is a simple C-methyl group, or a C-ethyl group, etc. Infrared spectroscopy (2) has been used to detect and to determine C-methyl groups, and also to differentiate between isopropyl, *tert*-butyl, and other C-methyl groups.

Both of the above methods have limitations for the differentiation of C-methyl groups. Proton nuclear magnetic resonance (N.M.R.) has already been applied to the problem (3) but little discussion of the scope and limitations of the method has been published. In the present paper the effect of coupling of a methyl group to other protons in a molecule is considered in detail.

The detection of C-methyl groups by means of N.M.R. spectroscopy is especially favorable for two reasons. In the first place, a strong signal is usually obtained because of the complete magnetic equivalence of the three protons as a result of the rapid internal rotation of the methyl group. Secondly, when the methyl group is attached to a saturated carbon atom, the chemical shift of the methyl group, which is about 1 p.p.m. downfield from tetramethylsilane, is usually different from that of other protons in the molecule. Exceptions occur in compounds containing certain structural features such as cyclopropane rings. *trans*-1,1-Dichloro-2,3-dimethylcyclopropane (4), for example, has an N.M.R. spectrum which is essentially a single line at 8.78 τ.

The N.M.R. spectra of compounds containing C-methyl groups attached to unsaturated carbon atoms have been discussed in some detail by several authors (5, 6, 7, 8, 9, 10) and will not be considered here.

When the methyl group is attached to a saturated carbon atom we may consider three separate cases, depending on whether the saturated carbon atom also carries (*a*) no hydrogen atom, (*b*) one hydrogen atom, or (*c*) two hydrogen atoms.

In class (*a*), when there is no hydrogen atom on the adjacent carbon atom, the methyl group generally gives rise to a single sharp line. Since all the intensity is concentrated in one line there is no difficulty in observing such a signal in a spectrum. Typical examples are the 18- and 19-methyl groups of steroids (11) and the methyl groups in camphane derivatives (12). In exceptional cases, the methyl group may show very weak coupling to

[1]*Manuscript received June 20, 1961.*
Contribution from the Department of Chemistry, University of Ottawa, Ottawa 2, Ontario.

other protons in the molecule, thus (4) the two non-equivalent *gem*-methyl groups of (I) are coupled together to the extent of 0.5 c.p.s. Roberts (13) has reported a value of 0.75 c.p.s. for the coupling constant of the C-methyl group to one of the protons of the methylene group in methyl 2-bromo-2-methylpropionate. In general, it may be anticipated that this type of coupling will be very small (<1 c.p.s.) and can be neglected for practical purposes.

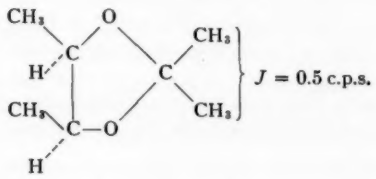

(I)

The second class is that of compounds containing the $CHCH_3$ group. The spectrum to be expected from such a system, in the absence of other magnetically active nuclei, has been dealt with in several places (cf. ref. 14). The simplest case, usually designated (15) by the symbols AX_3, occurs when the chemical shift of the two groups of protons is large compared with the coupling constant between them. The methyl group then gives rise to a doublet, and the separation is equal to the coupling constant. It may be mentioned here that the coupling constants of methyl groups to adjacent protons generally lie in the range of 6–8 c.p.s.

We may also place in this class the isopropyl group. If the two methyl groups are chemically identical and are well shifted from the CH proton, the situation is analogous to that just described. If the two methyl groups are not chemically identical, usually (but not necessarily) because of the presence of an asymmetric center in the molecule, two different methyl doublets, which may overlap, are obtained (16, 17). The non-equivalence of methyl groups in such systems is similar to that of two protons of a methylene group in certain molecules (18, 19).

When the chemical shift in the $CHCH_3$ group is not very large, the spectrum becomes an AB_3 type (15) and contains more lines. However, when the ratio of coupling constant to chemical shift is not more than about 0.25, the spectrum of the methyl group is still approximately a doublet. More exactly, each "line" of the doublet is now split into a number of lines, and the high-field component is split more and also is of lower intensity than the low-field component (assuming the CH group to be at low field of the methyl group). When the chemical shift is much less, a doublet is no longer recognizable. Jackman (3) has tried to rationalize the spectra of certain compounds (e.g. methylcyclohexane) containing $CHCH_3$ groups simply in terms of AB_3 systems. However, closer inspection shows that the observed and calculated spectra of the methyl groups cannot be made to agree completely, no matter what combination of chemical shifts and coupling constants are used. In each case there are other protons in the molecule which are appreciably coupled to, but only slightly chemically shifted from, the tertiary proton of the $CHCH_3$ group. These protons *must* be included in the analysis in order to obtain correct results. This is so even if, as is generally true, the methyl group is coupled only to the tertiary proton and not to the other protons of the molecule.

We shall first examine the spectrum to be expected for the methyl group in a molecule such as (II), where the R's are not involved in coupling with the system under consideration. We will assume that the methyl group is well chemically shifted from H(1) and

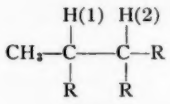

(II)

H(2) and that $J_{CH_3,H(2)}$ is zero. This is actually a special case of the X_3AB system, which has been treated by Fessenden and Waugh (9). Figure 1 shows the calculated spectra due

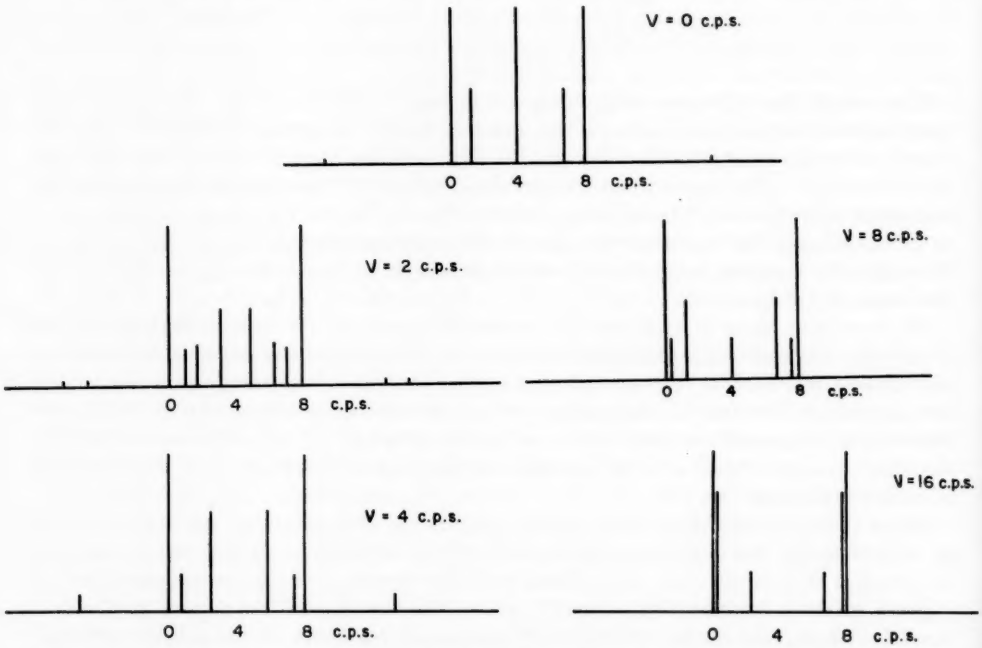

FIG. 1. Calculated spectra for compounds of type (II) for various values of the chemical shift (ν) between H(1) and H(2) and with $J_{CH_3,H(1)} = J_{H(1),H(2)} = 8$ c.p.s. and $J_{CH_3,H(2)} = 0$.

to the CH_3 group for various values of the chemical shift ($\nu_{H(1),H(2)}$) between H(1) and H(2), and, for simplicity, with $J_{CH_3,H(1)} = J_{H(1),H(2)} = 8.0$ c.p.s. Although the coupling constants are not generally equal, this does not affect the general conclusions drawn from the calculations.

When the chemical shift, $\nu_{H(1),H(2)}$, is very large the spectrum of the methyl group is a doublet, the lines being at $+1/2J_{CH_3,H(1)}$ and $-1/2J_{CH_3,H(1)}$ from the position of the methyl band in the absence of coupling. This is, of course, just the result expected from a first-order treatment. When the chemical shift is *not* large, only half of the intensity of the methyl band resides in the two lines at positions mentioned above. Most of the

remaining intensity is situated *between* these two lines, the exact distribution depending very markedly on the value of $\nu_{H(1),H(2)}$ (Fig. 1). The effect of H(2) is most pronounced when $\nu_{H(1),H(2)}$ is no greater than $J_{H(1),H(2)}$ and is negligible when $\nu_{H(1),H(2)} > 2J_{H(1),H(2)}$.

It can easily be understood why half of the intensity is in the lines at $\pm 1/2J_{CH_3,H(1)}$. There are four spin states for the protons H(1) and H(2), and the wave functions of the states with both protons having a spin of $+1/2$ or with both protons having a spin of $-1/2$ will not mix with any other functions, whereas the pairs of wave functions associated with one proton having a spin of $+1/2$ and the other a spin of $-1/2$ and vice versa do mix as they have the same total spin (15). From similar considerations it can be seen that if there are two protons similar to H(2), then only one quarter of the intensity of the methyl group lies in the "unperturbed" lines at $\pm 1/2J_{CH_3,H(1)}$. For three and four protons these fractions fall to 1/8 and 1/16 respectively. Complete solutions in these cases would be very laborious but it can be surmised that most of the remaining intensity, in the form of many lines, will be situated, as before, between the pair of unperturbed lines.

Therefore, the $CHCH_3$ group in a complex molecule may be expected to be a doublet or a doublet showing some additional lines, or in extreme cases, just a wide band with little resolved structure. This is the situation where the chemical shift between the CH_3 group and the adjacent proton is large compared with the coupling constant. When the chemical shift is not large, a similar effect is to be expected. The spectrum of the methyl group will correspond to the B_3 part of an AB_3 system only when A is not coupled to any protons other than the B protons. If the effects described above for the AX_3 system are important, a much more complex spectrum may be expected, which in extreme cases may reduce to a structureless wide band.

It should be noted that the observed splitting of the methyl band will not always be equal to the coupling constant. The splitting will usually be less because most of the intensity of the extra lines lies inside the two unperturbed lines whose separation gives the true coupling constant. This is probably the explanation for the wide variation in the "coupling constants"* of the methyl groups of 6α- and 6β-methyl steroids found by Slomp and McGarvey (20). In particular, for certain compounds some quite small splittings were found for which no explanation was presented. It would be expected that the coupling constant of the methyl group to the adjacent proton would not vary greatly in such a series of compounds. In agreement with the arguments presented in this paper is the fact that small splittings were not observed whenever the tertiary proton on C6 was likely to be chemically shifted (generally to low field) from the protons on C7, such as by the presence of a $\Delta^{4,5}$ double bond, or by the C6 proton being equatorial rather than axial (21). Unfortunately, the chemical shifts of the significant protons in such complex molecules cannot be observed directly, because the bands of a large number of other protons interfere.

Similar effects are found in the dimethylcyclohexanes examined recently by Musher (22). From the 40 Mc/sec N.M.R. spectra of the cis and trans isomers of 1,2-, 1,3-, and 1,4-dimethylcyclohexanes, Musher concluded that the coupling constants of equatorial methyl groups to the adjacent axial protons were zero or small (2.7 c.p.s.). In the alternative case of axial methyl groups and adjacent equatorial protons, appreciable (ca. 5 c.p.s.) coupling constants were observed. However, these "coupling constants" were merely the observed splittings of the methyl bands. Since the compounds used should be particularly liable to the effects discussed in this paper, the conclusions of Musher

**In cases of this type the term "splitting" would seem to be preferable to the term "coupling constant".*

regarding coupling constants cannot be regarded as correct. The correct constants could no doubt be obtained by preparing suitably deuterated derivatives, which is, unfortunately, not an easy task, but which has been achieved in the present work for some compounds discussed later in this paper. It may be noted that where zero splittings were observed by Musher, the methyl bands were in fact broad and not sharp as they should be if the coupling constants were zero. In order to obtain experimental confirmation of the deductions made, the N.M.R. spectra of a number of suitable compounds containing C-methyl groups have been examined.

A very simple spectrum (Fig. 2) is given by the 3,5-dinitrobenzoate of *erythro*-3-bromo-2-butanol. The spectrum shows two different methyl bands, each a well-defined doublet

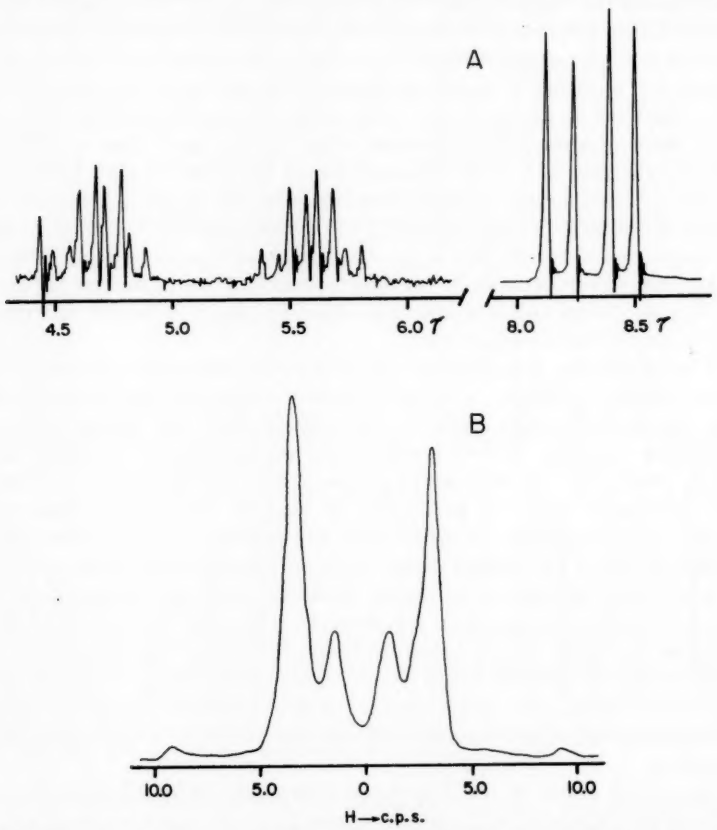

FIG. 2. A. Spectrum of 3,5-dinitrobenzoate and *erythro*-3-bromo-2-butanol, in chloroform solution. The sharp band at the extreme left is that of $C^{13}HCl_3$. The two parts of the spectrum were taken at different recorder gain.

B. Methyl band of meso-2,3-dibromobutane (pure liquid).

in accordance with the X_3 part of an AX_3 system. It should be noted that protons on C2 and C3 are well chemically shifted from one another and from the methyl groups and occur at low fields as doublets of quartets. In contrast to this case is the spectrum of the closely related meso-2,3-dibromobutane, where the chemical shift between the protons

on C2 and C3 is zero. The methyl groups here have the same chemical shift so only one methyl band is observed, but this is not a simple doublet (Fig. 2), for other lines appear. The spectrum of this molecule has already been discussed briefly (23) and fuller details will be published in a separate paper.

The spectra of methylsuccinic acid and β-methylglutaric acid are shown in Fig. 3.

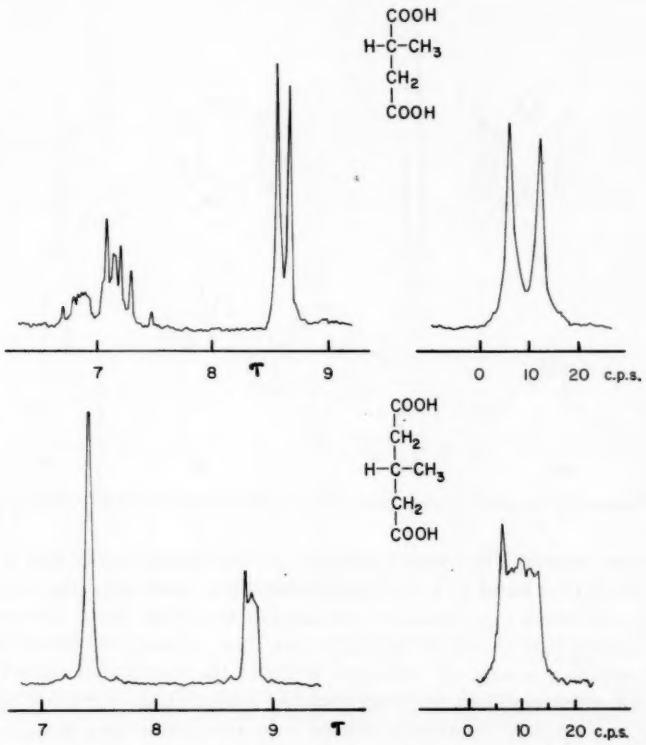

FIG. 3. Spectra of methylsuccinic acid and β-methylglutaric acid in trifluoroacetic acid. The bands of the carboxyl protons are not shown. The methyl bands at slow sweep are shown on the right.

These structurally related compounds give quite different bands for the methyl group. In methylsuccinic acid there is a distinct, though not large, chemical shift between the α and the two α′ protons and, as expected, the methyl group is a fairly good doublet. The coupling constant $J_{CH_3,H(2)}$ is probably a little larger than the observed splitting (6.6 c.p.s.) of the methyl band. In β-methylglutaric acid the α,α′ and β-protons must be only slightly chemically shifted from one another as they give rise to a single, slightly broad band. The result is that the methyl group does not give rise to a doublet at all, but to a wide band which obviously contains many lines.

Other examples of this type are the N.M.R. spectra of 2- and 3-methylcyclohexanone. The band of the methyl group of 2-methylcyclohexanone is a fairly good doublet, as expected, since the 2-proton should be chemically shifted from the 3-methylene protons by the proximity of the carbonyl group. On the other hand, in 3-methylcyclohexanone

the methyl group gives a very poor "doublet" (Fig. 4) which is a result of the carbonyl group shifting the position of the 2-methylene protons so that these are only slightly separated from the 3-proton. Support of this explanation was obtained by deuteration at position 2 (and incidentally at 6 also since an exchange method was used). The deuterated isomer gives a good doublet (Fig. 4) for the methyl group. This also shows that 1,3-coupling of the methyl group is not important as one methylene group (at C4) remains

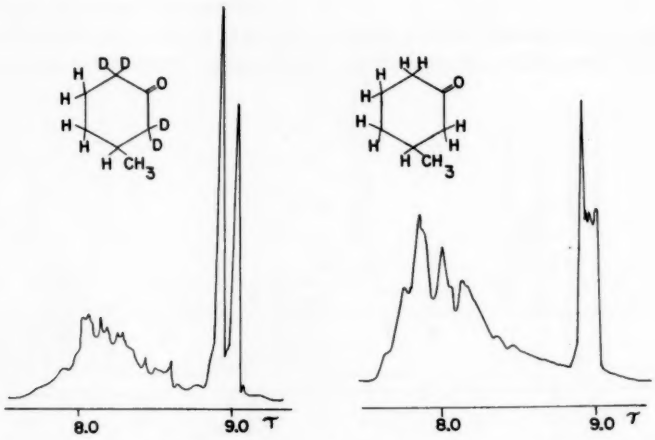

FIG. 4. Spectra of 3-methylcyclohexanone and of 2,2,6,6-tetradeuterio-3-methylcyclohexanone.

in the deuterated isomer. The methyl splitting for the deuterated isomer is 6.1 c.p.s. The splitting of the methyl band in 3-methylcyclohexanone itself depends very markedly on the resolution and sweep rate, owing to the asymmetry of the band. At very high resolution and slow sweep rate the splitting is 5.0 c.p.s., but at lower resolution or faster sweep the observed splitting is only ca. 4.0 c.p.s. Even in the deuterated isomer, the splitting is probably not quite equal to the true coupling constant, as there are still protons on C4 which are not strongly chemically shifted from the proton on C3.

In all the examples described above the chemical shift between the methyl group and the adjacent proton is reasonably large. In methylcyclohexane this shift is much smaller, resulting in a strong skewness in the intensity of the methyl band (Fig. 5) which is an extremely poor doublet with a separation of 4.7 c.p.s. However, this band does not agree with the B_3 part of an AB_3 spectrum. Methylcyclohexane is known to exist largely with the methyl group equatorial (24). It is also known (21) that axial protons are found at slightly higher field than equatorial protons, and that tertiary protons are at slightly lower field than methylene protons, other things being equal (3). These shifts should largely cancel out and the axial proton adjacent to the methyl group should be very close in chemical shift to the protons (especially the equatorial ones) on C2 and C6.

The spectrum (Fig. 5) of 2,2,6,6-tetradeuteriomethylcyclohexane (for isotopic purity see Experimental), on the other hand, gives a methyl band whose structure is consistent with the B_3 part of an AB_3 system. Calculation shows that $J = 6.8$ c.p.s. and that J/ν is about 0.25. It should again be noted that the value of the coupling constant is appreciably greater than the observed splitting in undeuterated methylcyclohexane.

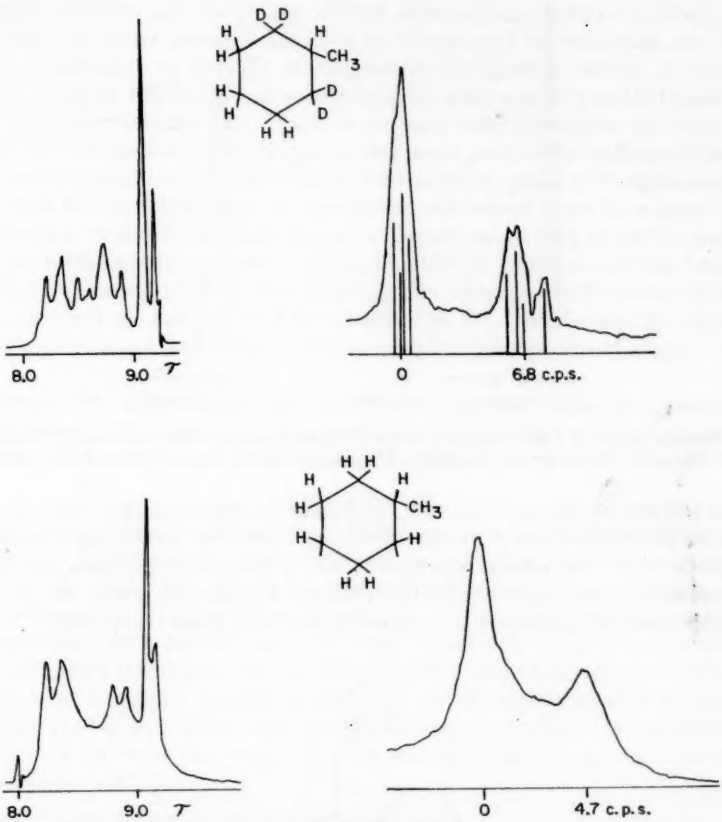

FIG. 5. Spectra of methylcyclohexane and 2,2,6,6-tetradeuteriomethylcyclohexane. The methyl bands at slow sweep are shown on the right. The sharp band at the left of the methylcyclohexane spectrum is a side band of tetramethylsilane.

The *Lycopodium* alkaloid lycodine (III*a*) (25) presents a good example of a natural product showing some of the effects discussed in this paper. In the first publication (26) on this alkaloid, the N.M.R. spectrum (40 Mc/sec) was taken as evidence that the methyl group, which was known to be present, was attached to a quaternary carbon atom, as the methyl band was unsplit. However, spectra (Fig. 6) taken (27) at 60 Mc/sec and under somewhat better resolution showed that the methyl band was quite broad and, in fact, could just be resolved as a doublet of separation 1.9 c.p.s. This splitting undoubtedly does not represent the coupling constant. In N-acetyllycodine (III*b*), the methyl band of the lycodine part of the molecule cannot even be resolved into a doublet under the best possible resolution. The band (Fig. 6) is nevertheless broad and does show an inflection on the high-field side. In contrast, the band of the methyl protons of the N-acetyl group is quite sharp and therefore also of much greater height. These effects can be ascribed to the smallness of the chemical shift of the CH proton to the adjacent pairs of methylene protons, partly as a result of the CH proton being shifted upfield from

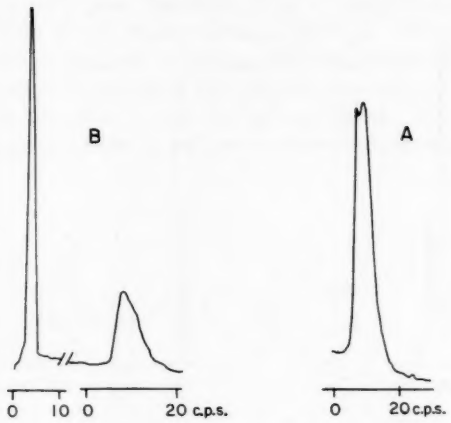

FIG. 6. Methyl bands of (A) lycodine and (B) N-acetyllycodine. The two methyl bands of B were taken under the same instrumental conditions. The magnetic field increases from left to right.

its normal position by the pyridine ring. Molecular models show that the CH proton lies in the region above the plane of the pyridine ring where the circulating π electrons cause a diamagnetic shift. The related alkaloids α- and β-obscurine (28) show the same apparently abnormal methyl band shown by lycodine. Further discussion on the spectra of these alkaloids will be published in a paper dealing with these compounds.

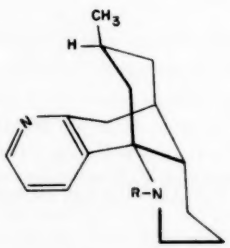

(IIIa) R = H
(IIIb) R = Ac

Another example of "abnormal" behavior is found in 1-β(3,5-dinitrobenzoyloxy)-2α-iodo-3α-methylcyclohexane prepared recently by Lemieux and Kavadias. The N.M.R. spectrum taken at a comparatively fast sweep (29) shows only a single, somewhat broad line for the methyl group. This can be understood if the proton on C3 is only slightly chemically shifted from the protons on C4. In agreement with this interpretation, the proton on C2 gives a broad line, instead of the doublet of doublets expected. In other isomers of the above compound the methyl group is a doublet and the C2 proton shows the expected fine structure.

The spectrum of compounds containing ethyl groups can be expected to show the same behavior as that of compounds containing the $CHCH_3$ group. The methyl group will only be a good triplet when it is well chemically shifted from the methylene protons, *and*

the methylene protons are chemically shifted from other protons to which they are coupled. When the ethyl group is attached to a saturated carbon atom not bearing a strongly electronegative or strongly electropositive substituent, neither of these conditions will generally be fulfilled. Thus valeric acid (3) gives rise to a methyl band which is wide and fairly shapeless. In fact, it is not too easy to differentiate this type of ethyl group from the "abnormal" $CHCH_3$ group discussed previously. *n*-Butyraldehyde (3), where the second condition above is fairly well fulfilled, gives a recognizable, if poor, triplet. Diethyl ketone fulfills both the conditions and indeed gives (3) a good triplet for the methyl group. It should be noted that in molecules containing an asymmetric carbon atom, the two methylene protons of an ethyl group are not identical and may have slightly different coupling constants to the methyl group. The ethyl group of some small molecules have been analyzed as A_3B_2 or A_3B_2X systems (30, 31), and during the course of the present work Cavanaugh and Dailey have investigated the spectra of propyl derivatives (32).

In this paper, the only magnetically active nuclei present have been assumed to be protons. However, the arguments presented can be extended readily to cases where fluorine, phosphorus, etc. occur in an organic compound.

EXPERIMENTAL

The spectra were taken at a frequency of 60 Mc/sec on a Varian V-4302 high-resolution spectrometer. The compounds were dissolved in carbon tetrachloride (except where otherwise stated) containing about 1% tetramethylsilane to make 10–15% solutions. Chemical shifts are reported on Tiers' τ scale (33) (i.e. in p.p.m. increasing to high field, with tetramethylsilane given the value of 10.00). Calibration of the spectra was carried out by the side-band technique. The frequency of the audio-oscillator was monitored on a Hewlett–Packard frequency counter, model 521C. In all cases a number of spectra were taken with increasing as well as with decreasing magnetic fields. The tetramethylsilane peak was always observed as a single, very sharp band. Coupling constants are estimated to be accurate to 0.15 c.p.s.

Preparation of 2,2,6,6-Tetradeuteriomethylcyclohexane

Cyclohexanone (10 g), deuterium oxide (15 ml, 99.7%), and anhydrous potassium carbonate (0.5 g) were refluxed for 2 hours. The cyclohexanone, recovered by ether extraction, was submitted to two more such treatments. The 2,2,6,6-tetradeuteriocyclohexanone was finally distilled through a small column, b.p. 93–96° (142 mm) (4 g), and was free of isomers containing protons α to the carbonyl group, as shown by the N.M.R. spectrum. Treatment of the deuterated cyclohexanone with triphenylphosphinemethylene according to the procedure described in *Organic Syntheses* (34) gave crude methylenecyclohexane, ca. 2 g, b.p. 80–100°. The only impurity was found to be benzene, both by gas chromatography and by the N.M.R. spectrum. The N.M.R. spectrum (bands at 5.52 τ and 8.48 τ only) also showed that the methylenecyclohexane was fully deuterated at positions 2 and 6. The above fraction was hydrogenated at room temperature and pressure in the presence of platinum oxide catalyst (10 mg). The product was shaken with concentrated sulphuric acid at 60° until gas chromatography showed that all the benzene was removed. The product gave a single peak with the same retention time as methylcyclohexane on gas chromatography using a silicone oil column at 110°. The mass spectrum (kindly taken by Dr. F. Lossing of the National Research Council, Ottawa) showed the presence of 65% tetradeuterated, 11% undeuterated, 10% pentadeuterated, 9% trideuterated, 3% monodeuterated, and 2% dideuterated methylcyclohexane. The

presence of unexpectedly large amounts of the undeuterated isomer can be explained most simply if some isomerization (35, 36) to 1-methylcyclohexene took place. This compound could then undergo an exchange of its allylic deuterium atoms prior to hydrogenation. Indeed, gas chromatography of the hydrogenation mixture contained a small peak, not present in the initial product, with a retention time consistent with that expected for 1-methylcyclohexene. This product disappeared, as expected, on treatment with sulphuric acid. Although the final product was only 65% isotopically pure, this should not affect the N.M.R. spectrum too much.

2,2,6,6-Tetradeuterio-3-methylcyclohexanone

3-Methylcyclohexanone was deuterated as described above for cyclohexanone.

3,5-Dinitrobenzoate of Erythro-3-bromo-2-butanol

The compound had m.p. 85° (lit. (37) m.p. 85°). In the N.M.R. spectrum (Fig. 2) the bands centered at 4.68 τ and 5.60 τ can be assigned to the protons on C2 and C3 respectively, and the doublets at 8.44 τ and 8.19 τ can be assigned to the 4- and 1-methyl groups respectively. The coupling constants are $J_{12} = 6.4$, $J_{34} = 6.9$, and $J_{23} = 4.2$ c.p.s. The assignments are consistent with the chemical-shift effects of bromine and oxygen atoms (38).

ACKNOWLEDGMENTS

I wish to thank Mrs. Osgerby for technical help in the preparation of deuterated cyclohexanone and deuterated methylcyclohexanone.

This research was supported by a grant from the National Research Council of Canada.

REFERENCES

1. H. Bickel, H. Schmid, and P. Karrer. Helv. Chim. Acta, **38**, 649 (1955).
2. L. J. Bellamy. The infra-red spectra of complex molecules. Methuen & Co., London. 1958. p. 24.
3. L. M. Jackman. Applications of nuclear magnetic resonance spectroscopy in organic chemistry. Pergamon Press, New York. 1959. p. 82.
4. F. A. L. Anet. Unpublished work.
5. M. S. Barber, J. B. Davis, L. M. Jackman, and B. C. L. Weedon. J. Chem. Soc. 2870 (1960).
6. L. M. Jackman and R. H. Wiley. J. Chem. Soc. 2881, 2886 (1960).
7. V. J. Kowalewski and D. G. deKowalewski. J. Chem. Phys. **33**, 1794 (1960).
8. R. R. Fraser and D. E. McGreer. Can. J. Chem. **39**, 505 (1961).
9. R. W. Fessenden and J. S. Waugh. J. Chem. Phys. **30**, 994 (1959).
10. R. B. Bates and D. M. Gale. J. Am. Chem. Soc. **82**, 5749 (1690).
11. J. N. Shoolery and M. T. Rogers. J. Am. Chem. Soc. **80**, 5121 (1958).
12. F. A. L. Anet. Can. J. Chem. **39**, 789 (1961).
13. D. R. Davis, R. P. Lutz, and J. D. Roberts. J. Am. Chem. Soc. **83**, 246 (1961).
14. P. L. Corio. Chem. Revs. **60**, 385 (1960).
15. J. A. Pople, W. G. Schneider, and H. J. Bernstein. High-resolution nuclear magnetic resonance. McGraw-Hill Book Co., New York. 1959.
16. S. Goodwin, J. N. Shoolery, and L. F. Johnson. J. Am. Chem. Soc. **81**, 3065 (1959).
17. R. Anet. J. Org. Chem. **26**, 246 (1961).
18. P. M. Nair and J. D. Roberts. J. Am. Chem. Soc. **79**, 4565 (1957).
19. J. S. Waugh and F. A. Cotton. J. Phys. Chem. **65**, 562 (1961).
20. G. Slomp and B. R. McGarvey. J. Am. Chem. Soc. **81**, 2200 (1959).
21. R. U. Lemieux, R. K. Kullnig, H. J. Bernstein, and W. G. Schneider. J. Am. Chem. Soc. **80**, 6098 (1958).
22. J. I. Musher. Spectrochim. Acta, **16**, 835 (1960).
23. F. A. L. Anet. Proc. Chem. Soc. 327 (1959).
24. C. W. Beckett, K. S. Pitzer, and R. Spitzer. J. Am. Chem. Soc. **69**, 977, 2488 (1947).
25. F. A. L. Anet and V. Rao. Tetrahedron Letters, No. 20, 9 (1960).
26. F. A. L. Anet and C. R. Eves. Can. J. Chem. **36**, 902 (1958).
27. F. A. L. Anet and V. Rao. To be published.
28. W. A. Ayer and G. G. Iverach. Tetrahedron Letters, No. 10, 19 (1960).
29. J. Kavadias. Ph.D. Thesis, University of Ottawa, Ottawa, Ont. 1961.
30. B. R. McGarvey and G. Slomp. J. Chem. Phys. **30**, 1586 (1959).
31. P. T. Narasimhan and M. T. Rogers. J. Am. Chem. Soc. **82**, 5983 (1960); J. Chem. Phys. **34**, 1049 (1961).

32. J. R. CAVANAUGH and B. P. DAILEY. J. Chem. Phys. **34**, 1094 (1961).
33. G. D. TIERS. J. Phys. Chem. **62**, 1151 (1958).
34. G. WITTIG and U. SCHOELLKOPF. Org. Syntheses, **40**, 66 (1960).
35. S. SIEGEL and G. V. SMITH. J. Am. Chem. Soc. **82**, 6087 (1960).
36. J. F. SAUVAGE, R. H. BARKER, and A. S. HUSSEY. J. Am. Chem. Soc. **82**, 6090 (1960).
37. S. WINSTEIN and H. J. LUCAS. J. Am. Chem. Soc. **61**, 1576 (1939).
38. J. R. CAVANAUGH and B. P. DAILEY. J. Chem. Phys. **34**, 1099 (1961).

EXTRACELLULAR ACIDIC POLYSACCHARIDES FROM C. INSIDIOSUM AND OTHER CORYNEBACTERIUM SPP.[1]

P. A. J. GORIN AND J. F. T. SPENCER

ABSTRACT

The extracellular polysaccharide of *Corynebacterium insidiosum*, the causative agent of alfalfa wilt, contains D-glucose, D-galactose, and L-fucose in the proportions 2:3:4, with smaller amounts of an unknown acid. Partial acid hydrolysis of the polysaccharide gives 4-*O*-β-D-glucopyranosyl-L-fucose and 4-*O*-β-D-glucopyranosyl-(3-*O*-D-galactopyranosyl)-L-fucose as neutral oligosaccharides. Also formed are D-galactose, substituted in the 4-position with an unknown acid, and 4-*O*-β-D-glucopyranosyl-(3-*O*-D-galactopyranosyl)-L-fucose, which has the 4-position of the galactopyranosyl moiety substituted in a similar way. It appears that the above oligosaccharides represent the structure of the polysaccharide to a considerable extent.

Phytopathogenic microorganisms of several genera have been shown to form extracellular polysaccharides in synthetic media and in some cases these materials appear to have a phytotoxic effect when they are formed in vivo (1). Three genera are being examined and structural determinations on the extracellular polysaccharides from *Xanthomonas* spp., *Agrobacterium* spp., and *Corynebacterium* spp. are being carried out. Within the latter two genera there is a consistency in the composition of the polysaccharides, as *Agrobacterium* spp. form mainly 1,2-β-D-glucopyranose polymers (2, 3) and the *Xanthomonas* spp. produce gummy polysaccharides containing glucuronic acid, glucose, and mannose in varying proportions and in one case glucuronic acid, galactose, and glucose (4).

In the present study the polysaccharides from *Corynebacterium* spp. have been examined and have been shown to be somewhat more heterogeneous in their properties than those in the other two genera. For instance, *C. insidiosum*, *C. sepedonicum*, and *C. michiganense* contain hexoses with a high proportion of methylpentose(s) and give, on partial acid hydrolysis, acidic sugars with color reactions unlike those given by uronic acids (Table I). However, *C. flaccumfaciens*, *C. tritici*, *C. rathayi*, and *C. poinsettia* appear to be in a different group, giving, on acidic hydrolysis, substances resembling aldobiouronic acids by their color reactions and mobilities on paper chromatograms. In this respect the latter three organisms form polysaccharides that seem to bear a resemblance to extracellular polysaccharides formed by phytopathogenic *Xanthomonas* spp. (4).

The extracellular polysaccharide from *Corynebacterium insidiosum*, the causative agent of alfalfa wilt, was examined in more detail since it had the unusual features described above when the organism was grown on a dialyzed yeast extract medium. The polymer was complex, yielding, on acid hydrolysis, galactose, glucose, and fucose in the proportion 3:2:4 and in addition contained an acidic grouping for every six sugar units. However, this acidic function was not of the usual uronic acid type since no aldobiouronic acids were detected after strong acid hydrolysis. Therefore it was evident that structural determinations on the polysaccharide should be carried out initially by other methods apart from the methylation route.

Much useful information was furnished by partial hydrolysis of the *C. insidiosum* polysaccharide and fractionation of the products by charcoal and cellulose chroma-

[1]*Manuscript received July 10, 1961.*
Contribution from the National Research Council of Canada, Prairie Regional Laboratory, Saskatoon, Saskatchewan.
Issued as N.R.C. No. 6526.

tography. Four main products were obtained, two being neutral and the other two sugars containing acidic functions which were not uronic in nature.

One of the neutral sugars was shown to be 4-*O*-β-D-glucopyranosyl-L-fucose (I), which must represent a large proportion of the polysaccharide since no free glucose was present in the partial hydrolyzate although much galactose and fucose were produced. The disaccharide was amorphous, but a crystalline heptaacetate was prepared and also the derived polyhydric alcohol (5) gave an octaacetate which crystallized. The 4-linkage was assigned to the disaccharide since it took up 2.0 moles of lead tetraacetate in acetic acid gradually (6). This was confirmed by periodate oxidation of the derived polyol, which consumed 3.8 moles of oxidant yielding 1.9 moles of formic acid and no acetaldehyde. Since the specific rotation of the 4-*O*-D-glucopyranosyl-L-fucitol was −30° it seemed probable that the linkage configuration was β (7).

The other neutral fragment proved to be a trisaccharide (II) containing galactose, glucose, and fucose. Partial acid hydrolysis, using conditions similar to those used in the preparation of the trisaccharide from the polysaccharide, gave galactose and 4-*O*-β-D-glucopyranosyl-L-fucose, thus suggesting that the trimer also represents structurally a large proportion of the polysaccharide. The reducing end of the sugar was shown to be fucose since it was the only part that was reduced by sodium borohydride. The fucose portion was then shown to be linked in the 3-position by lead tetraacetate oxidation, since the sugar consumed 1 mole of oxidant (6), suggesting a branched-chain 4-*O*-β-D-glucopyranosyl(3-*O*-D-galactopyranosyl)-L-fucose structure (II). This was confirmed by two methods, oxidation with lead tetraacetate in potassium acetate – acetic acid, which gave 2 moles of formic acid slowly by oxidation of the glucose and galactose non-reducing end units (8). In addition, oxidation with sodium periodate gave a product which, on sodium borohydride reduction followed by acid hydrolysis, was degraded to glycerol and 5-deoxy pentitol.

When the two acidic sugars obtained on partial hydrolysis of the polysaccharide were examined it was shown that the unknown acid was attached to the 4-position of the galactose molecule in each case. The sugar with the lower molecular weight (III) crystallized and was shown to contain galactose since this hexose was formed by strong acid hydrolysis. C-1 of the galactose was apparently free since the substance mutarotated from +70° to +49° in water. Titration with alkali indicated a neutral equivalent of 288 and, based on this figure, consumption of lead tetraacetate by the sugar was 0.31, 0.69, 1.13, and 1.32 moles after 2, 5, 10, and 20 minutes respectively, thus indicating 4-substitution. Carbon and hydrogen analyses suggested an empirical formula of $C_{11}H_{20}O_9$, corresponding to a hexose unit attached ethereally to a hydroxy group of a dihydroxypentanoic acid. This formulation, however, does not agree with the infrared data obtained on the free sugar or the derived alcohol, the latter being obtained by methylation (CH_2N_2) followed by sodium borohydride reduction (9). The free sugar has a band at 1705 cm^{-1} corresponding to a carboxyl carbonyl group and there also appears to be a partially obscured band at 1725 cm^{-1} to 1750 cm^{-1}, which could represent an ester carbonyl group. The derived methyl ester gave a sharp band at 1735 cm^{-1} and on treatment with sodium borohydride a neutral substance was obtained which gave a strong band at 1740 cm^{-1}. This product, according to paper chromatograms, contained a little hexitol as well as the expected material so that the weight of evidence so far obtained indicates an ester-type linkage at the 4-position of the galactose residue.

The higher molecular weight material (IV) was amorphous and gave galactose, glucose, and fucose on acid hydrolysis, and on partial hydrolysis 4-*O*-β-D-glucopyranosyl-L-fucose

and the acidic galactose derivative were detected on paper chromatograms (III). Fucose was again shown to be at the reducing end by sodium borohydride reduction and, if a molecular weight of 602* is assumed, lead tetraacetate oxidation studies indicated a 3-linked fucose residue. It thus seemed that a 4-*O*-β-D-glucopyranosyl(3-galactopyranosyl)-L-fucose structure with an unknown carboxyl derivative attached (IV) was likely and its position of substitution on the galactose was shown to be at 4 since periodate oxidation of the oligosaccharide followed by sodium borohydride reduction and acid hydrolysis gave erythritol in addition to glycerol and 5-deoxy pentitol.

Periodate oxidation of the polysaccharide gave little information, except to show that non-reducing end groups or 6-linked hexopyranosyl units only are oxidized, and since overoxidation takes place only a rough figure of 28% can be estimated for their presence in the total polysaccharide.

Thus the polysaccharide from *C. insidiosum* is complex, particularly so because of the attachment of an unknown acidic entity on the galactose position. However, this type of substituent appears to be quite widespread at least in the extracellular polysaccharides from *Corynebacterium* spp., and more work is needed to show their true identities.

EXPERIMENTAL

Evaporations were carried out at 50° C under reduced pressure and specific rotations measured at 23° C.

Cultural Methods for Polysaccharide Production

The cultures of *Corynebacterium* spp. were maintained on a medium containing 1.5% glucose, 1.0% yeast extract, 0.5% calcium carbonate, and 1.3% agar.

The organisms were grown in a medium containing 1.5% glucose, 1.0% yeast extract, and 0.2 to 0.5% calcium carbonate. The yeast extract solution was dialyzed before use to remove high molecular weight polysaccharides. Small quantities of gum-producing polysaccharide were produced in 500-ml Erlenmeyer flasks containing 100 ml medium, incubated at 25° C on a rotary shaker, eccentricity 1/2 inch, operated at 250 r.p.m. For production of larger quantities of polysaccharide the organisms were grown in 5-liter glass-jar-type stirred fermentors having a working volume of 3 liters or in 30-liter stainless steel fermentors having a working volume of 20 liters.

Cells were removed in a Sharples supercentrifuge or in a Spinco ultracentrifuge if necessary, generally after about 4 days. Culture supernatants which contained a good deal of suspended matter after concentration were again centrifuged in the ultracentrifuge. After centrifugation the solutions were evaporated under vacuum to as small a volume as possible and the polysaccharide was precipitated by addition of 5 volumes of ethanol. For *Corynebacterium insidiosum* the yields of crude product were approximately 3 g per liter. The precipitate was recovered and redissolved in a large quantity of water and the solution treated with Amberlite IR-120 and Dowex-1. After filtration and evaporation the purified polysaccharide was reprecipitated with excess ethanol, washed with ethanol, and dried.

General Examination Procedure for Polysaccharides

The polysaccharide from each fermentation was hydrolyzed with *N* sulphuric acid at 100° C overnight to obtain the over-all sugar composition as shown by paper chromatograms using *p*-anisidine hydrochloride (10) as spray reagent. Those that did not show

*Based on a trisaccharide with a carboxyl function attached in a manner similar to that on III.

aldobiouronic acids under these conditions were partially hydrolyzed for 6 hours with *N* sulphuric acid at 70° C, under which conditions other acidic components might be detected. The results are listed in Table I.

TABLE I

Properties of extracellular *Corynebacterium* spp. polysaccharides

Organism and its A.T.C.C. number	Constituent sugars	$[\alpha]_D$	Non-uronic acid acidic function
C. insidiosum 10253	Galactose (32%) Glucose (21%) Fucose (46%)	−98°	+ve
C. sepedonicum 9850	Galactose (45%) Glucose (27%) Fucose (29%)	+87°	+ve
C. michiganense 7433	Galactose Glucose Mannose Fucose (33.9% total)	−33°	+ve
C. fascians 12974	Mannose Glucose Tr. galactose	+60°	Not tested
C. flaccumfaciens 7392	Glucose Mannose Fucose Rhamnose Aldobiouronic acid	−12°	—
C. tritici 9682	Glucose Mannose Rhamnose Aldobiouronic acid	+13°	—
C. rathayi 80†	Glucose Mannose Aldobiouronic acid Unknown at $R_{rhamnose}$ 1.1*	+51°	—

*Solvent. Ethyl acetate – acetic acid – water 9:2:2 v/v.
†National Collection of Plant Pathogenic Bacteria, Ministry of Agriculture, Fisheries and Food, Plant Pathology Laboratory, Harpenden, Herts, England.

Complete Hydrolysis of C. insidiosum Polysaccharide

The polysaccharide (100 mg) was hydrolyzed for 18 hours at 100° C in *N* sulphuric acid. The solution was then neutralized ($BaCO_3$), filtered, and evaporated to give a mixture of galactose, glucose, and fucose. These components were separated on a sheet of Whatman No. 1 filter paper using ethyl acetate – pyridine – water (10:4:3 v/v) as solvent and the relative amounts of sugars present estimated colorimetrically by the benzidine method of Jones and Pridham (11). The ratio of galactose–glucose–fucose was 3:2:4, the fucose composition checking well with a C-methyl estimation on the mixture. A larger scale hydrolysis was carried out and the components were fractionated on a cellulose column using *n*-butanol half saturated with water to yield L-fucose, D-glucose, and D-galactose, which were crystallized and identified.

Partial Hydrolysis of C. insidiosum Polysaccharide

The polysaccharide (20 g) was dissolved in *N* sulphuric acid (2 liters) by stirring the mixture at 70° C for 6 hours. After neutralization ($BaCO_3$) and removal of cations with Amberlite IR-120, the solution was examined on paper chromatograms and was shown to contain galactose and fucose as the monosaccharide fraction. On a paper chromatogram

using the ethyl acetate – acetic acid – water (9:2:2 v/v) solvent a yellow-brown spot ($R_{galactose}$ 0.8) with the *p*-anisidine hydrochloride spray was evident with smaller amounts of yellow spots with $R_{lactose}$ 0.7 and 1.1. The solution was passed down a charcoal column and the galactose and fucose removed by washing with water. Thirty per cent aqueous

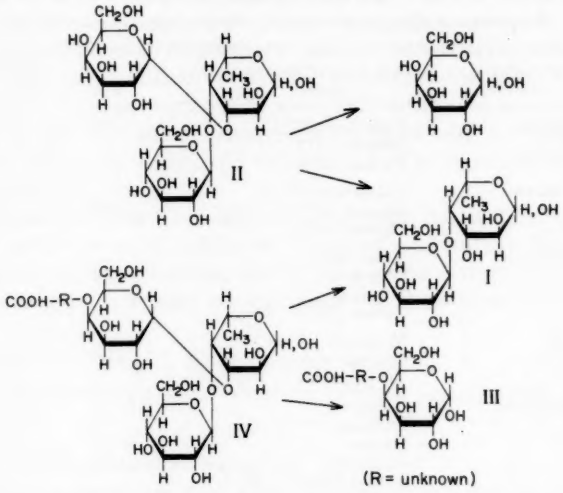

FIG. 1. Partial hydrolysis products of *C. insidiosum* polysaccharide.

ethanol eluted the compounds giving spots with $R_{galactose}$ 0.8 and $R_{lactose}$ 0.7 and 1.1, and in addition, a material running at the same speed as fucose and giving a yellow-brown spot with *p*-anisidine hydrochloride. The materials with $R_{lactose}$ 0.7 and R_{fucose} 1.0 proved to be acidic since they ran slowly in the ethyl acetate – pyridine – water (10:4:3 v/v) solvent.

The above components were fractionated on a cellulose column. Butanol saturated with water separated the materials with R_{fucose} 1.0 and $R_{galactose}$ 0.8 and butanol–ethanol–water (8:2:1 v/v) separated the other slower moving materials with $R_{lactose}$ 1.1 and 0.7. These partial hydrolysis products were examined for their chemical structures.

Identification of 4-O-β-D-Glucopyranosyl-L-fucose ($R_{galactose}$ 0.8) (I)

This material (3.4 g) was isolated in an amorphous form and a portion (300 mg) was converted to its heptaacetate by heating on a steam bath overnight in acetic anhydride (5 ml) containing sodium acetate (300 mg). After the excess anhydride was destroyed with ice-water, the solution was extracted with chloroform. The chloroform extract crystallized on evaporation and two recrystallizations from ethanol yielded a heptaacetate (123 mg) with m.p. 228–230° C and $[\alpha]_D$ −59° (*c*, 1.0, $CHCl_3$). Calculated for $C_{26}H_{36}O_{17}$: C, 50.3%; H, 5.85%. Found: C, 50.2%; H, 6.1%.

Deacetylation with a catalytic amount of sodium methoxide in methanol yielded, after neutralization with acetic acid, the free sugar with $[\alpha]_D$ −71° (*c*, 0.6, H_2O). Acid hydrolysis with *N* sulphuric acid at 100° C overnight yielded glucose and fucose (paper chromatograms). After 2, 5, 15, and 60 minutes the sugar consumed 0.81, 1.58, 1.99, and 2.06 moles of lead tetraacetate in acetic acid, respectively, giving strong indication of a 4-linked disaccharide.

The disaccharide (200 mg) was reduced with sodium borohydride (50 mg) in water (2 ml). After 4 hours the reductant was destroyed with acetic acid and cations were removed with Amberlite IR-120. The solution was filtered and evaporated to a crust which was repeatedly dissolved in methanol, which was then evaporated. The amorphous polyol was converted to its octaacetate by the acetylation procedure used above. Two recrystallizations from ethanol yielded crystals with m.p. 125–126° C and $[\alpha]_D$ −30° (*c*, 1.1, $CHCl_3$). Calculated for $C_{28}H_{40}O_{18}$: C, 50.6%; H, 6.1%. Found: C, 50.6%; H, 6.2%.

Deacetylation gave 4-*O*-β-D-glucopyranosyl-L-fucitol with $[\alpha]_D$ −30° (*c*, 1.1, H_2O), which was oxidized with aqueous sodium periodate and after 18 hours took up 3.8 moles of oxidant giving 1.9 moles of formic acid. No acetaldehyde could be detected (12) in the oxidation mixture.

Identification of 4-O-β-D-Glucopyranosyl(3-O-D-galactopyranosyl)-L-fucose ($R_{lactose}$ 0.7) (II)

This material ($[\alpha]_D$ +23° (*c*, 1.3, H_2O)) gave galactose, glucose, and fucose (paper chromatograms) on hydrolysis with *N* sulphuric acid at 100° C overnight. Reduction for 18 hours with sodium borohydride gave a polyol, which, on acid hydrolysis at 100° C with *N* sulphuric acid overnight gave, as reducing sugar, galactose and glucose and also some fucitol, detectable with the ammoniacal silver nitrate spray (13).

The fucose reducing end-unit was linked in the 3-position since, based on a molecular weight of 488, it took up 1.01, 1.04, and 1.09 moles of lead tetraacetate in acetic acid after 4, 15, and 30 minutes respectively. The trisaccharide was also oxidized with lead tetraacetate in 90% acetic acid containing potassium acetate and the formic acid produced measured as carbon dioxide in a Warburg respirometer (8). The production of carbon dioxide corresponded to the oxidation of two non-reducing end-units, one being oxidized more quickly than the other. At the end of the reaction 4.72 moles of oxidant had been consumed in glycol cleavage.

TABLE II

Time (minutes)	12	20	35	65	95	145	285	325	465
Moles CO_2 produced	0.43	0.64	0.80	0.95	1.08	1.38	1.78	1.87	2.11

The trisaccharide (10 mg) was oxidized overnight with excess aqueous sodium periodate and the ions then removed with mixed Amberlite IR-120 and Dowex-1 (bicarbonate form). The aldehyde was reduced with sodium borohydride by the method described previously and the product hydrolyzed with *N* sulphuric acid (5 ml) at 100° C overnight. The product, after neutralization ($BaCO_3$), was examined on a paper chromatogram (solvent *n*-butanol:ethanol:water, 40:11:19 v/v) and the only detectable spots using the ammoniacal silver nitrate spray corresponded to glycerol and a spot which could be 5-deoxylyxitol. These results agree with the above lead tetraacetate oxidation in that two non-reducing end-units are present.

A sample of the trisaccharide (70 mg) was partially hydrolyzed with *N* sulphuric acid (1 ml) at 70° C for 6 hours. After neutralization ($BaCO_3$) and filtration, the product corresponded to a mixture of 4-*O*-β-D-glucopyranosyl-L-fucose and galactose. These components were separated on sheets of Whatman No. 1 filter paper using *n*-butanol–ethanol–water (40:11:19 v/v) as solvent, and the two sugars were identified, the disaccharide as its heptaacetate and the galactose by its 1-methylphenylhydrazone (14). These were each compared with authentic specimens and had identical X-ray diffraction patterns.

Unknown Acidic Galactose Derivative (R_{fucose} 1.0) (III)

This product crystallized and two recrystallizations from ethanol yielded a material with m.p. 113–114° C and had $[\alpha]_D$ +70° → +49° (*c*, 0.6, H_2O, constant value). Acid hydrolysis at 100° C in *N* sulphuric acid for 18 hours yielded galactose (paper chromatograms). Its neutral equivalent was 288 and this figure and the analysis figures of C, 44.9%; H, 6.9% indicate a $C_{11}H_{20}O_9$ formula. Calculated for $C_{11}H_{20}O_9$: C, 44.6%; H, 6.8%. The infrared spectrum had strong absorption at 1705 cm^{-1} corresponding to acid carbonyl and a shoulder to this peak pointed to ester carbonyl absorption in the region 1725 cm^{-1} to 1750 cm^{-1}. Lead tetraacetate oxidation of the sugar resulted in uptake of 0.31, 0.69, 1.13, and 1.32 moles of oxidant after 2, 5, 10, and 20 minutes respectively based on a molecular weight of 288. These figures, even if this molecular weight is only approximate, indicate 4-substitution on the galactose molecule.

Treatment of the unknown acid (25 mg) in methanol with ethereal diazomethane yielded, on evaporation, its methyl ester (25 mg) having infrared absorption at 1735 cm^{-1}. The ester was dissolved in methanol (1 ml) containing 0.1 equivalent of sodium methoxide at 0° C, and sodium borohydride (20 mg) was added, the solution being kept in the refrigerator for 6 hours. The methanol was then removed by evaporation and the product isolated as described above. On paper chromatograms in *n*-butanol–ethanol–water (40:11:19 v/v) a main spot with $R_{rhamnose}$ 1.3, detectable with ammoniacal silver nitrate, was found together with a minor spot corresponding to a hexitol. Infrared absorption of the product at 1740 cm^{-1} indicated that an ester carboxyl group was still present.

Unknown Acidic 4-O-β-D-Glucopyranosyl-(3-O-galactopyranosyl)-L-fucose Derivative ($R_{lactose}$ 1.1) (IV)

This sugar, having $[\alpha]_D$ +9° (*c*, 0.6, H_2O) was cleaved using conditions identical with those for hydrolysis of the trisaccharide (II), giving galactose, glucose, and fucose. Partial acid hydrolysis gave 4-*O*-β-D-glucopyranosyl-L-fucose and the unknown acidic galactose derivative (III), all these sugars being identified by their chromatographic behavior. Fucose was identified as the reducing end of the sugar since sodium borohydride reduction followed by acid hydrolysis gave fucitol. The fucose was substituted in the 3-position since 0.90, 1.03, and 1.21 moles of lead tetraacetate in acetic acid were taken up after 2, 10, and 45 minutes, respectively, based on a molecular weight of 602. Sodium periodate oxidation* followed by sodium borohydride reduction, then hydrolysis, gave erythritol in addition to glycerol and 5-deoxy-lyxitol, indicating the unknown substituent was located in the 4-position of the galactose unit.

Sodium Periodate Oxidation of C. insidiosum Polysaccharide

The polysaccharide, $[\alpha]_D$ −98° (*c*, 0.7, H_2O), gave analysis figures of C 44.7%, H 6.9%, N 0.3%, ash 0.9%, and Cl 0.22%, and contained an acid group for every 912 of molecular weight. The sodium periodate oxidation data were as follows:

Time (days)	1	2	3	4	5	6	7
Sodium periodate uptake (moles)	0.42	0.46	0.53	—	0.55	0.59	0.60
Formic acid formed (moles)	0.16	0.17	0.21	0.23	0.24	0.25	0.28

The product on sodium borohydride reduction followed by acid hydrolysis in *N* sulphuric acid at 100° C overnight gave glycerol (on paper chromatograms) as the only non-reducing sugar, no erythritol being detected. Glucose, galactose, and fucose were also present.

**In this case sodium periodate and iodate were removed, first by treatment with Amberlite IR-120 and then with barium carbonate.*

ACKNOWLEDGMENTS

The authors wish to thank Mr. N. Gardner and Mrs. S. F. Hector for technical assistance, Mr. M. Mazurek for microanalytical determinations, and Miss I. M. Gaffney for carrying out infrared measurements.

REFERENCES

1. J. F. T. SPENCER and P. A. J. GORIN. Can. J. Microbiol. **7**, 185 (1961).
2. P. A. J. GORIN, J. F. T. SPENCER, and D. W. S. WESTLAKE. Can. J. Chem. **39**, 1067 (1961).
3. E. W. PUTMAN, A. L. POTTER, R. HODGSON, and W. Z. HASSID. J. Am. Chem. Soc. **72**, 5024 (1950).
4. P. A. J. GORIN and J. F. T. SPENCER. To be published.
5. M. L. WOLFROM and H. B. WOOD. J. Am. Chem. Soc. **73**, 2933 (1951).
6. A. J. CHARLSON and A. S. PERLIN. Can. J. Chem. **34**, 1200 (1956).
7. A. J. CHARLSON, P. A. J. GORIN, and A. S. PERLIN. Methods in carbohydrate chemistry. In press.
8. A. S. PERLIN. J. Am. Chem. Soc. **76**, 5505 (1954).
9. H. L. FRUSH and H. S. ISBELL. J. Am. Chem. Soc. **78**, 2844 (1956).
10. L. HOUGH, J. K. N. JONES, and W. H. WADMAN. J. Chem. Soc. 1702 (1950).
11. J. K. N. JONES and J. B. PRIDHAM. Biochem. J. **58**, 288 (1954).
12. P. DESNUELLE and M. NAUDET. Bull. soc. chim. France, **12**, 871 (1945).
13. S. M. PARTRIDGE. Nature, **158**, 270 (1946).
14. C. A. LOBRY DE BRUYN and W. A. VAN ECKENSTEIN. Rec. trav. chim. **15**, 226 (1896).

STRUCTURAL RELATIONSHIPS OF EXTRACELLULAR POLYSACCHARIDES FROM PHYTOPATHOGENIC XANTHOMONAS SPP.

PART I. STRUCTURE OF THE EXTRACELLULAR POLYSACCHARIDE FROM XANTHOMONAS STEWARTII[1]

P. A. J. GORIN AND J. F. T. SPENCER

ABSTRACT

Xanthomonas stewartii produces an extracellular polysaccharide which is markedly different from those formed by other *Xanthomonas* spp. examined in that it gave glucose, galactose, and an aldobiouronic acid on hydrolysis. Methylation followed by hydrolysis yielded 2,3,4,6-tetra-*O*-methyl-D-glucose (4 parts), 2,3,4-tri-*O*-methyl-D-glucose (2 parts), 2,4,6-tri-*O*-methyl-D-galactose (1 part), 2,3,4-tri-*O*-methyl-D-galactose (2 parts), and 2-*O*-methyl-D-galactose (1.8 parts). Partial acid hydrolysis yielded 6-*O*-β-D-glucopyranosyl-D-galactose, 3-*O*-β-D-glucopyranosyl-D-galactose, 3-*O*-β-D-galactopyranosyl-D-galactose, and 4-*O*-β-D-glucuronopyranosyl-D-galactose.

The extracellular polysaccharides from phytopathogenic species of *Xanthomonas* are being examined and a consistency of structure within the genus, at least as far as the sugar constituents of the polysaccharides are concerned, has been demonstrated. Nine of the 12 *Xanthomonas* spp. studied produce polysaccharides (on dialyzed yeast extract medium) which give viscous aqueous solutions and contain glucuronic acid, glucose, and mannose. Two species examined do not produce appreciable amounts of polysaccharide,* and *Xanthomonas stewartii* (formerly *Bacterium stewartii*), the corn wilt organism, forms a different type of polysaccharide containing glucuronic acid, galactose, and glucose (Table I). This polysaccharide also gives viscous solutions in water. These

TABLE I

Xanthomonas spp. and their extracellular polysaccharides

Polysaccharide-forming *Xanthomonas* spp. (with A.T.C.C. number) and their products of hydrolysis		
Aldobiouronic acid, glucose, and mannose	Aldobiouronic acid, galactose, and glucose	*Xanthomonas* spp. not forming polysaccharides
*X. campestris**	*X. stewartii* (8199)	*X. betticola* (10309)
X. carotae (10547)		*X. vasculorum*
X. hyacinthi (12612)		
X. maculofoliigardeniae (10201)		
X. malvacearum (12131)		
X. phaseoli†		
X. pruni (10016)		
X. translucens (10722)		
X. vignicola (11648)		

*Reference 18.
†Reference 17.

results agree with the reclassification of this organism described in the 1957 Bergey's Manual of Determinative Bacteriology (1). *Xanthomonas stewartii* is quoted to be a

[1]*Manuscript received July 10, 1961.*
Contribution from the National Research Council of Canada, Prairie Regional Laboratory, Saskatoon, Saskatchewan.
Issued as N.R.C. No. 6525.

**Any taxonomic deductions on non-polysaccharide-forming species should be made carefully since it is quite possible that other polysaccharide-forming strains of the same species exist.*

Xanthomonas species incertae sedis and plant pathologists have placed it in the *Xanthomonas* genus even though it does not possess all the characteristics of the genus.

Since a large proportion of *Xanthomonas* spp. (Table I) produce polysaccharides which give solutions of high viscosity, it is of interest to observe that the vascular systems of plants can be blocked to some extent by these solutions. This effect has been observed on tomato cuttings by Riker and co-workers (2), using several polysaccharides, and by Leach *et al.* (3), who showed that excised seedlings of tomato, sunflower, and bean wilted under the influence of an aqueous solution of *X. phaseoli* polysaccharide. Also, the authors of the present paper have demonstrated the wilting properties of the *Corynebacterium insidiosum* polysaccharide on alfalfa cuttings and the fact that the polymer is formed in the infected plant itself (4). This physiological action has been observed in a different way by Corey and Starr (5), who studied the morphology of four strains of *X. phaseoli* and showed that the amount of polysaccharide formed by each strain could be correlated with its virulence on the host plant.

Therefore a more detailed structural analysis on the extracellular polysaccharides of the *Xanthomonas* species is being carried out, starting with *X. stewartii*. It is hoped that the polysaccharides from some of the other species containing glucuronic acid, glucose, and mannose (Table I) can be studied later.

The polysaccharide from *X. stewartii* proved to be highly branched, approximately one-third of the sugar residues consisting of non-reducing glucose end units. Studies on the methyl glycosides obtained from the fully methylated polysaccharides were kindly carried out by Dr. C. T. Bishop (6) using the gas–liquid phase chromatography procedure. The presence of the methyl glycosides of 2,3,4,6-tetra-*O*-methyl-D-glucose (4 parts), 2,3,4-tri-*O*-methyl-D-glucose (2 parts), 2,4,6-tri-*O*-methyl-D-galactose (1 part), and 2,3,4-tri-*O*-methyl-D-galactose (2 parts) was shown. Cellulose chromatography (7) of the reducing methyl sugars showed the absence of di-*O*-methyl-D-glucose. However, 2-*O*-methyl-D-galactose was isolated in a proportion equivalent to 1.8 parts taking into account the glucuronic acid in the molecule which is equivalent to 1.3 parts. The above figures also give an estimate of the proportion of sugars in the polysaccharide, which amount to glucuronic acid (11%), glucose (51%), and galactose (32%).

Periodate oxidation of the polysaccharide showed an immediate uptake (18 hours) of oxidant and production of formic acid with little further oxidation over a week. A 1.20-mole quantity of oxidant was consumed with the evolution of 0.58 mole of formic acid, amounts which agree closely with a 1.30 molar uptake and 0.65-mole quantity of formic acid that would be calculated from the methylation results.

Since information was required on the sugar sequence in the polysaccharide, a partial acid hydrolysis was carried out at 80° C with *N* sulphuric acid. Two main disaccharide fractions were obtained by cellulose chromatography, one of which was 6-*O*-β-D-glucopyranosyl-D-galactose, isolated in 13% yield. Although it crystallized only with difficulty, it could be converted readily to crystalline 6-*O*-β-D-glucopyranosyl-D-galactitol nonaacetate by sodium borohydride reduction followed by acetylation. This compound proved to be identical with a specimen prepared similarly from the authentic reducing disaccharide (8). The other disaccharide, 3-*O*-β-D-glucopyranosyl-D-galactose, did not crystallize. However, it gave glucose and galactose on acid hydrolysis and glucose only on sodium borohydride reduction followed by acid hydrolysis. The position of substitution on the galactose reducing end was determined by lead tetraacetate oxidation and since 1 mole was taken up immediately (3 minutes) with little increase over 30

minutes, the linkage was evidently in the 3-position (9). For a glucose–galactose disaccharide its specific rotation of +35° was low, suggesting a β-configuration for the glycosidic linkage.

An aldobiouronic acid was obtained by an isolation procedure similar to that described above except that the hydrolysis in *N* sulphuric acid was carried out at 100° C. The aldobiouronic acid gave a uronic acid and galactose on vigorous acid hydrolysis and when the dimer was oxidized with lead tetraacetate it consumed 1.8 moles of oxidant (after 30 minutes) at a slower rate than that expected for a 6-linkage. The material was therefore 4-linked and the 4-*O*-glucuronopyranosyl-D-galactose structure seemed likely. Treatment with diazomethane and reduction of the methyl ester with sodium borohydride (10) gave a crystalline disaccharide alcohol with $[\alpha]_D$ −13°. Acid hydrolysis gave glucose as the only reducing sugar, thus identifying the uronic acid portion. Since the specific rotations of the neutral derivative (and the parent aldobiouronic acid) were low, the configuration of the glycosidic linkage should be β.

Another type of acid hydrolysis of the polysaccharide was carried out using the procedure of Smith and co-workers (11) wherein the polysaccharide was oxidized with sodium periodate. The oxypolysaccharide was then reduced with sodium borohydride and the product obtained hydrolyzed with acid. However, with this polysaccharide somewhat more vigorous conditions were needed than those recommended by the Minnesota group. The reducing sugars obtained were galactose and a disaccharide, and after cellulose chromatography the dimer was isolated and tentatively characterized as 3-*O*-β-D-galactopyranosyl-D-galactose (12). Although it could not be induced to crystallize, it gave galactose only on acid hydrolysis. When it was treated with lead tetraacetate, the consumption of oxidant corresponded to a 3-linked disaccharide and the product on hydrolysis contained galactose and lyxose. The specific rotation (+52°) corresponded closely to that of authentic 3-*O*-β-D-galactopyranosyl-D-galactose. Since no trisaccharide was obtained in the partial hydrolysis of the modified polysaccharide, it can be safely assumed that there were no more than two successive galactose residues in the starting polysaccharide that were linked in the 3-position.

Methylation of the galactose-containing polysaccharide obtained by successive sodium periodate oxidation and sodium borohydride reduction and hydrolysis under milder conditions than above gave a product which, on hydrolysis, gave three poly-*O*-methyl galactose derivatives. These were isolated from cellulose columns and shown to be 2,3,4,6-tetra-*O*-methyl-D-galactose (characterized as the aniline derivative), 2,4,6-tri-*O*-methyl-D-galactose, and 2,6-di-*O*-methyl-D-galactose in the proportion 1.7:1:1.15, thus confirming the isolation of 3-*O*-β-D-galactopyranosyl-D-galactose. These results also suggest that the 2,6-di-*O*-methyl-D-galactose represents the same fragment that yields 2-*O*-methyl-D-galactose from the undegraded methylated polysaccharide. Also, since the degraded polysaccharide contained galactose only, the glucuronic acid portion in the *X. stewartii* polysaccharide was linked in such a way as to permit periodate oxidation.

Summarizing, the polysaccharide is highly branched and contains no points of single branching, only double branching as represented by the 2-*O*-methyl galactose obtained in the methylation studies. The polymer contains at least four different linkage types. These were demonstrated by the isolation of 6-*O*-β- and 3-*O*-β-D-glucopyranosyl-D-galactose, 3-*O*-β-D-galactopyranosyl-D-galactose and 4-*O*-β-D-glucuronopyranosyl-D-galactose and by identification of the hydrolysis products of the methylated polysaccharide (Table II). The non-reducing end units consist of glucose (and glucuronic acid perhaps) and it seems likely that these are β-linked to galactopyranose residues in the

6-position. However, further deductions on the structure of this rather complex polysaccharide would be somewhat speculative and would require, for example, the isolation of trisaccharides in good yield in order to furnish a more comprehensive picture.

EXPERIMENTAL

Solutions were evaporated at 50° C under reduced pressure and specific rotations measured at 23° C.

Cultural Conditions for Xanthomonas spp.

The organisms were maintained and polysaccharide produced under conditions identical with those described in a previous paper (13). The yields were generally 1–4 g/liter of crude polysaccharide and this was purified as described previously (13).

Sugar Composition of Polysaccharides

The polysaccharides obtained from various species of *Xanthomonas* were hydrolyzed overnight on a steam bath in *N* sulphuric acid. After neutralization ($BaCO_3$), filtration, and evaporation the sugars were examined on paper chromatograms in various solvents using *p*-anisidine hydrochloride (14) as spray reagent. The results are recorded in Table I.

X. stewartii Polysaccharide and its Periodate Oxidation Characteristics

The polysaccharide had $[\alpha]_D$ +41° (*c*, 0.1, H_2O) and based on an anhydro hexose unit with mol. wt. 162 it contained, by titration, one acidic group per 9 units. Found: C, 43.4%; H, 6.6%; ash, 0.4%. It gave on acid hydrolysis at 100° C overnight in *N* sulphuric acid an aldobiouronic acid, galactose, and glucose. On oxidation with aqueous sodium periodate the following data were obtained:

Time, days	1	2	3	4	5	6
Uptake of oxidant, moles/mole	1.18	1.13	1.03	—	1.26	1.23
Formic acid produced, moles/mole	0.51	0.48	0.54	0.56	0.57	0.54

The end product was dialyzed to remove low molecular weight material and the sample consisting of roughly 50 mg of oxypolysaccharide in water (50 ml) was treated with sodium borohydride (50 mg). After a day, excess reductant was destroyed with acetic acid and the solution was then treated with Amberlite IR-120. The solution was filtered and evaporated to dryness, and the boric acid was removed by repeated evaporations with methanol. The product was hydrolyzed overnight at 100° C in *N* sulphuric acid (2 ml) and after neutralization ($BaCO_3$), filtration, and evaporation the product was examined on paper chromatograms (solvent: *n*-butanol–ethanol–water, 40:11:19 v/v). As would be expected from the periodate data, the only non-reducing sugar that appeared with the ammoniacal silver nitrate spray (15) was glycerol. The only reducing sugar detected was galactose.

Methylation and Hydrolysis of X. stewartii Polysaccharide

The polysaccharide (5.0 g) was dissolved in water (150 ml) to give a very viscous solution. Sodium hydroxide (30 g) in water (60 ml) was added and methylation was carried out by addition of dimethyl sulphate, in 11 separate aliquots of 3 cc each, once every 30 minutes. This process was repeated five times on successive days after which the solution was heated at 100° C for 3 hours. After cooling the methylation mixture was acidified slightly with dilute sulphuric acid and the gummy precipitate which formed was collected and dried. Yield, 3.8 g. The partially methylated polysaccharide was dissolved in dimethyl formamide (200 ml), methyl iodide (200 ml) was added, and the

solution shaken vigorously. Silver oxide was added on 6 successive days in 30-g portions and after this time chloroform (1 liter) was added and the solution filtered (16). The chloroform was evaporated to a crust, which was redissolved in chloroform and washed with aqueous potassium cyanide followed by water. The methylated residue, after evaporation, weighed 3.6 g.

This product was refluxed in 10% methanolic hydrogen chloride (50 ml) overnight and the solution neutralized (Ag_2CO_3), filtered, and evaporated to a syrup. This was further hydrolyzed by heating at 100° C in *N* sulphuric acid (20 ml) overnight. Neutralization ($BaCO_3$), filtration, and evaporation yielded a syrupy product with —OCH_3 40.2%.

(a) Cellulose Column Chromatography

The above product appeared to contain, by paper chromatography, tetramethyl, trimethyl, and monomethyl hexoses and a spot corresponding to a methylated substance containing uronic acid. Fractionation of a portion (1.1 g) on a cellulose column using *n*-butanol as solvent gave 2-*O*-methyl-D-galactose (68 mg) and 545 mg of other methylated sugars. Two recrystallizations of the monomethyl sugar from ethanol gave crystals with m.p. 152–155° C. Calculated for $C_6H_{11}O_5(OCH_3)$: OCH_3, 16.0%. Found: OCH_3, 16.0%. X-Ray diffraction patterns prepared on this and an authentic specimen were identical.

(b) Gas–Liquid Phase Chromatography

The mixture of reducing methylated sugars (1.0 g) was refluxed overnight in 3% methanolic hydrogen chloride (20 ml). The acid was neutralized with silver carbonate, and the solution then filtered and evaporated to a syrup. Using a standard Pye unit, Dr. C. T. Bishop carried out quantitative separations at 200° C with a column of Carbowax 20 M on Chromosorb P (1:4 w/w) and a flow rate of 40 ml per minute of helium. Tetra- and tri-methyl hexoses were separated and estimated by integration of the area under the peaks on the flow chart (Table II).

TABLE II

Methylation results on *Xanthomonas stewartii* polysaccharide

Substitution in polysaccharide from methylation data	Parts present on a molar basis
Glucose non-reducing end units	4
6-Substituted glucose units	2
3-Substituted galactose units	1
6-Substituted galactose units	2
3,4,6-Substituted galactose units	1.8
Glucuronic acid present*	1.3

*Based on titration against the original polysaccharide.

Partial Hydrolysis of X. stewartii Polysaccharide

(*a*) The polysaccharide (7.5 g) was partially hydrolyzed with *N* sulphuric acid at 80° C for 6 hours. The hydrolyzate was neutralized ($BaCO_3$), filtered, and deionized with Amberlite IR-120 and Dowex-1. The neutral portion (2.05 g) was fractionated on a cellulose column using *n*-butanol–ethanol–water (8:2:1 v/v) as the mobile phase. Two disaccharide fractions were obtained with $R_{lactose}$ 1.1 (1.05 g) and 0.9 (0.23 g) on paper chromatograms in the ethyl acetate – acetic acid – water (9:2:2 v/v) solvent.

Both sugars were amorphous and the one with $R_{lactose}$ 1.1 (150 mg) ($[\alpha]_D$ +10° (*c*, 2.0, H_2O)) was reduced with sodium borohydride by the method described earlier to 6-*O*-β-D-glucopyranosyl-D-galactitol (73 mg), which after two recrystallizations from ethanol had m.p. 160–162° C and $[\alpha]_D$ −17° (*c*, 0.7, H_2O). Calculated for $C_{12}H_{24}O_{11}$: C, 41.9%; H, 7.0%. Found: C, 41.9%; H, 7.1%. Conversion to the acetate was effected by heating the sugar (30 mg) at 100° C for 18 hours in acetic anhydride (1 ml) containing sodium acetate (50 mg). The anhydride was destroyed with ice-water and a chloroform extract of the mixture was evaporated. On two recrystallizations from ethanol the nonaacetate (13 mg) was isolated, having m.p. 149–150° C. Calculated for $C_{30}H_{42}O_{20}$: C, 49.9%; H, 5.9%. Found: C, 50.0%; H, 5.9%. Its X-ray diffraction pattern was identical with an authentic specimen prepared in a similar way from 6-*O*-β-D-glucopyranosyl-D-galactose (8).

The disaccharide $R_{lactose}$ 0.9 was hydrolyzed with *N* sulphuric acid at 100° C overnight to give galactose and glucose. After reduction with sodium borohydride and subsequent hydrolysis, glucose was the only remaining reducing sugar. The reducing galactose unit was linked in the 3-position since, when the disaccharide was oxidized with lead tetraacetate in acetic acid, 0.98, 0.98, and 1.02 moles/mole of oxidant were consumed after 3, 10, and 30 minutes, respectively. The specific rotation of the disaccharide was +35° (*c*, 1.2, H_2O).

(*b*) *X. stewartii* polysaccharide (10 g) was hydrolyzed by heating in *N* sulphuric acid (100 ml) at 100° C for 18 hours. The reaction mixture was neutralized with barium carbonate, and the solution was filtered, treated with Amberlite IR-120, filtered, and evaporated to a crust. This was fractionated on a cellulose column and neutral sugars were eluted with *n*-butanol–ethanol–water (4:1:1 v/v). An aldobiouronic acid fraction (0.90 g) was obtained by using ethyl acetate – acetic acid – water (9:2:2 v/v) as the solvent. This sugar, $[\alpha]_D$ +15° (*c*, 1.0, H_2O), was hydrolyzed overnight at 100° C with 6 *N* sulphuric acid to give a uronic acid and galactose. The galactose portion was 4-linked since the aldobiouronic acid consumed 0.90, 1.52, 1.75, and 1.83 moles/mole of lead tetraacetate in acetic acid after 2, 5, 15, and 30 minutes, respectively.

One hundred and fifty-one milligrams of the aldobiouronic acid in methanol was converted by ethereal diazomethane to its methyl ester (147 mg). This was reduced with sodium borohydride (100 mg) in water (10 ml) for 2 hours and the product was isolated by the method described previously. The product was fractionated on a cellulose column using *n*-butanol saturated with water as solvent to give crude 4-*O*-β-D-glucopyranosyl-D-galactitol, which was crystallized twice from methanol to give a material (15 mg) with m.p. 204° C and $[\alpha]_D$ −13° (*c*, 1.1, H_2O). Calculated for $C_{12}H_{24}O_{11}$: C, 41.9%; H, 7.0%. Found: C, 42.0%; H, 6.85%. Acid hydrolysis with *N* sulphuric acid at 100° C overnight gave glucose (paper chromatogram).

Partial Hydrolysis of Polysaccharide Modified by Periodate Oxidation and Borohydride Reduction

Crude *X. stewartii* polysaccharide (40 g) was stirred with periodic acid (100 g) in 4 liters of water for 3 days, by which time all the polysaccharide had dissolved. Then aqueous barium hydroxide was added until the solution was slightly acid and residual acidity was removed with barium carbonate. The solution was filtered and then treated with sodium borohydride (10 g). After 18 hours the solution was brought to pH 5 with acetic acid and evaporated to a crust that was repeatedly shaken in methanol, which was evaporated. The product was deionized in water with Amberlite IR-120 and Dowex-1

(bicarbonate form), and the solution filtered and evaporated to 200 ml. The polysaccharide was precipitated by addition of 5 volumes of ethanol, and collected on a filter. Yield, 17 g.

Half of this material was dissolved in 0.1 *N* sulphuric acid (2 liters) and the solution heated at 95° C for 4 hours, neutralized ($BaCO_3$), filtered, and evaporated to a small volume. Examination on paper chromatogram indicated the presence of glycerol, galactose, and a disaccharide and these materials were separated by fractionation on a cellulose column. *n*-Butanol saturated with water gave glycerol (2.16 g) and *n*-butanol–ethanol–water (4:1:1 v/v) separated galactose (0.79 g) and the disaccharide (1.74 g).

The disaccharide gave galactose (on paper chromatograms) after hydrolysis on a steam bath overnight with *N* sulphuric acid. It consumed 0.88, 1.03, and 1.19 moles/mole of lead tetraacetate in acetic acid after 3, 10, and 25 minutes, respectively, indicating a 3-linked disaccharide. Since its specific rotation was +52° (*c*, 0.9, H_2O), it appeared to be 3-*O*-β-D-galactopyranosyl-D-galactose.

Methylation of X. stewartii Polysaccharide Modified by Periodate Oxidation and Borohydride Reduction

A sample of crude modified polysaccharide (4.35 g), prepared by the method described above, was methylated in the standard way (see earlier method in this section) with aqueous sodium hydroxide – dimethyl sulphate. After destruction of excess dimethyl sulphate the solution was neutralized with acetic acid and extracted once with chloroform. The extract was evaporated to dryness yielding a material (1.16 g) which was refluxed for 3 days in methyl iodide (50 ml) containing silver oxide (20 g). The product (0.99 g) after filtration and evaporation had —OCH_3 45.6%.

The methylated polysaccharide was hydrolyzed by refluxing overnight in 10% methanolic hydrogen chloride (20 ml) and, to this, water (20 ml) was added and the methanol removed by evaporation. A further hydrolysis at 100° C for 18 hours was carried out and the product after neutralization ($BaCO_3$) and evaporation contained three reducing sugars (paper chromatograms). Fractionation on a cellulose column using benzene–ethanol–water (1000:50:1 v/v) as solvent yielded 2,3,4,6-tetra-*O*-methyl-D-galactose (136 mg), 2,4,6-tri-*O*-methyl-D-galactose (75 mg), and 2,6-di-*O*-methyl-D-galactose (82 mg).

The tetramethyl galactose was characterized as its aniline derivative, m.p. 191–193° C. 2,4,6-Tri-*O*-methyl-D-galactose was recrystallized twice from ether and had m.p. 103–105° C and $[\alpha]_D$ +85° (*c*, 0.9, H_2O). 2,6-Di-*O*-methyl-D-galactose was crystallized twice from ethyl acetate and had m.p. and mixed m.p. 116–119° C and $[\alpha]_D$ +92° → +87° (*c*, 1.0, H_2O, constant value).

ACKNOWLEDGMENTS

The authors appreciate the technical assistance of Mrs. S. F. Hector and Mr. N. R. Gardner. Microanalyses were carried out by Mr. M. Mazurek.

REFERENCES

1. R. S. Breed, E. G. D. Murray, and N. R. Smith (*Editors*). *In* Bergey's Manual of determinative bacteriology. 7th ed. The Williams & Wilkins Co., Baltimore. 1957.
2. R. Hodgson, A. J. Riker, and W. H. Peterson. Phytopathology, **37**, 301 (1947).
3. J. G. Leach, V. G. Lilly, H. A. Wilson, and M. R. Purvis, Jr. Phytopathology, **47**, 113 (1957).
4. J. F. T. Spencer and P. A. J. Gorin. Can. J. Microbiol. **7**. 185 (1961).
5. R. R. Corey and M. P. Starr. J. Bacteriol. **74**, 137 (1957).
6. C. T. Bishop. Unpublished results.
7. L. Hough, J. K. N. Jones, and W. H. Wadman. J. Chem. Soc. 2511 (1949).

8. K. FREUDENBERG, A. NOË, and E. KNOPF. Ber. B, **60**, 238 (1927).
9. A. J. CHARLSON and A. S. PERLIN. Can. J. Chem. **34**, 1200 (1956).
10. M. L. WOLFROM and K. ANNO. J. Am. Chem. Soc. **74**, 5583 (1952).
11. I. J. GOLDSTEIN, G. W. HAY, B. A. LEWIS, and F. SMITH. Am. Chem. Soc. 135th Meeting, Abstracts 3D (1959).
12. E. L. HIRST and A. S. PERLIN. J. Chem. Soc. 2622 (1954).
13. P. A. J. GORIN and J. F. T. SPENCER. To be published.
14. L. HOUGH, J. K. N. JONES, and W. H. WADMAN. J. Chem. Soc. 1702 (1950).
15. S. M. PARTRIDGE. Nature, **158**, 270 (1946).
16. R. KUHN, H. TRISCHMANN, and I. LÖW. Angew. Chem. **67**, 32 (1955).
17. S. M. LESLEY and R. M. HOCHSTER. Can. J. Biochem. and Physiol. **37**, 513 (1959).
18. A. JEANES, J. E. PITTSLEY, J. H. SLONEKER, and F. R. SENTI. Am. Chem. Soc. 136th Meeting, Abstracts 7D (1959).

THE ALUMINUM REDUCTION OF MAGNESIUM OXIDE

II. THE VAPOR PRESSURE OF MAGNESIUM OVER THE SYSTEM Al–MgO–CaO[1]

K. GRJOTHEIM, O. HERSTAD, AND J. M. TOGURI

ABSTRACT

The equilibrium vapor pressure of magnesium over the reaction between the calcined dolomite and aluminum was measured by means of the transportation method. In the temperature range 886–1035° C, the reaction was found to proceed according to the equilibrium

$$12CaO_{(s)} + 21MgO_{(s)} + 14Al_{(l)} = 12CaO.7Al_2O_{3(s)} + 21Mg_{(g)}$$

and the measured equilibrium pressure of magnesium can be expressed by the equation

$$\log P_{\text{mm of Hg}} = -(8754/T) + 8.462.$$

INTRODUCTION

Silicon as a reducing agent for magnesium-bearing compounds has been examined by a number of workers (1, 2, 3); however, an analogous examination of the reaction between calcined dolomite and aluminum does not appear to exist. The reaction is reported to proceed as follows (4):

$$5CaO + 9MgO + 6Al = 5CaO.3Al_2O_3 + 9Mg. \qquad [1]$$

In the present investigation, a continuation of the study of the reduction of magnesium compounds with aluminum, the equilibrium vapor pressure of magnesium over reaction [1] was determined and the solid products of the reaction were identified.

EXPERIMENTAL

Preliminary experiments indicated that the expected pressure of magnesium was of the order of 40 mm of Hg at 1000° C, a pressure suitable for the employment of the transportation method. This method of measuring vapor pressures has proved to be successful for a number of similar reactions (1, 2, 3, 5) provided the necessary precautions against diffusion errors and unsaturation of the carrier gas are observed.

The transportation apparatus and procedures adopted for the present study have been fully described previously (5).

The carrier gas utilized throughout this investigation was S-argon gas obtained from Norsk Hydro, the analysis given was 99.94%. The impurities CO_2 and H_2O were removed by passing the argon through ascarite and dehydrite towers respectively.

PREPARATION OF CHARGE

The calcined dolomite used in this investigation was obtained from Hammarfallene (Norway). The chemical analysis was, in weight per cent: 58.3% CaO, 40.3% MgO, 0.06% Al_2O_3, 0.16% Fe_2O_3, and 1.18% insolubles. The aluminum powder (99.9%) was obtained from Merck, Germany.

Before use, the calcined dolomite was dried at 1100° C for 24 hours to expell traces of CO_2 and H_2O. The calcined dolomite and aluminum were then mixed in a stoichiometric ratio (MgO/Al) according to equation [1], and ground in a ball mill for 12 hours. The mixture was then pressed into briquettes, 2.0 cm diameter by 1.0 cm in height, at a pressure of 500 kg/cm^2.

[1]*Manuscript received June 19, 1961.*
Contribution from the Institute of Inorganic Chemistry, The Technical University of Norway, Trondheim, Norway.

These briquettes were broken into approximately 5-mm particle size, and about 150 g of such pieces was used as a charge.

RESULTS AND DISCUSSION

(a) Vapor Pressure Measurements

The vapor pressure of magnesium over the mixture of calcined dolomite and metallic aluminum was measured over the temperature range 886–1035° C. A number of experiments at different flow rates were carried out at each temperature investigated in order to determine the equilibrium vapor pressure which is independent of the flow rate. The observed equilibrium pressures are tabulated in Table I. The estimated probable error in the measured vapor pressure is 1%.

TABLE I

Experimental vapor pressure of magnesium

Temp. (° C)	Pressure (mm of Hg)
887	8.30
925	14.00
955	20.40
968	25.70
992	34.80
1035	60.25

When the results from Table I were plotted as log P versus the reciprocal of the absolute temperature, Fig. 1 was obtained. The data may be represented as a straight line and

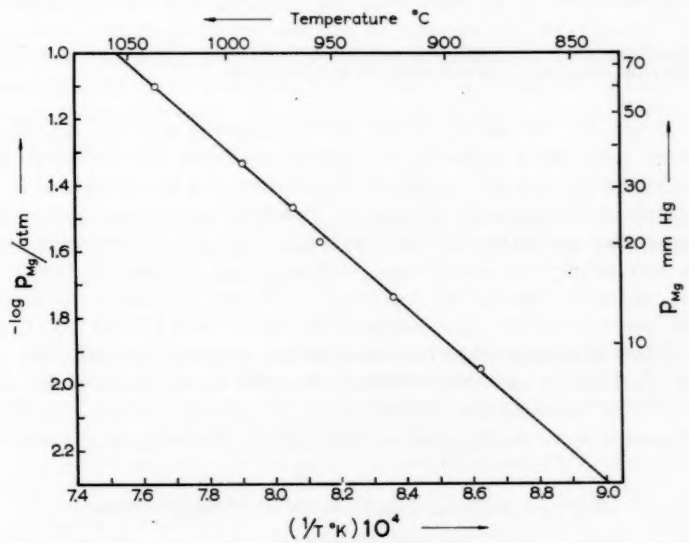

FIG. 1. Log P_{atm} of Mg versus $1/T°$ K.

fitted to the equation

$$\log P_{\text{mm of Hg}} = -(8754/T)+8.462,$$

where P is pressure in mm of Hg and T is the absolute temperature.

(b) Analysis of the Reaction Product

Chemical analysis of the condensed magnesium showed no traces of calcium.

The solid residue was analyzed by X-ray diffraction in order to confirm the reaction products of equation [1]. The diffraction patterns obtained (shown in Fig. 2) correspond

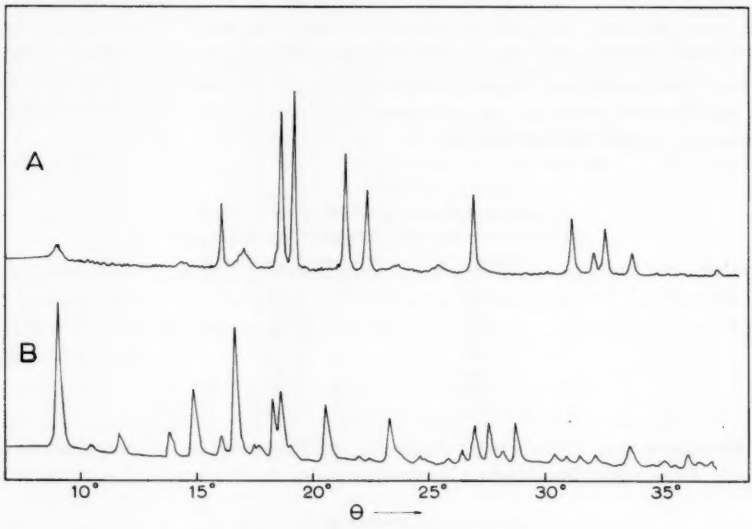

FIG. 2. X-Ray diffraction pattern (Cu target, Ni filter). A. Unreacted mixture of calcined dolomite and aluminum. B. Reacted mixture of calcined dolomite and aluminum.

only to CaO, MgO, Al, and $12CaO.7Al_2O_3$ when compared with the ASTM Index (6).

The literature indicates a difference in opinion regarding the similarity of the two compounds $5CaO.3Al_2O_3$ and $12CaO.7Al_2O_3$. The existence of the compound $5CaO.3Al_2O_3$ was first reported by Rankin and Wright (7). However, later investigators have found that this formula does not satisfy all the known characteristics of the compound. Bussem and Eitel (8) concluded, from a structural analysis of the compound, that it should be $12CaO.7Al_2O_3$. Recently, Aruja (9), following an X-ray analysis, concluded that the X-ray powder patterns of the compounds $5CaO.3Al_2O_3$ and $12CaO.7Al_2O_3$ showed no resemblance. There thus appears to be a controversy as to whether the two compounds are essentially identical or not. Nevertheless, since the X-ray patterns obtained, at all temperatures of this investigation, correspond to the powder pattern of $12CaO.7Al_2O_3$ reported by Swanson *et al.* (6, 10), this formula is used. The reaction is therefore written as follows:

$$12CaO_{(s)} + 21MgO_{(s)} + 14Al_{(l)} = 12CaO.7Al_2O_{3(s)} + 21Mg_{(g)}. \qquad [2]$$

The formation of the compound $12CaO.7Al_2O_3$ is not in accordance with the phase diagram of the system $CaO–MgO–Al_2O_3$ (11). The expected calcium aluminate is $3CaO.Al_2O_3$. However, no evidence could be obtained for its formation in the reaction studied. The possible reason for this might be either (I) that $3CaO.Al_2O_3$ is not a stable compound at the temperatures of the present investigation, or (II) that the kinetics of the formation of $12CaO.7Al_2O_3$ is much faster than that of $3CaO.Al_2O_3$.

A number of experiments were carried out in which $3CaO.Al_2O_3$, prepared by heating CaO and Al_2O_3 in stoichiometric amounts at 1350° C for 48 hours and then quenching to room temperature, was held at various temperatures for a period of time and then quenched. X-Ray diffraction patterns for these samples showed that below 1200° C traces of $12CaO.7Al_2O_3$ were formed. When 1% CaF_2 was added, the diffraction lines for $12CaO.7Al_2O_3$ were more intense than in the samples without CaF_2, held at the same temperature and for the same period of time.

When samples of the reaction mixture (calcined dolomite and aluminum) were heated to temperatures beyond 1200° C, both $12CaO.7Al_2O_3$ and $3CaO.Al_2O_3$ appeared, the amount of $3CaO.Al_2O_3$ increasing with longer period of heating.

It is interesting to compare the present results with the aluminum reduction of CaO (12), where $12CaO.7Al_2O_3$ was also obtained rather than $3CaO.Al_2O_3$ for temperatures below 1200° C. Above this temperature, in agreement with the results reported here, $3CaO.Al_2O_3$ was found. It thus appears that $3CaO.Al_2O_3$ disproportionates below 1200° C and that above 1200° C the reaction

$$12CaO.7Al_2O_{3(s)} + 9CaO_{(s)} = 7(3CaO.Al_2O_3)_{(s)}$$

occurs.

In the present case it was concluded that $12CaO.7Al_2O_3$ must be the stable calcium aluminate in equilibrium with CaO at the temperatures of the pressure measurements. The thermodynamic calculations are therefore based on the formation of $12CaO.7Al_2O_3$.

(c) Thermodynamic Considerations

Since the reactions were carried out at temperatures above the melting point of aluminum, some solution of magnesium would be expected. As described previously (1), liquid aluminum at these temperatures can be assumed to form an ideal solution with magnesium. Thus the activity of aluminum can be calculated at each temperature provided the equilibrium vapor pressure of magnesium is known. It was assumed that no solid solution occurred between the solid components; thus the equilibrium constant is written in the form

$$K = P_{Mg}^{21}/a_{Al}^{14}.$$

A "Σ plot" was carried out using the equilibrium constant derived from the experiments and the specific heat functions recommended by Kelley (13). The derived functions are shown in Table II for the over-all reaction.

TABLE II

Thermodynamic functions for the reaction $12CaO_{(s)}+21MgO_{(s)}+14Al_{(l)} = 12CaO.7Al_2O_{3(s)}+21Mg_{(g)}$ in the temperature range 1154–1308° K

ΔC_p	$= -45.49+16.00\times10^{-3}T-5.50\times10^{5}T^{-2}$
ΔH^0_T	$= 909{,}198-45.49T+8.0\times10^{-3}T^2+5.50\times10^{5}T^{-1}$
ΔG^0_T	$= 909{,}198+104.76T\log T-8.0\times10^{-3}T^2+2.75\times10^{5}T^{-1}-908.77T$
$\Delta H^0_{1225°\,K}$	$= +865{,}900$ cal
$\Delta G^0_{1225°\,K}$	$= +180{,}500$ cal
$\Delta S^0_{1225°\,K}$	$= +559.55$ e.u.

Combining the experimental data with the available data on CaO, on Al_2O_3, and on $12CaO.7Al_2O_3$, one obtains for the reaction

$$12CaO + 7Al_2O_3 = 12CaO.7Al_2O_3 \qquad [3]$$

the following data: $\Delta H^0_{298°\,K} = -18{,}500$ cal, and $\Delta S^0_{298°\,K} = 46.31$ e.u.

The entropy value reported by King (14) from low-temperature heat-capacity measurements is 50.6 e.u. Thus the value obtained in the present work is considered satisfactory when taking into account the errors involved in calculations of this type. The free energy of formation of the calcium aluminate from the oxides can be represented by the equation

$$\Delta G^0_T = -18{,}500 - 50.6\ T \pm 1.5 \text{ kcal.}$$

CONCLUSIONS

The reaction between calcined dolomite and metallic aluminum proceeds according to the equation

$$12CaO_{(s)} + 21MgO_{(s)} + 14Al_{(l)} = 12CaO.7Al_2O_{3(s)} + 21Mg_{(g)}$$

in the temperature range 886–1035° C. The corresponding equilibrium pressure of magnesium over this reaction can be represented by the equation

$$\log P_{\text{mm of Hg}} = -(8754/T) + 8.462$$

as determined by means of the transportation method.

ACKNOWLEDGMENT

This investigation has been sponsored by Norsk Metallurgisk Komite, for which the authors are grateful.

REFERENCES

1. L. M. Pidgeon and J. A. King. Discussions Faraday Soc. **4**, 197 (1948).
2. A. Schneider and E. Hesse. Z. Elektrochem. **46**, 279 (1940).
3. T. Rosenqvist and B. Ellingsaeter. J. Metals, **212**, 1111 (1956).
4. A. Yu. Tait. Tsvetnye Metal. **30**, 56 (1957).
5. K. Grjotheim, O. Herstad, and J. M. Toguri. Can. J. Chem. **39**, 443 (1961).
6. ASTM X-ray Powder Data. File 9-413.
7. G. A. Rankin and F. E. Wright. Am. J. Sci. **39**, 1 (1915).
8. W. Bussem and A. Eitel. Z. Krist. **95**, 175 (1936).
9. E. Aruja. Acta Cryst. **10**, 337 (1957).
10. H. E. Swanson, M. I. Cook, T. Isaacs, and E. H. Evans. Natl. Bur. Standards (U.S.), Circ. 539. 1960. p. 9.
11. E. Levin, H. McMurdie, and F. Hall. Phase diagrams for ceramists. Am. Ceram. Soc. Part I. 114 (1956).
12. P. Vignial and J. L. Andrieux. Compt. rend. **242**, 709 (1956).
13. K. K. Kelley. U.S. Bur. Mines, Bull. 584. 1960.
14. E. G. King. J. Phys. Chem. **59**, 218 (1955).

LIGHT ABSORPTION STUDIES

PART XIX. THE ULTRAVIOLET ABSORPTION SPECTRA OF IODOBENZENES[1]

W. F. Forbes

ABSTRACT

As a sequel to previous studies on the ultraviolet absorption spectra of halogen-substituted benzenes the spectra of iodobenzene in various solvents, and the spectra of a series of substituted iodobenzenes in cyclohexane solution, are reported. It is shown that these spectra can be rationalized qualitatively in terms of simple resonance theory, if the apparent mesomeric effect of the iodine atom is assumed to be greater for iodine than for the other halogen atoms.

INTRODUCTION

In previous papers on the ultraviolet spectra of bromobenzenes (1), chlorobenzenes (2), and fluorobenzenes (3), band nomenclature and other terms used were discussed. Since in the present paper the terms employed are identical, no further introduction is required concerning them. The above-mentioned three papers noted generalizations which could be deduced from the spectra, and the purpose of the present paper is to extend and summarize these observations, particularly those concerning the apparent mesomeric order of the halogen atoms, by the study of the ultraviolet absorption spectra of the iodobenzenes.

EXPERIMENTAL

The ultraviolet absorption spectra were determined by standard methods in matched 1-cm silica quartz cells using both a Beckman DK 2 spectrophotometer and a Unicam SP 500 spectrophotometer calibrated against a didymium filter and solutions of potassium chromate and potassium nitrate. Wavelength readings obtained on the two instruments were found to be within 1 mμ of each other. The accuracy of λ_{max} values is estimated to be ± 1 mμ, and the precision of molar absorptivities, $\pm 5\%$ or better. Most molar absorptivity values were reproducible to $\pm 2\%$. The solvents used were spectroanalyzed cyclohexane (Fisher) and other commercially available spectroanalyzed solvents.

The iodobenzenes were mostly commercial materials, purified by distillation or recrystallization until their boiling points and refractive indices or melting points showed them to be sufficiently pure. Some of the iodobenzenes, including iodobenzene itself, decomposed slightly and afforded a limited amount of iodine. The iodine thus liberated was estimated by its absorption maximum near 525 mμ in cyclohexane solution. The amount formed was usually less than 1%. Whenever possible, the iodobenzene spectra were determined under conditions similar to those under which previous spectra in this series had been determined. For each compound at least two independent sets of observations were made. The ultraviolet maxima are listed in Tables I and II. Some of the spectra have previously been described in this series or elsewhere (cf., for example, refs. 4, 5, and 6, and references cited therein).

THE SPECTRUM OF IODOBENZENE

The absorption characteristics of iodobenzene in different solvents are listed in Table I.

Comparison of the ultraviolet spectral data for iodobenzene and other halogen-substituted iodobenzenes (1, 2, 3) shows that the more intense absorption band of iodobenzene, the *B*-band (7), occurs at longer wavelength and with greater absorption

[1]*Manuscript received May 8, 1961.*
Contribution from the Division of Protein Chemistry, C.S.I.R.O., Wool Research Laboratories, Parkville, N.2 (Melbourne), Victoria, Australia.

TABLE I

Main ultraviolet absorption maxima of iodobenzene in various solvents*

Solvent	*B*-band		*C*-band	
	λ_{max}(mμ)	ϵ_{max}	λ_{max}(mμ)	ϵ_{max}
Vapor phase	ca. *219* 224 228	†	ca. *254* 258 264	†
Cyclohexane	ca. *224* 228.5 233.5	*11,000* 15,000 14,000	ca. *248* 253.5 258 ca. *263.5*	*700* 750 800 *700*
Ether	226.5 ca. *230.5*	16,000 *15,250*	252 257 ca. *263*	755 750 *650*
Ethanol	226.5 ca. *230*	13,500 *13,000*	252 257 ca. *262*	725 725 *600*
Water	227	8,000‡	ca. *251* ca. *256* ca. *263*	*650* *600* *500*

*Values in italics represent inflections in this and the subsequent table.
†Intensities not determined.
‡Sodium iodide has a maximum at similar wavelength (226 mμ) in aqueous solution. This maximum, however, is appreciably displaced in ethanolic solution (to 219.5 mμ) and in ether solution (to 248.5 mμ). The iodobenzene *B*-band is therefore not believed to be due to modified iodide ion absorption (cf. ref. 8).

intensity than for other halogen-substituted benzenes. These spectral changes can be interpreted in terms of an apparent mesomeric release of electrons in the order I > Br > Cl > F. Other ultraviolet spectral data (see refs. 1, 2, 3, and 9, and later discussion in this paper) also suggest this order, as do the intensities of the infrared carbonyl bands of halogen-substituted acetophenones (these intensities have been related to mesomeric interaction (10)) and some coupling constants and asymmetry parameters obtained from nuclear quadrupole resonance spectra (11).

On the other hand, it is well known that reactivity and dipole-moment data can best be interpreted by assuming a mesomeric release of electrons in the order F > Cl > Br > I (cf. also refs. 9, 12, and 13, and references cited therein). Other data, which provide information concerning electron density, such as the location and intensities of the ultraviolet *C*-bands and certain solvents effects on spectra (see below), reactivities (14), and ionization potentials (cf. ref. 15), afford various orders for the mesomeric effects of the halogen atoms. The absolute mesomeric order of the halogen atoms therefore remains unknown. In the meantime it may be assumed, as a working hypothesis, that the "apparent mesomeric effect" of the halogen atoms, as indicated by the present ultraviolet spectral data, corresponds to a mesomeric release of electrons in the *electronic excited state* in the order I > Br > Cl > F. The electronic excited state concerned is the state primarily involved in the transitions leading to the *B*-bands of the ultraviolet spectra. On this hypothesis it may be assumed that the net order of release of electrons for the halogens is different in the electronic excited state and in the ground state. The electronic excited state of iodobenzene may be visualized as involving resonance forms of type I, and this simplified resonance picture accounts satisfactorily for a number of the ultraviolet spectral changes.

The *B*-band of iodobenzene shows a characteristic, fine structure in most solvents (see Fig. 1). The wavelength displacement observed between solutions in cyclohexane

and the vapor phase is of the order of 5 mμ (see Table I), which is considerably greater than the corresponding displacements observed for fluorobenzene, chlorobenzene, and bromobenzene (refs. 1, 2, 3; cf. also ref. 16). This observation is consistent with the view that the C—I dipole makes a greater contribution to the relevant electronic excited

I

state of iodobenzene, probably by facilitating solvent orientation, than do the C—F, C—Cl, or C—Br dipoles to the corresponding excited states of the other halobenzenes. This, in turn, is consistent with the resonance picture described above.

Other spectral changes, with change of solvent, are illustrated in Fig. 1. As with bromobenzene and chlorobenzene (1, 2) no appreciable wavelength displacements are

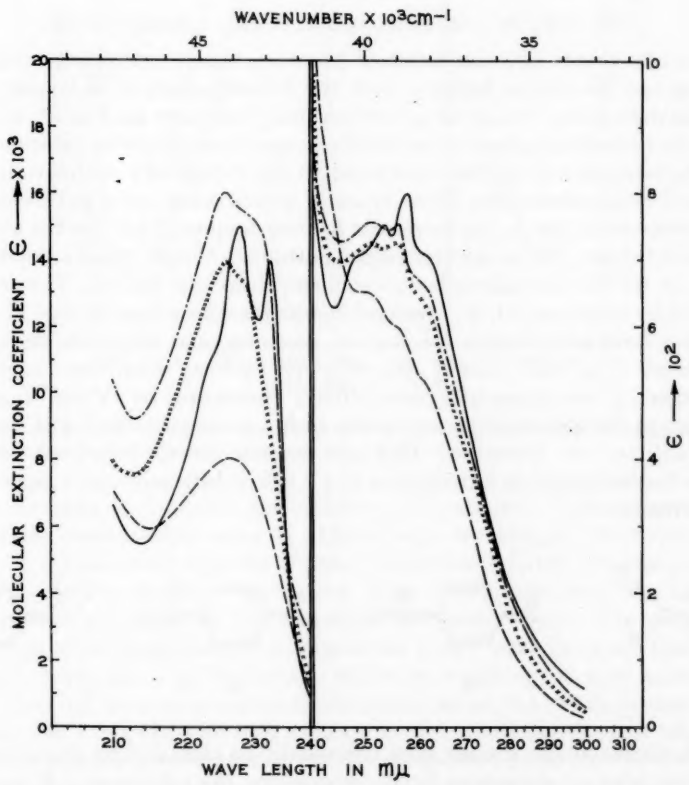

FIG. 1. The ultraviolet absorption spectra of iodobenzene in cyclohexane solution (——), in ether (—·), in ethanol (×××), and in water (— —).

observed on changing the solvent, although the maximal extinction coefficients are decreased in aqueous solution. This decrease, presumably caused by some form of intermolecular hydrogen bonding, appears to be general for halogen-substituted benzenes. Further, the fine structure is decreased in aqueous solution.

The *C*-band of iodobenzene (for band nomenclature used, see ref. 7) is considerably more intense than that of bromobenzene or chlorobenzene. However, in most solvents the band is approximately as intense as that of fluorobenzene (see Fig. 1 and cf. ref. 3). This indicates that the *C*-band of iodobenzene is determined by a combination of electronic interactions different from that used in determining the *B*-band (cf. refs. 13 and 17). Wavelength displacements of the *C*-band for the halogen-substituted benzenes also are not in a definite order with increasing molecular weight of the halogen substituent. However, the *C*-band fine structure in cyclohexane solution becomes progressively less pronounced on passing from fluorobenzene to iodobenzene. For fluorobenzene, the *C*-band fine structure resembles that of benzene (see Fig. 1 of ref. 3), whereas for iodobenzene this is much less pronounced. This may be because the iodo substituent more effectively disturbs the symmetrical vibrations of the benzene ring because of increased mesomeric interactions.

THE SPECTRA OF PARA-SUBSTITUTED IODOBENZENES

As previously noted, in *p*-disubstituted benzenes, where one substituent is electron withdrawing and the other a halogen atom, the *B*-band occurs at its longest wavelength in the iodine derivative. It may be noted that most functions, such as σ^*, σ_p, σ', but not $\sigma_p - \sigma'$, for electron-donating substituents differ in sign from the above-mentioned electron-withdrawing substituents. On the other hand, in the *B*-band of the ultraviolet spectra of *p*-substituted iodobenzenes *both* these types of substituents cause bathochromic wavelength displacements, that is, displacements to lower frequency (cf. also the work reported by Bloor and Copley (18) on spectroscopic constants). Simple valence bond theory can again account for this anomalous behavior in the ultraviolet spectra. This follows since, as illustrated by structure III, an extended dipolar resonance form of type II is no longer favored when both substituents are electron donating, and the molecule consequently tends to absorb to a *locally excited state* with the methoxy substituent exerting only a secondary effect. If resonance structures, crudely represented by IV and V, are assumed to contribute to the electronic excited state, such a secondary effect will, however, still normally facilitate the transition. This can account for the observed bathochromic wavelength displacements on introduction of a *p*-iodo substituent into a monosubstituted benzene derivative.

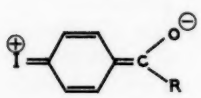

II

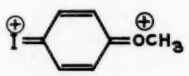

III

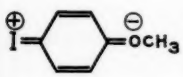

IV

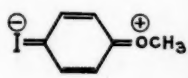

V

The predominant locally excited state can usually be identified by characteristic band features of the relevant absorption band; for example, the iodobenzene *B*-band in cyclohexane solution is a doublet with the twin peaks separated by ca. 5 mμ (see Fig. 1), and this doublet can still be discerned in some of the *p*-substituted iodobenzenes. This is

illustrated in Fig. 2, which shows the absorption spectra of *p*-chloroiodobenzene, *p*-bromoiodobenzene, *p*-diiodobenzene, and iodobenzene, all in cyclohexane solution. The *B*-bands

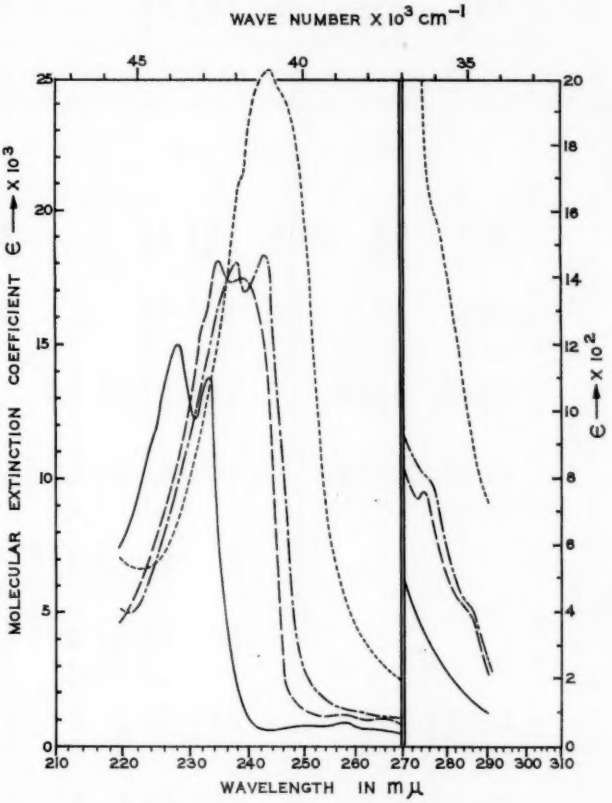

FIG. 2. The ultraviolet absorption spectra in cyclohexane solution of *p*-chloroiodobenzene (— —), *p*-bromoiodobenzene (—·), *p*-diiodobenzene (- -), and iodobenzene (——).

of the four compounds show that the *p*-chloro, *p*-bromo, and *p*-iodo substituents cause the iodobenzene absorption to occur at slightly longer wavelength. Moreover, this secondary effect of a *p*-substituent on the *B*-band absorption of iodobenzene is greater for an iodo than for a bromo or chloro substituent. This secondary effect of the halogen atom thus also follows the order of the apparent mesomeric effects. The maximal molar absorptivity of these *p*-substituted iodobenzenes shows large increases compared with that of iodobenzene (see Fig. 2), the ϵ_{max} values approaching, or even exceeding, those which are observed for *p*-substituted iodobenzenes when the *p*-substituent is electron withdrawing (see Table II). This may indicate a large transition moment which, in turn, suggests that electronic interactions, as crudely represented by structures of type III, and others, are important. Evidence that such structures contribute to the ground or electronic excited state of *p*-substituted iodobenzenes, when both substituents are electron donating, can also be deduced from the *B*-band solvent changes. For example, Fig. 3 shows that the

TABLE II

Main ultraviolet absorption maxima of substituted iodobenzenes in cyclohexane solution*

Sub-stituent	Para isomer				Meta isomer						Ortho isomer					
	B-band		*C*-band		*B*-band		2nd *B*-band		*C*-band		*B*-band		2nd *B*-band		*C*-band	
	λ_{max} (mμ)	ϵ_{max}	λ_{max} (mμ)	ϵ_{max}	λ_{max} (mμ)	ϵ_{max}	λ_{max} (mμ)	ϵ_{max}	λ_{max} (mμ)	ϵ_{max}	λ_{max} (mμ)	ϵ_{max}	λ_{max} (mμ)	ϵ_{max}	λ_{max} (mμ)	ϵ_{max}
—I	ca. *239* 243 ca. *247*	*21,000* 25,500 *24,000*	ca. *268* ca. *277*	*2,600* *1,600*	ca. *224* 228 ca. *232* 237 ca. *242*	*25,000* 31,500 *24,500* 19,000 *12,000*	—	—	260 ca. *269* *276.5* *285.5*	1,250 *1,100* *900* *525*	232 238 ca. *243*	13,000 13,000 *11,000*	—	—	*259* 266 ca. *273*	*1,200* 1,100 *900*
—CH_3	230.5 236	18,000 16,500	258 262 272 281	850 850 725 500	ca. *224* 229 *234*	*10,500* 13,000 *12,000*			256 261 270 278	800 800 700 500	228 233	12,500 12,250			ca. *255* 259 *265* *268* *276*	*750* 765 *700* *680* *500*
—OH	231.5 ca. *236.5*	15,000‡ *12,400*	276.5 283 291.5	1,300 1,450 1,100							224 229	8,300 6,500	218	9,250†	269 276.5 284.5	2,200 3,000 2,800
—OCH_3	234.5 ca. *239*	19,000 *15,800*	276 282 292	1,450 1,600 1,200	ca. *225* 231 ca. *237*	*9,250* 9,500 *6,500*	216	25,500†	271 277.5 285	1,950 2,700 2,550	ca. *229* 232.5 237	*8,700* 10,200 10,000			272 278.5 286	2,400 3,400 3,250
—NH_2	248	19,000	296.5 ca. *315*	1,700 *1,450*	ca. *233* ca. *244*	*10,000*† *8,000*	217 ca. *222*	35,000 *28,500*	294 ca. *302.5*	2,700 *2,200*	238 ca. *245*	8,400 *6,200*			293 ca. *302*	3,200 *2,800*
—$COCH_3$	264	19,500	ca. *278* ca. *280*	*14,500* *10,000*	224	24,500	ca. *246* ca. *251*	*6,800* *6,000*	292.5 302	1,050 950						
—CHO	ca. *268* ca. *276* ca. *283*	*19,500* *16,000* *14,500*	ca. *290*	*4,000*	228	25,000	ca. *242* ca. *251* ca. *256*	*8,000* *7,500* *7,000*	297.5 305	1,300 1,250						
—NO_2	ca. *284* 290.5	*12,500* 13,000	ca. *305*	*8,500*	232	22,500	ca. *257*	*7,500*	*300* 309 ca. *321*	*1,100* 1,200 *800*	230 ca. *235*	14,500 *13,000*	ca. *252*	*5,000*	306	1,750

*The values recorded are those obtained in the present investigations. Frequently, but not always, the data were in good agreement with recent values reported by other workers.
†Band assignment doubtful.
‡Indicates accompanying fine structure near the maximum.

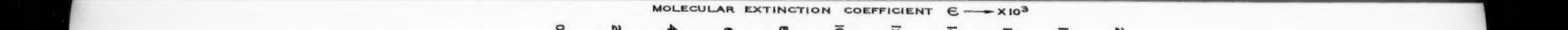

B-band of *p*-iodoanisole is displaced to slightly shorter wavelength, whereas the *B*-band of *p*-iodophenol is displaced to slightly longer wavelength, on passing from cyclohexane to ethanol solution. These displacements are characteristic of anisole and phenol absorption respectively (19, 20) and consequently indicate that the methoxy and hydroxy groups play a part in determining the transition of the relevant *B*-bands.

The *C*-bands of *p*-substituted iodobenzenes frequently show features of the *C*-bands of both the monosubstituted benzene parent compounds. For example, the *C*-bands of

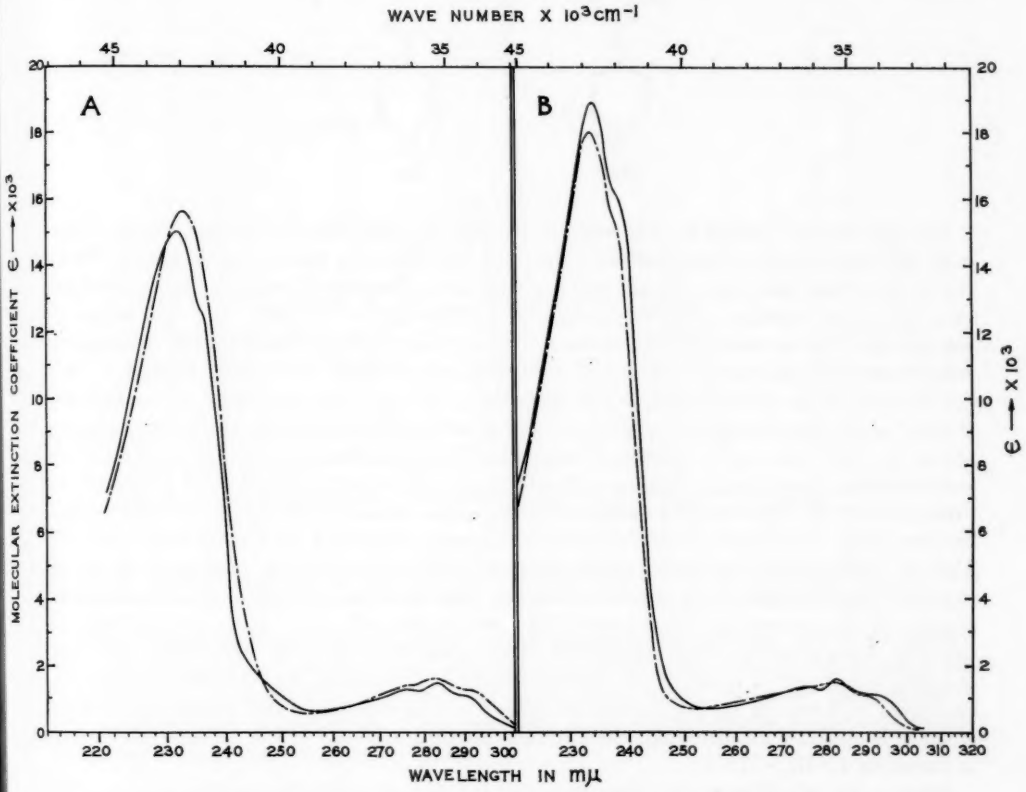

FIG. 3. The ultraviolet absorption spectra of (A) *p*-iodophenol and (B) *p*-iodoanisole in cyclohexane (—) and ethanol (—·) solutions.

p-iodophenol and *p*-iodoanisole (see Fig. 3) are similar to the *C*-bands of both iodobenzene (see Fig. 1) and, with respect to their locations of maximal absorptions, to the *C*-bands of either phenol or anisole (19, 20). However, the *C*-band of the *p*-substituted iodobenzenes generally occurs at longer wavelength than that of either of the two "component" *C*-bands.

THE SPECTRA OF META-SUBSTITUTED IODOBENZENES

The absorption characteristics of *m*-substituted iodobenzenes can again be rationalized in terms of simple resonance theory by observing that no extended dipolar resonance

form can be written. Hence one might expect a *m*-substituted iodobenzene, such as *m*-iodoacetophenone, to exhibit one or both of the *B*-bands corresponding either to iodobenzene or to acetophenone absorption. (The latter band is referred to as the second *B*-band in Table II.) In this way the two *B*-bands of *m*-iodoacetophenone for example, are associated with resonance forms of type VI and VII respectively, with the iodo or acetyl group, respectively, causing only a secondary effect.

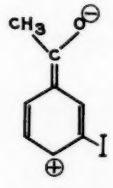

VI

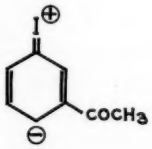

VII

The precise mechanism of this secondary effect remains obscure and appears to vary with different *m*-substituted iodobenzenes, but the following facts may be noted. First, the iodine atom decreases the intensity of the acetophenone absorption (acetophenone in cyclohexane solution absorbs maximally at 238 mμ, ϵ = 12,500), and this effect is paralleled in the decrease of the intensities of the infrared carbonyl bands of the *m*-halogen-substituted acetophenones compared with that of acetophenone (10). Secondly, the substitution of an iodine atom in the *m*-position reduces the ultraviolet acetophenone *B*-band absorption intensity more effectively than does the substitution of other halogen atoms (cf. refs. 1, 2, and 3). Hence, it seems that in the electronic excited state of *m*-iodo-acetophenone, forms which may be such as resonance forms of type VII, are preferred to those of type VI. This may be explained if the iodine atom, by *donating* electrons to the benzene ring, facilitates the electronic excited state involving structures such as VII. Also on passing from *m*-fluoroacetophenone to *m*-iodoacetophenone, resonance forms of type VII may be assumed to be more and more favored and this is reflected in the intensification of the absorption band associated with halobenzene absorption and the simultaneous diminution of that associated with acetophenone. The secondary spectral changes, occurring in some of the *m*-substituted iodobenzenes, can therefore again be explained in terms of simple resonance theory if it is assumed that, where the *m*-substituent is electron withdrawing, the electron-releasing abilities of the halogen atoms are in the order I > Br > Cl > F.

When both substituents in a *m*-substituted iodobenzene are electron donating as, for example, in *m*-chloroiodobenzene, the iodobenzene *B*-band intensity appears to be slightly reduced relative to the absorption intensity of iodobenzene. This also applies to the *B*-band of *o*-chloroiodobenzene, but not to *p*-chloroiodobenzene, since in the latter *B*-band the iodobenzene absorption clearly predominates (see Fig. 4). This is presumably because interactions associated with resonance forms of type VIII are sufficiently important in *p*-chloroiodobenzene to cause a predominance of iodobenzene *B*-band absorption.

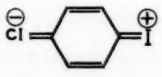

VIII

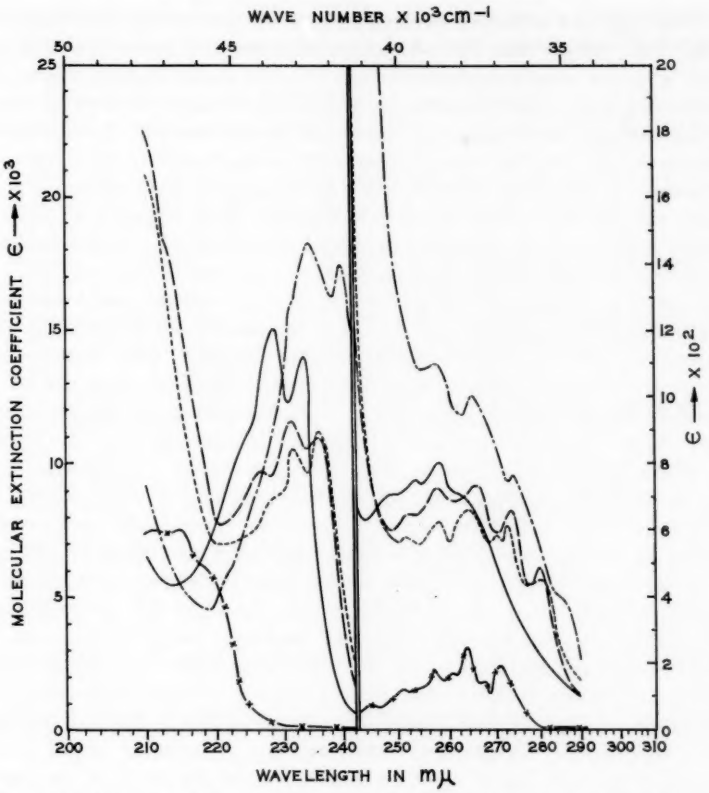

FIG. 4. The ultraviolet absorption spectra in cyclohexane solution of *m*-chloroiodobenzene (— —), *o*-chloroiodobenzene (- -), *p*-chloroiodobenzene (—·), iodobenzene (——), and chlorobenzene (—×).

The *C*-bands of *m*-substituted iodobenzenes appear to be additive as a first approximation, that is, the observed *C*-band approximates to the sum of the two *C*-bands of the corresponding monosubstituted benzenoid parent compounds. However, the *C*-band of the *m*-substituted iodobenzenes is also generally displaced to slightly longer wavelength (see, for example, the *C*-bands in Fig. 4).

THE SPECTRA OF ORTHO-SUBSTITUTED IODOBENZENES

It is well known that the *B*-bands of a number of *o*-disubstituted benzene derivatives frequently resemble the *B*-bands of the corresponding *m*-isomer, that is, two *B*-bands are often observed corresponding to the *B*-bands of the two monosubstituted benzene derivatives. The reason why electronic excitation should occur to locally excited states rather than to so-called electron-transfer states, as symbolized by resonance forms of type IX, is obscure.

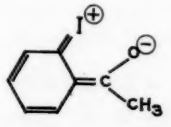

IX

Steric interactions are certainly evident from a number of spectral and other data. Ungnade (21) has shown that for *o*-halonitrobenzenes the band near 260 mμ occurs as a shoulder only for *o*-iodonitrobenzene and that its molar absorptivity at 260 mμ is the smallest among the *o*-halonitrobenzenes if the iodine absorption is taken into account. This band near 260 mμ corresponds to nitrobenzene absorption and its decreased intensity may be taken to imply that the *o*-iodo substituent twists the nitro group out of the plane of the benzene ring and thus inhibits the nitrobenzene *B*-band absorption. In other examples also, the "second" *B*-band of *o*-halogen-substituted benzene derivatives, if well defined, is least intense in the *o*-iodosubstituted compound (cf. ref. 22; for evidence of steric interactions in *o*-substituted iodobenzenes see also refs. 23, 24, and 25).

The spectrum of *o*-iodophenol, compared with that of *o*-iodoanisole, does not suggest intramolecular hydrogen bonding in the former compound, although there is evidence that weak intramolecular hydrogen bonding exists (26, 27). This therefore represents an example of an intramolecular hydrogen bond which does not give rise to a spectral change characteristic of hydrogen bonding (i.e. bathochromic wavelength displacement accompanied by an intensity increase) in the main ultraviolet maxima. It emphasizes the caution which is required before the lack of an ultraviolet spectral change is used to show the absence of intramolecular hydrogen bonding. One of the reasons why some intramolecular hydrogen bonds do not give rise to appreciable ultraviolet spectral changes is that a molecule may absorb to locally excited states which do not involve the part of the molecule which contains the intramolecular hydrogen bond (cf. ref. 28).

It may next be noted that in *o*-substituted halobenzenes the iodobenzene *B*-band, like the bromobenzene *B*-band (1), frequently no longer occurs, or occurs only with reduced absorption intensity. Moreover, in compounds such as *o*-iodonitrobenzene, a hypsochromic wavelength displacement also occurs relative to the *B*-band maxima in the corresponding *m*-isomers (see Table II). These spectral changes suggest steric interactions involving the iodobenzene chromophore. A possible explanation of the spectral changes is that the iodine atom is dislodged from the plane of the benzene ring in such a way that certain interactions between the π-orbitals of the benzene ring and the pseudo π-orbitals of the iodine atom are no longer possible.

The *C*-band in *o*-substituted iodobenzenes, on the other hand, sometimes occurs with decreased and sometimes with increased absorption intensity (see Table II). It has already been suggested (see the section on the spectrum of iodobenzene) that increased mesomeric interaction gives rise to a less pronounced *C*-band and this can account for the *C*-band changes in *o*-substituted iodobenzenes. That is, steric interactions may tend to inhibit mesomeric interaction between the substituents and the benzene ring, and this partial inhibition of mesomeric interaction may cause the frequently observed intensity increase of the *C*-band relative to the intensity of the *C*-band of the *m*-isomer (see, for example, the *C*-band of *o*-iodoaniline in Table II). As steric interactions become large, however, the interaction between the chromophores, which initially gives rise to the characteristic *C*-band, tends to be completely inhibited and the *C*-band intensity now *decreases* towards the intensity value observed in the *C*-band of the isolated benzene molecule (see, for example, the *C*-band of *o*-iodotoluene in Table II and also ref. 29). The hypothesis therefore predicts that steric interactions may either increase or decrease the *C*-band intensity of *o*-substituted iodobenzenes.

ACKNOWLEDGMENTS

The author is indebted to Miss V. R. Jellett for the careful determination of the ultraviolet spectral data. Some of the spectra have been determined at the Memorial

University of Newfoundland by Mr. J. C. Dearden, assisted by Miss Florence Jackman, in preparation for his Ph.D. thesis; the author is indebted to Mr. Dearden for making these data available.

Grateful acknowledgment for financial assistance in support of that part of these studies which was carried out in Canada is made to the National Research Council.

REFERENCES

1. W. F. Forbes. Can. J. Chem. **39**, 1131 (1961).
2. W. F. Forbes. Can. J. Chem. **38**, 1104 (1960).
3. W. F. Forbes. Can. J. Chem. **37**, 1977 (1959).
4. W. M. Schubert, H. Steadly, and J. M. Craven. J. Am. Chem. Soc. **82**, 1353 (1960).
5. W. M. Schubert and J. M. Craven. J. Am. Chem. Soc. **82**, 1357 (1960).
6. L. Goodman and L. J. Frolen. J. Chem. Phys. **30**, 1361 (1959).
7. W. F. Forbes and R. Shilton. *In* Symposium on spectroscopy—STP 269. ASTM (1959). p. 176.
8. F. M. Beringer and I. Lillien. J. Am. Chem. Soc. **82**, 5135 (1960).
9. V. Baliah and M. Uma. Naturwissenschaften, **45**, 512 (1958).
10. W. F. Forbes and W. A. Mueller. Can. J. Chem. **35**, 488 (1957).
11. W. G. Laurita and W. S. Koski. J. Am. Chem. Soc. **81**, 3179 (1959).
12. H. Shimizu, M. Katayama, and S. Fujiwara. Bull. Chem. Soc. Japan, **32**, 419 (1959).
13. J. Ferguson and T. Iredale. J. Chem. Soc. 2959 (1953).
14. R. W. Taft, Jr. J. Phys. Chem. **64**, 1805 (1960).
15. F. Meda. Spectrochim. Acta, **13**, 75 (1958).
16. J. C. Dearden and W. F. Forbes. Can. J. Chem. **38**, 896 (1960).
17. W. W. Robertson and F. A. Matsen. J. Am. Chem. Soc. **72**, 5252 (1950).
18. J. E. Bloor and D. B. Copley. Chem. & Ind. (London), 526 (1960).
19. J. C. Dearden and W. F. Forbes. Can. J. Chem. **37**, 1294 (1959).
20. J. C. Dearden and W. F. Forbes. Can. J. Chem. **37**, 1305 (1959).
21. H. E. Ungnade. J. Am. Chem. Soc. **76**, 1601 (1954).
22. H. E. Ungnade. J. Am. Chem. Soc. **76**, 5133 (1954).
23. S. Brownstein. J. Am. Chem. Soc. **80**, 2300 (1958).
24. J. Ferguson and T. Iredale. J. Chem. Soc. 2959 (1953).
25. G. H. Beaven and D. M. Hall. J. Chem. Soc. 4637 (1956).
26. D. A. K. Jones and J. G. Watkinson. Chem. & Ind. (London), 661 (1960).
27. A. W. Baker and W. W. Kaeding. J. Am. Chem. Soc. **81**, 5904 (1959).
28. J. C. Dearden and W. F. Forbes. Can. J. Chem. **38**, 1837 (1960).
29. E. Baciocchi and G. Illuminati. Ricerca sci. **26**, 3040 (1956).

THE ELECTRONIC SPECTRA OF $MoCl_5$ AND $NbCl_5$[1]

RICHARD F. W. BADER AND ALAN D. WESTLAND

ABSTRACT

The visible and ultraviolet spectra of $MoCl_5$ and $NbCl_5$ have been investigated in both the vapor state and solution. The number of bands observed indicates that a Jahn–Teller effect may be operative in the $^2E'$ state of $MoCl_5$.

INTRODUCTION

Early electron diffraction studies have indicated that, in the gas phase, both molybdenum and niobium pentachloride possess trigonal bypyramid structures (1, 2). The resulting D_{3h} symmetry produces an interesting splitting of the 4*d* metal orbitals in these compounds, the interest of which is enhanced by the fact that the single 4*d* electron present in the $MoCl_5$ molecule should bring about a Jahn–Teller distortion of the nuclear framework in both the ground and first excited states. For these reasons we have undertaken a complete spectroscopic investigation of $MoCl_5$ and $NbCl_5$. The results for the visible and ultraviolet regions are given here; the infrared investigations will be reported shortly.

A simple application of group theory shows that, in the crystalline field of the five halide ions, the 4*d* atomic orbitals of the metal ion are split into two sets of orbital doublets (e'' and e') and into an orbital singlet (a_1'). Furthermore, crystal-field calculations by Ballhausen and Klixbüll Jørgensen (3) have shown that the order of the orbital levels is $\bar{a}_1' > \bar{e}' > e''$, i.e., the e'' orbital is the most stable, as shown in Fig. 1 (the

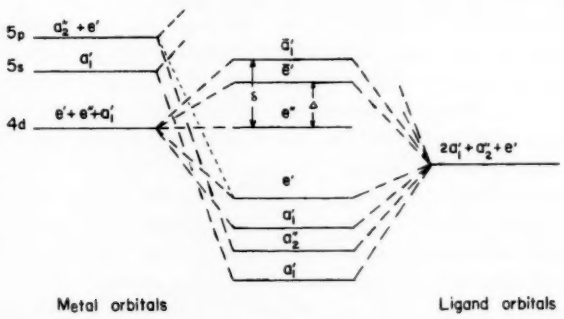

FIG. 1. The ligand field splitting diagram for a trigonal bipyramid molecule.

d–d orbital separations are designated by Δ and δ as shown). Also shown in the same figure are the ligand molecular orbitals for an MX_5 complex. It is seen that the five bonding σ molecular orbitals of the ligands are of symmetries a_1', a_2'', and e'. Thus, of the *d* orbitals, only those of a_1' (d_{z^2}) and e' ($d_{x^2-y^2}$, d_{xy}) symmetry may participate in the σ-bonding with the ligand molecules, corresponding to the fact that their antibonding combinations (designated by a bar) are raised in energy over that of the e'' (d_{xz}, d_{yz})

[1]*Manuscript received July 3, 1961.*
Contribution from the Department of Chemistry, University of Ottawa, Ottawa, Canada.

orbital. This electronic description may be related to the d^3sp configuration of Pauling.* The electronic structure of the metal ions is $Kr(4d)^n$, giving ground electronic states of $^1A_1'$ for Nb(V) ($n = 0$) and $^2E''$ for Mo(V) ($n = 1$, the single $4d$ electron will occupy the e'' orbital).

The theorem of Jahn and Teller (4) states that a non-linear molecule which possesses a spatial degeneracy in a symmetrical configuration will have an equilibrium configuration of some lower symmetry in which the electronic degeneracy has been lost. Therefore, both the ground electronic state of $MoCl_5$ (with one electron in the e'' orbital) and the first excited state (with one electron in the e' orbital) should exhibit Jahn–Teller distortions. (The electronic spectrum of $NbCl_5$, which possesses a closed shell structure identical with that of the molybdenum compound, was investigated as well to determine the character of the charge transfer bands and hence aid in the assignment of the d–d transitions.)

The Jahn–Teller effect represents a breakdown of the Born–Oppenheimer approximation, for it introduces an intimate coupling of certain of the nuclear motions with the electronic angular momentum, leading to the formation of vibronic states in which the concept of a potential surface has been lost.

The static problem (12) leading to the distortion may be treated as a first-order splitting of the electronic degeneracy by certain of the vibrational motions of the molecule. Which of the vibrational motions will provide such a perturbation is again best determined by the methods of group theory. The structure of the vibrational representation of a trigonal bipyramid is

$$\Gamma_{vib} = 2A_1' + 3E' + 2A_2'' + E''.$$

The only motions which resolve the degeneracy of the $^2E''$ and $^2E'$ electronic states are the three vibrations of E' symmetry. (Only the direct products of species $\Gamma_{E'}$ with $\Gamma_{E''}{}^2$ and $\Gamma_{E'}{}^2$ contain the identity representation aside from the identity representation itself.)

The representation of D_{3h} spanned by the even harmonics of order less than five contains the identity representation three times ($n = 0, 2, 4$). Therefore, the non-spherically symmetric crystal-field contribution to the Hamiltonian has the form

$$H_c = \Sigma_i(A Y_{20} + B Y_{40}) \qquad [1]$$

and in the general case two sets of constants A and B will be required, one set for the axial ligands and another for the equatorial ligands. The Y_{nm} are the usual spherical harmonics. Terms with m values different from zero do not appear in [1] due to the trigonal arrangement of the three ligands in the plane. The matrix of this perturbation will obviously have no off-diagonal elements in the $|l,m\rangle$ basis of the $4d$ orbitals. The orbitals are simply split into two doublets $|2,2\rangle,|2,-2\rangle(e')$, and $|2,1\rangle,|2,-1\rangle(e'')$ and into the singlet $|2,0\rangle$ (a_1'). We may thus conveniently employ the same basis functions to derive the Jahn–Teller splittings with the perturbation of required E' symmetry given by

$$H_{E'} = \Sigma_i[Y_{2\pm2}R_2(r_i) + Y_{4\pm4}R_4(r_i)]Q \qquad [2]$$

where Q is a normal co-ordinate of E' symmetry. It is easily seen that there are no diagonal

*The $5p_z$ and $5p_y$ metal orbitals may also participate to some extent in σ-bonding with the three equatorial ligands as indicated by the light dashed line joining the $5p$ and e' levels in Fig. 1. A trigonal bipyramid may also be formed using the dsp^3 orbitals of the metal. Thus there are in this case a total of seven orbitals (no more than three of them d orbitals) of proper symmetry to participate in the σ-bonding in an MX_5 molecule.

elements of this perturbation; there are only off-diagonal ones, between $|2,2\rangle$ and $|2,-2\rangle$, which are mixed under $Y_{4\pm4}$, and between $|2,1\rangle$ and $|2,-1\rangle$, which are mixed under $Y_{2\pm2}$. (The perturbation $H_{E'}$ will also mix in some of the $|2,0\rangle$ state with the $|2,\pm2\rangle$ states but this can be ignored because of the large energy separation between the two sets of states and, furthermore, it does not change the form of the results.) If we let the matrix elements $\langle l,m \mid H_{E'} \mid l,-m^* \rangle$ have the values kQ and $k'Q$ for $|m| = 1$ and 2 respectively, then the eigenvalues of the two perturbation problems combined with the harmonic restoring force $\frac{1}{2}KQ^2$ are

$$V = \tfrac{1}{2}KQ^2 \pm kQ \qquad \text{for the } E'' \text{ state,}$$

$$V = \tfrac{1}{2}KQ^2 \pm k'Q \qquad \text{for the } E' \text{ state.}$$

This shows that both the E'' and E' states are resolved under the influence of the E' vibrations and that the nuclear potential function is split into two branches. A plot of either value of V versus Q leads to a double cone potential surface with the potential minimum at $Q = k/K$ (or k'/K) as illustrated in the paper by Longuet-Higgins, Öpik, Pryce, and Sack (5). The nuclear motions of E' symmetry are shown in Fig. 2. The E'

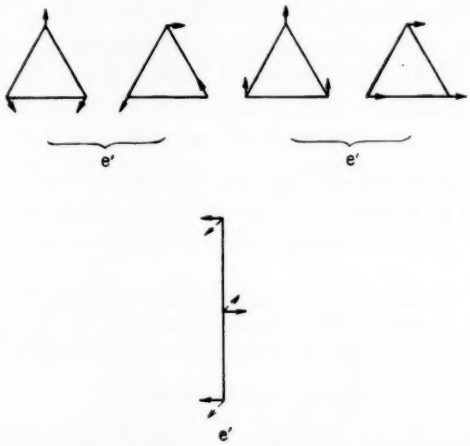

FIG. 2. The nuclear motions of E' symmetry for a trigonal bipyramid molecule.

vibrations will be combinations of these motions, the exact forms of which can only be deduced when the forms of the normal vibrations are known. One of the possible distortions is shown in Fig. 3. It is seen that the result is a lowering of the symmetry to C_{2v} which removes the degeneracy of all the levels.

Molybdenum is from the second transition series; therefore, one cannot overlook the possibility of a strong spin–orbit coupling upsetting the Jahn–Teller effect. As we point out in the Discussion, while we are confident that a large Jahn–Teller effect will be present in the first excited state due to the occupation of the e' antibonding orbital, the spin–orbit coupling may quite easily be of sufficient strength to prevent a distortion from occurring in the ground state where the degeneracy arises from the e'' non-bonding orbital. We restrict the following analysis then, to the $|\pm1\rangle$ states, but actually a similar treatment with corresponding results holds for the $|\pm2\rangle$ kets.

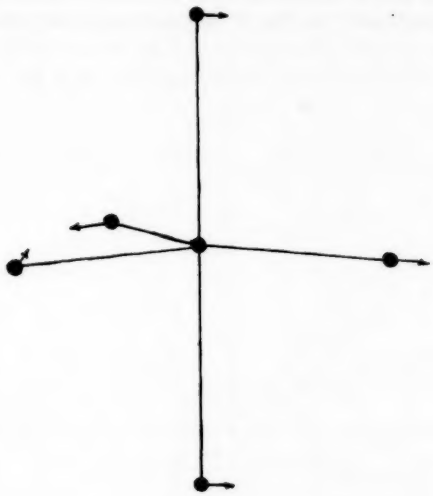

FIG. 3. A possible E' vibrational distortion of a trigonal bipyramid molecule.

In the absence of spin–orbit interactions, the ground state $^2E''$ is fourfold degenerate, $|\pm 1, \pm\frac{1}{2}\rangle$ (in the $|m_l, m_s\rangle$ notation). Spin–orbit coupling alone will result in the formation of two Kramers spin doublets, the degeneracy of which cannot be removed by any electrostatic field. We now investigate the problem of the simultaneous operation of a spin–orbit coupling and a Jahn–Teller effect of comparable magnitude. The secular matrix of the operator

$$H' = H_E' + \lambda \bar{L} \cdot \bar{S}$$

is

$$\begin{array}{c|cc|} & |\pm 1, \pm\frac{1}{2}\rangle & |\mp 1, \pm\frac{1}{2}\rangle \\ \hline \langle \pm 1, \pm\frac{1}{2}| & \frac{1}{2}\lambda & kQ \\ \langle \mp 1, \pm\frac{1}{2}| & kQ & -\frac{1}{2}\lambda \\ \hline \end{array} . \qquad [3]^*$$

The roots of the corresponding secular equation are (each root occurs twice as all the levels are still Kramers doublets)

$$E = \pm\tfrac{1}{2}(\lambda^2 + 4k^2Q^2)^{\frac{1}{2}}.$$

To obtain the total potential V, we add the harmonic restoring force $\frac{1}{2}KQ^2$ to these roots and obtain

$$V_\pm = \tfrac{1}{2}KQ^2 \pm \tfrac{1}{2}(\lambda^2 + 4k^2Q^2)^{\frac{1}{2}}.$$

Notice that, for $Q = 0$, the spin–orbit coupling has removed the degeneracy of the pairs of states on which the Jahn–Teller effect operates, i.e., $|+1, \frac{1}{2}\rangle$ is now an amount λ above $|-1, +\frac{1}{2}\rangle$ and similarly $|-1, -\frac{1}{2}\rangle$ is an amount λ above $|+1, -\frac{1}{2}\rangle$. The

*The $\bar{L} \cdot \bar{S}$ perturbation will introduce small admixtures of the $|0, \pm\frac{1}{2}\rangle$ states into the $|\pm 1, \mp\frac{1}{2}\rangle$ states and $|\pm 2, \mp\frac{1}{2}\rangle$ into the $|\pm 1, \pm\frac{1}{2}\rangle$ states. The coefficients of these admixtures will be small as they are determined by the ratios $\sqrt{\frac{1}{2}}\lambda/\delta$ and λ/Δ. Furthermore, their inclusion will not change the form of the results.

relative magnitudes of λ and k now determine two possibilities for the forms of V_+ and V_-. These are shown graphically in Fig. 4. Regardless of the relative values of λ and k,

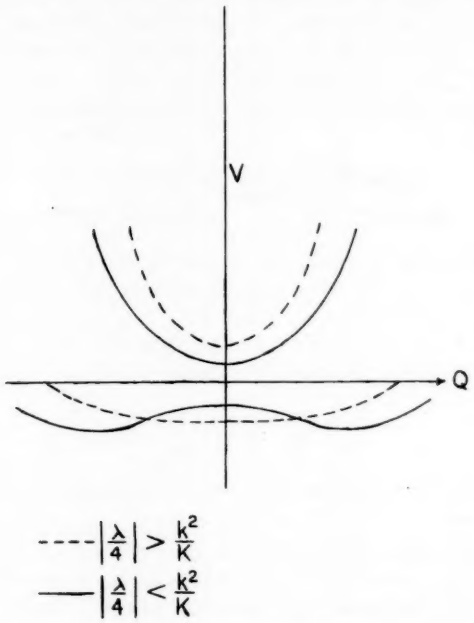

FIG. 4. The splitting of the fourfold degenerate potential level by spin–orbit and Jahn–Teller effects of comparable magnitude. In the text the upper curves are termed V_+ and the lower ones V_-.

the upper level in each case has but one minimum at $Q = 0$. However, the lower level may have two minima at values of $Q \neq 0$, or only one minimum at $Q = 0$, depending on the relative magnitudes of k^2/K and $|\lambda/4|$. Thus, when $k^2/K > |\lambda/4|$ and the Jahn–Teller effect is overriding, the molecule will distort even though the two levels are no longer degenerate but possess only a "near degeneracy". However, as λ is increased, a point is reached when the near degeneracy is, in a manner of speaking, no longer near enough and the Jahn–Teller distortion disappears. This will occur when $|\lambda/4| > k^2/K$. Thus, an absolute degeneracy is not necessary for the operation of the Jahn–Teller effect (12); a near degeneracy, if it fulfills the analytic requirement given above, will suffice. The analysis also shows that a sufficiently strong spin–orbit coupling will effectively quench a Jahn–Teller distortion. Jahn (14) has previously shown that a symmetrical configuration may be stabilized by large spin forces.

RESULTS

The visible and ultraviolet spectra of $MoCl_5$ and $NbCl_5$ vapors were obtained with a Beckmann DK-2 spectrophotometer using a 10-cm all-quartz cell which could be heated to the necessary temperatures (60–100° C).* The spectra of the two pentachlorides were also investigated in the infrared region, on a Perkin–Elmer single beam, double pass

*NOTE ADDED IN PROOF: *M. Gloor and K. Wieland (Helv. Chim. Acta, 44, 1098 (1961)) recently obtained a spectrum for* $NbCl_5$ *between the range 22,000–40,000 cm^{-1} which agrees with ours.*

instrument from 4000 to 723 cm^{-1}. A Perkin–Elmer prism grating instrument was employed to search the region from 2,500 to 12,000 cm^{-1} for the $MoCl_5$ compound. The visible and ultraviolet spectrum of $MoCl_5$ is shown in Fig. 5, and the positions of the observed band maxima for both compounds are listed in Table I. The band shown at

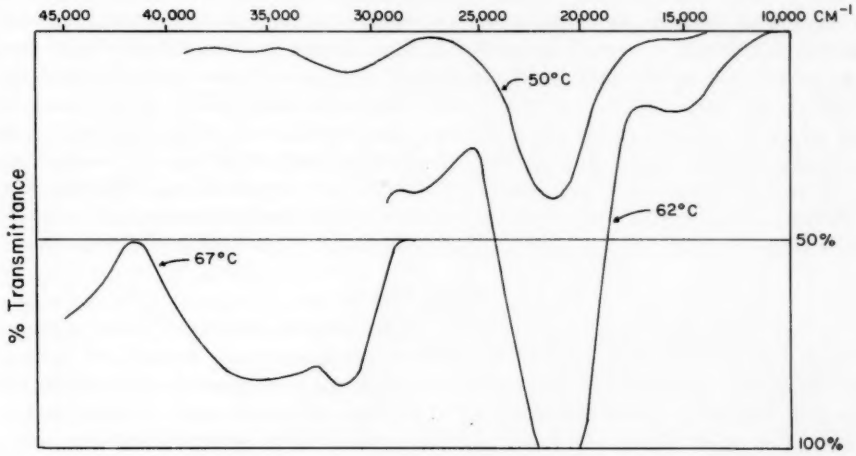

FIG. 5. The visible and ultraviolet spectrum of $MoCl_5$.

TABLE I

The visible and ultraviolet absorption bands of $MoCl_5$ and $NbCl_5$ and their extinction coefficients

$MoCl_5$		$NbCl_5$	
ν_{max} (in cm^{-1})	$\epsilon(\times 10^{-4})$ (l. $mole^{-1}$ cm^{-1})	ν_{max} (in cm^{-1})	$\epsilon(\times 10^{-4})$ (l. $mole^{-1}$ cm^{-1})
1,009	0.1		
15,200	0.4		
21,300	2.		
27,800	*		
35,700	2	35,100	1
42,600†	1	41,700†	1

*The extinction coefficient for this band cannot be accurately determined as the band occurs on the tail of the chlorine gas absorption. It is by far the least intense of all the bands.

†These bands occur just before the cutoff point of the instrument. The values entered in the table give the wavelength at the ½-peak height.

31,000 cm^{-1} in the spectrum of $MoCl_5$ was shown to be due to chlorine gas. The same band appeared to a lesser extent in the spectrum of $NbCl_5$ at higher temperatures. The dissociation of $MoCl_5$ in the gas phase according to the equation

$$2(MoCl_5)_{gas} \rightleftarrows 2(MoCl_4)_{solid} + Cl_2$$

has been investigated by Vasilkova and Sharupin (6). The result of heating molybdenum pentachloride is to produce chlorine gas at pressures comparable with those of the pentachloride itself. Apparently a similar decomposition occurs to a lesser extent in the case

of niobium pentachloride. Unfortunately, all the bands are broad and exhibit no vibrational structure. An initial attempt was made to record the spectrum of molybdenum pentachloride on an Hilger E2 spectrograph to obtain a high resolution spectrum. However, no detail was observed.

Spectra were also obtained for the two pentachlorides in solution. The solution spectrum of $MoCl_5$ in cyclohexane and carbon tetrachloride in the visible was unchanged from that of the gas phase but the band in the ultraviolet region was intensified. The solution spectrum of $NbCl_5$ in carbon tetrachloride was completely changed from that found in the gas phase. A very intense band appeared at 475 mμ and more intense absorption was found in the ultraviolet region. This is an interesting observation in that both $MoCl_5$ and $NbCl_5$ are known to exist as dimers in the solid state (7, 8) in the form of double octahedra having a common edge. We believe that, in solution, the dimerization persists in the case of the niobium compound but not in the case of the molybdenum. Further evidence to support this view was obtained from a reflection spectrum of the solid $NbCl_5$, which gave the same intense band at 475 mμ as found in the solution of this compound.*

DISCUSSION

The expected consequences of the Jahn–Teller effect on electronic spectra have been discussed by Longuet-Higgins *et al.* (5). These consequences are twofold. In cases where the vibrational structure of the transitions is resolved a progression in the distorting E' vibration should be observed along with the regular progression in the symmetrical modes. The Jahn–Teller effect, by lowering the effective symmetry of the molecule, breaks down the otherwise rigorous selection rule prohibiting single (or odd number) changes in the E' vibrational quantum number during a transition. The same authors have given the expected band shapes for transitions to Jahn–Teller degenerate states from a non-degenerate state for different values of the distortion parameter k in the cases where only one distorting vibration is allowed. Unfortunately neither of these more elaborate analyses may be carried out in the present case for, as noted above, the bands are very broad and exhibit no vibrational structure. However, we feel that the observed spectrum does indicate a large Jahn–Teller splitting in the first excited state of molybdenum pentachloride. In its simplest terms, the Jahn–Teller effect resolves the degeneracy of an orbital doublet and leads to the appearance of two maxima in the electronic spectrum, where but one would be observed in its absence. Longuet-Higgins *et al.* (5) have discussed how such a double maximum may be roughly interpreted in terms of the Franck–Condon principle. In a transition from a non-degenerate to a degenerate state, the molecule may arrive on either branch of the double cone potential surface referred to previously. Different amounts of vibrational energy will be involved in each case depending on which possibility is the most favorable. Such a situation will lead to a double maximum in the absorption spectrum. In the present case the lowest transition is from one degenerate state to another (the lowest state may well not be Jahn–Teller active because of the spin–orbit coupling). In the degenerate ground state the molecule will, if k (or λ) is of any reasonable magnitude at all, be in the neighborhood of the potential

**The infrared spectrum of niobium pentachloride in carbon disulphide solution was obtained by Gaunt and Ainscough (9) and the assignments so obtained were put forward as proof of the trigonal bypyramidal structure for this compound. We think that their results are not meaningful in this connection as an investigation of the ultraviolet spectrum of a carbon disulphide solution of the niobium pentachloride gave a spectrum radically different from that in the gas phase and different again from that found in carbon tetrachloride. Solution of the niobium compound in carbon disulphide leads to the formation of an intense yellow-orange solution as opposed to the pale yellow solution obtained in carbon tetrachloride, or the pale yellow color of the solid itself. We will report more fully on this point in the infrared investigation of these two pentachlorides.*

minimum with a well-defined nuclear configuration. Thus its transition to the degenerate excited state should give the appearance noted above for a transition from a non-degenerate (where again the ground state is in a well-defined configuration) to a doubly degenerate state. The intensities of the two bands at 15,200 and 21,300 cm^{-1} denote them as allowed, as expected for the E'–E'' transitions. Although the energy separation between the two band maxima of approximately 6000 cm^{-1} cannot be related in any simple way to the value of k', it does suggest a large distortion in the E' state. A very large distortion would also lead to the appearance of two maxima as it would correspond to a permanently distorted molecule of C_{2v} symmetry where the E' state has been split into two new states of B_1 and A_1 symmetries. It should be recalled that the $\bar{e}'$ orbital is a strongly antibonding one and thus a large splitting should be expected just as is observed in the cases of octahedral molecules exhibiting Jahn–Teller effects arising from occupation of the antibonding e_g orbitals. The $\bar{e}'$ orbitals point directly at the ligands in the plane and thus the electrostatic forces exerted on the ligands by an electron in the $\bar{e}'$ orbital will be quite large.

The splitting in the ground state due to the occupation of the e'' orbital will be small as this orbital is directed away from all of the ligands and is not involved in any σ bonding with the ligands. Thus the electrostatic repulsions exerted by the electron density in this orbital will be of much smaller magnitude. The same small splitting is also encountered in octahedral molecules when the degeneracy arises from the occupation of the t_{2g} orbitals as is evidenced by the so far unsuccessful search for distortions in these cases. In fact, there may not be any Jahn–Teller distortion in the ground state due to the presence of a strong spin–orbit coupling. As was pointed out in the Introduction, the spin–orbit interactions cause a splitting of the ground state potential function into two curves (V_+ and V_-) separated in energy by $(\lambda^2 + 4k^2Q^2)^{\frac{1}{2}}$. We suggest that the infrared band observed at 1009 cm^{-1} is due to a transition from V_- to V_+. We base the assignment on the following considerations. First, niobium pentachloride has no corresponding band and thus it is unlikely that the 1009 cm^{-1} band is due to a vibrational motion. Second, the value of λ for the Mo^{+4} ion is 887 cm^{-1} (11) and the value for Mo^{+5} should be somewhat larger. Such a value of λ, coupled with the contribution due to the $4k^2Q^2$ term, would place the band in the observed frequency range. In fact, the theoretical analysis of the spin–orbit coupling effect prompted our search for a band in this region.

The observation of a transition from V_- to V_+ does not necessarily imply the absence of a Jahn–Teller effect in the ground state of $MoCl_5$. As pointed out in the Introduction, k^2/K may still be larger than $|\lambda/4|$ and thus a distortion should still occur. This final question can only be answered by a complete investigation of the infrared spectra of $MoCl_5$ and $NbCl_5$ to see if any indications of band splittings can be determined in the former case. This work, together with a more detailed analysis of the 1009 cm^{-1} band, is now in progress.

The band found at 27,800 cm^{-1} which is superimposed on the tail of the strong absorption due to Cl_2 is assigned to the A_1'–E'' transition, an assignment which is consistent with the low intensity of this particular absorption. Unfortunately, the chlorine gas absorption interferes with this band and no detail beyond its presence may be obtained. The remaining bands at 35,700 and 42,600 cm^{-1} are attributed to charge transfer processes. These assignments are very reasonable because of their observed intensity, short wavelength, and similarity in these properties to the corresponding bands observed for niobium pentachloride (at 35,100 and 41,700 cm^{-1}), which possesses no d–d transitions.

The crystal-field splitting in a trigonal bipyramid molecule involves two parameters if

the five ligands are assumed to lie equidistant from the metal atom. In a simplified approach these may be related to the G_2 and G_4 (for the ionic case) or B_2 and B_4 (for the dipole case) parameters of Ballhausen (10). As in the octahedral cases, neither of these parameters will be determined entirely by simple electrostatic effects but must be interpreted as empirical separations determined by both the electrostatic interactions and the covalent bonding effects of the ligands. We have evaluated the integrals G_2 and G_4 for 4*d* hydrogen-like atomic orbitals to determine their ratio in a rough attempt to justify the above spectroscopic assignments by showing that they can be calculated from reasonable values of the parameters. Assuming the splitting to be linear in Q in the E' state, the mean of the two zero–zero levels in the E'–E'' transition is at approximately 13,500 cm^{-1}. This gives a ratio of the A_1'–E'' to the E'–E'' energy separations ($= \delta/\Delta$) of approximately two. The electron diffraction data for the $MoCl_5$ molecule gave an average over the five bond lengths as 2.27 Å (1). If all five chlorides are assumed to be equidistant from the metal ion, the δ/Δ ratio comes out in the neighborhood of 4.5, i.e., much too large. This discrepancy becomes even larger if it is assumed that the two axial ligands lie closer to the metal ion than do the three ligands in the plane. For example, an axial ligand to metal distance of 2.27 Å and an equatorial – metal ligand distance of 2.40 Å give a δ/Δ energy ratio of 6.6. However, it was found that any shortening of the equatorial bond length or any lengthening of the axial bond length pushes the energy ratio in the desired direction. In fact, an equatorial–metal bond length of 2.15 Å together with an axial–metal bond length of 2.40 Å (which averages to the observed value) gives the observed energy ratio of $\delta/\Delta = 2$. This shortening of the bonds in the plane and the lengthening along the axis in this empirical approach to adjusting the parameters would be equivalent to differing amounts of covalent bonding in the two directions. The apparent increase in bonding found for the equatorial ligands over that for the axial ligands can be related to the fact that the $5p_x$ and $5p_y$ metal orbitals may also contribute to the σ-bonding in the former case. Extra σ-bonding contributions to the axial ligands could only arise from the participation of much higher lying metal orbitals and thus be of little relative significance. It is interesting to note that in the trigonal bipyramid molecules for which all the bond lengths are accurately known, the equatorial bonds are shorter than the axial ones, as is predicted by the present fitting of the observed spectrum. We do not, of course, ascribe this inequality to any Jahn–Teller distortion.

The absorptions in the regions of 1000, 20,000, and 28,000 cm^{-1} are, therefore, reasonably assigned to *d*–*d* transitions. The appearance of the double maximum in the intermediate band is consistent with a Jahn–Teller splitting of the E' state.

The low-lying band implies a spin–orbit splitting of the ground state, with or without an accompanying Jahn–Teller distortion.

EXPERIMENTAL

Molybdenum pentachloride which was obtained commercially was analyzed gravimetrically and used without further purification. Anal. Calc.: Mo, 35.78%; Found: 35.74, 35.80%.

Niobium pentachloride was prepared from the oxide by the procedure of Schäfer and Pietruck (13) and purified by vacuum sublimation. The materials were handled exclusively under rigorously dried nitrogen.

In order to ascertain whether there was any interference from oxychlorides, a substance having the composition $MoOCl_3$ was prepared by controlled hydrolysis and its ultraviolet and infrared spectra determined. Cyclohexane used for the solution spectrum

was purified by passage through a column of silica gel and subsequent distillation from an excess of $MoCl_5$. The carbon tetrachloride and carbon disulphide were commercial spectral grade products.

REFERENCES

1. R. V. G. EWENS and M. W. LISTER. Trans. Faraday Soc. **34**, 1358 (1938).
2. H. A. SKINNER and L. E. SUTTON. Trans. Faraday Soc. **36**, 668 (1940).
3. C. J. BALLHAUSEN and C. KLIXBÜLL JØRGENSEN. Kgl. Danske Videnskab. Selskab, Mat.-fys. Medd. **29** (14), (1955).
4. H. A. JAHN and E. TELLER. Proc. Roy. Soc. A, **161**, 220 (1937).
5. H. C. LONGUET-HIGGINS, U. ÖPIK, M. H. L. PRYCE, and R. A. SACK. Proc. Roy. Soc. A, **244**, 1 (1958).
6. S. A. SHCHUHAREV, I. V. VASILKOVA, and B. N. SHARUPIN. J. Gen. Chem. U.S.S.R. **26**, 2335 (1956).
7. D. E. SANDS and A. ZALKIN. Acta. Cryst. **12**, 723 (1959).
8. D. E. SANDS and A. ZALKIN. Acta. Cryst. **11**, 615 (1958).
9. J. GAUNT and J. B. AINSCOUGH. Spectrochim. Acta, **10**, 52 (1957).
10. C. J. BALLHAUSEN. Kgl. Danske Videnskab. Selskab, Mat.-fys. Medd. **29** (4), (1954).
11. J. S. GRIFFITH. The theory of transition metal ions. Cambridge University Press, Cambridge. 1961.
12. U. ÖPIK and M. H. L. PRYCE. Proc. Roy. Soc. A, **238**, 425 (1957).
13. H. SCHÄFER and C. PIETRUCK. Z. anorg. u. allgem. Chem. **264**, 2 (1951).
14. H. A. JAHN. Proc. Roy. Soc. A, **164**, 117 (1938).

NOTES

THE N.M.R. SPECTRUM OF CYCLOPENTANONE

F. A. L. ANET

The high-resolution proton nuclear magnetic resonance (N.M.R.) spectrum of cyclopentanone has been stated (1, 2) to consist of a single line at 25 and 40 Mc/sec. Wiberg and Nist (3) have recently reported that at 60 Mc/sec cyclopentanone in carbon tetrachloride gave rise to a closely spaced doublet and concluded that the chemical shift between the α and β protons was very small. By comparison of the spectrum with that expected from an A_2B_2 system (4), these authors also concluded that the coupling constants were abnormally small (< 2.4 c.p.s.). However, this cannot be considered valid, as cyclopentanone is an example of an A_4B_4 system (4) or, by Corio's definition (5), an $AA'A''A'''BB'B''B'''$ system. Analysis as an A_2B_2 system would only be correct if the coupling constants between the vicinal β protons were all zero, which is highly unlikely.

The spectrum of cyclopentanone has been re-examined at 60 Mc/sec and it was observed that although the main band of the spectrum is a (rough) doublet, as reported by Wiberg, the spectrum is actually unsymmetrical, unlike that of an A_2B_2 system (4, 5). There are also a number of weak lines, not previously observed, at an appreciable distance from the main doublet. These lines are not due to impurities or spinning side bands, nor can they be ascribed to protons on C^{13}. Their presence shows that relatively large coupling constants must be present in cyclopentanone. That large coupling constants are present is shown even more clearly by the spectrum of cyclopentanone in benzene solution (Fig. 1). Now there is quite an appreciable chemical shift between the α and β protons and the spectrum is no longer even approximately a doublet.

Unfortunately, a complete analysis of the spectrum of cyclopentanone would be extremely tedious. As well as one (relative) chemical shift there are six different coupling constants to be determined, apart from the probably negligible 1,3-coupling constants. Nevertheless, it is possible to extract some information by the application of the moment method described by Anderson and McConnell (6). In a molecule, such as cyclopentanone, which has protons in only two different chemical environments, the moment method gives particularly simple results for the relative chemical shift ($\Delta\nu$) and for the sum of the squares of the coupling constants between *chemically shifted* protons. If M_2, M_3, and M_4 are respectively the reduced second, third, and fourth moments (i.e. moments taken from an origin where the first moment is zero) and J_{cis} and J_{trans} are the two different coupling constants between vicinal α and β protons, then the following expressions hold (6):

$$\nu = 2\sqrt{M_2},$$

$$J_{cis}^2 + J_{trans}^2 = \frac{M_4 - M_2^2}{M_2},$$

$$M_3 = 0.$$

Calculations on the spectrum in Fig. 1 and on a number of other spectra taken at

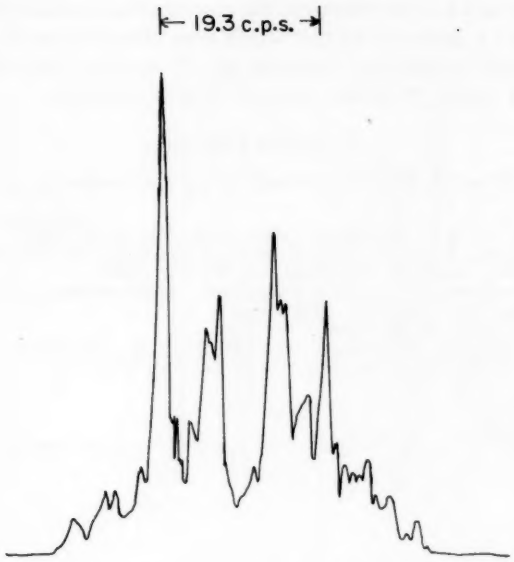

FIG. 1. N.M.R. spectrum of a 20% by volume solution of cyclopentanone in benzene. The magnetic field increases from left to right.

different sweep rates gave, for 20% by volume solutions of cyclopentanone in benzene, $\Delta\nu = 19.5\pm0.5$ c.p.s. and $(J_{cis}^2+J_{trans}^2)^{1/2} = 10.8\pm1.0$ c.p.s. In a solution containing equal volumes of cyclopentanone, benzene, and carbon tetrachloride, $\Delta\nu = 10.8\pm0.5$ c.p.s. and $(J_{cis}^2+J_{trans}^2)^{1/2} = 10.1\pm1.0$ c.p.s. Thus, as expected, the coupling constants do not vary appreciably on the changing of the solvent. One of these coupling constants must be larger than 6 c.p.s. and could be as large as 10 c.p.s. Correspondingly the other coupling constant must be smaller than 8 c.p.s. and could be zero. These values are entirely consistent with the coupling constants in flexible, five-membered rings (7). The fact that the spectrum of Fig. 1 is unsymmetrical and is much too complicated for an A_2B_2 system shows that the coupling constants between vicinal β protons must also have appreciable values.

EXPERIMENTAL

Spectra were measured on a Varian V-4302 high-resolution spectrometer. Care was taken to obtain a pure absorption mode and the radio-frequency power was set well below saturation level so as to obtain correct intensities. To calculate moments a millimeter grid was superposed on the spectrum, and the intensities (as measured by the heights) at small intervals, usually 1 mm, were measured from an arbitrary zero outside the spectrum. Depending on the case, from 60 to 120 readings were made. These values were fed to a computer (I.B.M. 650) which was programed to calculate M_2, M_3, and M_4. Calculations were made on a number of spectra with both increasing and decreasing magnetic fields and with various sweep rates.

The cyclopentanone (Eastman Kodak pure grade) showed only a single band on gas chromatography with a silicone oil column at 134°. The spectrum was unchanged after

the cyclopentanone had been purified via the recrystallized semicarbazone derivative. At high sensitivity and r.f. power no further bands were observed on the side of the spectrum of Fig. 1 except bands assignable to protons on C^{13}. Spectra taken in pyridine or aniline solutions were very similar to those taken in benzene solution.

ACKNOWLEDGMENT

I wish to thank Miss O. Boshko for setting up the computer program.

1. H. PRIMAS, K. FREI, and H. H. GÜNTHARD. Helv. Chim. Acta, **41**, 35 (1958).
2. J. D. ROBERTS. Nuclear magnetic resonance. McGraw-Hill Book Co., New York. 1959. p. 57.
3. K. B. WIBERG and B. J. NIST. J. Am. Chem. Soc. **83**, 1226 (1961).
4. J. A. POPLE, W. G. SCHNEIDER, and H. J. BERNSTEIN. High-resolution nuclear magnetic resonance. McGraw-Hill Book Co., New York. 1959. Chap. 6.
5. P. L. CORIO. Chem. Revs. **60**, 383 (1960).
6. W. A. ANDERSON and H. M. MCCONNELL. J. Chem. Phys. **26**, 1496 (1957).
7. N. SHEPPARD and J. J. TURNER. Proc. Roy. Soc. A, **252**, 506 (1959).

RECEIVED JULY 10, 1961.
DEPARTMENT OF CHEMISTRY,
UNIVERSITY OF OTTAWA,
OTTAWA, ONT.

PROTON RESONANCE SPECTRA OF 8-HYDROXY AND 8-METHYL QUINOLINE

L. W. REEVES AND K. O. STRØMME

The present study is a comparison of the behavior of 8-hydroxy and 8-methyl quinoline in various nonpolar solvents. The part played by the hydroxyl proton in the intermolecular associations of 8-hydroxy quinoline is of some interest in view of its importance as a chelating agent.

EXPERIMENTAL

8-Hydroxy quinoline of analytical grade was recrystallized and 8-methyl quinoline was used as analytical grade. The solvents were all fractionally distilled and stored over drying agents. A 40 Mc/s Varian spectrometer was used to take spectra, and the 'sideband technique' was used to determine peak positions. Absolute chemical shifts on the cyclohexane scale are accurate to ± 1.0 c.p.s. but internal chemical shifts are accurate to ± 0.2 c.p.s. A 1% cyclohexane internal standard was always included in the solution.

RESULTS

Chemical shifts of the hydroxyl proton and the α, β, and γ protons of the hetero ring have been measured. The hetero ring protons formed an ABX or AMX group (1), and some overlap occurred in most cases between the β-proton spectrum and the spectrum of the second aromatic ring. Chemical shifts in the second aromatic ring were very similar and the main feature was a large, single peak with several small satellites. It was always possible to assign transitions in the β-proton spectrum and thus obtain a complete analysis for the ABX or AMX spectrum.

To illustrate this, Fig. 1(a) shows a spectrum of 18.6 mole% 8-hydroxy quinoline in

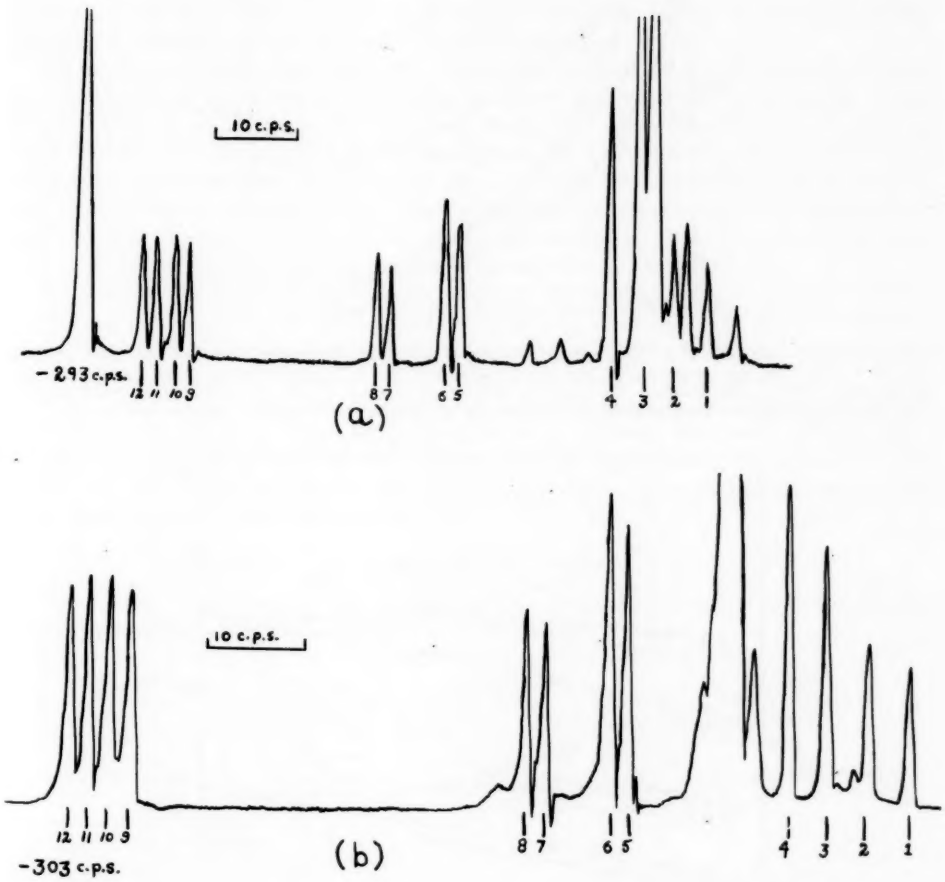

FIG. 1. (*a*) 8-Hydroxy quinoline, 18.6% in CCl_4; spectrum at 30° C. (*b*) 8-Methyl quinoline, pure; spectrum at 30° C.

CCl_4 and Fig. 1(*b*) shows a spectrum of pure 8-methyl quinoline with the methyl peak at high field omitted. The 12 transitions of the *ABX* spectrum are numbered according to the assignments of Bernstein, Schneider, and Pople (1) in each case. Figure 2 gives the results of dilution chemical shifts in CCl_4, benzene, and acetone for the hydroxyl proton resonance. Figure 3 indicates the dilution chemical shifts of the α, β, and γ protons for 8-hydroxy and 8-methyl quinoline in the various solvents and at the conditions given in the legend to this figure. The indirect spin–spin coupling constants evaluated were the same in all spectra analyzed. These were $|J_{\beta\gamma}| = 8.3$ c.p.s, $|J_{\alpha\beta}| = 4.4$ c.p.s., and $|J_{\alpha\gamma}| = 1.7$ c.p.s.

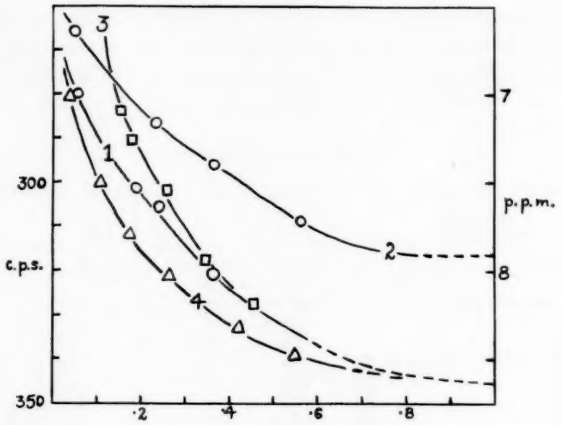

FIG. 2. Chemical shifts of —OH proton resonance of 8-hydroxy quinoline in various solvents: curve 1 (○), in CCl_4 at 29° C; curve 2 (○), in CCl_4 at 80° C; curve 3 (□), in acetone at 29° C; curve 4 (△), in benzene at 29° C. The abscissa of each point is the mole fraction of 8-hydroxy quinoline in the solvent and the ordinate is the chemical shift with respect to an internal cyclohexane standard.

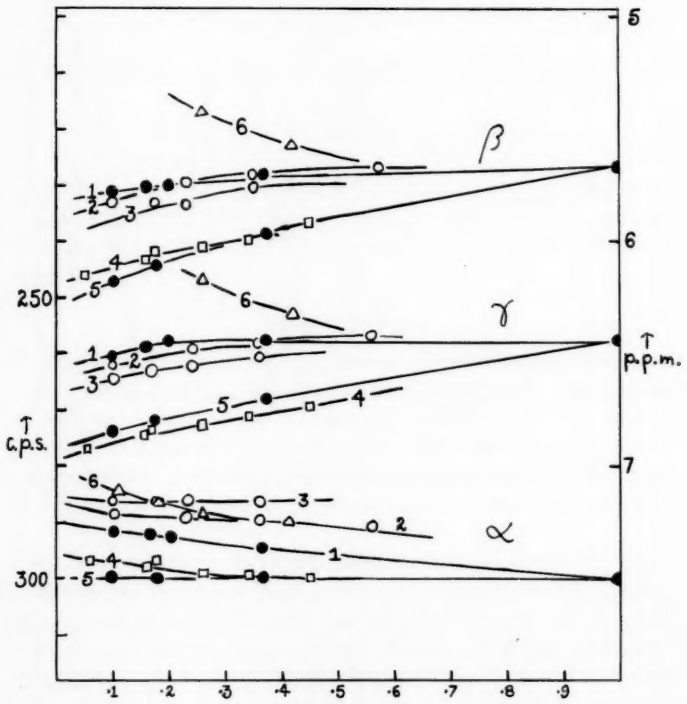

FIG. 3. Chemical shifts of α, β, and γ ring protons as a function of quinoline derivative; solvent and temperature with respect to concentration: curve 1 (●), 8-methyl quinoline in CCl_4 at 29° C; curve 2 (○), 8-hydroxy quinoline in CCl_4 at 80° C; curve 3 (○), 8-hydroxy quinoline in CCl_4 at 29° C; curve 4 (□), 8-hydroxy quinoline in acetone at 29° C; curve 5 (●), 8-methyl quinoline in acetone at 29° C; curve 6 (△), 8-hydroxy quinoline in benzene at 28° C.

DISCUSSION

The shape of the dilution chemical shift curves for the 8-hydroxy quinoline OH proton is indicative of exclusively intermolecular hydrogen bonding (2, 3). The estimation of interatomic distances would indicate little interaction within the same molecule between the hydroxyl proton and the nitrogen on the second ring (4).

The behavior of the hetero ring proton resonances of 8-methyl and 8-hydroxy quinoline is very similar in the same solvents (Fig. 3). There is a small shift to low field for the β and γ protons and to high field for the α proton in carbon tetrachloride solutions at room temperature. An increase in temperature of 50° C for the 8-hydroxy quinoline in CCl_4 solutions causes a low-field shift for the β and γ proton consistent with the concentration dependence of these shifts. The approximate extrapolation of these chemical shifts to mole fraction = 1 and 0 indicates a total shift of less than 10 c.p.s. in all cases. The small temperature coefficient amounted to only 2 c.p.s. in 50° C.

The direction of these chemical shift changes is the same in acetone solutions but the magnitude of the change is much larger for the β and γ protons. The dilution chemical shifts in benzene are in the direction of high field for all three protons in the hetero ring but again the magnitude of shifts is much larger for the β and γ protons.

These results are suggestive of preferential hydrogen bonding of solvent molecules at the β and γ positions in view of the fact that they represent difference shifts between cyclohexane and quinoline in the same solvent (5). The magnitude of the difference shifts due to van der Waals, anisotropy effects, and polar effects are probably comparable and difficult to estimate with any certainty (6).

ACKNOWLEDGMENTS

The support of the Research Corporation and the National Research Council of Canada is gratefully acknowledged.

1. H. J. Bernstein, J. A. Pople, and W. G. Schneider. Can. J. Chem. **35**, 65 (1957).
2. C. M. Huggins, G. C. Pimentel, and J. N. Shoolery. J. Chem. Phys. **23**, 311 (1956).
3. L. W. Reeves, E. A. Allan, and K. O. Strømme. Can. J. Chem. **38**, 1249 (1960).
4. Interatomic Distances. Spec. Publ. No. 11. Chemical Society, London.
5. T. Schaeffer and W. G. Schneider. J. Chem. Phys. **32**, 1224 (1960).
6. A. D. Buckingham, T. Schaeffer, and W. G. Schneider. J. Chem. Phys. **32**, 1227 (1960).

Received June 22, 1961.
Department of Chemistry,
University of British Columbia,
Vancouver, B.C.

CHEMICAL CONSTITUENTS OF CHICOZAPOTE*

E. Azpeitia, A. Bowers, P. Crabbé, O. Mancera, J. S. Matthews, J. Reynoso, and J. Salazar

The "chicozapote", *Achras sapota* L. of the Sapotaceae family, is a common tree of tropical regions of America, growing mainly in Brazil, Colombia, Guatemala, Honduras, Mexico, Peru, and Venezuela (1). Although the sapotilla tree or chicle tree (chicle from the original Maya word *sicté*) is well known since it constitutes the only source of natural

*This work constitutes a part of the undergraduate theses submitted by E. A. and J. R. to the Universidad Nacional Autónoma de México, and by J. S. to the Escuela Nacional de Ciencias Biólógicas.

chewing gum, little work has been done on the chemical constitution of the latex of this tree. This latex, also called "crude chicle" or "loaf chicle", is obtained by collecting the liquid exuded from the bark of *Achras sapota* L.

Stillwell, in an X-ray study of chicle (2), concluded that the latex was a mixture of gutta-percha, calcium oxalate monohydrate, and a resinous fraction. Schlesinger and Leeper have shown (3) that this gutta-percha was a mixture of cis and trans polyisoprenes. On the other hand, Lifschutz and Vietmeyer, by extraction of chicle with ethanol, obtained (4) a fraction which they called "isophytosterol" because of the similar behavior of this extract to color reactions with "isocholesterol", later identified as a mixture of lanosterol, agnosterol, and their side-chain dihydro analogues.

This paper reports the preliminary results of an investigation of the alcoholic extracts of chicle from different sources. Ethanol extraction with a Soxhlet of a crude chicle from Guatemala led to the isolation, in about 55% yield, of a yellow resin which crystallized spontaneously on standing. Although repeated crystallizations did not afford a pure compound, extensive chromatography over alumina, followed by several recrystallizations, led to the isolation and identification of two pentacyclic triterpenes and a steroid, namely lupeol acetate, β-amyrin acetate, and α-spinasterol acetate, in approximate yields of 70, 10, and 2–5% respectively.

These three compounds were purified rigorously, hydrolyzed to the corresponding 3β-alcohols, and then further characterized as their benzoates. Each derivative was compared with an authentic sample of the known compound (mixed melting point and infrared spectrum). The physical constants are listed in Table I.

TABLE I

Compound	Melting point		Optical rotation	
	This work	Literature value	This work	Literature value
Lupeol	213–215	215–216*	+27	+27*
Acetate	219–220	220*	+42	+47*
Benzoate	262–264	273–274*	+66	+61*
β-Amyrin	198–199	199–200†	+85	+89†
Acetate	239–241	241†	+82	+85†
Benzoate	233–235	233–234†	+105	+100†
α-Spinasterol	169–170	168–169‡	+2	−4‡
Acetate	183–184	186‡	−4	−5‡
Benzoate	196–197	200‡	+2	+2‡

*J. Simonsen and W. C. J. Ross. The terpenes. Vol. IV. Cambridge University Press. 1957. p. 331.
†J. Simonsen and W. C. J. Ross. The terpenes. Vol. IV. Cambridge University Press. 1957. p. 175.
‡L. F. Fieser, M. Fieser, and R. N. Chakravarti. J. Am. Chem. Soc. 71, 2226 (1949).

It is worth mentioning that α-spinasterol (Δ^7-stigmasterol or bessisterol) seems to be a more common steroid than suspected earlier (5). Besides spinach (6), *Polygala senega* roots (7), alfalfa (*Medicago sativa* L.) (8), and the rhizomes of *Mormordica cochinchinensis* Spreng. (9), this Δ^7-steroid has been identified recently in *Iresin pringlei* (10) and in *Chenopodium foetidum*, which also contains cineol and a very small amount of a ketone which seems to correspond to piperitenone (2,4-dinitrophenylhydrazone, m.p. 188–189°; calc. for $C_{16}H_{18}O_4N_4$: N, 16.96; found: N, 17.37) (11).

Another crude chicle, from Campeche, Mexico, was found to be a complex mixture; the major constituents, however, again were lupeol acetate and β-amyrin acetate. Interestingly enough, in this chicle no α-spinasterol could be identified.

The recent development of gas chromatography techniques in the steroid (12), alkaloid (13), and fatty- (14) and amino-acids (15) fields prompted us to apply this method to our chicle mixture. For comparison purposes, authentic samples of the pentacyclic triterpenes and the Δ^7-steroid were chromatographed using this technique, which was later applied to the crude crystalline chicle. Those compounds were analyzed on a Barber-Colman Model 10 gas chromatograph with an argon, β-ray ionization detector and a 6 ft$\times\frac{1}{4}$ in. column containing 1% QF-1 silicone (Vanden Heuvel, Haahti, and Horning (12)) on Gas-Chrom P (16) at 240° C. The retention times, in minutes, measured from the air peak were: α-spinasterol, 3.57; β-amyrin, 3.93; lupeol, 4.64; α-spinasterol acetate, 5.24; β-amyrin acetate, 6.31; lupeol acetate, 7.15. Chicle from Campeche, Mexico, was found to consist of approximately 79% of lupeol acetate, 12% of β-amyrin acetate, together with some unidentified components. The retention time of lupeol acetate on a 6 ft$\times\frac{1}{4}$ in. column of 1.5% SE-30 (Vanden Heuvel, Sweeley, and Horning (12)) on Gas-Chrom P at 240° was 3 minutes. The main component of chicle also had the same retention time.

Work is now in progress to determine the structure of some of the minor constituents in chicle.

1. M. Martinez. Las plantas medicinales de Mexico. *Edited by* Botas. Mexico. 1944. p. 386.
2. C. W. Stillwell. Ind. Eng. Chem. **23**, 703 (1931).
3. W. Schlesinger and H. M. Leeper. Ind. Eng. Chem. **43**, 398 (1951).
4. I. Lifschutz and O. Vietmeyer, Z. Physiol. Chem. **155**, 240 (1926).
5. L. F. Fieser and M. Fieser. Steroids. Reinhold Publishing Co., New York. 1959. p. 352. See also: Elsevier's Encyclopaedia of organic chemistry. Vol. 14. Elsevier Publishing Co., Amsterdam. 1954. Suppl. p. 1794.
6. M. C. Hart and F. W. Heyl. J. Biol. Chem. **95**, 311 (1932).
7. J. C. E. Simpson. J. Chem. Soc. 730 (1937).
8. H. Dam, A. Geiger, J. Glavind, P. Karrer, W. Karrer, E. Rotschild, and H. Salomon. Helv. Chim. Acta, **22**, 310 (1939). E. Fernholtz and M. L. Morre, J. Am. Chem. Soc. **61**, 2467 (1939).
9. S. Kuwada and S. Yosiki. J. Pharm. Soc. Japan, **60**, 407 (1940).
10. P. Crabbé, E. Azpeitia, and C. Djerassi. Bull soc. chim. Belg. **70**, 168 (1961).
11. P. Crabbé and E. Azpeitia. Unpublished observation.
12. R. K. Beerthuis and J. H. Recourt. Nature, **186**, 372 (1960). W. J. A. Vanden Heuvel, C. C. Sweeley, and E. C. Horning. J. Am. Chem. Soc. **82**, 3481 (1960). H. Ziffer, W. J. A. Vanden Heuvel, E. O. A. Haahti, and E. C. Horning. J. Am. Chem. Soc. **82**, 6411 (1960). H. H. Wotiz and H. F. Martin. J. Biol. Chem. **236**, 1312 (1961). W. J. A. Vanden Heuvel, E. O. A. Haahti, and E. C. Horning. J. Am. Chem. Soc. **83**, 1513 (1961).
13. H. H. Lloyd, H. M. Fales, P. F. Highet, W. J. A. Vanden Heuvel, and W. C. Wildman. J. Am. Chem. Soc. **82**, 3791 (1960).
14. M. L. Vorbeck, L. R. Mattick, F. A. Lee, and C. S. Pederson. Nature, **187**, 689 (1961).
15. D. E. Johnson, S. J. Scott, and A. Meister. Anal. Chem. **33**, 669 (1961).
16. Applied Science Laboratories, 140 North Barnard Street, State College, Penna.

Received July 7, 1961.
Research Laboratories,
Syntex. S. A.,
Apartado Postal 2679,
Mexico, D. F., Mexico.

Symposium on Co-ordination in Chemistry

The papers that follow were presented at the Symposium on Co-ordination in Chemistry, Inorganic Subject Division, Chemical Institute of Canada, held at McMaster University, Hamilton, Ontario, May 15, 16, 1961.

CO-ORDINATION COMPOUNDS OF HYDRAZINE

PART II. THE INTERACTION OF TRIMETHYLBORANE AND TRIMETHYLALUMINUM WITH HYDRAZINE[1, 2]

W. G. PATERSON[3] AND M. ONYSZCHUK

ABSTRACT

Trimethylborane and anhydrous hydrazine react at 25° in vacuum, yielding a 2:1 adduct, $2(CH_3)_3B \cdot N_2H_4$, which is stable at or below −78° and evolves trimethylborane slowly at higher temperatures, leaving a stable 1:1 adduct, $(CH_3)_3B \cdot N_2H_4$ (m.p. 42–43°). The thermal decomposition of the latter at 150–160° is complex, producing nitrogen, methane, ammonia, a mixture of butane and the isomeric butenes, and a heterogeneous solid. At 25° diborane displaces trimethylborane from the 1:1 adduct and reacts with it to form 1,1-dimethyldiborane, in addition to hydrogen, methane, and a heterogeneous solid.

Trimethylaluminum and hydrazine give a complex reaction in vacuum at 25°, but in diethyl ether solution the product was thought to be $(CH_3)_2AlNHNHAl(CH_3)_2$, which decomposes on being touched.

Recently (1) we reported that under appropriate conditions boron trifluoride, like the borane group (2, 3), forms stable 1:1 and 2:1 addition compounds with hydrazine, $BF_3 \cdot N_2H_4$ and $2BF_3 \cdot N_2H_4$, respectively. With the object of obtaining further information about the tendency of hydrazine to co-ordinate with other electron-deficient molecules, we have investigated the reactions of hydrazine with trimethylborane and trimethylaluminum. Since the electron-acceptor powers of trimethylborane and trimethylaluminum are considerably less than those of boron trifluoride or of the borane group (4, 5), hydrazine should form less stable adducts with trimethylborane or trimethylaluminum than with boron trifluoride or with the borane group. The results reported here confirm this expectation.

RESULTS AND DISCUSSION

The interaction of trimethylborane and hydrazine in vacuum at 25° produced the new co-ordination compound 2-trimethylborane-hydrazine (I), $2(CH_3)_3B \cdot N_2H_4$. This adduct was stable either in the presence of an excess of trimethylborane or at temperatures below −78°; otherwise, trimethylborane was evolved ultimately, leaving the new stable addition compound trimethylborane-hydrazine (II), $(CH_3)_3B \cdot N_2H_4$, which melted at 42–43°. By being allowed to react with an excess of trimethylborane, adduct II was converted into I, as represented by the following scheme:

$$2(CH_3)_3B + N_2H_4 \rightarrow 2(CH_3)_3B \cdot N_2H_4 \quad \text{I}$$

$$> -78° \quad \Big\downarrow\Big\uparrow \quad \text{excess } (CH_3)_3B$$

$$(CH_3)_3B + (CH_3)_3B \cdot N_2H_4.$$

$$\text{II}$$

[1]*Manuscript received June 30, 1961.*

Contribution from the Inorganic Chemistry Laboratory, McGill University, Montreal 2, Quebec, with financial assistance from the Defence Research Board of Canada, under Grant Number 9530-20, Project D46-95-30-20. Presented at the Symposium on Co-ordination in Chemistry, Chemical Institute of Canada, Hamilton, Ontario, May 15–16, 1961.

[2]*Part I: Can. J. Chem.* **39**, *986 (1961).*

[3]*Holder of N.R.C. Studentships, 1957–59. Present address: Department of Chemistry, University of Alberta, Edmonton, Alberta.*

These results suggest that the attraction exerted by trimethylborane on the lone electron pair of one nitrogen atom in the 1:1 adduct induces a significant decrease in the co-ordinating ability of the lone electron pair on the other nitrogen atom. This reduced reactivity of the second lone electron pair in hydrazine appears to be a general rule (6). The instability of I as compared with the analogous borane (2, 3) and boron trifluoride (1) adducts is in agreement with the following order of the electron-acceptor strengths of the three Lewis acids toward molecules in which nitrogen is the donor atom (5): $BH_3 \sim BF_3 > (CH_3)_3B$.

The complex II consisted of white, hygroscopic crystals which hydrolyzed readily. Strong acidification of the aqueous solution resulted in the displacement of trimethylborane, followed by its spontaneous and violent ignition in air.

A comparison of the infrared spectrum of II with that of trimethylborane-ammonia, given in Fig. 1, reveals marked similarities and confirms the presence of a B—N stretching

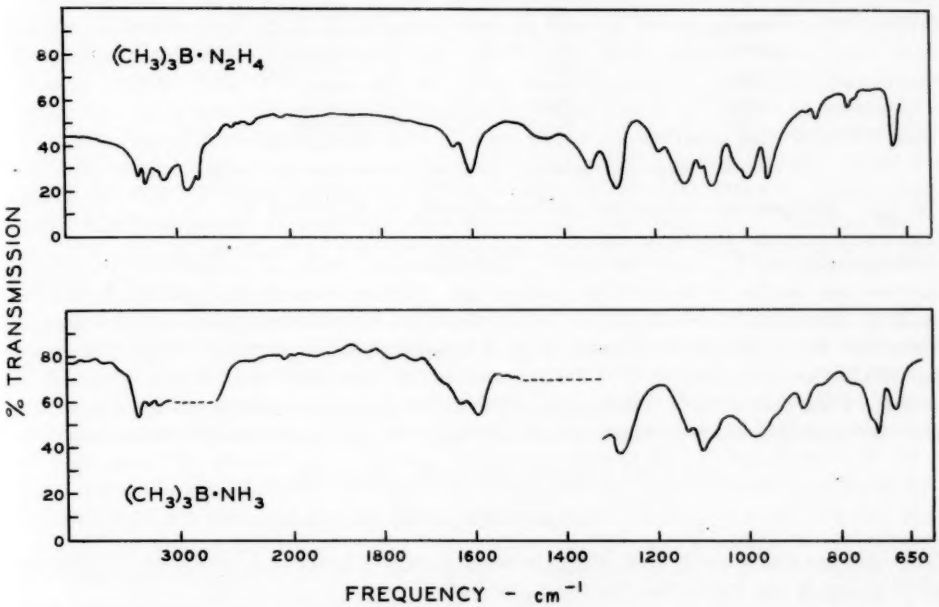

FIG. 1. Infrared spectra of $(CH_3)_3B \cdot N_2H_4$ (in KBr disk) and $(CH_3)_3B \cdot NH_3$ (in Nujol mull).

vibration in II at 1075 cm^{-1}. The frequency assignments listed in Table I were made by analogy with the assignments recorded in the literature for the infrared spectra of trimethylborane (7), hydrazine (8), and hydrazine hydrohalides (9, 10), and for the Raman spectrum of $(CH_3)_3B \cdot NH_3$ (11). Because trimethylborane-ammonia is so volatile at room temperature the potassium bromide pellet method could not be used to obtain its infrared spectrum; therefore, the Nujol mull technique was used instead, and the regions 3100–2800 cm^{-1} and 1500–1325 cm^{-1} were omitted due to interference from the Nujol absorption peaks.

The thermal decomposition of II in vacuum at 150–160° for 16 hours was complex, yielding methane, nitrogen, ammonia, butane, 1-butene, 2-butene, and an unidentified

TABLE I

Infrared vibration frequencies of $(CH_3)_3B \cdot NH_3$ and $(CH_3)_3B \cdot N_2H_4$

$(CH_3)_3B \cdot NH_3$* (cm^{-1})	$(CH_3)_3B \cdot N_2H_4$ (cm^{-1})	Assignment
3370 s	3342 s	N—H stretching (asym.)
3280 s	3277 s	N—H stretching (sym.)
3190 s	3110 s	N—H intermolecular ?
	2908 s	C—H stretching (asym.)
	2812 s	C—H stretching (sym.)
1638 m	1640 m	NH_3 deformation (asym.) or
1595 s	1602 s	NH_2 deformation (asym.)
	1440 w, b	CH_3 deformation (asym.) and NH_2 deformation (sym.)
	1343 s	NH_2 rocking (asym.)
1283 vs	1282 vs	CH_3 deformation (sym.)
	1192 m	NH_2 rocking (sym.)
1135 s	1135 vs	B—C stretching (asym.)
	1103 m	NH_2 wagging (asym.)
1103 vs	1075 vs	B—N stretching
985 s, b	997 s, b	CH_3 rocking
	956 s	N—N stretching
882 w	851 w	CH_3 rocking
730 s	782 w	NH_3 wagging or
716 s	768 w	NH_2 wagging
682 m	679 s	B—C stretching

s = strong m = medium w = weak v = very b = broad

*Nujol absorption peaks interfere in the regions 3100–2800 cm^{-1} and 1500–1325 cm^{-1}.

heterogeneous solid. The presence of C_4 hydrocarbons among the products is remarkable and we are unable to account for their origin. Neither trimethylborane nor hydrazine undergo appreciable decomposition when they are heated separately for 16 hours at 150–160°. The observed decomposition of II is more complex than that recently reported by Mikhailov and Bubnov (12) for complexes of the type $R_3B \cdot N_2H_4$, where R is *n*-C_3H_7, *i*-C_3H_7, or *n*-C_4H_9. These decompose in the presence of excess trialkylborane into the corresponding alkanes, alkenes, and hydrogen, according to the following scheme:

$$R_3B \cdot N_2H_4 \rightarrow [R_2BNHNH_2] + RH + R_{-H} + H_2$$
$$\downarrow R_2B$$
$$R_2BNHNHBR_2 + RH + R_{-H} + H_2.$$

Only alkanes and alkenes containing the same number of carbon atoms as in the original alkyl group of the trialkylborane were reported.

There was no reaction between I and diborane at −80°. At room temperature, however, diborane reacted with II to give trimethylborane, 1,1-dimethyldiborane, hydrogen, and a heterogeneous solid which evolved both methane and hydrogen on heating. Since free trimethylborane was obtained, it was certain that a displacement of trimethylborane from II by the borane group had occurred. Moreover, the formation of 1,1-dimethyldiborane, which could only have occurred by the following reaction (13),

$$2B_2H_6 + 2(CH_3)_3B \rightarrow 3(CH_3)_2B_2H_4,$$

showed that more trimethylborane had been displaced than that indicated by the amount of trimethylborane recovered. In fact the displacement of trimethylborane by the borane group was about 66%, based on the amounts of trimethylborane and 1,1-dimethyldiborane in the product mixture. These data show clearly that, toward hydrazine, the borane group is a stronger electron acceptor than trimethylborane. When the heterogeneous

solid product was heated, methane and hydrogen were evolved. This suggests that both II and 2-borane-hydrazine (2, 3) were present because these adducts when heated are known to yield methane and hydrogen, respectively.

The reaction of hydrazine with trimethylaluminum in vacuum at 25° produced methane, hydrogen, and a nonstoichiometric residue. In diethyl ether solution, the same reactants gave methane and a white solid, which was recovered after evaporation of the solvent and unreacted trimethylaluminum. The weight of the solid product and the amount of methane formed initially indicated that the solid was probably *sym*-bisdimethylaluminohydrazine, $(CH_3)_2AlNHNHAl(CH_3)_2$; since it decomposed on being touched, its composition could not be confirmed by analysis.

EXPERIMENTAL

The different experimental techniques have been described previously (1).

The method of Brown (14) for the preparation of trimethylborane was modified in that boron trichloride and methyl iodide were used in place of boron trifluoride and methyl bromide. (Yield: 79%. Found: molecular weight (M), 55.6; vapor pressure (v.p.), 30.7 mm at −78.3°. Calc. for $(CH_3)_3B$: M, 55.9; v.p., 31.3 mm at −78.3°.) Anhydrous hydrazine was prepared by refluxing the 95+% material over potassium hydroxide (1). The reduction of boron trichloride with lithium aluminum hydride in diethyl ether solution was used for the preparation of diborane. (Yield: 62%. Found: M, 27.7. Calc. for B_2H_6: M, 27.7.) Trimethylaluminum (Ethyl Corporation) was purified by several fractional distillations at 0° (Found: v.p., 13.2 mm at 24.7°. Lit. (15): v.p., 12.8 mm at 24.7°), and the infrared spectrum of the pure substance was identical with that reported previously (16).

Interaction of Trimethylborane with Hydrazine

In a typical experiment, trimethylborane (9.69 mmoles) and anhydrous hydrazine (3.26 mmoles) were combined in vacuum and kept at 25° overnight. The reaction was initially rapid, but a long time was required for its completion, as indicated by a slow decrease in the total pressure. A white crystalline material formed gradually on the walls of the vessel. The amount of unreacted trimethylborane (3.26 mmoles. Found: M, 55.2. Calc. for $(CH_3)_3B$: M, 55.9), recovered by distillation at −78°, showed that trimethylborane (6.43 mmoles) had reacted with hydrazine (3.26 mmoles) in a ratio of 2:1, thus forming the adduct $2(CH_3)_3B\cdot N_2H_4$. When this complex was warmed, it evolved trimethylborane slowly at −65 to −70°, but at 0°, trimethylborane (3.24 mmoles; M, 56.0) was removed rapidly. A residue containing trimethylborane (3.19 mmoles) and hydrazine (3.26 mmoles) in a ratio of 1:1, corresponding to the complex $(CH_3)_3B\cdot N_2H_4$, was left. Pressure measurements in the range −78 to 0° indicated that $2(CH_3)_3B\cdot N_2H_4$ did not dissociate reversibly.

However, when an excess of trimethylborane (7.46 mmoles) was added to a sample of $(CH_3)_3B\cdot N_2H_4$ (4.04 mmoles) and the mixture was kept at 25° overnight, the recovery of trimethylborane (3.40 mmoles; M, 55.8), by distillation at −78°, indicated that the compound $2(CH_3)_3B\cdot N_2H_4$ had been regenerated, since 4.04 mmoles of $(CH_3)_3B\cdot N_2H_4$ had absorbed an additional 4.06 mmoles of trimethylborane.

Pyrolysis of $(CH_3)_3B\cdot N_2H_4$

Trimethylborane (8.58 mmoles) and hydrazine (8.58 mmoles) were combined in an all-glass vessel and the white solid adduct, $(CH_3)_3B\cdot N_2H_4$, which formed was heated for 16 hours at 150–160°. The principal products were: (*a*) noncondensable gases (N_2 and

CH_4; 0.67 mmoles), (*b*) ammonia (0.42 mmoles. Found: M, 18.0; v.p., 35.6 mm at −79.5°. Calc. for NH_3: M, 17.0; v.p., 40.0 mm at −79.2° (17)), (*c*) a mixture of butane and the isomeric butenes (2.44 mmoles. Found: M, 56.3. Calc. for C_4H_8: M, 56.1; for C_4H_{10}: M, 58.1), and (*d*) an unidentified heterogeneous white solid. The composition of the C_4 hydrocarbon fraction was confirmed by infrared and mass spectra measurements. The latter indicated that the ratio of C_4H_{10} to C_4H_8 was approximately 1 to 3.

When trimethylborane (7.75 mmoles) was heated in a sealed tube for 16 hours at 150–160°, a quantitative recovery of the gas proved that no significant decomposition had taken place.

Hydrazine (9.33 mmoles) was heated in an all-glass vessel for 16 hours at 150–160°. The reaction products were nitrogen (0.14 mmole. Found: M, 32.8. Calc. for N_2: M, 28.0), ammonia (0.52 mmole. Found: M, 17.5. Calc. for NH_3: M, 17.0), and unchanged hydrazine (8.86 mmoles; analyzed by the iodate method (6)), in accordance with the decomposition (18)

$$3N_2H_4 \rightarrow 4NH_3 + N_2,$$

and the extent of decomposition of hydrazine was only 5%.

Interactions of $2(CH_3)_3B \cdot N_2H_4$ and $(CH_3)_3B \cdot N_2H_4$ with B_2H_6

After $2(CH_3)_3B \cdot N_2H_4$ (3.26 mmoles) and diborane (4.01 mmoles) had been maintained overnight at −80°, the quantitative recovery of diborane, by distillation at −78°, proved that no reaction had taken place.

In another experiment, $(CH_3)_3B \cdot N_2H_4$ (3.26 mmoles) and diborane (4.01 mmoles) were combined and left overnight at 25°. The reaction, which produced a solid and several volatile products, was stopped by surrounding a portion of the reaction vessel with a liquid-air bath. After all the volatile material had condensed, hydrogen (0.75 mmole) was left. The condensable substances were fractionated at −143°, yielding diborane (0.59 mmole; M, 26.6), and repeatedly at −115°, yielding trimethylborane (0.50 mmole) and 1,1-dimethyldiborane (2.46 mmoles. Found: M, 58.9; v.p., 11 mm at −79.5°. Calc. for $(CH_3)_2B_2H_4$: M, 55.7; v.p., 13 mm at −78.5° (19)). The infrared spectrum of the latter was identical with that reported by Lehmann *et al.* (20).

The solid residue was heated gradually, resulting in the evolution of noncondensable gas, as summarized in Table II. These data suggest that methane and hydrogen were

TABLE II

Temperature of residue (°C)	Amount of gas (mmoles)	Molecular weight
100	3.94	17.6
170	0.75	7.21
250	4.13	2.46

evolved. The quantity of condensable gas released during these operations was negligible.

Interaction of Trimethylaluminum with Hydrazine

(i) Reaction in vacuum.—Anhydrous hydrazine (4.72 mmoles) and trimethylaluminum (20.0 mmoles) were left at 25° overnight. The products of the reaction were: (*a*) a pale brown solid which did not change visibly on heating to 300°, (*b*) a mixture of non-condensable gases (20.0 mmoles: 18.58 mmoles CH_4 and 1.42 mmoles H_2. Found: M, 15.0. Calc. for CH_4: M, 16.0; for H_2: M, 2.0. Successive vapor pressure measurements on

this fraction gradually approached that of CH_4), and (*c*) unreacted trimethylaluminum (12.03 mmoles. Found: v.p., 15.9 mm at 26.7°. Lit. (15): v.p., 13.7 mm at 26.7°). The identity of the latter was also confirmed by its infrared spectrum.

(ii) Reaction in diethyl ether.—In a typical experiment, anhydrous diethyl ether (20 ml) was thoroughly degassed in vacuum and to it were added hydrazine (10.09 mmoles) and trimethylaluminum (27.9 mmoles). The apparatus was sealed and the reactants were stirred overnight at 25°. A white suspension formed in the ether solution. Methane (20.1 mmoles. Found: M, 16.3; v.p., 21.5 mm at −191°. Calc. for CH_4: M, 16.0; v.p., 20.0 mm at −191.8° (17)) was the only noncondensable gas produced. The solvent and unreacted trimethylaluminum were distilled at room temperature, leaving a white crystalline deposit. Analyses of the latter for aluminum were not reproducible, but the weight of the crude product (1.57 g) corresponded approximately to that required (1.46 g) for the formation of the substance *sym*-bisdimethylaluminohydrazine, $(CH_3)_2AlNHNHAl(CH_3)_2$. The formation of exactly 2 moles of methane per mole of hydrazine consumed was supporting evidence. Since the solid compound was extremely sensitive to touch, it could be neither purified nor analyzed.

ACKNOWLEDGMENTS

We are grateful for financial assistance from the Defence Research Board and for two Studentships to one of us (W.G.P.) from the National Research Council. We are indebted to Dr. L. Elias, formerly of the Physical Chemistry Laboratory, McGill University, for the measurement and interpretation of mass spectra.

REFERENCES

1. W. G. Paterson and M. Onyszchuk. Can. J. Chem. **39**, 986 (1961).
2. H. J. Emeléus and F. G. A. Stone. J. Chem. Soc. 840 (1951).
3. M. J. Steindler and H. I. Schlesinger. J. Am. Chem. Soc. **75**, 756 (1953).
4. R. E. McCoy and S. H. Bauer. J. Am. Chem. Soc. **78**, 2061 (1945).
5. F. G. A. Stone. Chem. Revs. **58**, 101 (1958).
6. L. F. Audrieth and B. A. Ogg. The chemistry of hydrazine. John Wiley & Sons, Inc., New York. 1951.
7. W. J. Lehmann, C. O. Wilson, Jr., and I. Shapiro. J. Chem. Phys. **28**, 777 (1958).
8. P. A. Giguère and I. D. Liu. J. Chem. Phys. **20**, 136 (1952).
9. J. C. Decius and D. P. Pearson. J. Am. Chem. Soc. **75**, 2436 (1953).
10. R. G. Snyder and J. C. Decius. Spectrochim. Acta, **13**, 280 (1959).
11. J. Goubeau and H. J. Becher. Z. anorg. u. allgem. Chem. **268**, 1 (1952).
12. B. M. Mikhailov and Y. N. Bubnov. Izvest. Akad. Nauk S.S.S.R., Otdel. Khim. Nauk. 370 (1960).
13. H. I. Schlesinger and A. O. Walker. J. Am. Chem. Soc. **57**, 621 (1935).
14. H. C. Brown. J. Am. Chem. Soc. **67**, 374 (1945).
15. C. H. Bamford, D. L. Levi, and D. M. Newitt. J. Chem. Soc. 468 (1946).
16. K. S. Pitzer and R. K. Sheline. J. Chem. Phys. **16**, 522, 668 (1948).
17. D. R. Stull. Ind. Eng. Chem. **39**, 517 (1947).
18. A. Kant and W. J. McMahon. J. Inorg. & Nuclear Chem. **15**, 305 (1960).
19. R. T. Sanderson. Vacuum manipulation of volatile compounds. John Wiley & Sons, Inc., New York. 1948.
20. W. J. Lehmann, C. O. Wilson, Jr., and I. Shapiro. J. Chem. Phys. **34**, 476 (1961).

COMPLEX PERIODATES AND TELLURATES[1]

M. W. LISTER

This paper is concerned with the complex periodates and tellurates formed by some of the transition metals in the first long period. Probably similar salts could be obtained from transition metals in the later periods, but so far only some silver salts have actually been prepared. Periodic acid, H_5IO_6, and telluric acid, H_6TeO_6, have similarities in formula which set them apart from the acids formed by earlier elements of their groups with the same valency, e.g. perchloric acid, $HClO_4$, and selenic acid, H_2SeO_4. They are also much weaker acids: H_5IO_6 has $pK_1 = 1.6$, $pK_2 = 7.0$; and telluric acid has $pK_1 = 6.1$ and $pK_2 = 10.4$. Consequently it is not surprising that they form complexes which do not find analogues in the chemistry of chlorine and selenium.

Periodic acid or periodates are fairly strong oxidizing agents, so that they oxidize the transition metals to their higher valencies. Some of the compounds described below contain the metals in unusually high valency states. However, to reach these valencies, still stronger oxidizing agents are sometimes required; and the periodate then acts rather as a stabilizing agent for these higher valencies, than as the oxidizing agent. The actual oxidizing agents which have been applied are sodium (or other) persulphate or hypochlorite, and electrolytic oxidation.

The compounds which have been prepared are listed in Table I. The oxidizing agent refers to the compound used in the preparation to reach the higher valency.

TABLE I

Central element	Compound	Oxidizing agent	Reference
Manganese	$Na_7H_4Mn(IO_6)_2.17H_2O$	NaOCl	1
	$K_7H_4Mn(IO_6)_2.8H_2O$	KOCl	1
	$Ba_5HMn(IO_6)_2.10H_2O$		1
	$Na_2Mn_2I_2O_{11}$	Periodate	2
	$K_2Mn_2I_2O_{11}$	Periodate	2
	$Na_7H_7Mn(TeO_6)_2.5H_2O$	NaOCl	10
	$K_6H_8Mn(TeO_6)_2.5H_2O$	KOCl	10
Iron	$Na_2FeIO_6.3H_2O$	—	3
Cobalt	$Na_5H_2Co(IO_6)_2.10H_2O$	NaOCl	4
	$K_4H_3Co(IO_6)_2.3H_2O$	KOCl	4
	$Ba_5[H_2Co(IO_6)_2].10H_2O$	—	4
	$Na_3Co_4(IO_6)_3.11H_2O$	Periodate	5
	$K_3Co_4(IO_6)_3.11H_2O$	Periodate	5
	$K_3H_6Co(TeO_6)_2.2H_2O$	KOCl	10
Nickel	$NaNiIO_6.H_2O$	Persulphate	6
	$KNiIO_6.H_2O$	Persulphate	6
Copper	$Na_7Cu(IO_6)_2.16H_2O$		8
	$Na_5H_2Cu(IO_6)_2.13H_2O$	NaOCl	7
	$K_7Cu(IO_6)_2.20H_2O$	$Na_2S_2O_8$	8
	$K_4H_2Cu(IO_6)_2.4H_2O$	Electrolytic	8
	$K_3H_4Cu(IO_6)_2.6H_2O$		8
	$Na_9Cu(TeO_6)_2.20H_2O$	Electrolytic	7
	$Na_7H_2Cu(TeO_6)_2.12H_2O$	Electrolytic	3, 8
	$Na_5H_4Cu(TeO_6)_2.18H_2O$	Electrolytic	3

[1]*Manuscript received June 30, 1961.*
Contribution from the Department of Chemistry, University of Toronto, Toronto, Ont. Presented at the Symposium on Co-ordination in Chemistry, Chemical Institute of Canada, Hamilton, Ontario, May 15–16, 1961.

The general method of preparation is to mix somewhat acidified solutions of a salt of the central metal and sodium (or potassium) periodate or tellurate, and then to add the oxidizing agent, for instance sodium hypochlorite containing considerable excess sodium hydroxide. The complex salts may crystallize rather slowly, and it is often useful to add alcohol to aid precipitation of them. They can usually be recrystallized from water or dilute sodium hydroxide solution. In practice difficulties arise because the compounds often come down as sticky, poorly crystallized precipitates; and the precipitate may also be contaminated with sodium periodate or tellurate, which has to be removed by recrystallization or reprecipitation.

Valency of Central Metal

As can be seen in Table I, some of these compounds contain Mn(IV), Ni(IV), or Cu(III), which are higher valencies than are common in the bulk of the complex compounds of these elements. The presence of these valencies can be demonstrated by the various methods given below.

1. Titration Methods

This type of method was used by Price in 1903 when he added potassium iodide and acid to $Na_2Mn_2I_2O_{11}$ and titrated the iodine liberated. With trivalent copper it is particularly useful, since sulphuric acid decomposes the compound to give divalent copper again, presumably with liberation of oxygen. Hence if potassium iodide is added to a solution of $Na_7Cu(IO_6)_2$, and then sulphuric acid is added, 18 equivalents of iodine are liberated per molecule; but if the acid is added first, only 17 equivalents are liberated. With the tellurate complex the corresponding numbers are 2 and 1 equivalents of iodine per molecule. Potentiometric titration with ferrous ammonium sulphate (and acid) is also useful since the periodate is then reduced to iodate, and the central metal to the divalent state. Another method along the same lines consists in bubbling in sulphur dioxide and titrating the sulphuric acid formed by its oxidation.

2. Magnetic Properties

A considerable number of magnetic measurements have been made on these compounds, with the results as given in Table II. These are all measurements of the magnetic

TABLE II

Compound	Molar susceptibility $\times 10^6$		Reference
$Na_7Cu(IO_6)_2.15H_2O$	−271		8
$Na_5H_2Cu(IO_6)_2.13H_2O$	−276		8
$Na_7H_2Cu(TeO_6)_2.14H_2O$	−310		8
$K_4H_3Cu(IO_6)_2.4H_2O$	−207		8
$K_3H_4Cu(IO_6)_2.6H_2O$	−187		8
$Na_7H_4Mn(IO_6)_2.17H_2O$	5611, at 3.0° C 5166, at 25.6° C 4964, at 39.7° C	3.84 Bohr magnetons	1
$K_6H_8Mn(TeO_6)_2.5H_2O$	4850, at 25.1° C 4530, at 39.6° C	4.03 Bohr magnetons	1
$Na_5H_2Co(IO_6)_2.10H_2O$ $K_3H_6Co(TeO_6)_2.3H_2O$	−290		4
$NaNiIO_6$	414, at 31° C 387, at 31° C	1.1 Bohr magnetons	6 6

susceptibility, using the ordinary Goüy apparatus. The results on Co(III) compounds make these diamagnetic, as is usual for Co(III). The results on Mn(IV) compounds

agree with the "spin-only" formula for a substance with three unpaired electron spins; this is what is to be expected for Mn(IV), which contains three 3*d* electrons.

It is interesting to note that the Cu(III) compounds are diamagnetic. Cu(III) has eight 3*d* electrons, as does Ni(II), and presumably (as with Ni(II)), there is a possibility of either paired or unpaired spins. If four ligands are arranged around Ni(II) in a plane, the compound is, in general, diamagnetic; presumably the diamagnetism of Cu(III) is evidence of planar stereochemistry in this case also.

The results in $NaNiIO_6$ and $KNiIO_6$ give magnetic moments of 1.1 Bohr magnetons (6). Ray and Sarma suggest that the pure compounds would be diamagnetic but that some dissociation has taken place. This implies that the pure compounds contain spin-paired Ni(IV) in an octrahedral field, a situation found for other tetravalent nickel complexes (9).

General Properties

These complex salts are crystalline solids, usually rather moderately soluble in water. Jensovsky has given solubility curves for a few of the copper complexes. The salts with many sodium or potassium atoms (as opposed to hydrogen) are markedly less soluble in water. It is also true of most of them that they are considerably less soluble in sodium hydroxide solutions than in pure water. They are colored compounds, with light-absorption curves of the same shape: the absorption is high in the ultraviolet, falls to a minimum as we go to longer wavelength, and then passes through a single maximum. Table III

TABLE III
Light absorption

Compound	Maximum	Minimum
$Na_7H_4Mn(IO_6)_3$	482	442 mμ
$Na_7H_7Mn(TeO_6)_3$	470	420
$Na_4H_4Mn(TeO_6)_2$	450 (shoulder)	—
$Na_5H_2Co(IO_6)_2$	625	535
$H_7Co(IO_6)_2$	610	545
$K_3H_6Co(TeO_6)_2$	635	562
$Na_7Cu(IO_6)_2$	420	316

gives the positions of the maxima and minima for aqueous solutions. The extinction coefficients are highest for the copper compound, less for manganese, and least for the cobalt compounds.

Acid–Base Reactions

Some of the complex salts are stable enough to exist in acid solution. For instance, it is possible to pass a solution of sodium periodatocobaltate through a cation exchange resin in its acid form and to obtain a stable solution of the free acid; presumably $H_7Co(IO_6)_2$. Consequently, solutions of sodium periodatocobaltate can be titrated against acids such as perchloric acid, and the pH followed, to obtain information on the ionization constants of the acid, and hence to some extent on the structure of the compounds.

The complex copper salts are too unstable to exist in acid solution, where they break up to give divalent copper. Jensovsky has shown that they are stable at least as far as pH = 8.5, when the salt $K_4H_3Cu(IO_6)_2$ can be crystallized out.

Sodium periodatomanganate is stable enough in acid to allow a complete pH curve to be found. In fairly dilute solution (2.5×10^{-3} *M*) the free acid is ionized to the extent of two hydrogens per molecule, i.e.($H_3O^+)_2.Mn(H_3IO_6)_3^{-2}$. The p*K* values for these first

two stages must be fairly low, certainly 1.5 or less. A detailed study of the pH curve gave for the successive pK values: pK_3 = 2.75, pK_4 = 4.35, pK_5 = 5.45, pK_6 = 9.55, pK_7 = 10.45. These make the main jumps in the ionization constant occur at the stages $Mn(H_3IO_6)_3^{-2}$, $Mn(H_2IO_6)_3^{-5}$, i.e. at the symmetrical ions. The difference between the other pK values is about that expected for hydrogen atoms separated by the number of atoms required by the formula (for instance, the hydrogens in citric acid are separated by the same number of intervening atoms, and have about the same differences in pK).

Unfortunately, this simple, and reasonably satisfactory, explanation is complicated by the observation that, if the solution of sodium periodatomanganate is acidified and the mixture is titrated with alkali, a higher pH curve is found over part of the range. The difference comes mostly in pK_5; pK_1, pK_2, and pK_3 are virtually unaltered, pK_4 is a little higher (5.2), but pK_5 is much higher (9.55). A possible explanation is that in acid the complex is partially dissociated, but that this is not a rapid process, except perhaps in very acid solutions, i.e. it is catalyzed by hydrogen ions. The type of dissociation might be from a ring structure to a structure with periodate attached through one oxygen:

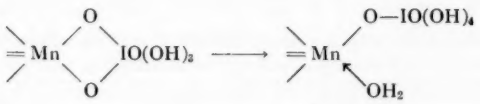

and it is possible to write structures, for the ions, which agree qualitatively with the observed ionization constants. However, the evidence at present is not sufficient to establish these suggestions.

A similar treatment of sodium telluratomanganate gives a similar type of curve, but this time the titration curves are the same in both directions. The acid $H_{14}Mn(TeO_6)_3$ has pK_1 and pK_2 fairly small (averaging 2.2), corresponding to ionization to $(H_3O^+)_2Mn(H_4TeO_6)_3^{-2}$. The values of p$K_3$ to pK_5 are not very different, averaging about 7.5; this involves ionization as far as $Mn(H_3TeO_6)_3^{-5}$. The next ionization constant is about $10^{-11.5}$. A summary of these pK values is in Table IV.

TABLE IV

$H_{14}Mn(TeO_6)_3$ pK_1 = pK_2 = 2.2 pK_3–pK_5 = 7.5 pK_6 = 11.5	$H_{11}Mn(IO_6)_3$ pK_1, pK_2, small pK_3 = 2.75, pK_4 = 4.35, pK_5 = 5.45 pK_6 = 9.55, pK_7 = 10.45
$H_9Co(TeO_6)_2$ pK_1 = 3.0 pK_2 = 8, pK_3 = 9	$H_7Co(IO_6)_2$ pK_1, small, pK_2 = 1.95 pK_3 = 7.1, pK_4 = 8.0 pK_5 = 12.1

A similar treatment of the complex cobalt salts gave the results which are also summarized in Table IV. The behavior of $H_9Co(TeO_6)_2$ is easily explained since the first ionization constant is fairly large, implying easy ionization to $Co(H_4TeO_6)^-$. Then follow two similar constants to give $Co(H_4TeO_6)^{-3}$. However, the acid $H_7Co(IO_6)_2$ has, unexpectedly, two fairly large ionization constants, followed by a pair of fairly similar values. This suggests that the structure of the acid is not as simple as might appear, but at present there is insufficient evidence for any detailed explanation.

Stability Constants of Complex Ions

Various measurements have been made on the stability constants of complex periodates and tellurates, the methods and results being as follows.

1. Copper Compounds

Here use can be made of the fact that uncomplexed copper catalyzes the decomposition of sodium hypochlorite to sodium chloride and oxygen (7). By measuring the rate of gas evolution from solutions containing sodium hypochlorite, sodium hydroxide, copper, and sodium periodate or tellurate in various proportions, it is possible to deduce the equilibrium constant. The uncomplexed copper is probably present as $Cu(OH_4)^-$, and the lack of dependence of the equilibrium constant on hydroxide concentration makes the equilibrium

$$Cu(IO_6)_2^{-7} + 4H_2O \rightleftharpoons Cu(OH)_4^- + 2H_2IO_6^{-3}.$$

With tellurate the main reaction is

$$Cu(HTeO_6)_2^{-7} + 2OH^- + 2H_2O \rightleftharpoons Cu(OH)_4^- + 2H_2TeO_6^{-4}.$$

The equilibrium constants (in 0.4 M NaOH for tellurate) are:

	Tellurate	Periodate	
K_1	1.8×10^{-6}	3.4×10^{-5},	40° C
K_2	1.1×10^{-11}	8.0×10^{-11},	40° C

K_1 and K_2 refer to the two stages of complexing:

$$K_1 = \frac{[Cu].[ligand]}{[1:1\ complex]}, \text{ and } K_2 = \frac{[Cu].[ligand]^2}{[1:2\ complex]}.$$

2. Cobalt Compounds

These are much more stable than the copper compounds; but because cobaltic hydroxide is relatively insoluble, the equilibrium is very slowly reached, starting with cobalt hydroxide and aqueous sodium periodate or tellurate. However, if a solution of the complex salt is added to aqueous sodium hypochlorite, it slightly increases the rate of oxygen evolution, and this increase corresponds to the equilibrium constants at 60° C:

$$\text{Cobalt periodate, } K_2 = 1.7\times10^{-16}$$

$$\text{Cobalt tellurate, } K_2 = 2.5\times10^{-16}.$$

These are for solutions containing 0.1 M sodium hydroxide. At present there is not enough information to write detailed equations for the reactions.

3. Manganese Compounds

The method of using the catalytic decomposition of hypochlorite ions will not work with manganese as this element does not seem to act as a catalyst. However, other methods are available.

Sodium periodatomanganate changes spontaneously in aqueous solution to sodium permanganate and sodium iodate and periodate by the reaction

$$2Na_7H_4Mn(IO_6)_3 + 2H_2O \rightarrow 2NaMnO_4 + 3NaIO_3 + 3Na_2H_3IO_6 + 3NaOH.$$

The rate of this reaction is found to be given by

$$\text{Rate} = K[\text{complex}].[Na_2H_3IO_6]^{-1}[NaOH]^{-2}.$$

This is probably because the complex ion breaks up, by the equation

$$H_4Mn(IO_6)_3^{-7} + 2H_2O \rightleftharpoons H_3Mn(IO_6)_2^{-3} + H_3IO_6^{-2} + 2OH^-$$

and the simpler ion, $H_3Mn(IO_6)_2^{-3}$, then reacts further. In the absence of added sodium periodate, the rate equation is apparently somewhat modified because the periodate is then derived solely from the complex present. From this, a value for the equilibrium constant of the above reaction can be calculated, and it is found to be 2×10^{-9} at 35° C.

This method cannot be applied to sodium telluratomanganate, since tellurate ions are not strongly oxidizing. However the dissociation of the telluratomanganate ion can be demonstrated in aqueous solution by spectrophotometric measurements. If solutions of sodium telluratomanganate are made up in aqueous solution, with and without added sodium tellurate, the apparent extinction coefficients vary considerably. Measurements made on these mixtures over a considerable range of concentration of sodium tellurate, sodium hydroxide, and the complex gave results agreeing with the equilibrium

$$H_7Mn(TeO_6)_3^{-7} + H_2O \rightleftharpoons H_4Mn(TeO_6)_2^{-4} + H_4TeO_6^{-2} + OH^-,$$

assuming that the complex ion had the same formula as in the solid compound $Na_7H_7Mn(TeO_6)_3\cdot 5H_2O$, and that telluric acid is dissociated to $H_4TeO_6^{-2}$ in roughly 0.1 *M* sodium hydroxide. There is evidence to support the contention that the main complex ion contains three tellurate groups since the optical density of a solution made by oxidizing a given amount of manganese in the presence of various amounts of sodium tellurate increases steadily up to three tellurates per manganese, but thereafter remains constant. The equilibrium constant for the foregoing dissociation of telluratomanganate ion is found to be 4.3×10^{-5} at 25° C. This makes the tellurate complex considerably more unstable than the periodate complex, unlike the situation with the cobalt and copper compounds where the stabilities are much the same.

REFERENCES

1. M. W. Lister and Y. Yoshino. Can. J. Chem. **38**, 1291 (1960).
2. W. B. Price. Am. Chem. J. **30**, 182 (1903).
3. L. Malatesta. Gazz. chim. ital. **71**, 467 (1941).
4. M. W. Lister and Y. Yoshino. Can. J. Chem. **38**, 45 (1960).
5. L. Malaprade. Compt. rend. **210**, 504 (1940); **204**, 979 (1937).
6. P. Ray and B. Sarma. J. Indian Chem. Soc. **25**, 205 (1948).
7. M. W. Lister. Can. J. Chem. **31**, 638 (1953).
8. L. Jensovsky. Z. anorg. u. allgem. Chem. **307**, 208 (1961).
9. R. S. Nyholm. J. Chem. Soc. 2602 (1951).
10. M. W. Lister and Y. Yoshino. Unpublished work.

THE STEREOCHEMISTRY OF EIGHT-CO-ORDINATION: THE NATURE OF THE BONDING IN THE $Mo_6Cl_8^{4+}$, $Nb_6Cl_{12}^{2+}$, AND RELATED IONS[1]

R. J. GILLESPIE

ABSTRACT

It is pointed out that the square-antiprism arrangement of eight ligands which is expected for an atom which has eight bonding electron pairs in its valency shell occurs in the polynuclear complex ions found in several basic salts of zirconium(IV), thorium(IV), cerium(IV), and uranium(IV). The nature of the bonding in $Mo_6Cl_8^{4+}$, $Nb_6Cl_{12}^{2+}$, and related ions is discussed, and it is shown that it may be described in a manner which is consistent with a square-antiprism arrangement of eight electron pairs around each metal atom.

The stereochemistry of an atom in a molecule is determined by the arrangements of the electron pairs in its valency shell. These arrangements are determined by the operation of the Pauli exclusion principle which causes electrons with the same spin to keep apart (1). The author has shown previously that on this basis eight electron pairs in a valency shell would be expected to adopt a square-antiprism arrangement (2). Thus the arrangement of the valencies of an atom with a total of eight bonding electron pairs and no non-bonding pairs in its valency shell would be expected to be that of a square antiprism. Only two simple mononuclear complexes have had their structure determined, namely the tantalum octafluoride ion TaF_8^{3-} and thorium acetylacetonate $Th(C_5H_7O_2)_4$; both have the predicted square-antiprism arrangement (3, 4). In this paper it is shown that the same arrangement of eight bonds around a central atom is found in a number of polynuclear complexes, and that the bonding in $Mo_6Cl_8^{4+}$, $Nb_6Cl_{12}^{2+}$, and related ions can be satisfactorily described on this basis; the effects of a non-bonding electron pair on the arrangement of eight bonding pairs are also discussed.

Basic Salts of Ce(IV) and Th(IV)

Lundgren has investigated the structures of a number of basic salts of Ce(IV) and Th(IV) (5, 6, 7). In $Th(OH)_2CrO_4.H_2O$, and $Th(OH)_2SO_4$, there are polynuclear complex ions with the formula $[Th(OH)_2^{2+}]_n$ in which each Th is bonded to four OH groups arranged in the form of a square (Fig. 1). Eight-co-ordination around each

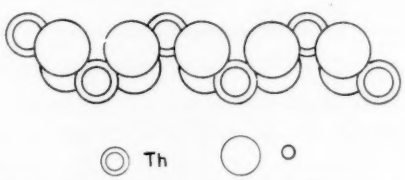

FIG. 1. The structure of the $[Th(OH)_2^{2+}]_n$ ion.

thorium is completed by four oxygen atoms from each of four separate chromate or sulphate groups, these four oxygen atoms being arranged at the corners of a square which is rotated through 45° with respect to the square formed by the OH groups, thus forming a square antiprism of oxygen atoms around each Th atom. The compound

[1]*Manuscript received June 30, 1961.*
Contribution from the Department of Chemistry, McMaster University, Hamilton, Ontario. Presented at the Symposium on Co-ordination in Chemistry, Chemical Institute of Canada, Hamilton, Ontario, May 15–16, 1961.

$CeOSO_4.H_2O$, however, contains infinite complex ions of the formula $(CeO^{2+})_n$ in which each Ce is co-ordinated to three oxygen atoms at three of the corners of a square (Fig. 2).

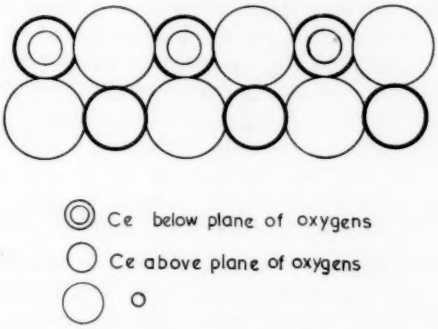

FIG. 2. The structure of the $(CeO^{2+})_n$ ion.

The square is completed by a water molecule, and, again, eight-co-ordination around the Ce is completed by four oxygen atoms from sulphate groups arranged at the corners of a square which is rotated through 45° with respect to the square formed by the oxygen atoms of the $[CeO^{2+}]_n$ chain and the water molecule. Thus there is a square-antiprism arrangement of oxygen atoms around the cerium atom. The basic sulphate with the formula $Ce_6O_4(OH)_4(SO_4)_6$, however, has a different structure containing the finite complex ion $Ce_6O_4(OH)_4^{12+}$. In this ion the metal atoms are situated at the corners of an octahedron, and are surrounded by eight oxygen atoms at the corners of a cube. Thus each cerium is co-ordinated to four oxygen atoms arranged at the corners of a square. Eight-co-ordination around the cerium is completed by four more oxygen atoms, one from each of four sulphate groups, which are arranged at the corners of a square rotated through 45° with respect to the four oxygen atoms in the complex cation. Thus each cerium is surrounded by a square-antiprism arrangement of eight oxygen atoms (Fig. 3).

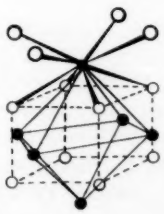

FIG. 3. The structure of $Ce_6O_4(OH)_4(SO_4)_6$.

$ZrOCl_2.8H_2O$

Crystalline hydrated zirconyl chloride has been found to contain the cyclic tetranuclear cation $[Zr_4(OH)_8(H_2O)_{16}]^{8+}$, which has the structure shown in Fig. 4 (8). The

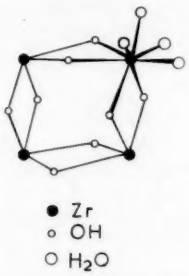

FIG. 4. The structure of the $[Zr_4(OH)_8(H_2O)_{16}]^{8+}$ ion.

four zirconium atoms are arranged in the form of a square, with two OH groups bridging each pair of zirconium atoms along the sides of the square, one OH being above and the other below the plane of the square. Four water molecules are also bonded to each zirconium and they are arranged in such a way as to complete a square-antiprism arrangement of ligands around the zirconium atom.

The $Mo_6Cl_8^{4+}$ Cation

Brosset (9, 10, 11) has determined the structures of crystalline hydrated molybdenum dichloride and also a similar basic hydrated molybdenum chloride and has shown that they should be formulated as $\{[Mo_6Cl_8]Cl_4(H_2O)_2\}6H_2O$ and $\{[Mo_6Cl_8](OH)_4(H_2O)_2\}$-$12H_2O$ respectively. The structure of the $Mo_6Cl_8^{4+}$ ion is shown in Fig. 5; it consists of

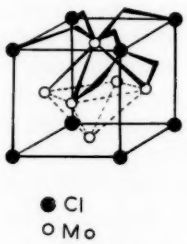

FIG. 5. The structure of the $Mo_6Cl_8^{4+}$ ion.

a regular octahedron of molybdenum atoms circumscribed by a cube of chlorine atoms, each molybdenum atom lying approximately in the plane of four chlorine atoms, constituting a face of the cube. Each molybdenum atom is thus surrounded by, and presumably bonded to, eight other atoms, four molybdenum atoms at the adjacent corners of the octahedron, and four chlorine atoms at the corners of a square which is parallel to, but rotated through 45° with respect to, the square formed by the four molybdenum atoms. There is, therefore, a very distorted square-antiprism arrangement of ligands around each molybdenum atom in which the four chlorine atoms lie in approximately the same plane as the central molybdenum atom. However, the arrangement of the bonding electron pairs is not necessarily the same as that of the ligands.

Sheldon (12) has made the very reasonable suggestion that the bonding of the chlorine atoms in the complex is essentially covalent since the ion retains its identity in solution and the chlorines show no tendency to ionize or to undergo replacement reactions. Each chlorine therefore appears to be forming three bonds to molybdenum atoms and the

Mo—Cl—Mo angles are only 60°. However, it is most unlikely that three of the four electron pairs in the valency shell of a chlorine atom could be so close together. The most probable arrangement for four equivalent electron pairs is tetrahedral (1, 2) and even for non-equivalent bonding and non-bonding pairs the angle between the bonding pairs is very unlikely to be less than 90° since, at this angle, repulsions between the electron pairs of a second-row element become relatively large (13). It is very probable that the angles between the three bonding pairs at each chlorine are somewhat greater than 90° and this can only be reconciled with the structure of the complex if the Mo—Cl bonds are bent, i.e. involve a non-linear overlap of appropriate orbitals on the metal and the chlorine atom (Fig. 5). If this is the case, then the arrangement of electron pairs around each molybdenum atom approximates closely the expected square antiprism. Some slight distortion of the regular square antiprism is in any case to be expected since the electron pairs bind either chlorine atoms or molybdenum atoms and are therefore not all equivalent to each other.

The $Mo_6Cl_8^{4+}$ ion is able to co-ordinate six ligands, one opposite each of the molybdenum atoms. In the compounds investigated by Brosset these additional ligands are $4Cl^-$ and $2H_2O$, or $4OH^-$ and $2H_2O$. The presence of an extra ligand will cause some distortion in the square-antiprism arrangement of the eight electron pairs around the molybdenum and if this ligand is attached to the molybdenum as strongly as the eight other ligands, the square-antiprism arrangement of eight bonding electron pairs passes over to the expected arrangement for nine bonding pairs, namely a triangular prism with an electron pair opposite the center of each of the three rectangular faces (2) (Fig. 6). This may also be described as a "3;3;3" arrangement; in this case the 3-fold axis of the trigonal prism is the y-axis.

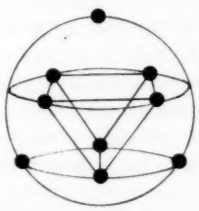

FIG. 6. The "3;3;3" trigonal prism arrangement for nine-co-ordination and its relation to the square-antiprism arrangement for eight-co-ordination.

This formulation of the structure of the $Mo_6Cl_8^{4+}$ ion implies that each molybdenum atom forms eight localized, at least partially covalent bonds, four of which are to other molybdenum atoms. Thus all the molybdenum valency electrons are used in bonding, and each molybdenum therefore has a d^0 configuration, which is consistent with the observed diamagnetism of the compounds containing this complex ion. Sheldon (12) has proposed that four chlorine atoms and one extra ligand are bound to each molybdenum by $d_{z^2-y^2}sp^3$ tetragonal, pyramidal orbitals and that the d_{xy} and d_{yz} orbitals form Mo—Mo bonds, leaving two electrons separately occupying essentially non-bonding d_{z^2} and d_{xy} orbitals, but nevertheless coupling their spins. This description of the bonding seems less satisfactory than that proposed above, for several reasons: it leads to an improbably small angle of 60° between three of the electron pairs on each chlorine atom; it necessitates a somewhat arbitrary assumption of pairing of the two electrons in the non-bonding

d_{z^2} and d_{xy} orbitals in order to explain the observed diamagnetism; and it implies somewhat weak Mo—Mo bonds since it allows only a total of 12 electrons for these 12 bonds which, however, have a length of 2.64 Å, which is close to the single bond value of 2.59 derived from the metal (14).

The $Nb_6Cl_{12}^{2+}$, $Ta_6Cl_{12}^{2+}$, and $Ta_6Br_{12}^{2+}$ Ions

The complex chlorides of niobium, $Nb_6Cl_{14}.7H_2O$ and $Ta_6Cl_{14}.7H_2O$, and the bromide $Ta_6Br_{14}.7H_2O$ have been shown to form the complex $Ta_6Cl_{12}^{2+}$, $Nb_6Cl_{12}^{2+}$, and $Ta_6Br_{12}^{2+}$ ions in aqueous solution (15). These ions have the structure shown in Fig. 7, in which

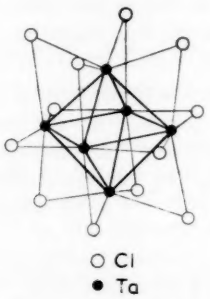

FIG. 7. The structure of the $Ta_6Cl_{12}^{2+}$ ion.

there is a regular octahedron of metal atoms, with a chlorine atom situated above each of the 12 edges of the octahedron. Thus each metal atom is surrounded by eight ligands, four chlorine atoms and four metal atoms arranged at the corners of a distorted cube. However, this is not the arrangement of the bonding electron pairs, firstly because the very small apparent bond angle at chlorine must imply that the metal–halogen bonds are bent and secondly because there are not enough electrons available to form 12 electron-pair bonds between the metal atoms. As only eight electron pairs are available for metal–metal bonds, their most probable arrangement would appear to be that in which there is one pair in the center of each face of the octahedron formed by the metal atoms, each electron pair binding three metal atoms and thus occupying a three-center orbital. If this is the case, the eight electron pairs surrounding the metal atom have the expected square-antiprism arrangement. It is probable that, in the solid, an additional ligand, e.g. Cl^- or H_2O, is bound to each of the metal atoms, thereby distorting the square-antiprism arrangement of eight electron pairs to the "3;3;3" arrangement expected for nine-co-ordination (Fig. 6).

The $U_6O_4(OH)_4^{12+}$ Ion

The basic sulphate of uranium of composition $U_6O_4(OH)_4(SO_4)_6$ has the same structure as the corresponding cerium compound, Fig. 3, and contains the complex cation $U_6O_4(OH)_4^{12+}$ (16). In this ion the metal atom has a valency shell containing eight bonding pairs and two non-bonding electrons.

The possible effect of the non-bonding electrons on the arrangement of the eight bonding pairs is most conveniently discussed in terms of the ligand-field theory. Figure 8 shows the splitting of the *d*-levels produced by the cubic, square-antiprism, and $Mo(CN)_8^{4-}$ arrangements of eight ligands. For the square-antiprism arrangement of ligands the d_{z^2} orbital has a lower energy than the other *d*-orbitals and could accommodate the unshared

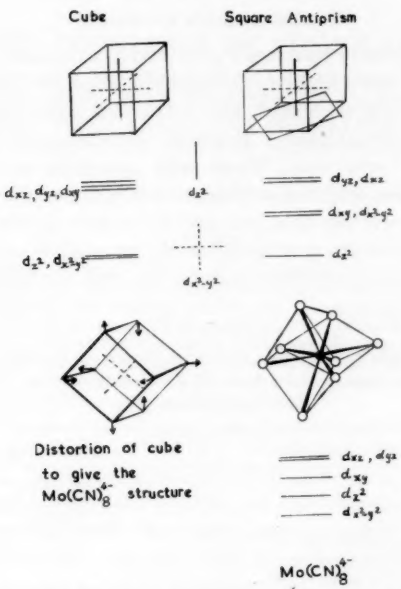

FIG. 8. Ligand-field "splittings" for the cube, square-antiprism, and $Mo(CN)_8^{4-}$ arrangements for eight-co-ordination.

pair without any appreciable distortion of the square-antiprism arrangement. Although this could, in principle, be the situation in the uranium compound, U(IV) compounds are generally paramagnetic and probably have an f^2 configuration with two unpaired electrons rather than a d^2 configuration. These electrons in the "inner" $5f$ orbitals have a negligible effect on the stereochemistry of the eight bonding electron pairs in the "outer" $6d7s7p$ orbitals and this may therefore be described as a weak-field or "outer"-orbital complex.

The $Mo(CN)_8^{4-}$ Ion

This ion does not have the square-antiprism structure but has the dodecahedral, or distorted cube, structure shown in Fig. 8 (17). Although the antiprism has been predicted to be the most stable arrangement for eight-co-ordination it may easily be seen that the dodecahedral structure must have very nearly the same stability, since the smallest bond angles for the square antiprism and the $Mo(CN)_8^{4-}$ structures are 74° 52′ and 74° respectively, whereas the smallest bond angle in the less-stable cubic arrangement is only 70° 32′. Since the interactions between the bonding electron pairs which arise from the operation of the Pauli exclusion principle are of such a nature that they increase very rapidly with decreasing separation of the electron pairs (18) the stability of a given arrangement is particularly dependent on the size of its smallest bond angle.

In the dodecahedral structure two non-bonding electrons may be accommodated in the $d_{x^2-y^2}$ orbital and they would not be expected to cause any appreciable distortion of the structure. In $Mo(CN)_8^{4-}$ the non-bonding pair is almost certainly involved to some extent in double bonding with the CN groups. It does not seem possible at the present time to decide what factors are of importance in determining the relative stabilities of the dodecahedral and square-antiprism structures.

NOTE ADDED IN PROOF

Since this paper was written I have been informed of some new, unpublished determinations of the structures of some eight-co-ordinated complexes: zirconium acetylacetonate (19) has a square-antiprism structure but tetrakisoxalatozirconate(IV) (20) and bis-diarsinetitanium (IV) tetrachloride (diarsine = o-$C_6H_4[As(CH_3)_2]_2$) (21) have the dodecahedral $Mo(CN)_8^{4-}$ structure. These new examples of both types of eight-co-ordinated structures further emphasize their very similar stabilities.

Table I lists all the known mononuclear and finite polynuclear molecules and complex ions in which the stereochemistry is determined by the square-antiprism and dodecahedral arrangements of eight bonding electron pairs in the valency shell of a central atom.

TABLE I

Molecules and complex ions with structures based on the square-antiprism and dodecahedral arrangements of eight bonding electron pairs

Square antiprism	Dodecahedron
TaF_8^{3-}	$Zr(oxalate)_4^{4-}$
$Th(acac)_4$	$Ti(diarsine)_2Cl_4$
$Zr(acac)_4$	$Mo(CN)_8^{4-}$
$[Ce_6O_4(OH)_4]^{12+}$	
$[U_6O_4(OH)_4]^{12+}$	
$[Zr_4(OH)_8(H_2O)_{16}]^{8+}$	
$Mo_6Cl_8^{4+}$	
$Nb_6Cl_{12}^{2+}$, $Ta_6Cl_{12}^{2+}$, $Ta_6Br_{12}^{2+}$	

ACKNOWLEDGMENT

I am greatly indebted to Professor J. L. Hoard and to Professor R. S. Nyholm for information concerning their results in advance of publication.

REFERENCES

1. J. W. Linnett. Wave mechanics and valency. Methuen, London. 1960.
2. R. J. Gillespie. Can. J. Chem. **38**, 818 (1960).
3. J. L. Hoard, W. H. Martin, M. E. Smith, and J. F. Whitney. J. Am. Chem. Soc. **76**, 3820 (1954).
4. D. Grdenic and B. Matokovic. Nature, **182**, 465 (1958).
5. G. Lundgren. Arkiv Kemi, **2**, 535 (1950).
6. G. Lundgren. Arkiv Kemi, **6**, 59 (1954).
7. G. Lundgren. Rec. trav. chim. **75**, 585 (1956).
8. A. Clearfield and P. A. Vaughan. Acta Cryst. **9**, 555 (1956).
9. C. Brosset. Arkiv Kemi, Mineral. Geol. A, **20**, 7 (1946).
10. C. Brosset. Arkiv Kemi, Mineral. Geol. A, **22**, 11 (1947).
11. C. Brosset. Arkiv Kemi, **1**, 353 (1950).
12. J. C. Sheldon. Nature, **184**, 1210 (1959).
13. R. J. Gillespie. J. Am. Chem. Soc. **82**, 5978 (1960).
14. L. Pauling. Nature of the chemical bond. 3rd ed. Cornell University Press, Ithaca, New York. 1960. p. 403.
15. P. A. Vaughan, J. H. Sturdivant, and L. Pauling. J. Am. Chem. Soc. **72**, 5477 (1950).
16. G. Lundgren. Arkiv Kemi, **5**, 349 (1953).
17. J. L. Hoard and H. H. Nordsieck. J. Am. Chem. Soc. **61**, 2853 (1939).
18. R. J. Gillespie. Can. J. Chem. **38**, 318 (1961).
19. J. L. Hoard and J. V. Silverton. Private communication.
20. J. L. Hoard. Private communication.
21. R. J. H. Clark, J. Lewis, R. S. Nyholm, P. Pauling, and G. B. Robertson. Private communication.

CO-ORDINATION COMPLEXES OF TITANIUM (IV) HALIDES

II. PREPARATION AND INFRARED SPECTRA OF THE COMPLEXES OF TITANIUM TETRACHLORIDE WITH DIESTERS OF α,ω-DICARBOXYLIC ACIDS AND COMPARISON WITH ANALOGOUS COMPLEXES OF ZIRCONIUM TETRACHLORIDE AND TIN TETRACHLORIDE[1]

ERNEST RIVET,[2] REAL AUBIN,[3] AND ROLAND RIVEST

ABSTRACT

Co-ordination complexes between diesters of α,ω-dicarboxylic acids and titanium tetrachloride, tin tetrachloride, and zirconium tetrachloride have been prepared. The analytical results, the infrared spectra, the melting points, and the molecular-weight determinations indicate that for the titanium and zirconium complexes, two types of complexes are obtained, one having a general formula $MX_4.1$ diester in which chelate rings from five to nine atoms are formed and the other one, $2MX_4.1$ diester in which there are two 4-membered rings per complex molecule. With tin tetrachloride only one type of complex is formed, which has two tin tetrachlorides and two diesters per complex molecule.

INTRODUCTION

In a previous paper (1) the reaction of diethyl oxalate with titanium tetrachloride has been studied and it was found that a chelated complex involving the two carbonyl groups of the oxalate was formed. The study was extended to diesters of the general formula $CO_2R—(CH_2)_n—CO_2R$, where n varies from 0 to 9, in order to see if very large chelate rings of the same type could be prepared.

In these diesters, the relative independance of every ester group makes it possible to consider that what is true for an ester should apply to a diester. In a carboxylic acid, the acidity is largely due to the possible resonance between the free electron pairs of the oxygen atoms. This makes the implication of the two oxygens of a monocarboxylic acid in the formation of a complex very unlikely. However, an ester is very different from a carboxylic acid. Although Pauling (2) and Wheland (3) mention that the resonance energy of an ester should be of the same order of magnitude as that of a carboxylic acid, Cook (4), using empirical results, has well established the absence of resonance in the esters, and he explained also this finding in terms of orbitals. It is not possible for the π orbitals of the carbonyl group to overlap the sp^3 orbitals of the other oxygen of the ester. Fieser (5) has reached the same conclusion by measuring ultraviolet absorption spectra: the molar extinction coefficients of the esters were larger than those of the corresponding carboxylic acids, thus indicating the presence of an unsaturated bond which is the double bond of the carbonyl group. It is then reasonable to assume that the four oxygen atoms of a diester are almost identical as far as their donor ability is concerned, except for the slight priority of the oxygens of the two carbonyl groups due to the possible steric hindrance of the radical on the two other oxygens. It becomes, then, possible to prepare complexes of diesters with titanium tetrachloride where two 4-membered-ring chelates will be formed. If one does a series of experiments with the diesters $CO_2R—(CH_2)_n—CO_2R$, he measures the relative ease of formation of large rings of seven, eight, nine, or more atoms compared to the formation of two 4-membered rings per diester molecule.

The formation of a four-membered-ring chelate on a Lewis acid requires that the two

[1]*Manuscript received June 30, 1961.*
Contribution from the Department of Chemistry, University of Montreal, Montreal, Que. Presented at the Symposium on Co-ordination in Chemistry, Chemical Institute of Canada, Hamilton, Ontario, May 15–16, 1961.
[2]*Present address: Radiation Laboratory, University of California, Berkeley 4, California.*
[3]*Present address: Séminaire de Joliette, Joliette, Que.*

donor atoms be accepted in a cis position. The work of Osipov (6) and co-workers, in which they obtained a one-to-one addition compound of titanium tetrachloride with ethyl propionate, indicates that this is very possible with $TiCl_4$. However, if the Lewis acid used is tin tetrachloride, the complex formed is $SnCl_4.2$ monoesters and the proposed structure is a trans one. In such a case, it should not be possible to observe the formation of a four-membered ring at both ends of the diester molecule. This was found to be so, and we prepared for the whole series of diesters, one-to-one addition compounds with tin tetrachlorides. In order to see if this difference in behavior between tin tetrachloride and titanium tetrachloride was a size effect, we prepared the same complex with zirconium tetrachloride; this was found not to be the case since zirconium and titanium tetrachlorides behaved similarly.

EXPERIMENTAL

Materials and Manipulation

Titanium tetrachloride was purified as mentioned before (7) and tin tetrachloride was purified by the method patented by Pittsburg Plate Glass Company (8). Commercial zirconium tetrachloride was sublimed in a nitrogen atmosphere at 200° C. The compound so obtained was a white powder. The analytical results were Zr, 39.60%; Cl, 60.49%, the theoretical values being 39.14% for zirconium and 60.84% for chlorine. The esters used were dried over magnesium sulphate or magnesium perchlorate and vacuum-distilled over magnesium perchlorate. One diester, diethyl suberate, was prepared in our laboratory using the esterification method described in *Organic syntheses* (9). It was dried and distilled, as were the other ones. The solvents used were purified by standard methods, dried, and distilled over a suitable drying agent. The water-sensitive complexes were prepared and handled in a dry box continuously flushed with dry nitrogen.

The methods of analysis for titanium and chlorine have been described previously (7); for the determination of tin the method described in Vogel's *Textbook of quantitative inorganic analysis* (10) was used. Zirconium was determined by precipitation with ammonium hydroxide, and ignition to the dioxide (11). All the analytical results are included in Table I.

TABLE I

		% Metal		% Cl	
Lewis acid	Lewis base	Theoretical	Found	Theoretical	Found
$TiCl_4$ (s)	Diethyl oxalate	14.26	14.40	41.27	41.26
$TiCl_4$ (s)	Diethyl malonate	13.69	13.69	40.53	40.81
$TiCl_4$ (s)	Diethyl succinate	13.16	13.51	38.97	38.56
$TiCl_4$ (s)	Diethyl glutarate	12.67	13.50	37.60	38.80
$TiCl_4$ (s)	Diethyl adipate (s)	—	14.40	—	40.3
$TiCl_4$	Diethyl adipate (e)	12.22	12.40	36.20	35.21
$TiCl_4$ (e)	Diethyl adipate	16.5	16.60	48.80	47.30
$TiCl_4$ (s)	Diethyl pimelate	16.06	16.08	48.10	44.15
$TiCl_4$	Diethyl suberate	15.00	14.90	46.40	42.30
$TiCl_4$	Diethyl azelate	15.30	15.12	45.46	42.80
$TiCl_4$	Diethyl sebacate	15.02	15.13	42.90	41.10
$TiCl_4$	Diethyl butyrate	15.67	15.67	46.41	44.80
$SnCl_4$	Diethyl succinate	27.3	27.4	32.60	30.20
$SnCl_4$	Diethyl adipate	25.60	24.90	30.60	30.10
$SnCl_4$	Diethyl azelate	23.50	23.40	28.10	28.10
$ZrCl_4$	Diethyl oxalate	24.04	24.34	37.39	30.52
$ZrCl_4$	Diethyl succinate	22.39	22.51	34.82	33.59
$ZrCl_4$	Ethyl butyrate	26.12	25.10	40.60	36.55
$ZrCl_4$	Diethyl sebacate	25.18	25.19	37.77	36.20

NOTE: s= stoichiometric; e= excess.

The setup used to prepare the complexes was the same as the one used in previous experiments (12).

The spectrophotometric measurements were carried out on a Perkin–Elmer infrared spectrophotomer, model 21, using a sodium chloride prism. The spectra of the complexes were determined in solutions of suitable solvents or by the KBr disk method. The melting point determinations were made with a Thiele apparatus. The molecular-weight determinations were made either by cryoscopy or ebullioscopy.

Preparation of the Complexes

The System $SnCl_4$ – Diethyl Succinate

Pure $SnCl_4$ was added dropwise to a certain quantity of the diester. The precipitate formed instantaneously as $SnCl_4$ was added. As the stoichiometric value of $SnCl_4$ for a one-to-one addition compound was approached, the liquid phase became very viscous and then the whole mass more or less solidified. It was washed very carefully with hexane and dried in vacuum at room temperature, leaving a white powder.

The System $SnCl_4$ – Diethyl Adipate

The reaction was performed by the dropwise addition of $SnCl_4$ to the pure ester.

The reaction rate was slower than in the previous case but led to a white solid which, when filtered, washed with hexane, and dried in vacuum at room temperature, gave a white powder.

The System $SnCl_4$ – Diethyl Azelate

This reaction was performed by the previous method, but no precipitation occurred even after many days of agitation. If the reaction mixture is washed with hexane, then there is precipitation of a white powder. This powder was filtered, washed with hexane, and dried in vacuum at room temperature.

The Systems $TiCl_4$–Oxalate and $TiCl_4$–Malonate

Thirty milliliters of a 10% solution of titanium chloride in hexane was added dropwise to 30 ml of a solution of the diester in the same solvent. Precipitation occurred at the very beginning of the addition, giving a yellow powder. The powder was filtered, washed many times on the filter with pure hexane, and dried in vacuum at room temperature.

The Systems $TiCl_4$ – Diethyl Succinate and $TiCl_4$ – Diethyl Glutarate

Thirty-eight milliliters of a 10% solution of titanium tetrachloride was added dropwise to 35 ml of a 10% solution of the diester. A yellow powder was formed at the beginning of the addition, and when the stoichiometric value for one-to-one addition was reached, another compound, somewhat lighter in color, was formed in small quantity. This explains the high values obtained for titanium and chlorine. It indicates that a very small proportion of the solid is probably a two-to-one addition compound of $TiCl_4$ to the diester.

The System $TiCl_4$ – Diethyl Adipate

By using 10% solutions of the reactants in hexane, as for previous preparations, one can obtain three analytical results. One obtains, in stoichiometric proportions, a mixture of compounds, which can be separated by extraction with benzene. The analytical values indicate that a mixture of two compounds, $TiCl_4$.1 diester and $2TiCl_4$.1 diester, was obtained; by using excess diester, one obtains the one-to-one addition compound almost exclusively and by using excess $TiCl_4$, one obtains the two-to-one addition compound. The two compounds have different melting points and their color is different, the first one being yellow, the other one being light yellow.

The Systems $TiCl_4$ – Diethyl Pimelate, $TiCl_4$ – Diethyl Suberate, $TiCl_4$ – Diethyl Azelate, and $TiCl_4$ – Diethyl Sebacate

The preparation of these complexes was performed in hexane with 10% solutions of the reactants. The complexes prepared are all similar in appearance, being light yellow powders. The analytical results indicate that they are all complexes of the two-to-one stoichiometric compositions. If one tries to prepare the one-to-one addition complexes, which would have been very large chelate rings, there is then dissolution of the complex in the excess diester and one obtains a very viscous, dark brown liquid which seems to be the solvated two-to-one addition compound. These results indicate that with these diesters only one compound can be isolated. However, if one uses CCl_4 as solvent and prepares a complex from stoichiometric values for a one-to-one addition compound, one can see that there are really two compounds, one being almost insoluble in CCl_4, the other being soluble. If one tries to isolate this small precipitate by decantation and then filtration, there is a modification of the precipitate on the filter and one gets a very viscous solid which cannot be properly dried. Qualitatively, this insoluble part is almost nil for the last two terms of the series, but is somewhat larger for the pimelate system.

The Systems $ZrCl_4$ – Diethyl Oxalate, $ZrCl_4$ – Diethyl Succinate, and $ZrCl_4$ – Ethyl Butyrate

To 2 g of powdered zirconium tetrachloride partially dissolved in carbon tetrachloride was added dropwise a 10% solution of the ester in the same solvent till a slight excess of the diester was obtained. The reactants were left in contact with each other for 2 or 3 days, then the white powder obtained was filtered, washed with dry carbon tetrachloride, and dried in vacuum at room temperature.

The System $ZrCl_4$ – Diethyl Sebacate

To 2 g of powdered zirconium tetrachloride partially dissolved in hexane was added dropwise a 10% solution of the sebacate, in the same solvent. The reactants were left in contact with each other for 2 or 3 days, then the white powder obtained was filtered, washed with hexane, and dried in vacuum at room temperature.

The analytical results as shown in Table I indicate that for the titanium tetrachloride complexes there is a progressive change from the monochelated complex of the first terms to the dichelated complexes as the length of the diester chain increases. By comparing the experimental results of the stoichiometric preparations with the theoretical values, one can calculate the relative amount of the two possible complexes for a given diester. These values were calculated using the following equations:

$$T_1 \times A + T_2 \times B = F \qquad [1]$$

$$A + B = 1. \qquad [2]$$

In these equations A is the mole fraction of titanium present as one-to-one addition compound, B is the mole fraction of titanium present as two-to-one addition compound, T_1 represents the theoretical value of the percentage of titanium for a one-to-one addition compound, T_2 the theoretical percentage of titanium in a two-to-one addition compound, and F the value of titanium found for the complex. The values so calculated are tabulated in Table II and illustrated in Fig. 1.

Infrared Spectra

The infrared spectra of the titanium complexes have been studied in solutions and by the KBr disk method. With methylene chloride solutions, we have studied the lowering

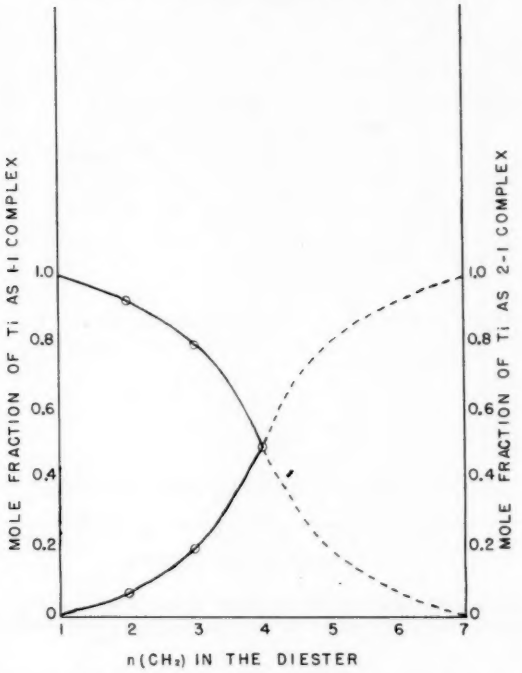

FIG. 1. Variation of the relative yield of the 1–1 and 2–1 titanium complexes as a function of the length of the diester chain.

TABLE II

Ester in the complex	T_1	T_2	F	A	B
Malonate	13.69		13.69	1.00	.0
Succinate	13.16	17.30	13.51	.93	.7
Glutarate	12.67	16.87	13.50	.80	.20
Adipate	12.22	16.50	14.40	.50	.50

of the carbonyl stretching frequency of the diesters, due to complexing. These results are included in Table III and illustrated in Figs. 2, 3, and 4.

TABLE III

Bathochrome effect of the carbonyl frequency in methylene chloride solutions of the titanium complexes

Ester in the complex	$\nu_{C=O}$		$\Delta\nu_{C=O}$
	Pure esters	Complexes	
Oxalate	1774, 1746	1708	57
Malonate	1748, 1731	1699, 1686	47
Succinate	1733	1669	64
Glutarate	1732	1652	80
Adipate	1729	1640	89
Pimelate	1731	1620	111
Azelate	1728	1620	108
Sebacate	1725	1620	105
Butyrate	1737	1635	102

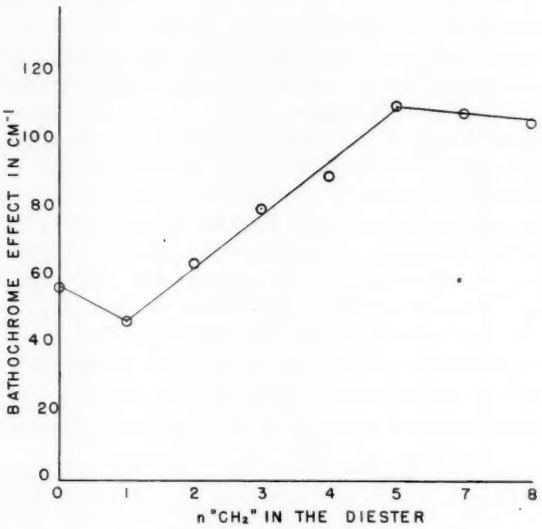

FIG. 2. Infrared spectra in methylene chloride solutions: variation of the bathochrome effect of the carbonyl stretching vibration when co-ordinated to titanium, as a function of the length of the diester chain.

By studying the infrared spectra of co-ordinated complexes containing cyclic ethers as the donor molecules, Sisler (13) has observed that the band attributed to C—O—C vibrations disappears in the spectrum of the complex. In order to see if the ethered oxygens of the diesters were involved in complexing, the spectrum of the diethyl sebacate ester in methylene chloride solution has been compared with the spectrum of the titanium complex dissolved in the same solvent. One can observe in Fig. 3 that in the region of 1200–1100 cm^{-1}, usually attributed to ν_{C-O} and ν_{C-O-C} vibrations (14), there is strong absorption in the spectrum of the ester which almost completely disappears in the spectrum of the complex. This seems to be a confirmation of the fact that the two oxygens of the ester groups of the sebacate act as donor atoms to form a four-membered-ring chelate.

In Fig. 4, we compare the spectrum of diethyl oxalate in *n*-butyl chloride solution with the spectrum of the $TiCl_4$–oxalate complex in the same solvent. The band located at 1165 cm^{-1} and attributed to ν_{C-O}, and the band located at 1152 cm^{-1} and attributed to ν_{C-O-C}, are much stronger in the spectrum of the ester than in the spectrum of the complex, but they still are easily located in the spectrum of the complex. This seems to confirm the proposed difference in the structure of the two types of complexes involved.

The spectra of the solid complexes of titanium studied by the KBr disk method gave different results. Four complexes were studied and all of them gave about the same bathochrome effect: 110 cm^{-1} for the succinate complex, 106 cm^{-1} for the adipate complex, 110 cm^{-1} for the sebacate complex.

The infrared spectra of tin complexes were also studied and the bathochrome effect did not change appreciably for the whole series, being about 100 cm^{-1}.

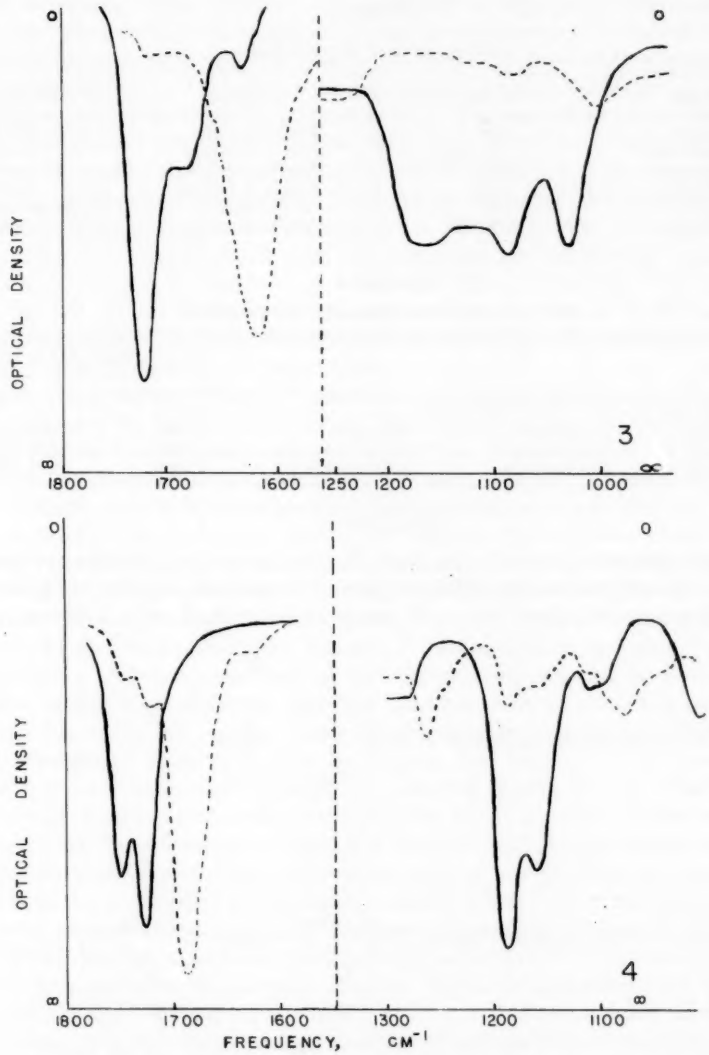

FIG. 3. Infrared spectra in methylene chloride solutions: —diethyl sebacate; - - - $2TiCl_4$. diethyl sebacate.
FIG. 4. Infrared spectra in *n*-butyl chloride solutions: —diethyl oxalate; - - - $TiCl_4$. diethyl oxalate.

Melting Points of the Complexes

The results of the melting-point measurements are included in Table IV.

Molecular-Weight Determinations

The determination of the molecular weight of some of the titanium complexes was very important in the proof of the monomeric nature of the complexes. The results are included in Table V.

TABLE IV

Melting points of the complexes

Complexes	Melting points	Complexes	Melting points
$TiCl_4$.oxalate	104°	$2TiCl_4$.azelate	92–95°
$TiCl_4$.malonate	121–122°	$2TiCl_4$.sebacate	99–100°
$TiCl_4$.succinate	138–139°	$2SnCl_4$.2 succinate	79–80°
$TiCl_4$.adipate	130°	$2SnCl_4$.2 azelate	54–56°
$2TiCl_4$.adipate	89°	$ZrCl_4$.oxalate	Decomposes at 280°
$2TiCl_4$.suberate	87–90°	$ZrCl_4$.succinate	360°

TABLE V

Molecular weights of some titanium complexes

Complexes	Method	Solvent	Molecular weight	
			Theoretical	Found
$TiCl_4$.succinate	Cryoscopy	Benzene	363.9	359, 317, 332
$TiCl_4$.sebacate	Ebullioscopy	*n*-Butyl chloride	638	613, 591, 630
$TiCl_4$.butyrate	Ebullioscopy	*n*-Butyl chloride	305	275, 281, 269

DISCUSSION

The results tabulated here indicate that the reactions of the diesters studied with titanium tetrachloride lead to two different types of compounds, represented by equations [3] and [4]. The transition from (*a*) to (*b*) seems to be gradual, as it is shown in Fig. 1.

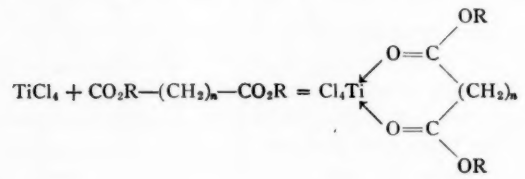

[3]

(*a*)

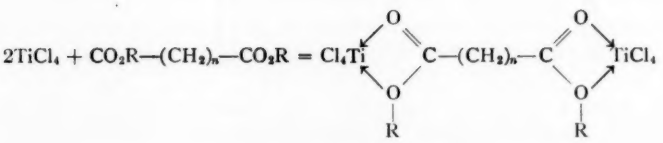

[4]

(*b*)

This graphical representation is not precise but at least gives an idea of what is happening. The values of A and B for the complexes of the diesters for which the value of n is larger than 4 could not be determined. If one tries to obtain a mixture of (*a*) and (*b*), the (*b*) complex dissolves in the diester and it is not possible to get rid of this diester because of its very low vapor pressure at room temperature. It has been attempted to wash out the diester with suitable solvents but it was found that it is part of a solvated molecule and as such is not removable by solvents.

Figure 2, in which the variation of the bathochrome effect is plotted against the n

values of the diester chain, illustrates a variation in the type of complexes obtained. The value of the carbonyl shift is the lowest for the six-membered-ring chelate for which the strain should be at a minimum. For this complex the carbonyl shift is equal in value to the shift observed for the $TiCl_4.2$ acetone complex. As the ring size increases, the carbonyl shift increases until it becomes about equal to the shift observed for a four-membered-ring complex. This is confirmed by the similar shift obtained for the complex $TiCl_4$–butyrate and by vanishing of the band attributed to C—O—C vibration in the type (*b*) complexes.

It is noticeable that in the solid state, the carbonyl frequency shifts are about the same for the whole series of titanium complexes. This is certainly due to the fact that in the solid state the OR groups in the type (*a*) complexes are involved in co-ordination to titanium somewhat as ammonia is in complexes like $TiCl_4.4NH_3$. This co-ordination through the OR groups in the solid state explains also the break in the melting points as one arrives at the (*b*) type complexes where this is not possible because the OR groups are already co-ordinated to a titanium atom.

In dilute solutions, the different molecules of complexes are well separated from each other as indicated by the molecular-weight determinations listed in Table V. Great care was taken in these determinations to avoid hydrolysis, which would give a lower molecular weight than the theoretical one. Every solvent used was checked with the Karl Fisher reagent, and the amount of water present could not change appreciably the thermometer readings leading to the molecular weight, but explains the fact that all the values are a little lower than the theoretical ones. The fact that the butyrate complex has a molecular weight which is about half that of the sebacate complex indicates that the formula proposed for the complexes similar to the sebacate one is probably adequate since there should not be any doubt about the formula of the monoester complex.

The behavior of tin tetrachloride in its reaction with diesters is different. The tin complexes obtained are different from the titanium ones as indicated by the melting points and the analytical results. Many experiments were performed to determine the molecular weight of these complexes in solution, but because of the lack of suitable solvents, it has not been possible to get reproducible results. So, we relied on the work of Hieber and Reindl (15), who have proved that $SnCl_4$ gives two-to-two addition compounds with the diesters we used. Since it is possible to obtain complexes $SnCl_4.2$ monoesters, the impossibility of obtaining chelate rings of the (*a*) type can be explained by the fact that the complexing of two ligands with $SnCl_4$ is done in the trans positions; it is then very possible that the four chlorine atoms lie equatorially on the plane of the tin atom and that the two axial co-ordinating positions are longer distances than the Sn—Cl distances, thus giving an elongated octahedron. This is in agreement with the conclusion of Sumarokova and Yarmukhamedova (16) in their work on complexes of stannic halides with thiourea, in which they mention that the complexes $SnX_4.2$ thiourea have a trans configuration.

ACKNOWLEDGMENTS

The authors are indebted to Professor Camille Sandorfy for valuable discussion on the infrared spectra and to Mr. Gilles Murphy for the preparation and analysis of some of the complexes.

The authors also wish to thank the National Research Council for the grants to one of us (R. R.) and l'Office des Recherches Scientifiques de la Province de Québec for the fellowships to E. R. and R. A.

SOMMAIRE

On a préparé des complexes de coordination entre des esters des acides α,ω-dicarboxyliques normaux et du tétrachlorure de titane, du tétrachlorure d'étain et du tétrachlorure de zirconium. Les résultats analytiques, les spectres infrarouges, les mesures de points de fusion indiquent que le tétrachlorure de titane et le tétrachlorure de zirconium donnent, par leur réaction avec les diesters, deux sortes de complexes de formule $MX_4.1$ diester et $2MX_4.1$ diester respectivement. Les complexes $MX_4.1$ diester sont des chelates contenant cinq à neuf atomes par anneau alors que les complexes $2MX_4.1$ diester contiennent par molecule deux anneaux a quatre situés en bouts de chaine du diester. Avec le tétrachlorure d'étain, on obtient seulement un genre de complexe de formule $2SnCl_4.2$ diesters.

REFERENCES

1. R. Aubin and R. Rivest. Can. J. Chem. **36**, 915 (1958).
2. L. Pauling. The nature of the chemical bond. 2nd ed. Cornell University Press. 1945. p. 202.
3. G. W. Wheland. Resonance in organic chemistry. John Wiley & Sons. 1955. p. 109.
4. D. Cook. J. Am. Chem. Soc. **80**, 49 (1958).
5. L. F. Fieser and M. Fieser. Organic chemistry. 3rd ed. D. C. Heath & Co., Boston. 1956. p. 175.
6. O. A. Osipov. Zhur. Obshcheĭ Khim. **26**, 322 (1956).
7. J. Archambault and R. Rivest. Can. J. Chem. **36**, 1461 (1958).
8. Pittsburg Plate Glass Co. Brit. Patent No. 600,003 (1948).
9. J. R. Johnson (*Editor*). Organic syntheses. Vol. XIX. John Wiley & Sons. 1939. p. 46.
10. A. I. Vogel. A text-book of quantitative inorganic analysis. 2nd ed. Longmans Green & Co., London. 1953. p. 358.
11. I. M. Kolthoff and E. B. Sandell. Textbook of quantitative inorganic analysis. 3rd ed. The Macmillan Co. 1959. p. 316.
12. J. Archambault and R. Rivest. Can. J. Chem. **38**, 1331 (1960).
13. F. R. Rolsten and H. H. Sisler. J. Am. Chem. Soc. **79**, 1819 (1957).
14. P. J. Corish and W. H. T. Davison. J. Chem. Soc. 927 (1958).
15. W. Hieber and E. Reindl. Z. Elektrochem. **46**, 559 (1940).
16. T. Sumarokova and E. Yarmukhamedova. J. Gen. Chem. U. S. S. R. Eng. Transl. 3663 (1956).

π-BONDING IN INORGANIC COMPOUNDS

IV. ROLE OF UNPAIRED ELECTRONS IN HEXAHALO COMPLEXES[1, 2]

A. D. WESTLAND AND N. C. BHIWANDKER[3]

ABSTRACT

A study of d_π–p_π bonding in paramagnetic compounds having the potassium chloroplatinate structure is described. It is shown that the magnetic superexchange effect is approximately proportional to the number of unpaired electrons in t_{2g}^5 and t_{2g}^4 systems but there is an irregularity in the t_{2g}^3 system of potassium chlororhenate. This singularity of the t_{2g}^3 case is considered to be a result of the orbital and crystal symmetries. The magnetic properties of the compounds are related to the extent of π-bonding stabilization in octahedral complexes having various configurations t_{2g}^n on their central atoms.

As part of a program to obtain quantitative or semiquantitative estimates of the extent of π-bonding in inorganic compounds, we have undertaken studies of the effects of certain variables such as principal quantum number of the orbitals involved and effective nuclear charge of the participating atoms. In the present paper we provide evidence which suggests that the extent of d_π–p_π bonding of the type defined as "semicovalent" (1) varies in proportion to the number of unpaired d-electrons provided that these are contained in orbitals of the appropriate symmetry. This result is not entirely trivial for in some of the cases in which electron-pair π-bonding is invoked to account for enhanced compound stability, there seems to be poor correlation between that stability and electron structure (2). In view of the results of the present investigation, it would seem feasible to ascribe the stability of complexes such as $Cr(CN)_6^{3-}$, in which there are no d-electron pairs, to a system of single electron or "half" π-bonds.

The present study compares the extent of magnetic superexchange in compounds K_2MeCl_6 in which the central atom possesses one, two, or three unpaired $5d_\epsilon$-electrons. In a previous publication (3) it was shown that there is extensive superexchange in K_2OsCl_6, K_2OsBr_6, and K_2ReCl_6. This apparently operates through d_π–p_π bonding orbitals which encompass the metal atom and its ligands and, as well, p_π–p_π overlap between the ligands of the neighboring complex groups (4). This latter exchange is shown by means of diagonal broken lines in Fig. 1. The previous results are herein supplemented with those for K_2IrCl_6, again employing the technique of isomorphous dilution with K_2PtCl_6.

It has been shown that K_2IrCl_6 is antiferromagnetic at low temperatures (5), and the electron spin resonance spectrum likewise provides evidence of a π-bonding mechanism (6, 7, 8). In order to obtain an estimate of the magnitude of d_π–p_π bonding in K_2IrCl_6, we have measured the change in the effective magnetic moment of the chloroiridate ion when it is put into solid solution at high dilution in K_2PtCl_6. The assumption that the change in effective magnetic moment is a measure of the superexchange and, in turn, of the extent of π-bonding in the Me—Cl link is justified as follows.

In order for the superexchange coupling to occur, it is necessary that quantum mechanical exchange should take place between neighboring chlorine atoms on adjacent $MeCl_6^{2-}$ groups as well as within the groups. Since there is only a very small change in lattice constant along this series of isomorphous compounds K_2IrCl_6, K_2OsCl_6, and

[1]*Manuscript received April 20, 1961.*
Contribution from the Department of Chemistry, University of Ottawa, Ottawa, Ontario. Presented at the Symposium on Co-ordination in Chemistry, Hamilton, Ontario, May 15–16, 1961.
[2]*Part III. Can. J. Chem.* **39**, *1284 (1961).*
[3]*Present address: Department of Chemistry, McGill University, Montreal, Que.*

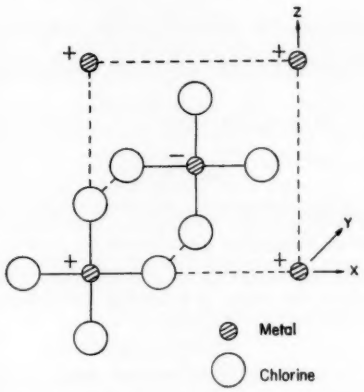

FIG. 1. Orientation of complex groups in crystal lattices of the potassium chloroplatinate type. A section through the plane (0,1,0) is shown.

K_2ReCl_6, it seems justified to assume that the Cl—Cl distance of adjacent anions is so nearly constant that all differences in the exchange effect are due to differences in the Me—Cl bonds.

RESULTS AND DISCUSSION

Pure Potassium Chloroiridate (IV)

The values of the susceptibilities and effective moments at three temperatures for the pure substance are shown in Table I. These data agree well with the values obtained by

TABLE I

Magnetic susceptibilities and effective moments of K_2IrCl_6

Temperature, °K	Gram susceptibility, $\chi_g \times 10^6$	Mole susceptibility, $\chi_M \times 10^3$	Effective moment, B.M.
298	2.15	1.25	1.72
224	2.96	1.63	1.71
90	5.41	2.86	1.44

Cooke *et al.* (5) but differ slightly from those of Norman and Morrow (9), who obtained μ_{eff} = 1.64 B.M. at 298° K. It was our experience that unless oxidizing conditions were maintained at all times during the crystallization of the compound, slightly low results were obtained.* Cooke *et al.* made no measurements between the boiling point of oxygen and room temperature, and assumed that the spin-only value of the moment obtains in the compound but that a large temperature-independent paramagnetism is present. The former assumption is not justified as will be shown.

It is to be expected that the compound should obey the theories of Kotani (10) or Figgis (11), which take account of spin–orbit coupling. The former predicts that the spin-only value of the moment will be observed for the t_{2g}^5 configuration when kT is small with respect to the spin–orbit coupling constant, λ, and that μ_{eff} should vary in nearly linear fashion with kT/λ for temperatures up to 300° K. Figgis' more detailed theory

*K_2IrCl_6 *is diamagnetic.*

takes account of electron delocalization and states that the moment at 0° K should be progressively lower than the spin-only value, the greater is the delocalization, $1-k$. The plot of μ_{eff} for the pure compound in Fig. 2 shows that moment is far from linear in tem-

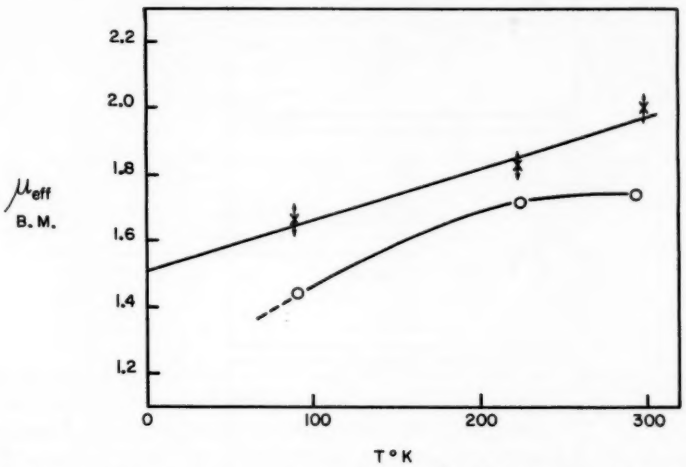

FIG. 2. Plots of effective moment against temperature: ○ pure K_2IrCl_6; × K_2IrCl_6 at infinite dilution in K_2PtCl_6.

perature and that the value at 0° K is much too low to correspond to a reasonable degree of delocalization ($\mu(0°\text{ K}) = 1.41$ B.M. for $k = 0.7$, for example).

The theories of Kotani and Figgis involve the assumption that there is no exchange between neighboring paramagnetic atoms. It was therefore thought that the discrepancy was the result of superexchange. Some indication of superexchange quenching in Na_2IrCl_6 was provided by Sloth and Garner (12), who found that the moment of the solid was 1.58 B.M. while in aqueous solutions it was 1.75 B.M. A study over an extensive temperature range can be carried out only in solid solution, however.

The System K_2IrCl_6/K_2PtCl_6

The effective moment of the iridium atom in solid solution rises with increasing dilution. The course of this quantity with change of concentration is shown in Fig. 3 for three different temperatures. It is apparent that the paramagnetism is partially quenched in the magnetically concentrated systems and that the behavior is essentially the same as that of the system K_2OsCl_6/K_2PtCl_6. There appears to be initially a slight decrease in the paramagnetism from 100 mole% down to about 50 mole%. We can suggest no convincing explanation for this effect if, indeed, it is real.

The data do not afford a very accurate extrapolation to infinite dilution, for the paramagnetism of the most dilute sample measured (12.5 mole%) is of the same order of magnitude as the accompanying diamagnetism. However, the values obtained from the graphs are given in Table II. The effective moment is plotted in Fig. 2, against temperature, along with the values for pure K_2IrCl_6. It may be seen that in contrast with the pure compound, the infinitely dilute chloroiridate (IV) ion behaves at least within the limits of experimental error, in the manner expected for a substance to which Figgis' theory should apply. The line in the figure has been drawn through the value $\mu = 1.5$ at

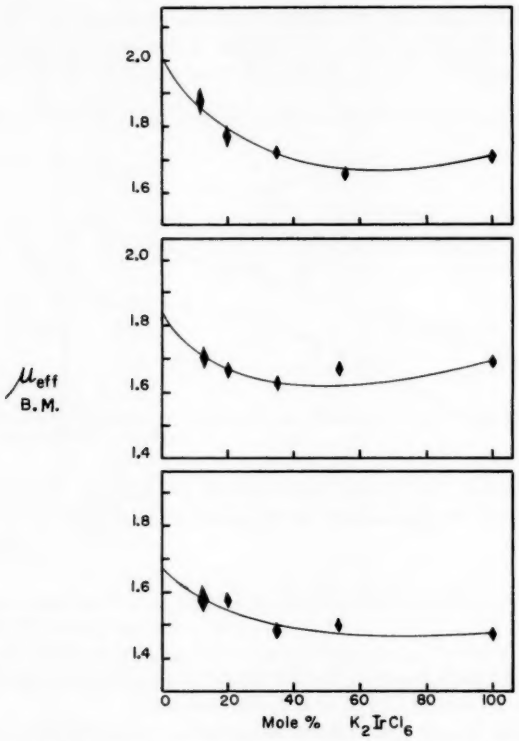

FIG. 3. Plots of the effective moment against concentration of K_2IrCl_6 dissolved in K_2PtCl_6.

$T = 0°$, corresponding to a value of $k = 0.7_6$. This would mean that the electron hole is ~24% in p_π orbitals of the ligands. Griffiths, Owen, and Ward obtained a value of $k = 0.7$ from paramagnetic resonance experiments (6). Although we feel our figure has little accuracy, it is in semiquantitative agreement with the previous results.

From the slope of the line, a value of 630 cm^{-1} is obtained for the spin–orbit coupling constant. This is an extraordinarily low value and makes us doubt the reliability of the estimate. A value of 2000–3000 would seem reasonable. The discrepancy may be the result of an underlying temperature-independent paramagnetism of the order of 0.4×10^3.

Comparison of K_2IrCl_6, K_2OsCl_6, and K_2ReCl_6

We may now compare the extent of superexchange in the compounds K_2MeCl_6. In the case of K_2ReCl_6, the investigation described previously (3) and subsequent measurements (13) suffice to show that the effective moment of chlororhenate (IV) at infinite dilution is 3.75±0.03 B.M. In Table III the room temperature moments of the three pure compounds and the complexes at infinite dilution are presented together with the values of the Weiss constant, Δ, calculated, in the case of iridium and osmium, on the assumption that

$$\mu_{eff} = 2.86[\chi_M(T+\Delta)]^{1/2},$$

where μ_{eff} is the moment for the complex at infinite dilution and χ_M is the mole susceptibility of the pure compound.

TABLE II

Paramagnetism of $IrCl_6^{2-}$ at infinite dilution in K_2PtCl_6

Temperature	Mole susceptibility $\times 10^3$	Effective moment, B.M.
298°	1.68	2.0 ±0.06
224°	1.85	1.82±0.06
90°	3.82	1.66±0.07

TABLE III

	No. of unpaired electrons	Moment of pure K_2MeCl_6, B.M.	Moment at infinite dilution, B.M.	Derived Weiss constant, Δ
Ir (IV)	1	1.7	2.1	104
Os (IV)	2	1.44	2.13	340
Re (IV)	3	3.26	3.75	90

It can be seen that the quenching of the paramagnetism does not depend simply on the number of unpaired electrons. However, the value of the Weiss constant is more than doubled in going from one unpaired electron to two.

Although this quenching is apparently not simply related to the electronic configuration, we believe that there is, in fact, an approximate proportionality between the super-exchange and the extent of π-bonding with the number of unpaired electrons, except for an irregularity at rhenium because of the geometry of the magnetic structure. We shall consider this structure forthwith.

Magnetic Structure of the Compounds K_2IrCl_6, K_2OsCl_6, and K_2ReCl_6

Anderson (14) has discussed the possible modes of antiferromagnetic ordering in the face-centered cubic type of lattice which can occur below the Néel temperature and has pointed out that the structure may be described by means of four sublattices, designated A, B, C, and D in Fig. 4. He has further shown that the ordering of the electron spins

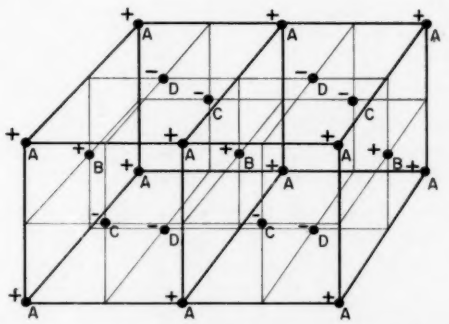

FIG. 4. Magnetic ordering in a face-centered cubic lattice.

in these sublattices may be one of three types depending upon the relative magnitudes of nearest-neighbor and next-nearest-neighbor interactions. Although neutron diffraction shows that the next-nearest-neighbor interactions are more important in many binary

compounds, such as NiO,MnSe, etc., the superexchange mechanism responsible for this, namely an Me ↑ — X — Me ↓ atomic sequence in which X is an anion possessing an occupied *p*-orbital lying in the axial direction, is not present in the compounds K_2MeCl_6. In these ternary complexes, the π-orbitals important to the superexchange mechanism are geometrically oriented so as to favor nearest-neighbor interactions. This is pictured in Fig. 1.

A given atom site in the face-centered cubic structure possesses 12 nearest-neighbor sites distributed equally among the other 3 sublattices. It is impossible to find an ordered arrangement in which the atom spin is antiparallel to that of all its nearest neighbors. At best, it can be antiparallel to only two thirds of them. If it be assumed that next-nearest-neighbor interaction is of minor importance, a favorable arrangement is found, with all spins in sublattices A and B, say, pointing west and those in C and D pointing east, as shown in Fig. 4. This will be allowed when the atoms of all four sublattices have an unpaired electron in either or both of the orbitals d_{xy} and d_{yz}. If such is the case, the magnetic structure would consist of an ordered system composed of sublattices A and C with antiparallel spins and, distinct from this, another like system composed of sublattices B and D. It can be seen from the diagram that an atom in sublattice B has four nearest neighbor atoms in sublattice A with the same spin. The same relation is found between the atoms of sublattices C and D. However, as long as *d*-electrons occupy only the pairs of orbitals d_{xy} and d_{yz}, there is no opportunity for superexchange between nearest-neighbor atoms with parallel spins.

In the event that each central atom possesses three unpaired t_{2g}-electrons, one of these must be accommodated in the d_{xz} orbital. In such a case, coupling between an atom and all of its nearest neighbors is possible. It is clear that this third unpaired electron will work against the ordering process and will decrease the magnitude of the asymptotic Curie temperature, $-\theta$, i.e. the Weiss constant, Δ.

Other ordering schemes can be proposed for the lattice, but the best schemes have the essential features in common, namely, that the ordering is perfect in the (1,0,0), (0,1,0), or (0,0,1) planes, but that each plane is not correlated with adjacent parallel planes except inasmuch as next-nearest-neighbor interactions may be favored, e.g. Anderson's "ordering of the third kind". An analogous arrangement of occupied orbitals will be set up in any case. Thus the irregularity at K_2ReCl_6 is accounted for.

SUMMARY

We conclude that the extent of π-bonding as revealed in the degree of superexchange cannot increase in proportion to the number of unpaired t_{2g}-electrons for more than two such electrons in compounds having a face-centered cubic lattice of paramagnetic atoms. It is presumed, however, that in *isolated* hexaco-ordinated complexes each t_{2g}-electron contributes equally up to the configuration t_{2g}^3 and from the configuration t_{2g}^4 to t_{2g}^6. This would likewise make feasible singly occupied π-bonds of "back-co-ordination" type, for example, in $Cr(CN)_6^{3-}$, and would account for the thermodynamic stability of such compounds.

EXPERIMENTAL

Magnetic measurements were made using a balance of the Gouy type. The maximum field strength was 5320 oersteds. Temperatures were checked by means of a thermocouple. Corrections for the underlying diamagnetism were made by using an experimental value obtained from potassium chloroplatinate. This was prepared from the same stock

chemicals as were used in the preparation of the solid solutions. The possible error due to uncertainty in the diamagnetism of the sample having the lowest iridium concentration was estimated at ±4%. The amount of ferromagnetic impurities in the samples was found to be negligible.

Potassium Hexachloroiridate (IV)

Potassium hexachloroiridate (IV) was prepared from iridium sponge supplied by Johnson, Matthey and Mallory, Limited. The metal was heated in a stream of chlorine and the resulting trichloride was dissolved in dilute hydrochloric acid. The solution was saturated with chlorine, and excess saturated potassium chloride solution was added. Anal. Calc. for K_2IrCl_6: Ir, 39.77. Found: Ir, 39.51.

Solid Solutions of K_2IrCl_6 in K_2PtCl_6

Solid solutions of K_2IrCl_6 in K_2PtCl_6 were prepared in a manner similar to that used previously for the osmium and rhenium systems (3) except that the solution of chloroiridic acid was saturated with chlorine at the time of crystallization. Debye–Scherrer diffraction patterns failed to yield an indication of heterogeneity of the products.

The separation of iridium from platinum, and its determination, were carried out using Gilchrist's procedure (15). Platinum was determined by reduction with formic acid (16).

ACKNOWLEDGMENT

This work was made possible through the support of the National Research Council.

REFERENCES

1. J. B. GOODENOUGH. Phys. Rev. **100**, 564 (1955).
2. R. N. KELLER and R. W. PARRY. *In* Chemistry of coordination compounds. *Edited by* J. C. Bailar. Reinhold, New York. 1956. p. 190.
3. A. D. WESTLAND and N. C. BHIWANDKER. Can. J. Chem. **39**, 1284 (1961).
4. B. R. JUDD. Proc. Roy. Soc. (London), A, **250**, 110 (1959).
5. A. H. COOKE, R. LAZENBY, F. R. MCKIM, J. OWEN, and W. P. WOLF. Proc. Roy. Soc. (London), A, **250**, 97 (1959).
6. J. H. E. GRIFFITHS, J. OWEN, and I. M. WARD. Proc. Roy. Soc. (London), A, **219**, 526 (1953).
7. J. H. E. GRIFFITHS and J. OWEN. Proc. Roy. Soc. (London), A, **226**, 96 (1954).
8. J. H. E. GRIFFITHS, J. OWEN, J. G. PARK, and M. F. PARTRIDGE. Proc. Roy. Soc. (London), A, **250**, 84 (1959).
9. V. NORMAN and J. C. MORROW. J. Chem. Phys. **31**, 455 (1959).
10. M. KOTANI. J. Phys. Soc. Japan, **4**, 293 (1949).
11. B. N. FIGGIS. Trans. Faraday Soc. **57**, 198 (1961).
12. E. N. SLOTH and C. S. GARNER. J. Chem. Phys. **22**, 2064 (1954).
13. A. D. WESTLAND. Unpublished results.
14. P. W. ANDERSON. Phys. Rev. **79**, 350, 705 (1950).
15. R. GILCHRIST. J. Am. Chem. Soc. **57**, 2565 (1935).
16. A. P. BLACKMORE, M. A. MARKS, R. R. BAREFOOT, and F. E. BEAMISH. Anal. Chem. **24**, 1815 (1952).

THE EFFECTS OF OPTICALLY INACTIVE IONS ON THE ROTATORY DISPERSION OF ASYMMETRIC COMPLEX IONS[1]

MARVIN J. ALBINAK,[2] DINESH C. BHATNAGAR, STANLEY KIRSCHNER, AND ANTHONY J. SONNESSA[3]

ABSTRACT

Considerable interest in the optical rotatory dispersion of asymmetric organic and inorganic compounds and its application to the elucidation of their structures has arisen in recent years. In order to study the effects of optically inactive ions on the rotatory dispersion of asymmetric complex ions, a series of salts was prepared of two active cations: levo *cis*-oxalato-bis(ethylenediamine)cobalt(III) and levo tris(ethylenediamine)chromium(III). Salts prepared included the fluoride, chloride, bromide, iodide, tetrafluoroborate, perchlorate, sulphate, and phosphate. In order to study this effect on an optically active anion, the lithium, sodium, potassium, rubidium, cesium, magnesium, calcium, and barium salts of dextro and levo tris(oxalato)-rhodate(III) were also prepared. Rotatory dispersion curves and absorption spectra were obtained for all salts in water solution. A comparison of the curves within a series showed definite trends in changes of wavelength and intensity of maxima of rotation and absorption with changes in both the ionic charge/size ratio (ionic potential) and polarizability of the optically inactive ions.

INTRODUCTION

It has been known since the time of Biot (1) that the rotation of the plane of polarized light by an optically active compound is a function of the wavelength of the incident light. This relationship between optical rotation and wavelength is known as rotatory dispersion and has been studied by several workers. Drude (2) has given an empirical equation which is sometimes useful in describing the optical rotatory dispersion of substances in wavelength regions outside the vicinity of optically active absorption bands. Reviews of optical rotatory dispersion have been published by Levene and Rothen (3), Lowry (4), Heller (5), Klyne and Parker (6), Moscowitz (7), and others (8). Cotton (9) has described the so-called "anomalous rotatory dispersion" of asymmetric compounds in the vicinity of their optically active absorption bands, and several workers (10, 5, 6, 7, 8, 11) have studied this effect in an effort to correlate it with various structural aspects of the compounds studied.

The rotatory dispersion of asymmetric complex inorganic compounds has been studied by several investigators, including Shimura (12), Izumiya (13), Jaeger (11), O'Brien and co-workers (14), Jonassen and Bailar (15), Martinette and Bailar (16), Pfeiffer (17), Mellor (18), and others.

Kirschner and co-workers (19, 20), Albinak (21), and Sonnessa (22) have noticed that the optical rotation and rotatory dispersion of an asymmetric complex ion change when the optically inactive ion associated with it is changed. A further study of this effect resulted in the initiation of an investigation to determine the effects of optically inactive ions on the rotatory dispersion of asymmetric complex ions. In order to facilitate the study of rotatory dispersion of complexes, a special spectrophotometric photoelectric polarimeter was constructed (19).

In this investigation, it was decided first to prepare and resolve several asymmetric complex cations, each with various optically inactive anions, and then to do the same

[1]*Manuscript received June 30, 1961.*
Contribution from the Department of Chemistry, Wayne State University, Detroit, Michigan, U.S.A. Presented in part before the Symposium on Co-ordination in Chemistry, Chemical Institute of Canada, Hamilton, Ontario, May 15–16, 1961.
[2]*Present address: Department of Chemistry, University of Detroit, Detroit 21, Michigan, U.S.A.*
[3]*Present address: Department of Chemistry, Seton Hall University, South Orange, New Jersey, U.S.A.*

for several asymmetric complex anions, each with various optically inactive cations. The rotatory dispersions of all these series of complexes were measured, and they were studied with a view toward determining which characteristics of the optically inactive ions contributed most to the rotatory dispersion changes and which were less important. The first series of asymmetric ions studied contained no asymmetric ligands and their asymmetry was due solely to the configuration of the optically inactive ligands about the central metal ion. Subsequent series of complexes contained asymmetric ligands, e.g., $[Co(NH_3)_4(d\text{-tart})]^+$, but these ions did not have the asymmetric configuration about the metal ion which is found in ions such as tris(ethylenediamine)cobalt(III), $[Co(en)_3]^{+3}$. Additional studies are underway to determine the effects of solvent polarity on rotatory dispersion changes as well as the effects of "loading" a solution containing an asymmetric complex ion with an optically inactive ion of opposite charge on the rotatory dispersion. Further studies are also underway to examine the effects of optically inactive ions on the rotatory dispersion of asymmetric inner complexes and the effects of absolute configuration changes on rotatory dispersion.

EXPERIMENTAL

A High Precision Spectrophotometric Photoelectric Polarimeter for the Determination of Optical Rotation and Optical Rotatory Dispersion

. Although photographic spectropolarimetry has certain unique advantages (5) with respect to long exposure possibilities in cases of low intensity, relatively wide spectral range, high sensitivity, and relative ease of measuring extremely large rotations (e.g., 360°) the procedures involved are usually quite inconvenient and time consuming. Consequently, most of the commercially available spectropolarimeters, as well as those constructed by individual research investigators, utilize photoelectric cells as light receptors. Some of the commercially available instruments include those manufactured by the Photovolt Corporation (95 Madison Ave., New York 16, N.Y.) based on an instrument described by Crumpler, Dyre, and Spell (23); Carl Zeiss, Inc. (485 Fifth Ave., New York 17, N.Y.) (24); Bellingham and Stanley (71, Hornsey Rise, London N. 19, England; Epic Inc., 154 Nassau St., New York 38, N.Y.); O. C. Rudolph and Sons, Inc. (P.O. Box 446, Caldwell, N.J., and Little Falls, N.J.) (25, 26); Perkin–Elmer Corp. (Norwalk, Conn.) (27); and others. Several interesting and unique photoelectric polarimeters, spectrophotometric polarimeters, and recording spectropolarimeters have been constructed in research laboratories throughout the world. Among these are those of Gillham (28), Malcolm and Elliott (29), Burer, Kohler, and Gunthard (30), Gates (31), Bruhat and co-workers (32), von Halban (33), Landt and Hirschmuller (34), Levy (35), Brode (36), Gutowski (37), Woldbye (38), and others (39). The foregoing instruments, however, may have, for many scientists engaged in research in optical rotatory dispersion today, one or more of the following shortcomings: (*a*) a limited wavelength range not extending into the ultraviolet region; (*b*) a precision no better than 0.01°; (*c*) a high degree of elaborateness and complexity, often making it impractical for many investigators to reconstruct such an instrument without the aid of professional technicians; (*d*) the need for time-consuming manipulations to operate the instrument; and (*e*) relatively high cost.

An interesting, commercially available attachment for the Beckman DU spectrophotometer has been developed by the Standard Polarimeter Company (6 Banta Place, Hackensack, N.J.), according to a design by Keston (40). This unit has been evaluated by Poulsen (41, 42). It utilizes light sources which are normally associated with the

Beckman spectrophotometer, and Polaroid plates (rather than polarizing prisms) which severely restrict the use of the instrument to solutions of relatively low optical density, to a limited range of wavelengths in the visible region, and sometimes to low precision.

The authors have described the construction and operation of a spectrophotometric polarimeter of high precision which can be assembled in most laboratories at relatively low cost (19, 43). It has a wavelength region of 2,600 Å to 10,000 Å; a precision of 0.002° when measuring small observed angles of rotation (< 1°); completely variable angles between transmission planes of polarizer and analyzer prisms, allowing for the measurement of observed angles of rotation greater than 1°; and it requires only about 30 minutes to determine an "average" rotatory dispersion curve from 2,600 Å to 7,000 Å. The mathematical principles of operation governing this type of instrument are in the literature (5, 41, 42, 44).

INSTRUMENTAL RESULTS

Table I shows a comparison between the optical rotations of various solutions determined with a high-precision visual polarimeter equipped with a sodium lamp and filter

TABLE I

Comparison of optical rotations of sugar solutions

Sample number	Observed rotation,* deg (visual polarimeter)	Observed rotation,† deg (spectrophotometric polarimeter)
1	0.053±0.003	0.050±0.002
2	0.102±0.003	0.100±0.002
3	0.184±0.003	0.180±0.002
4	0.213±0.003	0.213±0.002
5	0.368±0.003	0.369±0.002

*Na_D line; Rudolph High Precision Visual Polarimeter, Model 80.
†Na_D line.

for the D line, and those determined with the instrument constructed by the authors at the same wavelength.

The average deviation of individual determinations of angles less than 1° is 0.002° with this instrument. Although, theoretically, a high degree of elliptical polarization in the region of a strong Cotton effect (9) would produce a shift in the rotatory dispersion (5), the small angles of rotation measured and the small angle used for the sweep of the analyzer prism of this instrument minimize this effect. Actually, this effect was not observed in the optically active absorption band of potassium chromium tartrate, the very compound studied by Cotton (9) in his work on anomalous rotatory dispersion (Fig. 1).

Compounds Studied

A list of the optically active complex ions studied, along with the optically inactive ions associated with them, is given in Table II.

Preparations

1. *L-cis*-$[Co(en)_2(NO_2)_2]Br$ was prepared and resolved according to the method of Dwyer, Gyarfas, and Mellor (45).

2. *L*-$[Co(en)_3]Cl_3$ was prepared and resolved according to the method of Werner (46).

TABLE II

Optically active complex ions studied and their associated optically inactive ions

Optically active complex ion*	Associated optically inactive ions
L-cis-$[Co(en)_2(NO_2)_2]^+$	F^-, Cl^-, Br^-, I^-, $SO_4^=$, PO_4^{-3}, ClO_4^-, ClO_3^-, NO_3^-, $(C_6H_5)_4B^-$
L-$[Co(en)_3]^{+3}$	F^-, Cl^-, Br^-, I^-, $SO_4^=$, ClO_4^-, ClO_3^-, NO_3^-, PO_4^{-3}
L-$[Co(edta)]^-$	Li^+, Na^+, K^+, Rb^+, Cs^+, Mg^{++}, Ba^{++}, Al^{+3}
L-$[Cr(en)_3]^{+3}$	F^-, Cl^-, Br^-, I^-, BF_4^-, ClO_4^-, $SO_4^=$, PO_4^{-3}
D-$[Rh(ox)_3]^{-3}$	Li^+, Na^+, K^+, Rb^+, Cs^+, Mg^{++}, Ca^{++}, Ba^{++}
$[Co(NH_3)_4(d\text{-tart})]^+$	F^-, Cl^-, Br^-, I^-, BF_4^-, NO_3^-, ClO_4^-, $SO_4^=$, PO_4^{-3}
$[Pt(l\text{-alan})Cl_2]^-$	Li^+, Na^+, K^+, Rb^+, Cs^+, Mg^{++}, Ca^{++}, Ba^{++}, Al^{+3}
$[Pt(d\text{-glut})_2]^=$	Li^+, Na^+, K^+, Rb^+, Cs^+, Mg^{++}, Ca^{++}, Ba^{++}, Al^{+3}
$[Co(NH_3)_5(d\text{-tart})]^+$	F^-, Cl^-, Br^-, I^-, BF_4^-, NO_3^-, ClO_4^-, $SO_4^=$, PO_4^{-3}

*Abbreviations used: en = ethylenediamine; edta = ethylenediaminetetraacetate anion; ox = oxalate anion; *d*-tart = dextro tartrate anion; *l*-alan = levo alaninate anion; *d*-glut = dextro glutamate anion.

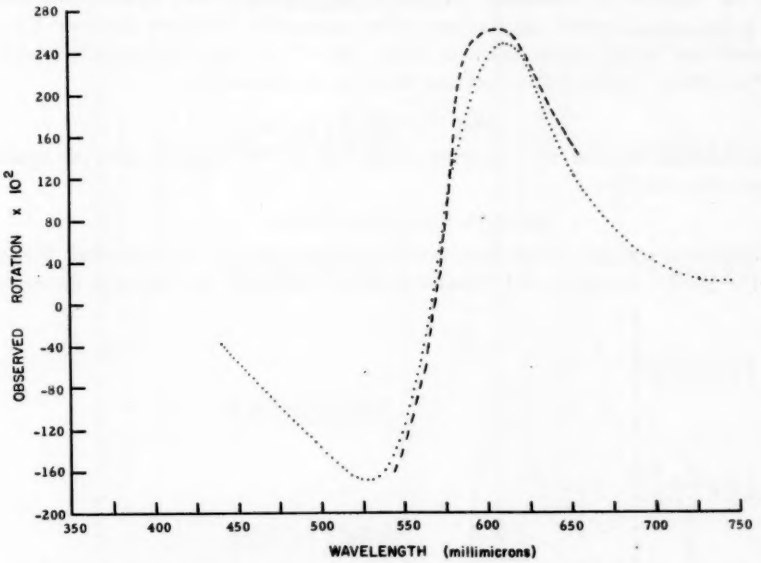

FIG. 1. Elliptical polarization and the Cotton effect. The rotatory dispersion of potassium chromium tartrate: ... curve from spectropolarimeter; – – – curve by Cotton.

3. *L*-K[Co(edta)] was prepared and resolved according to the method of Dwyer and Garvan (47).

4. *L*-$[Co(en)_2Cl_2]Cl$ was prepared and resolved according to the method of Bailar (48). It was converted to *L*-$[Co(en)_2(ox)]Cl$ according to the method of Werner (49).

5. *L*-$[Cr(en)_3]I_3$ was prepared and resolved by Albinak and co-workers of the University of Detroit and presented as a gift to this research group.

6. *D*-$K_3[Rh(ox)_3]$ was prepared and resolved by Dwyer (50).

7. $K[Pt(l\text{-alan})Cl_2]$ was prepared according to the method of Ley and Ficken (51).

8. $H_2[Pt(d\text{-glut})_2]$ was prepared according to the method of Grinberg (52).

9. $[Co(NH_3)_5(d\text{-tart})]Cl$ was prepared according to the method of Duff (53).

10. $[Co(NH_3)_4CO_3]Cl$ was prepared according to the method of Lamb (54). It was converted to $[Co(NH_3)_4(d\text{-tart})]Cl$ by treating 6.0 g of the carbonato complex in 100 ml

of water with 100 ml of an aqueous solution containing 4.1 g of dextro tartaric acid. This solution was added dropwise with continuous stirring. After the bubbles of carbon dioxide had ceased to be evolved, the solution was evaporated almost to dryness by passage of a stream of dry air over it. The resulting dark red, viscous semisolid substance was washed with 100 ml of ethanol and then ground in a mortar under absolute ethanol (the compound is hygroscopic). It was then filtered, washed with ether, and dried under vacuum. The yield of the dark red powder was 5.7 g (62%). Analysis: Calc. for $[Co(NH_3)_4(d\text{-tart})]Cl \cdot H_2O$: C, 14.60; H, 5.48; N, 17.02; Cl, 10.80. Found: C, 15.22; H, 5.71; N, 16.82; Cl, 11.33.

Rotatory Dispersion Curves

These were determined either on the instrument constructed by the authors or on a manual Rudolph High Precision Photoelectric Spectropolarimeter (26). The curves show wavelength vs. "equivalent molecular rotation", $[\alpha]_E$, which is used to eliminate nonreal differences in ion effects which may appear when molecular rotations are used for compounds where the cation:anion ratio is other than 1:1, e.g., $[Co(en)_2(NO_2)_2]Cl$ vs. $[Co(en)_2(NO_2)_2]_2SO_4$. Equivalent molecular rotation is defined as

$$[\alpha]_E = [\alpha]M/n,$$

where M = molecular weight, n = number of optically active complex ions per molecule, and $[\alpha]$ = specific rotation.

RESULTS AND DISCUSSION

A typical series of rotatory dispersion curves is shown in Fig. 2. In general, the wavelengths of the peaks, troughs, and crossover points (positive to negative crossover in

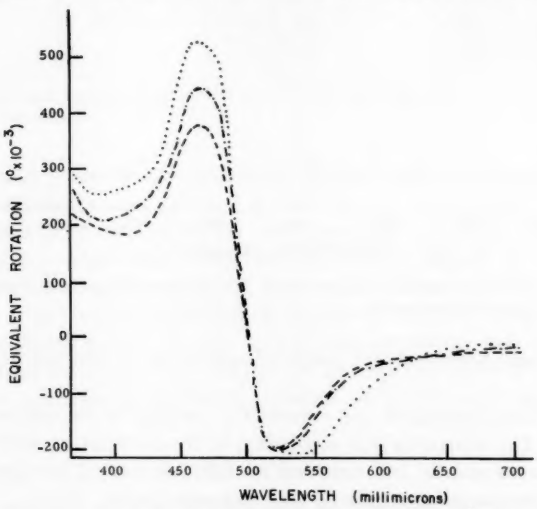

FIG. 2. Optical rotatory dispersion of L-$[Co(en)_3]^{+3}$ salts: – – – chloride; –·– bromide; . . . iodide.

sign of rotation, or vice versa) are fairly constant with change of optically inactive ion, but the magnitudes of rotation at these locations often vary considerably. Data on these magnitudes are given in Tables III–VIII along with the optical absorption maxima.

TABLE III

Comparison of rotatory dispersion of salts of levo tris(ethylenediamine)cobalt(III) ion

Anion	"Zero"	Negative maximum		"Zero"	Positive maximum		Trough		Absorption maximum
	λ	λ	$[\alpha]_E^0 \times 10^{-3}$	λ	λ	$[\alpha]_E^0 \times 10^{-3}$	λ	$[\alpha]_E^0 \times 10^{-3}$	λ
F^-	—	521	−250	497	463	480	380	214M	420
Cl^-	—	523	−205	494	463	380	400	183	470
Br^-	645	515	−225	496	455	445	380	204	470
I^-	—	(515–530)	−250	497	455	535	380	256	470
$SO_4^=$	—	520	−220	494	470	448	390	200	470
ClO_4^-	—	515	−263	495	460	500	393	229	470
ClO_3^-	—	520	−250	497	463	490	380	223	470
NO_3^-	—	520	−220	495	460	450	395	220	470
$PO_4^{\equiv}$	—	518	−250	497	470	460	395	150	470

TABLE IV

Comparison of rotatory dispersion of salts of levo ethylenedinitrilotetraacetatocobaltate(III) ion

Cation	First positive maximum		Zero I	Negative maximum		Zero II	Second positive maximum		Trough		Absorption maximum
	λ	$[\alpha]_E^0 \times 10^{-3}$	λ	λ	$[\alpha]_E^0 \times 10^{-3}$	λ	λ	$[\alpha]_E^0 \times 10^{-3}$	λ	$[\alpha]_E^0 \times 10^{-3}$	λ
Li^+	625	230	585	555	−285	494	440	175	410	65	538
Na^+	625	212	587	545	−282	495	443	170	410	82	538
K^+	625	171	592	545	−350	495	462	130	410	50	537
Rb^+	625	218	587	545	−277	497	440	176	410	104	537
Mg^{++}	625	143	589	550	−275	495	440	124	405	67	518
Al^{+++}	625	180	587	550	−260	496	440	158	400	35	537
Ba^{++}	625	122	588	548	−195	503	437	140	410	35	538

NOTE: all wavelengths are in millimicrons.

TABLE V

Wavelengths and magnitude of selected points on rotatory dispersion and absorption curves of salts of levo *cis*-oxalato-bis(ethylenediamine)cobalt(III) ion

	Maximum		Zero	First minimum		Saddle point	Second minimum		Absorption maximum	
Anion	λ	$[\alpha]_E^0 \times 10^{-4}$	λ	λ	$[\alpha]_E^0 \times 10^{-4}$	λ	λ	$[\alpha]_E^0 \times 10^{-4}$	λ	a_E
F^-	560	13.7	528	480	−19.0	370	305	−33.0	495	220
Cl^-	558	12.0	526	478	−14.6	380	305	−30.6	495	216
Br^-	560	10.9	526	480	−15.1	375	305	−28.2	495	210
I^-	560	8.5	527	480	−11.3	370	305	−22.5	495	229
BF_4^-	563	9.0	528	485	−13.6	375	305	−24.6	495	201
ClO_4^-	560	14.8	527	478	−21.2	375	305	−34.8	495	213
$SO_4^=$	560	7.0	528	480	−10.2	373	305	−16.8	495	222
$PO_4^=$	565	10.6	527	485	−13.7	375	305	−27.8	495	162

NOTE: all wavelengths are in millimicrons.

TABLE VI

Wavelengths and magnitude of selected points on rotatory dispersion and absorption curves of salts of levo tris(ethylenediamine)chromium(III) ion

	Minimum		Zero	Maximum		Trough	First absorption maximum		Second absorption maximum	
Anion	λ	$[\alpha]_E^0 \times 10^{-4}$	λ	λ	$[\alpha]_E^0 \times 10^{-4}$	λ	λ	a_E	λ	$a_E \times 10^{-3}$
F^-	490	−10.5	464	420	21.0	355	460	115	350	4.9
Cl^-	490	− 8.1	466	420	14.3	355	460	86.5	350	2.6
Br^-	490	−10.0	465	420	20.6	358	460	125	350	4.0
I^-	490	−13.4	463	418	24.2	355	460	136	350	2.5
BF_4^-	490	− 6.1	464	418	11.9	355	460	114	350	3.4
ClO_4^-	490	−11.6	464	420	22.8	358	460	132	350	5.3
$SO_4^=$	490	− 9.7	464	420	17.8	360	460	125	350	4.0
$PO_4^=$	490	− 6.3	464	420	11.8	360	460	110	350	2.0

NOTE: all wavelengths are in millimicrons.

TABLE VII

Wavelengths and magnitude of selected points on rotatory dispersion and absorption curves of salts of dextro tris(oxalato)rhodate(III) ion

	Zero I	Maximum		Zero II	Minimum		Absorption maximum	
Cation	λ	λ	$[\alpha]^0_E \times 10^{-4}$	λ	λ	$[\alpha]^0_E \times 10^{-4}$	λ	a_E
Li^+	590	460	12.0	427	360	−48.3	400	225
Na^+	589	460	13.7	427	360	−52.8	400	360
K^+	589	460	17.7	427	360	−65.3	400	435
Rb^+	589	460	14.4	427	360	−59.2	400	522
Cs^+	589	460	14.7	427	350	−61.8	400	480
Mg^{++}	595	455	3.9	420	370	− 9.5	400	291
Ca^{++}	595	460	14.4	426	360	−51.6	400	330
Ba^{++}	590	460	19.5	422	360	−54.6	400	465

NOTE: all wavelengths are in millimicrons.

TABLE VIII

Wavelengths and magnitude of selected points on rotatory dispersion and absorption curves of salts of dextro tartrato-tetramminecobalt(III) ion

	First maximum		Zero I	Minimum		Zero II	Absorption maximum
Anion	λ	$[\alpha]^0_E \times 10^{-2}$	λ	λ	$[\alpha]^0_E \times 10^{-2}$	λ	λ
F^-	540	+495	503	480	−180	440	520
Cl^-	540	+305	498	480	− 65	452	520
Br^-	540	+310	487	480	− 65	458	520
I^-	540	+430	500	480	−140	450	520
BF_4^-	540	+305	494	480	− 42	465	520
ClO_4^-	540	+215	500	480	− 65	478	520
$SO_4^=$	540	+245	494	480	− 80	450	520
$PO_4^{\equiv}$	540	+495	502	480	− 65	460	520
NO_3^-	540	+305	460	480	0	470	0

NOTE: all wavelengths are in millimicrons.

It appears that the changes in the magnitudes of optical rotation are related to the degree of ion pairing between the optically active and optically inactive ions. Illustrative of this are the plots of equivalent molecular rotation vs. "ionic potential" (ionic charge/ionic radius) (55), an example of which is given in Fig. 3. This effect is observed whether

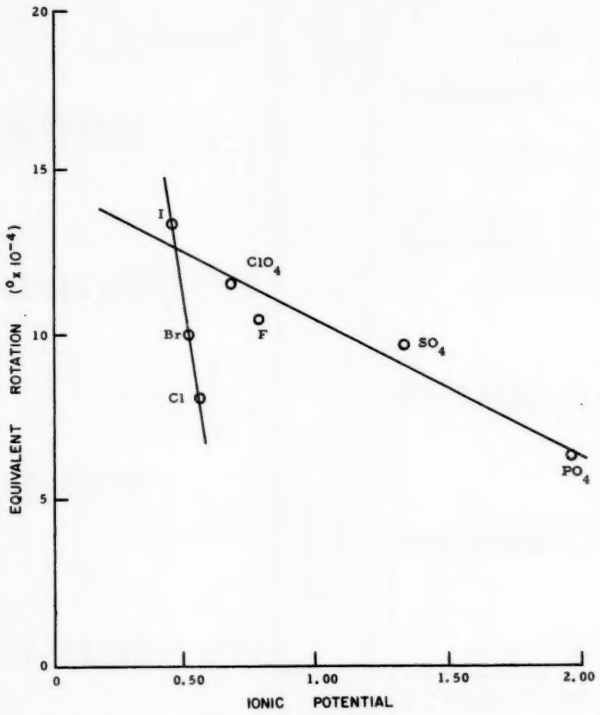

FIG. 3. Equivalent rotation vs. ionic potential for L-$[Cr(en)_3]^{+3}$ cation series.

the optically active complex ions are asymmetric solely because of the configuration of optically inactive ligands about a metal ion or because of the presence of optically active ligands without this type of configuration, e.g., $[Co(NH_3)_4(d\text{-tart})]^+$.

ACKNOWLEDGMENTS

The authors wish to express their sincere appreciation to the National Science Foundation for a grant without which this work could not have been carried out, to the American Cancer Society for an emergency grant which permitted the purchase of an important part of the instrument for which funds were unavailable, to Professor Wilfried Heller of Wayne State University for his helpful suggestions and comments on theory and design, and to Mr. Lee Peterson of Wayne State University for his help in the design and construction of the prism brackets and other metal parts.

REFERENCES

1. J. BIOT. Mem. Inst. **13**, *i*, 1 (1812).
2. P. DRUDE. Lehrbuch der Optik. 2nd ed. S. Hirzel, Verlag, Leipzig. 1906.
3. P. LEVENE and A. ROTHEN. *In* Organic chemistry, an advanced treatise. *Edited by* H. Gilman. John Wiley & Sons, New York. 1938.

4. T. LOWRY. Optical rotatory power. Longmans, Green and Co., Ltd., London. 1935.
5. W. HELLER and D. FITTS. *In* Physical methods of organic chemistry. 3rd ed. Vol. 1. Part 3. *Edited by* A. Weissberger. Interscience Publishers, New York. 1960. Chap. 33.
6. W. KLYNE and A. PARKER. *In* Physical methods of organic chemistry. 3rd ed. Vol. 1. Part 3. *Edited by* A. Weissberger. Interscience Publishers, New York. 1960. Chap. 34.
7. A. MOSCOWITZ. *In* Optical rotatory dispersion. *By* C. Djerassi. McGraw-Hill Book Co., Inc., New York. 1960. Chap. 12.
8. W. KAUZMANN, J. WALTER, and H. EYRING. Chem. Revs. **26**, 339 (1940). E. CONDON. Revs. Modern Phys. **9**, 432 (1937). W. KUHN. Ann. Rev. Phys. Chem. **9**, 417 (1958). W. MOFFITT. J. Chem. Phys. **25**, 1189 (1956). M. POWELL. Endeavor, **15**, 20 (1956). M. VOL'KENSHTEIN. Zhur. Eksptl. i Teoret. Fiz. **20**, 342 (1950). R. SERVANT. J. phys. radium, **3** (8), 90 (1942). J. KIRKWOOD. J. Chem. Phys. **5**, 479 (1937). M. BORN. Proc. Roy. Soc. (London), A, **150**, 84 (1935); A, **153**, 339 (1936). M. BETTI. Trans. Faraday Soc. **26**, 337 (1930). C. DJERASSI. Optical rotatory dispersion. McGraw-Hill Book Co., Inc., New York. 1960.
9. A. COTTON. Compt. rend. **120**, 989, 1044 (1895); Ann. chim. et phys. **8**, 347 (1896).
10. C. DJERASSI. Optical rotatory dispersion. McGraw-Hill Book Co., Inc., New York. 1960.
11. F. JAEGER. Optical activity and high temperature measurements. McGraw-Hill Book Co., Inc., New York. 1930.
12. Y. SHIMURA. Bull. Chem. Soc. Japan, **31**, 315 (1958).
13. N. IZUMIYA. J. Am. Chem. Soc. **78**, 1602 (1956).
14. T. O'BRIEN and R. TOOL. J. Am. Chem. Soc. **77**, 1368 (1955). T. O'BRIEN, J. MCREYNOLDS, and J. BAILAR, JR. J. Am. Chem. Soc. **70**, 749 (1948).
15. H. JONASSEN and J. BAILAR, JR. J. Am. Chem. Soc. **70**, 756 (1948).
16. SR. M. MARTINETTE and J. BAILAR, JR. J. Am. Chem. Soc. **74**, 1054 (1952).
17. P. PFEIFFER. J. prakt. Chem. **150**, 261 (1938).
18. D. P. MELLOR. Australian J. Sci. **3**, 99 (1941); J. Proc. Roy. Soc. N. S. Wales, **75**, 157 (1942).
19. S. KIRSCHNER, A. J. SONNESSA, D. BHATNAGAR, and D. MOY. Abstracts of Papers, 14N, Division of Inorganic Chemistry, 138th Meeting of the American Chemical Society, New York. 1960.
20. S. KIRSCHNER and D. BHATNAGAR. Abstracts of Papers, 11B, Division of Analytical Chemistry, 138th Meeting of the American Chemical Society, New York. 1960.
21. M. ALBINAK. Dissertation, Wayne State University, Detroit, Mich. 1958.
22. A. SONNESSA. Dissertation, Wayne State University, Detroit, Mich. 1960.
23. T. CRUMPLER, W. DYRE, and A. SPELL. Anal. Chem. **27**, 1645 (1955).
24. ZEISS WERKZEITSCHRIFT, **26**, 103 (1957).
25. H. RUDOLPH. J. Opt. Soc. Am. **45**, 50 (1955).
26. E. BRAND, E. WASHBURN, B. ERLANGER, E. ELLENBOGEN, F. LIPPMAN, and M. SCHEU. J. Am. Chem. Soc. **76**, 5037 (1954).
27. A. SAVITZKY, W. SLAVIN, and R. SALINGER. Pittsburgh Conference on Analytical Chemistry and Applied Spectroscopy. Mar. 3, 1959.
28. E. J. GILLHAM. Nature, **178**, 1412 (1956); J. Sci. Instr. **34**, 435 (1957).
29. B. MALCOLM and H. ELLIOTT. J. Sci. Instr. **34**, 48 (1957).
30. T. BURER, M. KOHLER, and H. GUNTHARD. Helv. Chim. Acta, **41**, 2216 (1958). H. HEDRIGER and H. GUNTHARD. Helv. Chim. Acta, **37**, 1125 (1954).
31. J. GATES. Chem. & Ind. (London), 190 (1958).
32. G. BRUHAT, A. BLANC-LAPIERRE, J. SCHLITZ, and G. RAOULT. Compt. rend. **214**, 615 (1942). G. BRUHAT and M. PAUTHENIER. Rev. opt. **6**, 163 (1927).
33. H. VON HALBAN. Nature, **119**, 86 (1927).
34. E. LANDT and H. HIRSCHMULLER. Deut. Zuckerind. **62**, 647 (1937).
35. G. LEVY. Anal. Chem. **23**, 1089 (1951). G. LEVY, P. SCHWED, and D. FERGUS. Rev. Sci. Instr. **21**, 693 (1950).
36. W. BRODE. J. Opt. Soc. Am. **41**, 987 (1951).
37. H. GUTOWSKI. J. Chem. Phys. **19**, 438 (1951).
38. F. WOLDBYE. Acta Chem. Scand. **13**, 2137 (1959).
39. S. MITCHELL and J. VEITCH. Nature, **168**, 662 (1951). D. RANK. J. Sci. Instr. **27**, 270 (1950). E. WILLEY. J. Sci. Instr. **20**, 74 (1943). G. LANDEGREN. Rev. Sci. Instr. **26**, 502, 578 (1955). H. WENKING. Z. Instrumentenk. **66**, 1 (1958). D. RANK, J. LIGHT, and P. YODOR. J. Sci. Instr. **27**, 270 (1950).
40. A. KESTON. Abstract of Papers, 18C, Division of Biological Chemistry, 127th Meeting of the American Chemical Society, Cincinnati, Ohio. 1955. A. KESTON and J. LOSPALLUTO. Federation Proc. **12**, 229 (1953).
41. K. POULSEN. Anal. Chem. **32**, 410 (1960).
42. P. GALLOP. Rev. Sci. Instr. **28**, 209 (1957).
43. M. J. ALBINAK, D. C. BHATNAGAR, S. KIRSCHNER, and A. J. SONNESSA. *In* Advances in the chemistry of the coordination compounds. *Edited by* S. KIRSCHNER. Macmillan Co., New York, N.Y. 1961.
44. STANDARD POLARIMETER COMPANY. Bulletin No. 2.
45. F. DWYER, E. GYARFAS, and D. MELLOR. J. Phys. Chem. **59**, 296 (1955). F. DWYER and F. GARVAN. *In* Inorganic syntheses. Vol. 6. *Edited by* E. Rochow. McGraw-Hill Book Co., Inc., New York. 1960. p. 195.
46. A. WERNER. Ber. **45**, 121 (1912).
47. F. DWYER and F. GARVAN. *In* Inorganic syntheses. Vol. 6. *Edited by* E. Rochow. McGraw-Hill Book Co., Inc., New York. 1960. p. 192.
48. J. BAILAR, JR. *In* Inorganic syntheses. Vol. 2. *Edited by* W. Fernelius. McGraw-Hill Book Co., Inc., New York. 1946. p. 222.

49. A. WERNER. Ber. **45**, 3286 (1912).
50. F. DWYER. J. Phys. Chem. **60**, 1331 (1956).
51. H. LEY and K. FICKEN. Ber. **45**, 380 (1912).
52. A. GRINBERG. Neorg. Khim. Akad. Nauk, S.S.S.R. No. 29, 37 (1955).
53. J. DUFF. J. Chem. Soc. **123**, 563, 569 (1923).
54. A. LAMB. J. Am. Chem. Soc. **59**, 385 (1937).
55. G. CARTLEDGE. J. Am. Chem. Soc. **50**, 2855, 2863, (1928); **52**, 3076 (1930).

SUBSTITUTION AT OCTAHEDRAL CENTERS

II. EFFECT OF SALTS UPON THE RATE OF HYDROLYSIS OF THE HALOPENTAMMINECHROMIUM(III) IONS[1,2]

T. P. JONES,[3] W. E. HARRIS, AND W. J. WALLACE

ABSTRACT

A study of the hydrolysis of the halopentamminechromium(III) ions in the presence of the sodium salts of weak acids reveals a rate acceleration due to specific ion-pair formation. The acceleration is due partly to a charge-transfer effect and partly to the fact that the ion helps to maintain the octahedral configuration of the complex in the transition state. It is concluded that the reaction occurs by dissociation, but without collapse of the structure to a five-co-ordinated intermediate.

INTRODUCTION

In many of the studies of reactions in inorganic systems which have appeared in recent years, the problem of incidental electrolyte has been taken into account by means of a constant "swamping" concentration of some "inert" electrolyte (1). Frequently, but not universally, sodium perchlorate has been used for this purpose. As a result, the literature shows data obtained under circumstances in which both the nature and concentration of the added salts differ markedly. Any attempt to intercompare such data is necessarily attended by assumptions about the effect of the electrolyte upon the reaction. In recent years a number of investigations have indicated a specificity in the influence of electrolytes upon the kinetics of both ionic and non-ionic reactions. Olson and Simonson (2) have shown that such effects are related to the ion which is opposite in charge to the one which is undergoing reaction. The influence of nitrate and sulphate upon the rate of hydrolysis of chloropentamminecobalt(III) had been observed earlier by Garrick (3). Sulphate was observed to have a marked accelerating effect upon the reaction, while nitrate at equivalent concentration exerted only a minor catalytic effect.

Recently, Taube and Posey (4) showed that reaction I, which proceeds predominantly through the ion pair (B), is sensitive to the presence of excess electrolyte. Thus, the rate of formation of the sulphato complex (A) is markedly decreased by the addition of sodium perchlorate. This is not surprising for a reaction which proceeds through the ion-pair intermediate (B). The addition of electrolyte reduces the activity coefficient of the ions in (C) so that the concentration of the ion-pair intermediate is decreased. It is perhaps

$$\underset{(A)}{Co(NH_3)_5SO_4^+} + H_2O \leftrightarrows \underset{(B)}{(Co(NH_3)_5H_2O^{+++}SO_4^{=})} \leftrightarrows \underset{(C)}{Co(NH_3)_5H_2O^{+++}} + SO_4^{=} \qquad [I]$$

surprising, however, that the rate of the hydrolysis was also decreased. There is no theoretical precedent for this. In these circumstances it is tempting to attribute this change in rate to a decrease in the concentration of ion pairs formed by the sulphato complex (A). The force of this interpretation is increased by the observation that both the sulphation and hydrolysis reactions are faster in the presence of increasing concentrations of sulphate. Although such observations as these do not demonstrate conclusively

[1]*Manuscript received June 30, 1961.*
Contribution from the Department of Chemistry, University of Alberta, Edmonton, Alberta. Presented at the Symposium on Co-ordination in Chemistry, Chemical Institute of Canada, Hamilton, Ontario, May 15–16, 1961.

[2]*The first paper in this series is considered to be reference 7.*

[3]*International Nickel Company Fellow, 1960–61; holder of National Research Council of Canada summer fellowships, 1959, 1961.*

that specific interaction complexes described as outer sphere ion pairs (4) participate in the rate-determining step of ionic reactions in solution they certainly do not argue against it. The specificity of the electrolyte effect is further borne out by the observations of other workers (5, 6).

The work reported in this paper is an outgrowth of that reported earlier (7) on the pH-independent hydrolysis of the halopentamminechromium(III) ions. It was found that the pH-independent hydrolysis reaction extended far up into the high pH region. Consequently the system proved convenient for the study of the effect of anions of a number of weak acids upon the rate of an uncomplicated hydrolysis reaction. In this way it has been possible to study the specificity of electrolyte effect in hydrolysis reactions on the basis of the base strength of the anion which was involved.

EXPERIMENTAL

Preparation of Materials

The chloro-, bromo-, and iodo-pentamminechromium(III) halides and perchlorates were prepared as described previously (7). Other materials were reagent grade and were used without further purification.

Kinetic Measurements

Solutions were prepared by mixing, in a volumetric flask, the calculated volume of stock solution of the sodium salt of the anion under investigation and enough halopentamminechromium(III) salt to make the final solution 10^{-3} *M* in chromium, agitating the mixture to dissolve the chromium salt, and diluting it to volume. The solution was placed in a water bath and allowed to come to temperature (10–20 minutes) before measurements were initiated by withdrawing a sample. In those solutions in which the anion concentration was below 0.005 *M* it was found desirable to increase the buffer capacity of the solution by the addition of an ammonia – ammonium perchlorate buffer. In these cases a pH of 8 was maintained by a buffer mixture whose ammonium perchlorate concentration was 0.01 *M*.

Samples withdrawn for analysis were run into a polarographic cell maintained at 0° C in a Dewar. The polarographic cell contained sufficient sulphuric or perchloric acid to convert all of the anion to the acid form and leave the final solution 0.1 *M* in hydrogen ion. The amount of acid required depended upon the nature and concentration of the anion in the reactive solution, but was never great enough to cause significant dilution. The concentrations of chromium species remaining in the solution were then determined polarographically as described previously (7). The initial polarographic measurements were made in the presence of perchloric acid and the later measurements with sulphuric acid. The change from perchloric to sulphuric acid was made when it was found that a better separation between the halo- and aquo-pentamminechromium(III) reduction waves was obtained in a sulphate-containing medium. Presumably this is related to the fact that the aquo complex would be expected to form a stronger ion pair than the chloro complex with sulphate. The anion present during the polarographic measurements did not influence the results in any way other than to increase the ease of interpretation of the polarograms.

The only anions which were polarographically reducible in the potential range of the chromium complexes under the conditions of low pH described above were fumarate and maleate. Fortunately the reduction potential for these anions was pH dependent, and by variation of the acidity of the solution it was possible to change the potential at

which reduction of these anions occurred to a value where they did not interfere with the determination of the concentration of the chromium species in the solution. The most convenient pH for the polarographic analysis of the fumarate solution was 6 and for the maleate was 8. In the analysis of these solutions the procedure involved quenching the reaction with ice-cold concentrated buffer of the appropriate pH instead of concentrated acid.

EXPERIMENTAL RESULTS

The effect exerted by a number of monovalent anions upon the rate of the reaction represented by equation [II], where X is Cl, Br, or I is shown in Fig. 1.

$$Cr(NH_3)_5X^{++} + H_2O \xrightarrow[\text{base}]{\text{anion}} Cr(NH_3)_5OH^{++} + X^- + \text{base } H^+ \qquad [II]$$

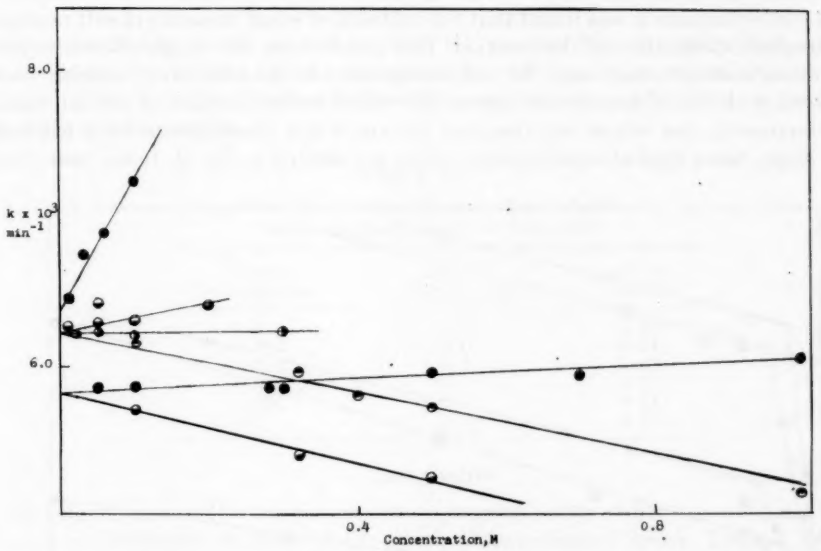

FIG. 1. The effect of monovalent anions upon the rate of hydrolysis of $Cr(NH_3)_5Br^{++}$ (upper set of curves) at 25° and $Cr(NH_3)_5Cl^{++}$ (lower set of curves) at 45°.
Upper curves: ● benzoate, ◒ acetate, ◑ bromide, ◓ perchlorate.
Lower curves: ● chloride, ◒ perchlorate.

The linear dependence of rate upon concentration of salt is evident from the data. Perhaps more surprising than the linearity of the salt effect is the marked variation of the influence of different salts upon the reaction rate. This variation is conveniently reported in terms of the slopes of the curves. The slopes calculated on the basis of a least-squares treatment of the data shown in Fig. 1 are reported in Table I. The specificity of the catalytic effect has been shown to be associated with the anion part of the salt (7).

The data for the monovalent anions are in sharp contrast with those obtained for polyvalent anions. The curves obtained by plotting rate of reaction [II] against concentration do not extrapolate back to a common k_0 at zero concentration of polyvalent anion. Instead the extrapolated value of the rate constant, which will be called $k_{0\ \text{extrap}}$,

TABLE I

The effect of monovalent salts upon the rate of hydrolysis of $Cr(NH_3)_5X^{++}$

X	Salt	Slope$\times 10^4$ (liter mole^{-1} min^{-1})	$k_0\times 10^3$ (min^{-1})
Cl*	NaCl	1.8	5.82
Cl*	$NaClO_4$	−15	5.87
Br†	$NaClO_4$	−11	6.24
Br†	NaBr	1.0	6.21
Br†	NaOAc	21	6.28
Br†	Na benzoate	48	6.51
I†	$NaClO_4$	−120	—

*At 45° C.
†At 25° C.

is a characteristic property of the catalyzing salt. When the behavior was examined at low salt concentrations it was found that the addition of small amounts of salt produced a very marked acceleration of the reaction. This acceleration was roughly linear in polyvalent anion concentration until the salt was present in the solution at roughly molar equivalence with the chromium salt (about 10^{-3} M). Further addition of the salt caused further increase in the rate of reaction, but the curve was characterized by a markedly smaller slope. Some typical experimental results are plotted in Fig. 2. It has been found

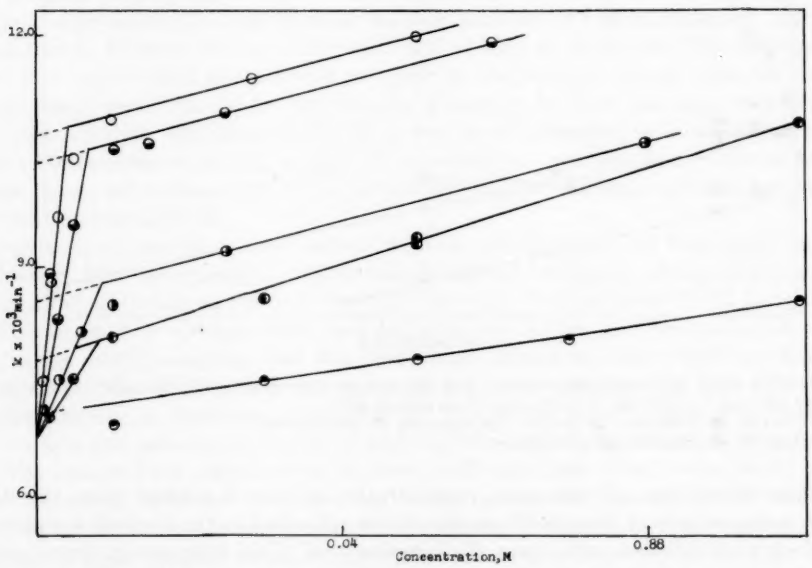

FIG. 2. The effect of various anions upon the rate of hydrolysis of $Cr(NH_3)_5Br^{++}$ at 25°: ○ citrate, ◒ maleate, ◑ sulphate, ◐ *o*-phthalate, ◓ fumarate.

convenient to characterize these curves in terms of $k_{0\ \text{extrap}}$ and the slope of the portion of the curve at higher salt concentration. The values of these parameters obtained by a least-squares analysis of the experimental data are shown in Table II.

TABLE II

The effect of polyvalent anions upon the rate of hydrolysis of $Cr(NH_3)_5Br^{++}$ at 25°

Salt*	$k_{0\ extrap} \times 10^3$ (min^{-1})	Slope $\times 10^3$ (liter min^{-1} $mole^{-1}$)
p-Phthalate	6.33	0.98
Adipate	6.56	2.21
Fumarate	6.90	1.67
Succinate	6.98	1.48
Oxalate	7.38	1.75
Malonate	7.47	2.59
o-Phthalate	7.85	2.97
Sulphate	8.94	1.12
Maleate	10.18	2.84
Citrate	10.70	2.52

*The sodium salt of the listed anion was used in all cases.

The enhancement in the rate of reaction [II] produced by the polyvalent anions is extremely sensitive to the total ionic strength of the solution. Some typical data are shown in Table III for the effect of sodium perchlorate upon the catalysis by citrate in the hydrolysis of the chloro complex.

TABLE III

Effect of ionic strength upon citrate catalysis of the acid hydrolysis of $Cr(NH_3)_5Cl^{++}$

Citrate concentration	$NaClO_4$ concentration	$k \times 10^3$ (min^{-1})
0.0	0.01	5.85
0.004	0.0	8.74
0.004	0.1	6.65
0.0	0.1	5.70
0.004	1.0	4.54
0.0	1.0	4.30

DISCUSSION

The rate of reaction [II] has been shown to respond to the addition of salts in a manner which is not explicable in terms of the simple Debye–Huckel theory. There is, however, some indication that the extended form, involving a term linear in electrolyte concentration, could be applied to the results obtained over the range 0.01 to 0.5 *M*. Alternatively and perhaps somewhat more conveniently, the ideas suggested by Ingold (8) to cover salt effects in the solvolysis of alkyl halides might be applied. Both of these suggestions suffer from the disadvantage, in the present application, of not allowing for specificity of the salt effect. Nevertheless, there is probably sufficient indication that the effect observed is due to the reacting species developing an ion atmosphere. This ion atmosphere promotes the stability of the transition state and suggests charge separation in the reaction intermediate. Such an observation is not surprising for a reaction which results in a net increase in the total number of ions in the solution regardless of the intimate mechanism of the reaction. Such charge separation is expected to be more important in a reaction which occurs by dissociation than in one which occurs by displacement. It is suggested, then, that the catalysis of reaction [II], produced by various salts at high concentration, is an indication of a dissociation mechanism.

More surprising and perhaps more useful in a diagnostic way was the observation of the rapid rise in rate produced by polyvalent anions in a concentration range which was comparable to that of the reacting species. Although this general kind of observation has been made by a number of other workers (3, 6, 9, 10), it has been investigated in somewhat more detail in the present work than previously. These salt effects have been attributed to specific ion-pair formation. It now appears necessary to divide salt effects into two categories. The first of these is the general ionic atmosphere effect discussed above. Ion-pair formation may play a role in this kind of salt effect since a dependence upon the nature of the anion involved was observed, but it does not seem to be the primary factor. The second category suggested involves the formation of specific ion pairs. In this case, it is assumed there are recognizable association units with integral numbers of ions to which ion pair formation constants could be applied. The simplest unit which could be considered in this way is one positive and one negative ion. Since this kind of unit is most easily visualized from a kinetic point of view it is proposed to treat our data on the basis of this model. The alternative of a bimolecular attack upon the halopentammine chromium(III) ion does not need to be seriously considered since the reaction is first order even in the presence of small concentrations of added salt. Furthermore the sole primary product of the reaction is observed to be the hydroxopentamminechromium(III) ion.

Reaction [II] follows the rate law [III], where k_1 is the rate constant for the uncatalyzed

$$\text{Rate} = \frac{(k_1+k_2K[\text{A}])}{1+K[\text{A}]}\,[\text{RX}] \qquad [\text{III}]$$

reaction, k_2 is the rate constant for the catalyzed reaction, K is the ion-pair association constant, [A] is the concentration of added anion, and [RX] is total concentration of halopentamminechromium(III) ion. Using relationship [III] it is possible to estimate a value for K. This has been done and when citrate is the catalyzing anion the association constant was calculated to be 233. This agrees very well with the value 248 determined experimentally (11). In Fig. 3 are plotted the experimentally observed values of $k_{0\,\text{extrap}}$ for reaction [II] against the constants for association of some of the ions used with the hexamminecobalt(III) ion (12). The order of the agreement is seen to be excellent.

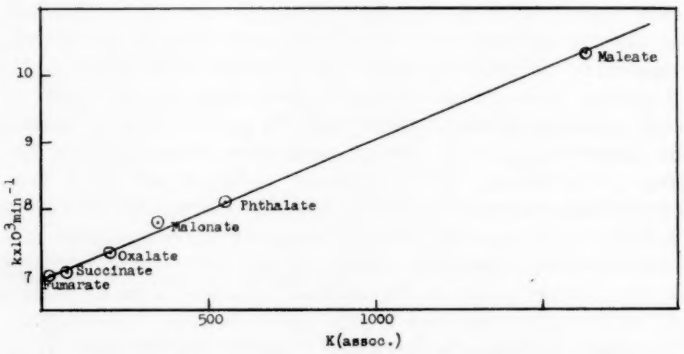

FIG. 3. Relation between the rate constant for the hydrolysis of $Cr(NH_3)_5Br^{++}$ at 25° and the magnitude of the ion-pair formation constant between anions and $Co(NH_3)_6^{+++}$. Data for the ion-pair formation constants are taken from reference 12.

Similar agreement has been obtained between the rate constants and ion-association constants (11) for the interaction between the chloropentamminechromium(III) ion and the polyvalent anions used in this study.

The sensitivity of the salt effect to the total ionic strength of the solution, shown in Table III, is a further indication of the rationality of the suggestion that ion pairs are involved. Unfortunately, the effect of sodium perchlorate upon the activity coefficient of the halopentamminechromium(III) ion is not known. However, the effect of sodium perchlorate upon the rate of the citrate-catalyzed reaction is in agreement with its effect upon the experimentally determined ion-pair formation constant (11).

If the ion pairs promote the hydrolysis reaction they must do so either through charge transfer or by stabilizing the transition state. Charge transfer might occur in a number of ways, but regardless of the mechanism, the result must be an increase in the electron density on the chromium. Such an increase in electron density would not be expected to promote attack upon the chromium by an electron-rich reagent such as water. Stabilization of the transition state might result because the associating anion tends to hold the complex ion in its normal octahedral configuration. This, of course, would tend to prevent the loss of ligand-field stabilization energy (13) which is attendant upon the distortion of the regular octahedron as the molecule proceeds through the transition state. Such stabilization is not compatible with the expansion of the co-ordination sphere which would be necessary to accommodate a displacement reaction. It seems, then, that the rate acceleration produced by ion-pair formation is incompatible with an S_N2 mechanism for reaction [II]. The explanation for the results must be sought in terms of a dissociation mechanism.

$$\begin{array}{ccccccc} & & \begin{array}{c} RH_2O^+ + X^- \\ H_2O \,\updownarrow \\ R^+X^- \\ A^- \,\updownarrow \\ RA + X^- \end{array} & & \begin{array}{c} RH_2O^+ + X^- \\ H_2O \,\updownarrow \\ R^+ \; X^- \\ \updownarrow A \\ RA + X^- \end{array} & & \begin{array}{c} RH_2O^+ + X^- \\ H_2O \,\updownarrow \\ R^+ + X^- \\ A \,\updownarrow \\ RA + X^- \end{array} \\ RX & \rightleftarrows & & \rightleftarrows & & \rightleftarrows & \end{array} \qquad [IV]$$

Fainberg and Winstein (14) have shown that the steps indicated in reaction [IV] need to be considered in a reaction which proceeds by a dissociation mechanism. These steps are intended to represent the sequence of events in which the two ionic fragments of the reaction first become separate identities in intimate contact (internal ion pair (14)), then ions in contact but each ion with an independent solvation sheath, and finally separated and independent ions. The stereochemistry of each of these intermediates is shown in Fig. 4. In the initial stage of separation the ions have sufficient influence upon one another that the original stereochemistry is maintained in spite of the lengthening metal to halogen bond. In the other two stages of separation the original octahedron has collapsed to a five-co-ordinate structure which is considered to be the trigonal bipyramid.

Bateman, Hughes, and Ingold (15) have shown that if a reactive intermediate of low co-ordination number is sufficiently stable to have independent existence in solution it should be possible to detect the presence of such an intermediate by a mass law effect. That such an effect is absent in the present case is evident from the data for the effect of chloride, bromide, and iodide salts on the rate of hydrolysis of the chloro, bromo, and iodo complexes. Separated ions do not seem to be involved in the rate-determining step of reaction [II].

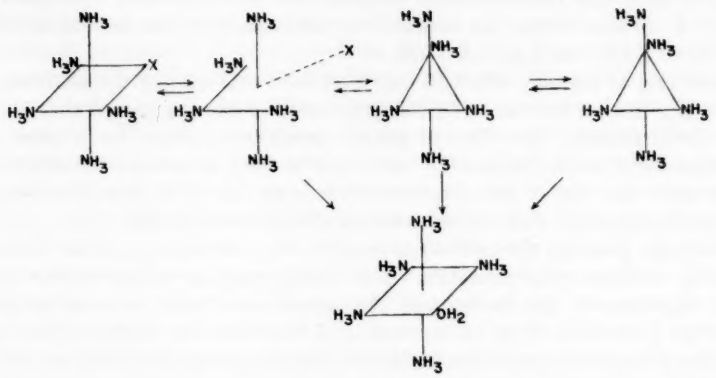

FIG. 4. Configuration relationships among the possible intermediates in the hydrolysis of $Cr(NH_3)_4X^{++}$.

If the octahedral structure collapses to yield the solvent-separated ion pair there are three equivalent positions at which water is able to attack the intermediate to produce the aquo ion. In the case under consideration this intermediate of reduced co-ordination number forms an ion pair with the anion of the salt present. The structure of such an ion pair becomes important. It seems reasonable to place the anion on the side of the complex away from the halogen. This conclusion was reached on the basis that *trans*-dichlorobis(ethylenediamine)cobalt(III) solvolysis is not accelerated by basic anions, whereas that of the corresponding cis complex is accelerated. The cis complex has a permanent dipole, whereas the trans complex does not, and it seems that a permanent dipole is necessary in order to obtain rate acceleration from ion-pair formation. Coupled with this is the observation that maleate produces a much greater change in the reaction rate than fumarate and that *o*-phthalate produces a much greater change than *p*-phthalate. In each case it is the anion with π orbitals suitably situated for overlap with the t_{2g} orbitals of the chromium which has the greater influence upon the reaction rate. This suggests that, in these cases at least, π bonding to the chromium is important and as a consequence the anion must be stretched across the face of the original octahedron. On the basis of these considerations the ion-pairing anion is thought to be stretched across the back side of the chromium complex in such a way that a reactive end is adjacent to each of two of the reactive sites and the body of the anion shields the third such site. Under these circumstances it would be surprising indeed if the ion-paired anion was not able to compete with water for some of these reactive sites. Such competition ought to make its appearance in the form of the aniono complex as one of the primary products of the reaction. For example, the fact that citrato complexes do not appear as primary products in the presence of citrate anion argues against a five-co-ordinated structure having an important role in the transition state. It might conceivably be argued that the anion does enter the complex in the initial step but is quickly eliminated by a subsequent hydrolysis. This seems unlikely because it has been observed that each of the anions reacts slowly with the product hydroxo complex to produce an aniono complex which is not hydrolyzed under the conditions of the experiment (16).

Acceleration of the reaction due to charge transfer is compatible with a dissociation reaction and acceleration due to the anion helping to maintain the original octahedral

configuration is compatible with the internal ion-pair intermediate. The internal ion-pair intermediate (14) is also compatible with the observation that the accelerating anion does not appear in the original reaction product. In this intermediate not all potential positions of attack on the molecule are equivalent. The position being vacated by the leaving group, which is most remote from the anion, is most vulnerable to attack. As a consequence one would not expect the accelerating anion to appear in the original reaction product and this is compatible with the experimental observations.

It is suggested that the reaction occurs via a stretching of the chromium to halogen bond. If, when the bond reaches a critical distance, there is a properly oriented water molecule this molecule enters to replace the halide ion. If there is not a properly oriented water molecule the halogen returns to its original position and no reaction occurs. The reaction might be considered to proceed via the following model.

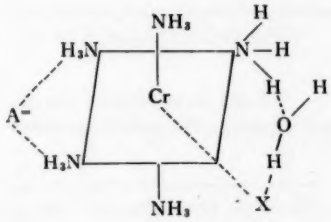

This model represents a reaction which is primarily S_N1 but one which requires the intervention of solvent for completion. The name solvent-assisted S_N1 is suggested.

REFERENCES

1. G. Biederman and L. G. Sillen. Arkiv Kemi, **5**, No. 40, 425 (1953).
2. A. R. Olson and R. T. Simonson. J. Chem. Phys. **17**, 1167 (1949).
3. F. J. Garrick. Trans. Faraday Soc. **34**, 1088 (1938).
4. H. Taube and F. A. Posey. J. Am. Chem. Soc. **75**, 1463 (1953).
5. M. Ikuta, H. G. McAdie, and W. McF. Smith. Can. J. Chem. **34**, 1361 (1956).
6. R. G. Pearson, P. M. Henry, and F. Basolo. J. Am. Chem. Soc. **79**, 5382 (1957).
7. M. A. Levine, T. P. Jones, W. E. Harris, and W. J. Wallace. J. Am. Chem. Soc. **83**, 2453 (1961).
8. C. K. Ingold. Structure and mechanism in organic chemistry. Cornell University Press. 1953. p. 362.
9. R. A. Plane and H. Taube. J. Phys. Chem. **56**, 33 (1952).
10. F. Basolo, B. D. Stone, J. G. Bergman, and R. G. Pearson. J. Am. Chem. Soc. **76**, 3079 (1954).
11. In preparation.
12. J. M. Peacock and J. C. James. J. Chem. Soc. 2233 (1951).
13. F. Basolo and R. G. Pearson. Mechanism of inorganic reactions. John Wiley & Sons, New York. 1958.
14. A. H. Fainberg and S. Winstein. J. Am. Chem. Soc. **78**, 2764 (1956).
15. L. C. Bateman, E. D. Hughes, and C. K. Ingold. J. Chem. Soc. 974 (1940).
16. Unpublished observations.

HELVETICA CHIMICA ACTA

SCHWEIZERISCHE
CHEMISCHE GESELLSCHAFT
Verlag Helvetica Chimica Acta
Basel 7 (Schweiz)

Seit 1918 **43** Jahre

Abonnemente: Jahrgang 1961, Vol. XLIV $31.50 incl. Porto

Es sind noch lieferbar:

Neudruck ab Lager
Vol. I–XXVII (1918–1944)

Originalausgaben, druckfrisch und antiquarisch.
Vol. XXVIII–XLIII (1945–1960)

Diverse Einzelhefte ab Vol. XX
Preise auf Anfrage. Nur solange Vorrat.

Das wissenschaftliche Organ der SCHWEIZERISCHEN CHEMISCHEN GESELLSCHAFT

Recueil des travaux chimiques des Pays-Bas

FONDÉ EN 1882 PAR

W. A. VAN DORP, A. P. N. FRANCHIMONT, S. HOOGEWERFF, E. MULDER ET A. C. OUDEMANS

EDITED BY THE ROYAL NETHERLANDS CHEMICAL SOCIETY

Generally the "Recueil des travaux chimiques des Pays-Bas" only accepts papers for publication from members of the Royal Netherlands Chemical Society who are also subscribers to the Recueil. Applications for membership of this society should be sent to The Secretariate, Lange Voorhout 5, The Hague.

The Recueil contains papers written in English, French or German and appears if possible monthly except in August and September, in issues of varying size. It is obtainable from D. B. Centen's Uitgeversmaatschappij, P.O.B. 507, Hilversum (the Netherlands), or through any bookseller in Holland or abroad. The subscription is 50.— guilders for Holland and 52.50 guilders abroad. Authors receive 75 reprints of their papers free of charge.

Editorial Office: Lange Voorhout 5, The Hague.

NOTES TO CONTRIBUTORS

Canadian Journal of Chemistry

MANUSCRIPTS

General.—Manuscripts, in English or French, should be typewritten, double spaced, on paper 8½×11 in. **The original and one copy are to be submitted.** Tables and captions for the figures should be placed at the end of the manuscript. Every sheet of the manuscript should be numbered. Style, arrangement, spelling, and abbreviations should conform to the usage of recent numbers of this journal. Greek letters or unusual signs should be written plainly or explained by marginal notes. Characters to be set in bold face type should be indicated by a wavy line below the characters. Superscripts and subscripts must be legible and carefully placed. Manuscripts and illustrations should be carefully checked before they are submitted. Authors will be charged for unnecessary deviations from the usual format and for changes made in the proof that are considered excessive or unnecessary.

Abstract.—An abstract of not more than about 200 words, indicating the scope of the work and the principal findings, is required, except in Notes.

References.—These should be designated in the text by a key number and listed at the end of the paper, with the number, in the order in which they are cited. The form of the citations should be that used in this journal; in references to papers in periodicals, titles should not be given and only initial page numbers are required. The names of periodicals should be abbreviated in the form given in the most recent *List of Periodicals Abstracted by Chemical Abstracts*. All citations should be checked with the original articles and each one referred to in the text by the key number.

Tables.—Tables should be numbered in roman numerals and each table referred to in the text. Titles should always be given but should be brief; column headings should be brief and descriptive matter in the tables confined to a minimum. Vertical rules should not be used. Numerous small tables should be avoided.

ILLUSTRATIONS

General.—All figures (including each figure of the plates) should be numbered consecutively from 1 up, in arabic figures, and each figure referred to in the text. The author's name, title of the paper, and figure number should be written in the lower left corner of the sheets on which the illustrations appear. Captions should not be written on the illustrations.

Line drawings.—Drawings should be carefully made with India ink on white drawing paper, blue tracing paper, or co-ordinate paper ruled in blue only; any co-ordinate lines that are to appear in the reproduction should be ruled in black ink. Paper ruled in green, yellow, or red should not be used. All lines must be of sufficient thickness to reproduce well. Decimal points, periods, and stippled dots must be solid black circles large enough to be reduced if necessary. Letters and numerals should be neatly made, preferably with a stencil (**do NOT use typewriting**), and be of such size that the smallest lettering will not be less than 1 mm high when the figure is reduced to a suitable size. Many drawings are made too large; originals should not be more than 2 or 3 times the size of the desired reproduction. Wherever possible two or more drawings should be grouped to reduce the number of cuts required. In such groups of drawings, or in large drawings, full use of the space available should be made; the ratio of height to width should conform to that of a journal page (5½×7¾ in.), but allowance must be made for the captions. **The original drawings and one set of clear copies (e.g. small photographs) are to be submitted.**

Photographs.—Prints should be made on glossy paper, with strong contrasts. They should be trimmed so that essential features only are shown and mounted carefully, with rubber cement, on white cardboard, with no space between those arranged in groups. In mounting, full use of the space available should be made. **Photographs are to be submitted in duplicate;** if they are to be reproduced in groups one set should be mounted, the duplicate set unmounted.

REPRINTS

A total of 100 reprints of each paper, without covers, are supplied free. Additional reprints, with or without covers, may be purchased at the time of publication.

Charges for reprints are based on the number of printed pages, which may be calculated approximately by multiplying by 0.5 the number of manuscript pages (double-space typewritten sheets, 8½×11 in.) and including the space occupied by illustrations. Prices and instructions for ordering reprints are sent out with the galley proof.

Contents

D. W. Davidson—Dielectric relaxation in liquids. II. Isomeric pentanediols - 2139

P. M. Laughton and R. E. Robertson—Solvolysis in hydrogen and deuterium oxide. IV. Halides with neighboring groups - - - - - - - - - - 2155

P. J. Dyne and W. M. Jenkinson—Radiation chemistry of cyclohexane. III. Effect of benzene and iodine on the isotopic composition of radiolytic hydrogen from C_6D_{12}–C_6H_{12} mixtures - - - - - - - - - - - - 2163

R. J. Gillespie and E. A. Robinson—The vibrational spectra of sulphuryl and thionyl halides - - - - - - - - - - - - - - - - - - 2171

R. J. Gillespie and E. A. Robinson—The Raman spectra of some polysulphuryl chlorides and fluorides - - - - - - - - - - - - - - - 2179

R. J. Gillespie and E. A. Robinson—The Raman spectra of liquid sulphur trioxide and solutions of sulphur trioxide in inert solvents - - - - - 2189

K. Noack and R. Norman Jones—Some stereochemical studies on α,β-unsaturated ketones using Raman spectrophotometry - - - - - - - 2201

R. Norman Jones and K. Noack—Conformational equilibria in diethyl ketone 2214

K. Noack and R. Norman Jones—Conformational equilibria in open-chain α,β-unsaturated ketones - - - - - - - - - - - - - - - 2225

R. C. Kapoor, O. P. Agrawal, and T. D. Seth—Polarographic determination of the dissociation constant of the sulphydryl group and diffusion coefficient measurements of thiomalic acid - - - - - - - - - - - - 2236

J. M. G. Cowie and P. M. Toporowski—Association in the binary liquid system dimethyl sulphoxide – water - - - - - - - - - - - - - - 2240

Otto P. Strausz and Harry E. Gunning—The decomposition of carbon dioxide by Hg $6(^3P_1)$ and Hg $6(^3P_0)$ atoms - - - - - - - - - - - 2244

Arthur R. Knight and Harry E. Gunning—Primary quantum yield determination by intermittent illumination in the reaction of methanol vapor with Hg $6(^3P_1)$ atoms - - - - - - - - - - - - - - - - - - - 2251

J. E. Bloor—Theoretical studies on the electronic spectra of substituted aromatic molecules. Part I. The intramolecular electron transfer model 2256

F. A. L. Anet—Some aspects of the nuclear magnetic resonance spectra of compounds containing C-methyl groups - - - - - - - - - - - 2262

P. A. J. Gorin and J. F. T. Spencer—Extracellular acidic polysaccharides from *C. insidiosum* and other *Corynebacterium* spp. - - - - - - - - - 2274

P. A. J. Gorin and J. F. T. Spencer—Structural relationships of extracellular polysaccharides from phytopathogenic *Xanthomonas* spp. Part I. Structure of the extracellular polysaccharide from *Xanthomonas stewartii* 2282

K. Grjotheim, O. Herstad, and J. M. Toguri—The aluminum reduction of magnesium oxide. II. The vapor pressure of magnesium over the system Al–MgO–CaO - - - - - - - - - - - - - - - - - - - 2290

W. F. Forbes—Light absorption studies. Part XIX. The ultraviolet absorption spectra of iodobenzenes - - - - - - - - - - - - - - - - 2295

Richard F. W. Bader and Alan D. Westland—The electronic spectra of $MoCl_4$ and $NbCl_4$ - - - - - - - - - - - - - - - - - - - 2306

Notes:

F. A. L. Anet—The N.M.R. spectrum of cyclopentanone - - - - - - 2316

L. W. Reeves and K. O. Strømme—Proton resonance spectra of 8-hydroxy and 8-methyl quinoline - - - - - - - - - - - - - - - 2318

E. Aspeitia, A. Bowers, P. Crabbé, O. Mancera, J. S. Matthews, J. Reynoso, and J. Salazar—Chemical constituents of chicozapote - - - - - 2321

SYMPOSIUM ON CO-ORDINATION IN CHEMISTRY

W. G. Paterson and M. Onyszchuk—Co-ordination compounds of hydrazine. Part II. The interaction of trimethylborane and trimethylaluminum with hydrazine - - - - - - - - - - - - - - - - - - - 2324

M. W. Lister—Complex periodates and tellurates - - - - - - - - - 2330

R. J. Gillespie—The stereochemistry of eight-co-ordination: the nature of the bonding in the $Mo_2Cl_8^{4+}$, $Nb_6Cl_{12}^{2+}$, and related ions - - - - - - - - 2336

Ernest Rivet, Real Aubin, and Roland Rivest—Co-ordination complexes of titanium (IV) halides. II. Preparation and infrared spectra of the complexes of titanium tetrachloride with diesters of α,ω-dicarboxylic acids and comparison with analogous complexes of zirconium tetrachloride and tin tetrachloride - - - - - - - - - - - - - - - - - - - 2343

A. D. Westland and N. C. Bhiwandker—π-Bonding in inorganic compounds. IV. Role of unpaired electrons in hexahalo complexes - - - - - - - 2353

Marvin J. Albinak, Dinesh C. Bhatnagar, Stanley Kirschner, and Anthony J. Sonnessa—The effects of optically inactive ions on the rotatory dispersion of asymmetric complex ions - - - - - - - - - - - - - - - 2360

T. P. Jones, W. E. Harris, and W. J. Wallace—Substitution at octahedral centers. II. Effect of salts upon the rate of hydrolysis of the halopentamminechromium(III) ions - - - - - - - - - - - - - - - - 2371

Printed in Canada *by* University of Toronto Press